Stringy ER = EPR

A dissertation presented

by

Elliot Schneider

to

The Department of Physics

in partial fulfillment of the requirements

for the degree of

Doctor of Philosophy

in the subject of

Physics

Harvard University

Cambridge, Massachusetts

May 2021

Dissertation Advisor: Daniel Louis Jafferis Elliot Schneider

Stringy ER = EPR

Abstract

The ER = EPR correspondence asserts that quantum entanglement and geometric spatial connection are closely related. A two-sided black hole, for example, is equivalent to an entangled superposition of disconnected geometries. In this dissertation, we construct perturbative string dualities that give explicit examples of this equivalence.

The string dualities are obtained by continuation in the sense of the target time coordinate of CFT dualities for the $\mathrm{SL}(2,\mathbb{R})_k/\mathrm{U}(1)$ and $\mathbb{Z}\backslash\mathrm{SL}(2,\mathbb{C})_k/\mathrm{SU}(2)$ coset WZW models. For large k, these CFTs admit a weakly-coupled description as a string in a Euclidean black hole target space of two-dimensional dilaton-gravity and three-dimensional AdS gravity, respectively. They also admit dual, strongly-coupled descriptions with a non-contractible target Euclidean time circle and a condensate of winding strings that wrap it. The latter description is the sine-Liouville background of Fateev, Zamolodchikov, and Zamolodchikov in the case of $\mathrm{SL}(2,\mathbb{R})_k/\mathrm{U}(1)$, and a similar dual that we propose for $\mathbb{Z}\backslash\mathrm{SL}(2,\mathbb{C})_k/\mathrm{SU}(2)$. By continuing the target Euclidean time coordinate on both sides of these dual backgrounds, we obtain Lorentzian dualities relating an ER description of a string in a connected black hole and an EPR description in a disconnected target with a condensate of entangled strings.

The first part of the dissertation is devoted to a study of the $\mathrm{SL}(2,\mathbb{R})_k/\mathrm{U}(1)$ CFT itself in the semi-classical limit. We construct the saddle-point expansion for the functional integral

that computes the reflection coefficient of the CFT. To do so requires that we complexify the target space and sum over complex-valued saddles, which, remarkably, include configurations that hit the singularity of the Lorentzian black hole within the complexified target.

The second part of the dissertation proposes the sine-Liouville dual description of the $\mathbb{Z}\backslash \mathrm{SL}(2,\mathbb{C})_k/\mathrm{SU}(2)$ CFT, and develops the tools necessary to establish the string dualities for ER = EPR by continuation. Part of the construction relies on understanding string perturbation theory in different spacetime states—the Hartle-Hawking state in the connected ER description of the black hole and the thermofield-double state in the disconnected EPR description. The state dependence is encoded in the choice of Schwinger-Keldysh contour for the worldsheet functional integral. We show that the sine-Liouville Euclidean time winding condensate leads in the Lorentzian continuation to a condensate of pairs of entangled folded strings, one on each side of the disconnected target and emanating from a strong-coupling region in place of a horizon. Each pair of strings is prepared in the worldsheet thermofield-double state in the sense of angular quantization, and a related angular deformation of the string moduli contour of integration is required to define string perturbation theory in the thermal EPR microstates. Finally, we discuss an infinitesimal interpretation of the dualities that gives equivalent semi-classical descriptions of a conformal perturbation that shifts the mass of the black hole.

Contents

Citations to Previously Published Work

The work described in this dissertation was completed in collaboration with Daniel Jafferis. Much of the content of Ch. 2 has appeared previously in

> D. L. Jafferis and E. Schneider, "Semi-Classical Analysis of the String Theory Cigar," April 2020, arXiv:hep-th/2004.05223,

and much of the content of Chs. 3-4 has appeared previously in

> D. L. Jafferis and E. Schneider, "Stringy ER = EPR," April 2021, arXiv:hep-th/2104.07233.

Acknowledgements

I could not have completed this degree without the help of a great many people to whom I am deeply grateful.

Foremost, I must thank my advisor, Daniel Jafferis, for sharing so much of his time, insight, and ideas with me. Daniel has some of the most remarkable intuition for physics of anyone that I have ever encountered, and I consider myself extremely fortunate to have had the opportunity to learn with him these past years. Thank you so much.

I have also learned an enormous amount from the many faculty members, post-docs, graduate students, and undergraduate students I have had the chance to interact with, both in graduate school and when I was an undergraduate at Caltech. Thank you all for everything you have taught me.

Thank you so much to the many staff members at Harvard who keep our department running. I would like to single out in particular Jacob Barandes and Lisa Cacciabaudo, whose support over the years has been invaluable.

I owe an immeasurable debt of gratitude to the many teachers who have inspired me throughout my life—far too many than I can name and thank properly here. But I would especially like to thank Andy Bramante, David Proctor, and Joe Wesney for nurturing my scientific curiosity as a high school student long ago.

Finally, thank you so much to my parents for making everything possible, and to my entire family for your continual love and support.

For Dad & Mom,
Allison, Jeff, & Rebecca,
Harrison & Ruby,
and even Mae

1 Introduction

The remarkable relationship between quantum entanglement and geometric spatial connection is a profound feature of quantum gravity [1–6]. The link between these two naively disparate subjects goes by the moniker "ER = EPR" [4]—ER for Einstein and Rosen [7], whose Einstein-Rosen bridge connects the left and right regions of a two-sided black hole, and EPR for Einstein, Podolsky, and Rosen [8], whose famous thought experiment was one of the early works that considered the consequences of entanglement in quantum mechanics. The prototypical example of this correspondence is that a pair of black holes that are entangled with one another are joined in their interiors by an Einstein-Rosen bridge, as in the two-sided Schwarzschild black hole shown in Fig. 1.1a. The principal goal of the work described in this dissertation is to construct examples of this equivalence of entanglement and spatial connection in string theory.

Black holes play fascinating dual roles in the landscape of physics. Our understanding of the laws of nature is organized, both historically and practically, by scale. At the very

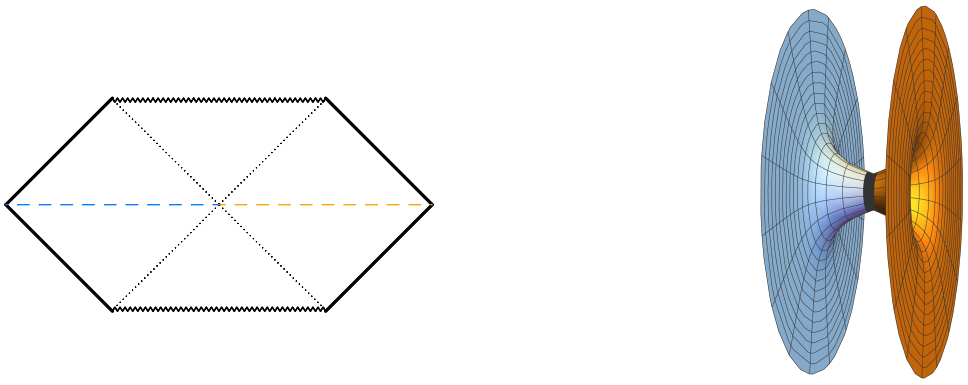

(a) **(b)**

Figure 1.1: Schwarzschild Black Hole. The Schwarzschild black hole is a solution of Einstein gravity in asymptotically flat space (left). It is a two-sided geometry, asymptoting to one Minkowski-space universe to the right, and to another on the left. Spatial slices of these two universes corresponding to the horizontal dashed lines are shown on the right. The two sides are joined at the horizon bifurcation point where the diagonal dotted lines intersect on the left, which corresponds to the black band gluing together the two throats on the right. The connection is called a wormhole or an Einstein-Rosen bridge. They are not causally connected, however, because no signal can pass from the left region to the right or vice-versa without exceeding the speed of light. The region behind the horizons is the interior of the black hole, ending at the past and future singularities represented by the zigzag lines.

largest distance scales—equivalently, the lowest energy scales—gravity is the dominant force in the universe, dictating the behavior of galaxies, and the stars, planets, and black holes that comprise them. Being the densest objects in the universe, black holes play a major role in this arena. At smaller distance scales, however, gravity becomes far less important than the other forces. For colliding protons at the Large Hadron Collider, for example, at energy scales of order 10 TeV, the gravitational force is so feeble compared to the strong and electroweak forces that gravity is typically ignored altogether in the study of particle physics at these energy scales. Above the Planck scale of order 10^{16} TeV, however, far beyond any energy scale ever likely to be accessed in a particle accelerator built on Earth, gravity reasserts itself: colliding particles with such enormous energies would form black holes.

Black holes therefore tie high and low energy physics together in an intricate way, and they serve as an essential guidepost in our efforts to understand the laws of physics at all

scales. Although we do not know the fully quantum theory of gravity that describes our universe, the fact that in the vicinity of the horizon of a large black hole—the point-of-no-return beyond which nothing, not even light, can escape its gravitational pull—spacetime is only weakly curved enables us to learn a great deal by applying the lower-energy physics we already understand. This line of reasoning has driven much research in theoretical physics in recent decades. It lead to Hawking's discovery that black holes radiate like blackbodies [9], which in turn spawned the information paradox [10] that to this day remains one of the overarching questions informing research on quantum gravity. Namely, if a black hole eventually evaporates away, how is the data of the quantum state of whatever matter had fallen into it encoded in the outgoing radiation?

Hawking's calculations, together with the work of Bekenstein [11, 12], showed that black holes behave as ordinary thermodynamic objects. In particular, they carry entropy—a great deal of it, in fact—given by the Bekenstein-Hawking formula $S = \frac{A}{4G_{\mathrm{N}}}$, with A the area of the horizon surface. In classical general relativity, black hole solutions are uniquely labeled by their mass, angular momentum, and charge [13, 14], meaning that the data of the initial configuration of collapsing matter that formed the black hole is not encoded in the classical solution. Instead, one concludes that a black hole has a huge number e^S of quantum-mechanical microstates which reflect the large number of initial configurations that may have formed it. A complete theory of quantum gravity should therefore be able to account for these black hole microstates.

The fact that the black hole entropy scales with the area of the horizon is quite surprising

at first. In field theory, for example, one has degrees of freedom associated to each point in space, and thus the entropy in a given region is proportional to its volume. Once gravity is taken into account, however, one arrives at an unexpected consequence: there is an upper bound on the amount of entropy that can be packed into any volume—the Bekenstein-Hawking entropy of a black hole whose horizon area is the boundary of that volume [15, 16]. For if that were not the case, by piling more junk into the volume until it collapses into a black hole, the entropy would suddenly drop to the Bekenstein-Hawking level, down from its supposedly larger initial value, in violation of the second law of thermodynamics. One concludes that the maximum entropy in a region of space is proportional not to its volume where the degrees of freedom were assumed to live, but to its boundary area. This leads to the idea of holography [15, 17], which claims that the degrees of freedom in a gravitational system in fact live on the boundary, i.e. in one lower dimension than the bulk.

Over the past twenty years, the idea of holography has been borne out through the gauge/gravity correspondence [18–20], which has transformed the way we think about quantum gravity. The correspondence says that gravity in a $d+1$ dimensional spacetime[1] is equivalent to a field theory living in d dimensions. The best known special case is the AdS/CFT correspondence, which relates gravity in an asymptotically Anti de Sitter (AdS) spacetime to a conformal field theory (CFT) on its boundary. A CFT is a special kind of quantum field theory which is invariant under local rescalings of the metric, while AdS is a particular manifold that solves Einstein's equations with negative cosmological constant while preserving as many symmetries as possible. AdS_3, for example, may be thought of as

[1] Potentially together with some additional compact manifold.

a solid cylinder, with Lorentzian time running along its length. Its dual, two-dimensional CFT description therefore naturally lives on the cylindrical surface at its boundary.[2] In other words, the dual CFT is quantized on a circle S^1 times time $\mathbb{R}$. In fact, at present the duality is elevated to a definition of the bulk theory of quantum gravity by equating it to the boundary CFT. At low energies, the bulk theory is described by Einstein gravity, coupled to additional light fields.

The two-sided black hole referenced in the description of ER = EPR at the beginning of the introduction and pictured in Fig. 1.1a is not an example of an astrophysical black hole formed by collapsing matter. It is an eternal solution of Einstein's equations that exists for all time. It is ER = EPR that captures the physical significance of this solution: it describes two black holes in separate universes that have been entangled with one another, and the entanglement is responsible for the Einstein-Rosen bridge that forms between them.

Each side of the black hole approaches a copy of its own asymptotically Minkowski-space universe, causally disconnected from the universe on the opposite side. However, the two sides are spatially connected at the horizon bifurcation point, where the two diagonal dotted lines in the figure intersect, and they share common past and future interior regions behind these horizons that terminate in the past and future singularities. This spatial connection is the Einstein-Rosen bridge, also known as a (non-traversable) wormhole. A spatial slice of the wormhole is shown in Fig. 1.1b, corresponding to the zero-time slice of the two-sided black hole indicated by the horizontal dashed line in Fig. 1.1a. Although the two sides are

[2] More precisely, the conformal boundary surface—the cylinder is at infinite distance in the AdS metric.

spatially connected, no signal can pass from one to the other, because it is impossible to cross the bridge without exceeding the speed of light. In particular, as time evolves upward on the Schwarzschild diagram, the wormhole grows ever-longer, and any signal one attempts to send from one side to the other becomes trapped in the interior region behind the horizons. Two intrepid astronauts who jump into the black hole from either side could meet in the interior, but they cannot transmit the content of their conversation back to their home space stations before they meet their unfortunate end in the singularity.

Each side of the geometry may be thought of as a black hole living in its own universe. If the black holes were not entangled with one another, there would be no connection between them, corresponding to erasing the black band in middle of Fig. 1.1b. For the two-sided black hole, however, the left and right sides are entangled, and the horizons of the black holes are glued together. According to ER = EPR, it is this entanglement that leads to the wormhole that connects the two.

To make this idea concrete, let us discuss the analogous two-sided black hole in asymptotic AdS_{d+1} space, so that we may apply the technology of AdS/CFT. Choose $d = 2$ for simplicity; the asymptotically AdS_3 black hole is also known as BTZ after its discoverers [21, 22]. This two-sided AdS_3 black hole has two asymptotically AdS_3 regions, and is therefore related to two copies of the dual CFT, one on the left and one on the right. The two-sided black hole is dual to a particular state in these two copies of the CFT, known as the thermofield-double (TFD) state [23, 24].[3]

[3] Above the Hawking-Page transition temperature [25].

To understand this statement, consider first a thermal state of a single CFT on a circle. It is a mixed state in the Hilbert space $\mathcal{H}(\mathrm{S}^1)$, described by a density matrix $\rho = e^{-\beta H}$, where $1/\beta$ is the temperature of the state. A thermal state on a spatial manifold Σ is in general prepared by the Euclidean functional integral on $\Sigma \times \mathrm{S}^1_\beta$. β is the circumference of the Euclidean time circle, corresponding to the evolution by $e^{-\beta H}$, and the Euclidean time is periodic because a thermal correlation function is computed by $\mathrm{tr}(e^{-\beta H} \cdots)$. Then the thermal state for the CFT on $\Sigma = \mathrm{S}^1$ is prepared by a Euclidean functional integral on a torus $\mathrm{S}^1 \times \mathrm{S}^1_\beta$. By cutting the Euclidean torus at a single spatial slice S^1 and gluing it to the S^1 cross-section of the Lorentzian cylinder, one prepares the thermal state in the Hilbert space of the CFT on the circle.

Alternatively, one may make multiple cuts on the torus to prepare states in the product Hilbert space of multiple copies of the CFT. For the TFD, one slices the torus in half, preparing a state in $\mathcal{H}_\mathrm{L}(\mathrm{S}^1) \otimes \mathcal{H}_\mathrm{R}(\mathrm{S}^1)$ describing two copies of the CFT. In other words, the TFD state is prepared by the Euclidean functional integral on $[0, \beta/2] \times \mathrm{S}^1$, consisting of an interval times a circle.

If one were to sew the second cut in the torus back up, one would recover the thermal state in the single copy of the CFT on the remaining circle. Thus, the thermal density matrix $e^{-\beta H}$ on $\mathcal{H}_\mathrm{R}(\mathrm{S}^1)$ corresponds to the reduced density matrix of the TFD state in $\mathcal{H}_\mathrm{L}(\mathrm{S}^1) \otimes \mathcal{H}_\mathrm{R}(\mathrm{S}^1)$ with respect to $\mathcal{H}_\mathrm{L}$: $e^{-\beta H} \propto \mathrm{tr}_{\mathcal{H}_\mathrm{L}} |\mathrm{TFD}\rangle \langle \mathrm{TFD}|$. $|\mathrm{TFD}\rangle$ is therefore called a purification of the thermal state, because it lifts the mixed state $e^{-\beta H}$ in one copy of the CFT to a pure state in two copies.

One may show that $|\mathrm{TFD}\rangle$ as defined by this Euclidean functional integral is equivalently expressed as a sum over energy eigenstates of the two CFT copies:[4]

$$|\mathrm{TFD}\rangle \propto \sum_n e^{-\beta E_n/2} |n\rangle_{\mathrm{L}} \otimes |n\rangle_{\mathrm{R}} \,. \tag{1.1}$$

Each term is simply a product of a state $|n\rangle_{\mathrm{L}}$ from $\mathcal{H}_{\mathrm{L}}$ and a state $|n\rangle_{\mathrm{R}}$ from $\mathcal{H}_{\mathrm{R}}$. The sum, however, is an entangled state in $\mathcal{H}_{\mathrm{L}} \otimes \mathcal{H}_{\mathrm{R}}$. In other words, $|\mathrm{TFD}\rangle$ cannot be written as a product of a single state in $\mathcal{H}_{\mathrm{L}}$ with a single state in $\mathcal{H}_{\mathrm{R}}$—it gives the state of the whole system, but not the state of the left and right CFTs individually. Such entangled states are ubiquitous in quantum mechanics; a familiar example is the spin singlet $|\uparrow\rangle \otimes |\downarrow\rangle - |\downarrow\rangle \otimes |\uparrow\rangle$ of the two-state system encountered in a first quantum mechanics course. The two Hilbert spaces are not coupled and are completely independent of one another, but the entanglement of the state ties them together in an intricate way.

The assertion of [23] is that the TFD state of the two CFT copies is dual to the two-sided black hole in its Hartle-Hawking (HH) state (Fig. 1.2) [26, 27]. The latter may likewise be prepared by a Euclidean functional integral, now in the sense of bulk quantum gravity. Namely, one takes the Euclidean continuation of the black hole, which has the topology of a solid torus, cuts it in half to form a manifold in the shape of a half-bagel, and glues this Euclidean cap to the zero-time slice of the black hole to prepare the HH state.[5] This state is

[4] One should more properly include the action of CPT conjugation on one factor, which we omit here for simplicity of exposition.

[5] More precisely, the Hartle-Hawking state may be regarded as a wavefunctional defined by the bulk gravity Euclidean functional integral with thermal boundary conditions at infinity and ending on a spatial slice bounded by the two circles. Then the claim is that above the Hawking-Page temperature, this wavefunctional is sharply peaked on the black hole background, whose zero-time slice is an annulus. Below the Hawking-Page temperature, the same wavefunctional instead peaks on two disconnected copies of AdS_3 in the bulk TFD state.

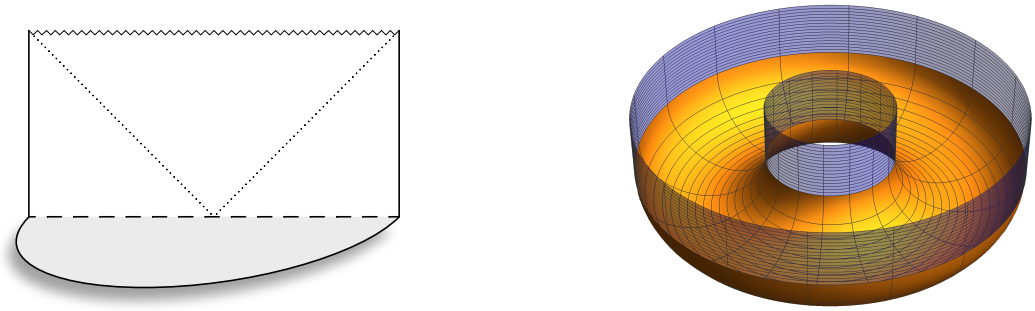

(a) **(b)**

Figure 1.2: The AdS_3 HH State and the Dual TFD. The conformal diagram of the asymptotic AdS_3 two-sided black hole (or, rather, its top half) is shown on the left. Over each point is an additional circle, which is suppressed in the figure. The left and right asymptotic AdS_3 regions are causally separated by the horizons, represented by the diagonal dotted lines. The future singularity is the zigzag line at the top of the diagram. The Hartle-Hawking state is prepared by halving the Euclidean continuation of the black hole, shown by the half-disk, and gluing it to the zero-time slice of the black hole on the horizontal dashed line. The Euclidean time periodicity is β, the inverse Hawking temperature of the black hole. The zero-time slice has the topology of an annulus and the halved Euclidean black hole resembles a half-bagel, obtained by revolving the dashed line and half-disk around the suppressed circle. Above the Hawking-Page temperature, this bulk state is dual to the thermofield-double state in two copies of the boundary CFT on a circle (times time), shown on the right. The yellow half-torus prepares the state on its two circle boundaries, which then evolve forward in Lorentzian time along the two blue cylinders. The Hartle-Hawking cap that prepared the bulk state corresponds to the solid half-torus obtained by filling in the interior of the yellow surface.

pictured in Fig. 1.2a, with the non-contractible circle direction of the solid torus suppressed. The "crust" of the half-bagel is a half-torus $[0, \beta/2] \times S^1$, which coincides with the boundary Euclidean cap that prepares the dual TFD state (Fig. 1.2b).

In this correspondence, the temperature $1/\beta$ defining the TFD state is set to the Hawking temperature [9] of the black hole. Upon reducing to a single side of the geometry and a single copy of the dual CFT, one obtains a thermal state at this temperature in the bulk and on the boundary. In this way, it is very natural that the two-sided black hole should be dual to a purification of a thermal state of the CFT at that temperature. Moreover, that the two-sided black hole is dual to a state in two independent copies of the CFT is a boundary manifestation of the fact that the left and right regions in the bulk are causally separated by the horizons.

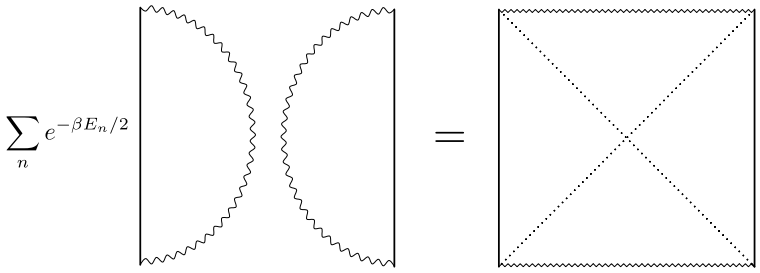

Figure 1.3: Schematic of ER = EPR. The connected, two-sided, asymptotically AdS black hole admits a dual description as an entangled superposition of disconnected spacetimes, represented schematically by the wedges on the left, each of which is dual to an energy eigenstate $|n\rangle_{\rm L}, |n\rangle_{\rm R}$ of the two copies of the boundary CFT. The ER = EPR correspondence asserts that this equivalence of entangled quantum states to connected spacetimes holds more generally. We find examples of string dualities of this type, relating a string in a connected target space to a string in an entangled superposition of disconnected targets.

At the same time, it is very surprising that a superposition of product states in two uncoupled CFTs as in $|\text{TFD}\rangle \propto \sum e^{-\beta E_n/2} |n\rangle_{\rm L} \otimes |n\rangle_{\rm R}$ should admit a bulk description as a single connected spacetime [1, 2]. Each CFT state $|n\rangle_{\rm L}$ is dual to some spacetime, as is each $|n\rangle_{\rm R}$, and so the product state $|n\rangle_{\rm L} \otimes |n\rangle_{\rm R}$ from these two uncoupled CFTs corresponds to a pair of disconnected spacetimes. Thus, the linearity of quantum mechanics would seem to imply that their superposition would in turn be dual to a superposition of disconnected geometries. And yet, the superposition admits a connected description as a two-sided black hole due to the entanglement[6] between the two sides, so the existence of an Einstein-Rosen bridge is a non-linear property of the state. Here then is an example of ER = EPR: the two-sided black hole is equivalent to an entangled superposition of disconnected geometries (Fig. 1.3).

This quantum equivalence of connected and disconnected geometries is quite unexpected from the perspective of classical gravity [28–30]. It can be traced [31] to the fact that the naive field basis $\{|g\rangle\}$ of the Hilbert space of the effective quantum gravity theory is

[6]Below the Hawking-Page temperature, the boundary TFD state is instead dual to the bulk TFD in two disconnected copies of AdS (Fig. 3.3a). Then the boundary TFD, and likewise the bulk disconnected superposition, is not sufficiently entangled to admit a dual semi-classical connected description.

overcomplete. In other words, a state prepared by a Euclidean functional integral like the HH state may be written as a wavefunctional $\Psi[g] = \langle g|\Psi\rangle$, defined by performing the integral over spacetime metrics ending on a slice with spatial metric g and with thermal AdS boundary conditions at infinity. For the HH state, the claim is that this wavefunctional is sharply peaked on the connected black hole metric at sufficiently high temperatures. g here represents a gauge equivalence class of metrics on the spatial slice with respect to spatial coordinate reparameterizations. The temporal coordinate redundancy is not fixed, however, and as a result the field eigenstates $\{|g\rangle\}$ form an overcomplete set. The outcome is that the HH state, which is peaked on the connected black hole, can equivalently be expressed as a sum over kets $|g\rangle$ with disconnected topologies.

Thus, there is no linear operator of the quantum theory that measures the "spatial connectedness" of a state [28–31], and there is no grading of the Hilbert space of quantum gravity by the number of spatial connected components. Likewise, as required for consistency with ER = EPR, there is no linear operator that measures the entanglement of a state. For an entangled state such as $|\text{TFD}\rangle$ may be written as a sum over product states, each of which is unentangled, and thus a linear operator cannot return "1" on an entangled state and "0" on an unentangled state.

All this suggests that there should exist examples of quantum gravity dualities, relating a connected spacetime to an entangled superposition of disconnected spacetimes. In this work, we exhibit exact string theory dualities of this type. The form of the relations is between string theory in a two-sided black hole[7] made of fundamental strings in the HH

[7]Or more simply in a two-sided Rindler decomposition of AdS_3, with asymptotic AdS_3 regions separated by coordinate

state (Fig. 1.2a), and string theory in a pair of disconnected spacetimes in the TFD state (in the bulk sense), with an entangled condensate of folded strings (Fig. 1.5a). Expanding the condensate, one indeed finds a dual EPR-like description of the black hole given by a superposition of disconnected geometries, each with a number of entangled strings. These entangled string backgrounds describe the thermal microstates that build up the black hole.

These ER = EPR string dualities are defined by Lorentzian continuation of CFT dualities for Euclidean black hole target spaces in two and three dimensions. Here we are referring to dualities of the worldsheet CFT of a string theory, not to be confused with the CFT that lives on the boundary of spacetime in the sense of the AdS/CFT duality. The worldsheet CFTs we will discuss are the $\mathrm{SL}(2,\mathbb{R})_k/\mathrm{U}(1)$ and $\mathbb{Z}\backslash\mathrm{SL}(2,\mathbb{C})_k/\mathrm{SU}(2)$ coset WZW models. They describe a string propagating in a two-dimensional asymptotically flat Euclidean black hole and three-dimensional Euclidean AdS black hole, respectively.

Before coming to that construction of the ER = EPR dualities, the first part of the dissertation is devoted to a study of the $\mathrm{SL}(2,\mathbb{R})_k/\mathrm{U}(1)$ CFT in its own right. This CFT has been a subject of great interest for thirty years, since it was shown to describe a Euclidean black hole for large k [32]. The Lie group $\mathrm{SL}(2,\mathbb{R})$ is equivalent to the manifold AdS_3, and thus the $\mathrm{SL}(2,\mathbb{R})_k$ WZW model describes a string in AdS_3, where $k = l^2_{\mathrm{AdS}}/l^2_{\mathrm{s}}$ sets the length scale of the geometry. The coset by U(1) gauges the time-translation isometry along the length of the AdS_3 cylinder, yielding a target space with the topology of a disk. At large k, it admits a weakly-coupled Lagrangian description given by a sigma-model into a

horizons.

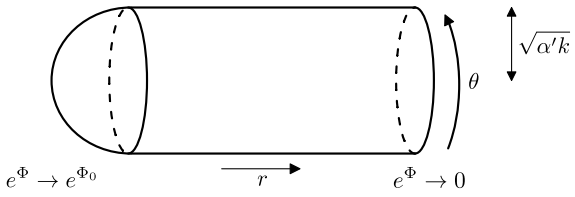

(a) The Cigar Background. The cigar sigma-model is a weakly-coupled Lagrangian description of the $\mathrm{SL}(2,\mathbb{R})_k/\mathrm{U}(1)$ CFT when k is large. For large r, the geometry is a cylinder of radius $\sqrt{\alpha' k}$, and as $r \to 0$ the cylinder smoothly caps off. The dilaton is a monotonically decreasing function of r. Its maximal value Φ_0 is attained at the tip, and at large r it falls off linearly as $-r$ and the string coupling goes to zero. Although a string in the weak-coupling region appears to be able to wind around the cylinder, there is no conserved topological charge because the string can unwind at the tip.

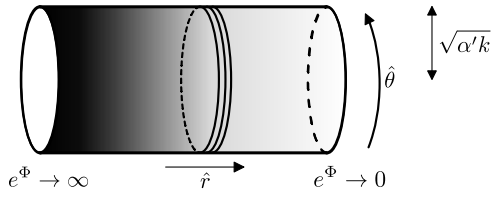

(b) The sine-Liouville Background. According to the FZZ duality, the sine-Liouville sigma-model is a dual description of the $\mathrm{SL}(2,\mathbb{R})_k/\mathrm{U}(1)$ CFT, better suited when k is small (compared to 2). The geometry is an infinite cylinder of radius $\sqrt{\alpha' k}$. The dilaton is $\Phi = -Q\hat{r}$, so that the string coupling e^{Φ} diverges as $\hat{r} \to -\infty$ and vanishes as $\hat{r} \to \infty$. The sine-Liouville potential $e^{-\sqrt{(k-2)/\alpha'}\hat{r}} \mathrm{Re}\, e^{i\sqrt{k/\alpha'}(\hat{\theta}_{\mathrm{L}} - \hat{\theta}_{\mathrm{R}})}$ includes a pure-winding mode of $\hat{\theta}$ (represented by the circles wrapping the middle of the cylinder), times a linear-dilaton primary (represented by the gradient).

Figure 1.4

cigar-shaped geometry with an asymptotically linear dilaton (Fig. 1.4a) [32].

The large k limit where this cigar description is best corresponds to the semi-classical limit of the CFT, and we study the functional integral in this limit by applying saddle-point methods. We focus on the simplest interesting observable: the reflection coefficient that describes the amplitude for a string sent in from infinity to reflect off the tip of the cigar and return to infinity.

In order to compute the saddle-point expansion of a functional integral one must, in general, complexify the integral and sum over complex saddles [33–42]. The necessity of complexification is familiar from the analogous problem for finite-dimensional integrals. For example, when evaluating the asymptotic expansion of a real integral $\int_{\mathcal{C}=\mathbb{R}} \mathrm{d}X\, e^{-kS[X]}$, one typically continues $S[X]$ to a holomorphic function on the complex X-plane, identifies its saddle points $S'[X_n] = 0$, constructs the steepest-descent contours $\mathcal{C}_n$ attached to each saddle, and deforms the original integration contour into the sum of steepest-descent contours

$\mathcal{C} = \sum_{n\in D} \mathcal{C}_n$ that is Cauchy-equivalent. In the $k \to \infty$ limit, the integral along a steepest-descent contour $\mathcal{C}_n$ is dominated by the contribution from its saddle, $e^{-kS[X_n]}$. Thus, in such favorable circumstances the asymptotic expansion of the original integral is given by the sum $\sum_{n\in D} e^{-kS[X_n]}$ of contributions from the subset of saddles that lie on the deformed integration contour.[8]

One may apply analogous methods to extract the asymptotic expansions of functional integrals [33–37]. The main complication in the infinite-dimensional case is that it is challenging to derive from first principles which sum of steepest-descent contours is equivalent to the original contour, and therefore which subset of saddles one should sum over in computing the asymptotic expansion [34]. In the case of the $\mathrm{SL}(2,\mathbb{R})_k/\mathrm{U}(1)$ CFT, however, the exact reflection coefficient is known [43–46], and one may therefore take its semi-classical limit and identify the set of saddles that reproduce it. That is the approach we take here. A similar analysis of the Liouville CFT reflection coefficient was performed in [35].

We again find that one must sum over complex saddles to reproduce the $\mathrm{SL}(2,\mathbb{R})_k/\mathrm{U}(1)$ reflection coefficient. In fact, as has long been known in Liouville CFT [47] and is also the case in the $\mathrm{SL}(2,\mathbb{R})_k/\mathrm{U}(1)$ CFT, the functional integral over real fields for the two-point function is divergent.[9] Instead, the functional integral for these and related (asymptotic) linear-dilaton backgrounds should in general be defined by an integral over a contour in complexified field space [35]. By identifying the complex saddles that contribute to the functional integral, one may in fact define the appropriate integration cycle by the sum of

[8] And the integral along each steepest-descent contour is equal to the Borel resummation of the perturbative expansion around the corresponding saddle.

[9] As is the partition function.

steepest-descent contours attached to the contributing saddles [35].

Part of the increased difficulty of the $\mathrm{SL}(2,\mathbb{R})_k/\mathrm{U}(1)$ problem compared to Liouville is due to the existence of bound states in the spectrum of the former CFT, which manifest as poles of its reflection coefficient. To reproduce these poles in the saddle-point expansion, we find that we must sum over configurations that hit the singularity of the black hole in the complexified target space.[10]

The $\mathrm{SL}(2,\mathbb{R})_k/\mathrm{U}(1)$ CFT admits a dual description, due to Fateev, Zamolodchikov, and Zamolodchikov (FZZ) [48, 49], given by a sigma-model into a cylinder, now with an infinite linear-dilaton direction, plus a condensate of winding strings (Fig. 1.4b). It is known as the sine-Liouville background, and the condensate is called the sine-Liouville potential. Whereas the cigar description is weakly coupled for large k in the sense of α' perturbation theory of the field theory, the sine-Liouville description is strongly coupled. Both backgrounds asymptote to identical cylinders in the region where the linear dilaton Φ goes to minus infinity and the string coupling e^{Φ} subsequently vanishes. But while the cigar geometry terminates at finite string coupling at its tip, in sine-Liouville the cylinder extends forever and the string coupling diverges. In this description it is instead the sine-Liouville potential that is responsible for suppressing string configurations that extend into the strong-coupling region. In both backgrounds the apparent winding number conservation law of the common asymptotic cylinder region is violated—in the cigar because a wound string may unwind at the tip, and in sine-Liouville because the winding potential explicitly breaks the symmetry.

[10] Similar complex contours hitting the black hole singularity were considered in Hartle and Hawking's path integral derivation of Hawking radiation [26].

(a) (b)

Figure 1.5: The Bulk TFD State. The infinite cylinder geometry of the sine-Liouville background has the topology of an annulus (right). The linear dilaton implies that the string coupling vanishes at one asymptotic boundary and diverges at the other, represented by the solid and dotted circles. When the annulus is halved and glued to the Lorentzian continuation, it prepares the TFD state in two disconnected copies of flat linear-dilaton spacetime (left). The state prepared by halving the dual EBTZ background is similar but with an additional circle suppressed. Also pictured is the embedding of a string worldsheet with a pair of Euclidean time winding operator insertions from the sine-Liouville potential. The image of the worldsheet wraps the Euclidean time circle, extending out from the dotted strong-coupling boundary toward finite coupling, before folding back on itself and falling back to strong coupling. When the worldsheet is sliced in angular quantization, each spatial slice is then mapped to a folded string, shown in red, that comes in and out of the strong-coupling region. The full sine-Liouville potential adds a condensate of such folded strings on top of the disconnected union of linear-dilaton $\times$ time backgrounds. Expanding the condensate, one obtains an EPR description of a string in a superposition of entangled disconnected spacetimes, dual to string theory in the connected black hole.

These are the essential features a Euclidean duality must exhibit in order to realize ER = EPR upon continuation. The contractible Euclidean time circle on one side of the duality leads to the HH state in a two-sided black hole when the target time coordinate is continued (Fig. 1.2a). The non-contractible Euclidean time circle in the dual description, meanwhile, yields a state in a disconnected geometry when its Euclidean annulus topology is cut in half and glued to the Lorentzian continuation (Fig. 1.5)—this is another TFD state, now in the bulk sense. By consistency, the non-contractible description must feature a mechanism that violates the winding number conservation law around the Euclidean time circle, since the string can unwind in the contractible dual. In the FZZ duality, this is accomplished by the condensate of Euclidean time winding strings.

In three-dimensional spacetime, we propose a similar duality of the $\mathbb{Z}\backslash \mathrm{SL}(2,\mathbb{C})_k/\mathrm{SU}(2)$

CFT that describes a string in the asymptotic Euclidean AdS_3 black hole, known as Euclidean BTZ (EBTZ), which, as mentioned earlier, has the topology of a solid torus (Fig. 1.6a). The duality in fact applies as well to $SL(2,\mathbb{C})_k/SU(2)$ itself, prior to the $\mathbb{Z}$ quotient. The latter describes a string in Euclidean AdS_3 ($EAdS_3$), which is equivalent to the $SL(2,\mathbb{C})/SU(2)$ coset manifold. $EAdS_3$ is again a solid cylinder, and compactifying its length yields the EBTZ solid torus $\mathbb{Z}\backslash SL(2,\mathbb{C})/SU(2)$, where the circumference $4\pi^2/\beta$ of the compactification is fixed by the inverse Hawking temperature β of the black hole. In the dual description, the radial direction of the torus or cylinder is replaced by an infinite linear-dilaton direction as in the sine-Liouville background, and a condensate of winding strings wrapping the resulting non-contractible cycle is again added (Fig. 1.6b).[11] The original description is weakly coupled for large k while the dual description is strongly coupled, and once again g_s diverges at the strong-coupling boundary of the dual geometry.[12] Gauging the translation symmetry around the original non-contractible cycle of the torus or the length of the cylinder in the two descriptions reproduces the cigar and sine-Liouville backgrounds. Thus, this duality may be thought of as a three-dimensional uplift of the FZZ duality.[13][14][15]

These dualities share the essential feature that the two related target spaces are of different

[11] As we explain in Sec. 4.1, the duality requires that we express the boundary cylinder or torus variables of $SL(2,\mathbb{C})_k/SU(2)$ or $\mathbb{Z}\backslash SL(2,\mathbb{C})_k/SU(2)$ in the first-order formalism.

[12] For small k (relative to its minimal value $k=2$), on the other hand, the original description of $SL(2,\mathbb{C})_k/SU(2)$ is strongly coupled. Then we expect that the dual sigma-model is the better description of the AdS_3 vacuum for small k. It would be interesting to understand the connection between the sine-Liouville description and recent work on string theory in AdS_3 at small k [50–53].

[13] $SL(2,\mathbb{C})/SU(2)$ is a Euclidean continuation of $SL(2,\mathbb{R}) = AdS_3$, and the two-dimensional black hole may equivalently be thought of as a coset of the former.

[14] Potentially related work on a three-dimensional uplift of the FZZ duality was discussed in [54].

[15] We expect there is also a supersymmetric version of this duality, as in the supersymmetric FZZ duality of [55]. We focus on the bosonic string in this work for simplicity, though we expect similar examples of ER = EPR would hold for the superstring in the cigar and the supersymmetric $AdS_3 \times S^3$ background.

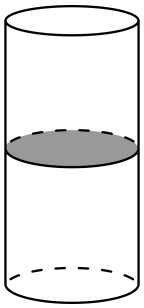

(a) The Euclidean AdS_3 Black Hole. $EAdS_3$ may be described as a solid cylinder. Compactifying the length of the cylinder to form a solid torus yields the Euclidean continuation of the asymptotic AdS_3 black hole, where the continuation is performed with respect to the contractible cycle. The inverse Hawking temperature β of the black hole fixes the periodicity $4\pi^2/\beta$ of the non-contractible cycle of the torus. The coset manifold $SL(2,\mathbb{C})/SU(2)$ is equivalent to $EAdS_3$, and a string in $EAdS_3$ may therefore be described by the $SL(2,\mathbb{C})_k/SU(2)$ coset WZW model, where $\alpha' k = l^2_{AdS}$ sets the AdS length. The quotient $\mathbb{Z}\backslash SL(2,\mathbb{C})_k/SU(2)$ thus describes a string in the asymptotic $EAdS_3$ black hole, known as Euclidean BTZ (EBTZ).

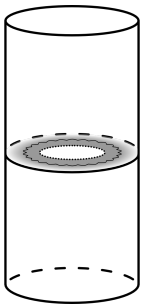

(b) The 3D sine-Liouville Background. In the dual description we propose for the $SL(2,\mathbb{C})_k/SU(2)$ CFT and its black hole quotient $\mathbb{Z}\backslash SL(2,\mathbb{C})_k/SU(2)$, the radial direction of the cylinder or solid torus is replaced by an infinite linear-dilaton direction, and a condensate of strings winding the resulting non-contractible cycle is added. Gauging the translation symmetry along the length of the cylinder produces the two-dimensional sine-Liouville background (Fig. 1.4b), whereas gauging the same symmetry in the first description yields the two-dimensional cigar (Fig. 1.4a). Thus, this duality is an uplift of the FZZ duality to a three-dimensional target space.

Figure 1.6

topologies. In the cigar description of $SL(2,\mathbb{R})_k/U(1)$, the geometry has the topology of a disk, with the asymptotic cylinder capping off at the origin. In the sine-Liouville description, the cylinder is infinite, and the topology is an annulus. Thus, the circle direction of the two geometries, which is defined as the Euclidean time, is contractible on one side of the duality and non-contractible on the other. Similarly, in the $\mathbb{Z}\backslash SL(2,\mathbb{C})_k/SU(2)$ duality the contractible cycle of the torus in the original description is replaced by a non-contractible cycle in the dual, exchanging the disk $\times$ S^1 topology with an annulus $\times$ S^1. It is again this cycle that one defines as the Euclidean time in order to obtain the Lorentzian black hole upon continuation.[16]

When the dual sine-Liouville background is cut and continued, one obtains the bulk TFD

[16] In the three-dimensional case one may alternatively continue with respect to the other cycle, which prepares a thermal state in AdS_3, or simply the vacuum state prior to the $\mathbb{Z}$ quotient. See Ft. 12.

state in the disconnected union of two copies of $\mathbb{R}^{1,1}$ in the two-dimensional case and $\mathbb{R}^{1,1} \times \mathrm{S}^1$ in the three-dimensional case (Fig. 1.5). On each copy of the spatial slice $\mathbb{R}$ one has a linear dilaton, with one asymptotic boundary at weak string coupling and the other at strong coupling, represented by the solid and dotted lines in the figure. On top of each free-field background, one has the condensate of strings that wind the non-contractible Euclidean time circle, which by the duality is equivalent to the connected black hole. A winding string worldsheet is also shown in the figure. An important aspect of our construction is to explain the interpretation of these winding strings in the Lorentzian continuation, which we will argue produce pairs of entangled folded strings emanating from the strong-coupling boundaries.

Complexified spacetimes such as Fig. 1.2a and 1.5a are familiar in quantum field theory. The Euclidean cap specifies the domain on which the fields in the functional integral are defined, and by gluing two Euclidean caps together with a Lorentzian excursion in between, one obtains a Schwinger-Keldysh contour on which the functional integral computes expectation values in the states specified by the caps [56, 57]. Such expectation values may be obtained by computing the Euclidean correlation function and then continuing the operator insertions to the Lorentzian section.

From the point of view of string theory, the Schwinger-Keldysh contour is now interpreted as the integration cycle in a complexification of the target space over which the worldsheet functional integral is evaluated. Note that it is imprecise to merely ask for a string amplitude in e.g. the black hole background—one must also specify a state in order to define a string

perturbation theory. For example, one could ask for a string amplitude in AdS_3 in the vacuum state or in a thermal state; the Lorentzian section is the same in both cases, but the string perturbation theories are different. The state is fixed by the incoming and outgoing Euclidean segments of the target space Schwinger-Keldysh contour. Thus, the target space contour obtained by gluing together two copies of Fig. 1.2a produces string amplitudes for the black hole background in the HH state. Similarly, the contour obtained by gluing together two copies of Fig. 1.5a—prior to adding the condensate—computes amplitudes for string theory in $\mathbb{R}^{1,1} \cup \mathbb{R}^{1,1}$ in the TFD state, or $\mathbb{R}^{1,1} \times \mathrm{S}^1 \cup \mathbb{R}^{1,1} \times \mathrm{S}^1$ in the three-dimensional case.

In this way, cutting and continuing the dual descriptions of the $\mathrm{SL}(2,\mathbb{R})_k/\mathrm{U}(1)$ and $\mathbb{Z}\backslash\mathrm{SL}(2,\mathbb{C})_k/\mathrm{SU}(2)$ CFTs yield Schwinger-Keldysh contours for the ER = EPR dual string theories. The condensate is the most subtle aspect of the continuation; it is built of strings that wind the Euclidean time circle, and therefore its interpretation in the Lorentzian continuation is not obvious. In two dimensions, it takes the form $V_{\mathrm{sL}} \propto W_+ + W_-$, where $W_\pm = e^{-2b_{\mathrm{sL}}\hat{r}} e^{\pm ik(\theta_{\mathrm{L}} - \theta_{\mathrm{R}})}$ are linear-dilaton $\times$ S^1 vertex operators for a string with unit winding around the Euclidean time circle θ, times a Liouville-like factor in the linear-dilaton direction $\hat{r}$ (Fig. 1.4b). The latter serves to reflect strings away from the strong-coupling region $\hat{r} \to -\infty$, where b_{sL} is a positive real number chosen such that these vertex operators are marginal. Let us treat the condensate as a large deformation of the free linear-dilaton $\times$ S^1 background; one obtains a series of W_+W_- insertions of the form $e^{-\int V_{\mathrm{sL}}} \sim \sum \frac{1}{(N!)^2} \left(\int W_+W_-\right)^N$.[17] Note that only paired operators W_+W_- contribute to the

[17] This expansion is formal and requires regularization in the strong-coupling region. Our aim, however, is to give an abstract

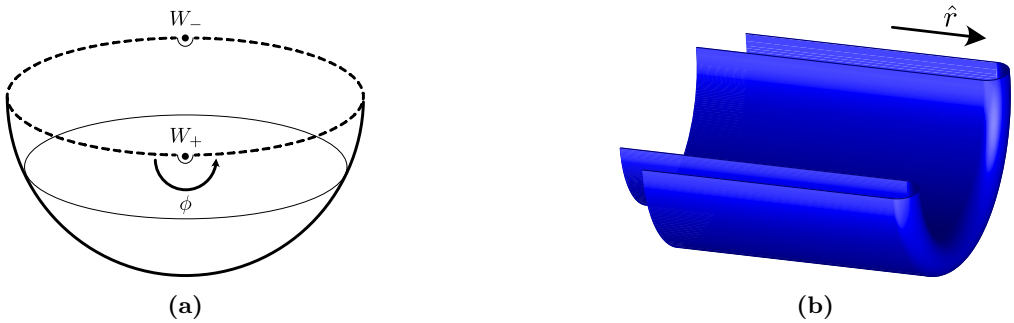

(a) **(b)**

Figure 1.7: The TFD State of a Pair of Folded Strings. With insertions of Euclidean time winding operators W_+, W_-, the worldsheet should be treated in angular quantization to discuss the continuation to Lorentzian target time. One foliates the worldsheet in radial lines, such as the two dashed semi-circles shown on the left, with the angular direction interpreted as Euclidean time. The resulting Hilbert space $\mathcal{H}_{+-}(\mathbb{R})$ lives on a line, labeled by asymptotic conditions associated to the operator insertions at either end. The functional integral over the halved worldsheet shown prepares the TFD state in two copies of $\mathcal{H}_{+-}(\mathbb{R})$. The asymptotic conditions for $W_\pm$ send $\hat{r} \to -\infty$ with winding ± 1. A schematic of the spacetime image of the halved worldsheet is shown on the right. In particular, the two dashed spatial slices map to the folded strings bounding the blue figure, emanating from the strong-coupling region.

expansion due to the winding number conservation law of the undeformed cylinder. We emphasize that it is only after resumming the series that one recovers the black hole CFT.

Consider therefore the effect of a pair of W_+, W_- insertions in the Lorentzian continuation of the linear-dilaton $\times$ S^1 string theory. Let W_+ be inserted at the origin and W_- at the point-at-infinity on the worldsheet (Fig. 1.7a). These operators insert sources in the worldsheet equations of motion that dictate the behavior of the string in their vicinity. As one approaches the $W_\pm$ insertion point on the worldsheet, the image of the string in the target is mapped to the strong-coupling region with winding ± 1. In angular gauge $\theta = \phi$ then, where θ is the compact target Euclidean time coordinate and ϕ is the worldsheet angular coordinate, the slices at $\phi = 0$ and π that bound the diagram in Fig. 1.7a map to folded strings in spacetime at $\theta = 0$ and π emanating from the strong-coupling region (Fig. 1.7b). The Lorentzian interpretation of the pair of Euclidean time winding insertions is thus that,

picture of the EPR string background, not a practical scheme for computing amplitudes.

atop the disconnected union of $\mathbb{R}^{1,1}$ backgrounds in the bulk TFD state, a pair of folded strings is added, one in the left and one in the right, with their ends at strong coupling. The strings are entangled with one another, being prepared by the Euclidean cap Fig. 1.7a, which is a TFD state on the worldsheet in the sense of angular quantization. In angular quantization, one interprets the angle ϕ as the worldsheet Euclidean time coordinate, so that the boundaries of the cap at $\phi = 0$ and π are spatial slices on which the TFD state is prepared. The sine-Liouville potential introduces a condensate of these entangled pairs of folded strings on top of the disconnected target.[18]

Thus, the Lorentzian string dualities we propose are as follows. The weakly-coupled side (in the α' sense) is string theory in the connected two-dimensional linear-dilaton (or three-dimensional AdS) black hole in the HH state. The strongly-coupled side is string theory in the disconnected union of two copies of linear-dilaton $\times$ time (or linear-dilaton $\times$ time $\times$ S^1) in the bulk TFD state, with a condensate of pairs of entangled folded strings emanating from the strong-coupling boundaries, themselves in the worldsheet TFD state of angular quantization.[19] By expanding the condensate, one obtains a superposition of entangled disconnected microstates. The dualities are therefore explicit examples of ER = EPR, each relating a connected, two-sided spacetime to an entangled superposition of disconnected geometries.

[18] Recent potentially related work involving a condensate of folded strings behind the black hole horizon and the Lorentzian continuation of the FZZ duality has appeared in [58–65]. It would be very interesting to establish the precise connection between these results.

[19] By continuing the duality of $SL(2,\mathbb{C})_k/SU(2)$ with respect to the same cycle, but prior to the $\mathbb{Z}$ quotient that makes the Euclidean black hole, one likewise obtains an even simpler duality between string theory in a connected Rindler decomposition of AdS_3 and the analogous EPR theory in linear-dilaton $\times$ time $\times \mathbb{R}$. The quotient replaces the ER side with the black hole and compactifies $\mathbb{R}$ to S^1 on the EPR side.

The outline of the remainder of the dissertation is as follows. In Ch. 2 we study the large k limit of the $\mathrm{SL}(2,\mathbb{R})_k/\mathrm{U}(1)$ CFT. We show that local operators of the CFT may be described by asymptotic conditions that cut out the neighborhood of an insertion and replace it by a boundary term in the cigar action. We then construct the saddle-point expansion of the functional integral for the two-point function of operators described by these asymptotic conditions.

In Ch. 3 we discuss the Schwinger-Keldysh contours that enable the definition of string perturbation theory in various states, including the TFD and HH states that appear in the statement of our ER = EPR dualities. We focus here on examples of string perturbation theory in AdS_3, which is the best understood case.

Having developed the necessary tools, in Ch. 4 we construct our examples of Lorentzian string dualities for ER = EPR. We begin by establishing the uplift of the FZZ duality to $\mathrm{SL}(2,\mathbb{C})_k/\mathrm{SU}(2)$ and $\mathbb{Z}\backslash\mathrm{SL}(2,\mathbb{C})_k/\mathrm{SU}(2)$. Then we introduce the angular quantization of Euclidean time winding operators, and a related deformation of the string moduli integration contour, that explain the Lorentzian meaning of the sine-Liouville condensate. After discussing the remaining details of the Lorentzian dualities, we conclude by describing an infinitesimal interpretation of these dualities in terms of conformal perturbation theory.

2 Semi-Classical Analysis of the 2D Black Hole

In this chapter, we investigate the semi-classical limit of the $\mathrm{SL}(2,\mathbb{R})_k/\mathrm{U}(1)$ CFT. For large k, this CFT describes a string propagating in a cigar-shaped two-dimensional Euclidean black hole [32]. In the following chapters, we will be interested in the Lorentzian continuation of this background with respect to the target time coordinate, which therefore describes a string in a two-dimensional Lorentzian black hole. Then the continued theory will yield the ER description in one of our examples of ER = EPR string dualities. An important role in that discussion is played by "asymptotic conditions" that enable a convenient functional integral description of local operator insertions in the CFT. In preparation for those applications, and because the analysis of the cigar in the semi-classical limit is interesting in its own right, in this chapter we compute the saddle-point expansion of the $\mathrm{SL}(2,\mathbb{R})_k/\mathrm{U}(1)$ functional integral for the simplest interesting observable: the reflection coefficient that describes the amplitude for a string sent in from infinity to reflect off the tip of the cigar.

The chapter is organized as follows. In Sec. 2.1 we review the free linear-dilaton back-

ground, which will play a ubiquitous role throughout the entirety of this dissertation. In Sec. 2.2 we review the Liouville CFT, which consists of the linear-dilaton background plus an exponential potential, and we perform the saddle-point expansion of its reflection coefficient. In Sec. 2.3 we review the $\mathrm{SL}(2,\mathbb{R})_k/\mathrm{U}(1)$ CFT, its cigar description, and the asymptotic conditions that describe operator insertions in the associated functional integral. In Sec. 2.4 we come to the saddle-point expansion of the cigar reflection coefficient. Finally, in Sec. 2.5 we discuss the dual formulation of the $\mathrm{SL}(2,\mathbb{R})_k/\mathrm{U}(1)$ CFT known as the sine-Liouville background due to Fateev, Zamolodchikov, and Zamolodchikov [48, 49], and we consider what may be said about the saddle-point expansion in the dual limit. This FZZ duality will also play an essential role in the discussion of ER = EPR string dualities in the remainder of the dissertation.

2.1 Review of the Free Linear Dilaton

Much of the work described in this dissertation will involve sigma-models into target geometries with a linear, or asymptotically-linear, dilaton along one direction. It is therefore useful to begin by reviewing some relevant details of the free linear-dilaton theory.

2.1.1 A Family of Free Bosons

The linear-dilaton conformal field theory (CFT) is a generalization of the free-boson CFT, labeled by a positive number[20] Q called the background charge. Namely, one considers a

[20] When we consider the bosonization of the bc ghost CFT in Eqn. 4.38 we will need to allow for imaginary Q, but for now we take Q real.

non-compact boson $X(z,\bar{z})$ with the usual operator-product expansion (OPE),

$$X(z,\bar{z})X(0) \sim -\frac{\alpha'}{2}\log|z|^2, \tag{2.1}$$

but with the modified holomorphic stress tensor

$$T(z) = -\frac{1}{\alpha'}(\partial X)^2 - Q\partial^2 X, \tag{2.2}$$

and similarly for the anti-holomorphic stress tensor $\bar{T}(\bar{z})$. The deformed stress tensor obeys the usual Virasoro OPE,

$$T(z)T(0) \sim \frac{c/2}{z^4} + \frac{2}{z^2}T(0) + \frac{1}{z}\partial T(0), \tag{2.3}$$

but with the free-boson central charge $c = 1$ modified as

$$c_{\mathrm{LD}} = 1 + 6\alpha' Q^2. \tag{2.4}$$

The deformation also modifies the OPE of T and X, with the consequence

$$T(z)j(0) \sim -\frac{iQ}{z^3} + \frac{1}{z^2}j(0) + \frac{1}{z}\partial j(0), \tag{2.5}$$

where $j(z) = \frac{i}{\alpha'}\partial X(z)$ is the holomorphic component of the current for the translation symmetry in X of the free boson. The addition of the z^{-3} term implies that $j(z)$ is no longer a Virasoro primary when Q is turned on, and the symmetry becomes anomalous in the linear-dilaton background. In particular, under the conformal transformation $z = e^w$

between the plane and the cylinder, the current transforms not as $j_w(w) = zj_z(z)$, but rather

$$j_w(w) = zj_z(z) - \frac{iQ}{2}. \tag{2.6}$$

The charges under the symmetry (i.e. the target momenta) of states on the cylinder as measured by $\oint j_w$ and local operators on the plane as measured by $\oint j_z$ will therefore differ by a shift proportional to Q, as spelled out below.

Exponential operators, conveniently written as $V_\alpha(z,\bar{z}) = e^{-2\alpha X(z,\bar{z})}$, remain Virasoro primary, however:

$$T(z)V_\alpha(0) \sim \frac{h_\alpha}{z^2}V_\alpha(0) + \frac{1}{z}\partial V_\alpha(0), \tag{2.7}$$

where

$$h_\alpha = \bar{h}_\alpha = \alpha'\alpha(Q-\alpha). \tag{2.8}$$

Compared to the conventional notation $e^{ipX(z,\bar{z})}$ for the ordinary free-boson vertex operators, one has $\alpha = -\frac{1}{2}ip$, and $h_\alpha|_{Q=0} = \frac{\alpha'}{4}p^2$ reproduces the familiar free-boson weight. The weights $h_\alpha, \bar{h}_\alpha$ are real when $\alpha \in \mathbb{R}$ or $\alpha \in \frac{Q}{2} + i\mathbb{R}$, which are referred to as the real and complex branches of vertex operators. On the complex branch, $h_\alpha = \alpha'|\alpha|^2 \geq \alpha'\frac{Q^2}{4}$ is always positive. On the real branch, the weight is only positive in the window $0 < \alpha < Q$, its maximal value coinciding with the minimal weight on the complex branch. We will consider the continuation of α to general complex values, however, regardless of whether the weights are

real and positive. Note also that the conformal weights are symmetric under reflection about $\alpha = \frac{Q}{2}$: $h_\alpha = h_{Q-\alpha}$. In the free theory, α and $Q - \alpha$ label independent operators, though in the interacting theories we will eventually be interested in they will in fact correspond to two components of the same operator.

Whereas the operator $e^{-2\alpha X}$ carries momentum $p = 2i\alpha$ as measured on the plane, due to the anomalous transformation law Eqn. 2.6 the state $\left|e^{-2\alpha X}\right\rangle \in \mathcal{H}(\mathrm{S}^1)$ prepared by inserting the operator in the far past on the cylinder carries momentum $p - iQ$:

$$P\left|e^{-2\alpha X}\right\rangle = 2i\left(\alpha - \frac{Q}{2}\right)\left|e^{-2\alpha X}\right\rangle. \tag{2.9}$$

In particular, a state of momentum s, with zero-mode wavefunction

$$\Psi(X_0) = e^{isX_0} = e^{-2\left(\alpha - \frac{Q}{2}\right)X_0}, \tag{2.10}$$

is prepared by inserting the operator with $\alpha = \frac{Q}{2} - i\frac{s}{2}$. Note that the wavefunction is of the form $e^{QX}V_\alpha$. The additional factor may be thought of as an insertion of the "background-charge operator" $V_{-Q/2}$ fixed in the far past, as further explained below.

The delta-function normalizable scattering states of the linear-dilaton background therefore correspond to the complex branch operators $\alpha \in \frac{Q}{2} + i\mathbb{R}$, and carry positive conformal weights. Away from this line, the wavefunction is non-normalizable, exponentially diverging either at $X \to \infty$ for $\mathrm{Re}(\alpha) < \frac{Q}{2}$, or $X \to -\infty$ for $\mathrm{Re}(\alpha) > \frac{Q}{2}$. Although they prepare non-normalizable states, such operators are nevertheless interesting.

2.1.2 Lagrangian Formulation

It is also useful to understand how these properties of the linear-dilaton CFT follow from its Lagrangian formulation. The deformation $-Q\partial^2 X$ of the free-boson stress tensor in Eqn. 2.2 arises from a coupling $\int \mathcal{R}\Phi$ between the worldsheet curvature and a linear dilaton $\Phi(X) = -QX$, hence the CFT's name. The action on a worldsheet Σ with metric h is

$$S[X;h] = \frac{1}{4\pi\alpha'}\int_\Sigma \mathrm{d}^2\sigma\,\sqrt{h}\;h^{ab}\partial_a X\partial_b X + \frac{1}{4\pi}\int_\Sigma \mathrm{d}^2\sigma\,\sqrt{h}\,\mathcal{R}\Phi + \frac{1}{2\pi}\int_{\partial\Sigma}\mathrm{d}\phi\,\sqrt{\gamma}\,\mathcal{K}\Phi. \tag{2.11}$$

We allow here for the possibility of a boundary $\partial\Sigma$, where $\mathcal{K}$ is the trace of the extrinsic curvature of the boundary, γ is the induced metric of the boundary, and $\mathrm{d}\phi\,\sqrt{\gamma}$ is the induced volume form.

Note that with Q real and positive the effective string coupling $e^{\Phi(X)}$ decays at $X \to \infty$ and diverges at $X \to -\infty$, which we refer to as the weak and strong-coupling regions. The divergence of the string coupling implies that the free linear dilaton is not a well-behaved background for string perturbation theory, and must be modified in a way that regulates the strong-coupling region.

The free-boson action alone is of course Weyl invariant under $h_{ab} \to e^{2\omega}h_{ab}$. With the addition of the linear dilaton, using $\mathcal{R} \to e^{-2\omega}(\mathcal{R} - 2\nabla^2\omega)$ and $\mathcal{K} \to e^{-\omega}(\mathcal{K} + n^a\partial_a\omega)$, one finds that the deformed action is Weyl invariant up to a field-independent anomaly, provided

that X simultaneously transforms as a Goldstone boson,

$$S\left[X+\alpha' Q\omega; e^{2\omega}h\right] = S\left[X;h\right] - S\left[-\alpha' Q\omega; h\right]. \tag{2.12}$$

By varying the action with respect to X and h^{ab}, one obtains the bulk equation of motion

$$\nabla^2 X = -\frac{1}{2}\alpha' Q\mathcal{R}, \tag{2.13}$$

and the stress tensor

$$T_{ab} = -\frac{1}{\alpha'}\left(\nabla_a X\nabla_b X - \frac{1}{2}h_{ab}\left(\nabla X\right)^2\right) + \left(\nabla_a\nabla_b - h_{ab}\nabla^2\right)\Phi. \tag{2.14}$$

The trace of the stress tensor is $h^{ab}T_{ab} = Q\nabla^2 X$, which, using the equation of motion, may be written

$$h^{ab}T_{ab} = -\frac{1}{12}(6\alpha' Q^2)\mathcal{R}. \tag{2.15}$$

Combined with the $c = 1$ Weyl anomaly of the ordinary free boson, we reproduce the Q-corrected Weyl anomaly

$$h^{ab}T_{ab}|_{\text{quantum}} = -\frac{c_{\text{LD}}}{12}\mathcal{R}, \tag{2.16}$$

where $c_{\text{LD}} = 1 + 6\alpha' Q^2$ as in Eqn. 2.4.

The curvature coupling in Eqn. 2.11 makes evident that the target translation symmetry

of the free boson $(\nabla X)^2$ is violated in the linear-dilaton background:

$$S[X+\varepsilon;h] = S[X;h] - \varepsilon Q\chi, \tag{2.17}$$

where

$$\chi = \frac{1}{4\pi}\int_{\Sigma} \mathrm{d}^2\sigma\,\sqrt{h}\,\mathcal{R} + \frac{1}{2\pi}\int_{\partial\Sigma} \mathrm{d}\phi\,\sqrt{\gamma}\,\mathcal{K}, \tag{2.18}$$

is the Euler characteristic of Σ. It follows that a correlation function of operators $\prod_j V_{\alpha_j}$ obeys the anomalous conservation law

$$\sum_j \alpha_j = \frac{1}{2}Q\chi, \tag{2.19}$$

since

$$\begin{aligned}\left\langle \prod_j V_{\alpha_j}(z_j,\bar{z}_j)\right\rangle &= \int \mathrm{D}X\, e^{-S[X,h]} \prod_j e^{-2\alpha_j X(z_j,\bar{z}_j)} \\ &= \int \mathrm{D}X\, e^{-S[X+\varepsilon,h]} \prod_j e^{-2\alpha_j X(z_j,\bar{z}_j) - 2\alpha_j\varepsilon} \\ &= e^{2\varepsilon\left(\frac{1}{2}Q\chi - \sum_j \alpha_j\right)} \int \mathrm{D}X\, e^{-S[X,h]} \prod_j e^{-2\alpha_j X(z_j,\bar{z}_j)}.\end{aligned} \tag{2.20}$$

Equivalently, the integral $\int \mathrm{d}x\, e^{2\left(\frac{1}{2}Q\chi - \sum_j \alpha_j\right)x}$ over the zero-mode of X is a Lagrange multiplier that imposes the constraint Eqn. 2.19.

With the flat metric $\mathrm{d}s^2 = \mathrm{d}z\mathrm{d}\bar{z}$, Eqn. 2.11 apparently reduces to the familiar free-boson

action

$$S = \frac{1}{2\pi\alpha'} \int \mathrm{d}^2 z \, \partial X \bar{\partial} X. \tag{2.21}$$

However, we are interested in the theory at string tree-level, for which Σ has the topology of a sphere, and there does not exist a globally flat metric on the sphere. In particular, the coordinate z does not cover the neighborhood of the point-at-infinity, and the "flat" metric is singular there: $\mathrm{d}s^2 = \frac{\mathrm{d}u \, \mathrm{d}\bar{u}}{(u\bar{u})^2}$, with a local coordinate $u = \frac{1}{z}$. This singularity contributes a delta-function source of curvature, $\mathcal{R} = 16\pi(u\bar{u})^2\delta(u, \bar{u}) = 16\pi\delta(z - z_\infty, \bar{z} - \bar{z}_\infty)$, as required by the Gauss-Bonnet to reproduce the Euler characteristic of the sphere:

$$\chi = \frac{1}{4\pi} \int \frac{\mathrm{d}^2 z}{2} 16\pi\delta(z - z_\infty, \bar{z} - \bar{z}_\infty) = 2. \tag{2.22}$$

The effect of the curvature singularity in Eqn. 2.11 is to shift the free-boson action Eqn. 2.21 on the plane by $-2QX(z_\infty, \bar{z}_\infty)$, which amounts to an insertion of V_{-Q} at the point-at-infinity in the functional integral. Thus, one can study the linear-dilaton background in flat coordinates, provided that one keeps track of this background-charge operator. It inserts a fixed source in the equation of motion at the point-at-infinity:

$$\partial\bar{\partial} X = -2\pi\alpha' Q \delta(z - z_\infty, \bar{z} - \bar{z}_\infty), \tag{2.23}$$

which likewise reflects the anomalous conservation of the currents ∂X and $\bar{\partial} X$.

One could avoid this singular behavior at the point-at-infinity by instead choosing the

round metric $\mathrm{d}s^2 = \frac{4}{(1+z\bar{z})^2}\mathrm{d}z\mathrm{d}\bar{z}$, for which $\mathcal{R} = 2$ is a constant. However, the dilaton term then produces a linear potential, which is slightly awkward. It is instead common practice in studying the linear-dilaton CFT to work with the plane metric $\mathrm{d}z\mathrm{d}\bar{z}$ or the cylinder metric $\frac{\mathrm{d}z\mathrm{d}\bar{z}}{z\bar{z}}$, which are related to the round metric by singular Weyl transformations that push all the curvature of the sphere to the point-at-infinity or the two ends of the cylinder.

With the cylinder metric, $\mathcal{R} = 8\pi z\bar{z}\left(\delta(z,\bar{z}) + \delta(z - z_\infty, \bar{z} - \bar{z}_\infty)\right)$, the background charge is now split symmetrically between the two ends with insertions of $V_{-Q/2}(0)$ and $V_{-Q/2}(z_\infty, \bar{z}_\infty)$, and the equation of motion becomes

$$\partial\bar{\partial}X = -\pi\alpha' Q\left(\delta(z,\bar{z}) + \delta(z - z_\infty, \bar{z} - \bar{z}_\infty)\right). \tag{2.24}$$

The background-charge insertion $V_{-Q/2}(0)$ is responsible for the factor e^{QX} that appears in the zero-mode wavefunction prepared by inserting $e^{-2\alpha X}$ on the cylinder (Eqn. 2.10).

With either the plane or cylinder metric, the anomalous conservation law $\sum \alpha_j = Q$ at genus zero amounts to requiring that the operator insertions $\prod V_{\alpha_j}$ offset the fixed contribution $V_{-Q}(z_\infty, \bar{z}_\infty)$ or $V_{-Q/2}(0), V_{-Q/2}(z_\infty, \bar{z}_\infty)$ from the background-charge insertions. Note also that the 1-point function of the operator $V_Q(z,\bar{z})$ is not required to vanish, which is compatible with conformal symmetry because $h_Q = \bar{h}_Q = 0$.

2.1.3 Asymptotic Conditions

As in Eqns. 2.23-2.24, when a general primary $V_\alpha(z', \bar{z}')$ is inserted in the functional integral,

$$\begin{aligned} &\int \mathrm{D}X\, e^{-S} V_\alpha(z', \bar{z}') \\ &\quad = \int \mathrm{D}X\, \exp\left\{ -\frac{1}{2\pi\alpha'} \int \mathrm{d}^2 z\, \left(\partial X \bar{\partial} X + 4\pi\alpha'\alpha\delta(z - z', \bar{z} - \bar{z}') X(z, \bar{z}) + \cdots \right) \right\}, \end{aligned} \tag{2.25}$$

a source term is introduced in the bulk equation of motion,

$$\partial\bar{\partial} X = 2\pi\alpha'\alpha\delta(z - z', \bar{z} - \bar{z}'). \tag{2.26}$$

Recalling the Green function for the two-dimensional wave equation, $\partial\bar{\partial}\log(z\bar{z}) = 2\pi\delta(z, \bar{z})$, one finds that in the neighborhood of the insertion point on the worldsheet the solution of the equation of motion is

$$X(z, \bar{z}) \overset{|z-z'|\to 0}{\longrightarrow} 2\alpha'\alpha \log|z - z'| + \mathcal{O}(1). \tag{2.27}$$

Evaluating the stress tensor Eqn. 2.2 on this solution one finds

$$z^2 T(z) \to \alpha'\alpha(Q - \alpha), \tag{2.28}$$

reproducing the conformal weight Eqn. 2.8. In local cylinder coordinates $z - z' \equiv e^{\rho + i\phi}$, Eqn. 2.27 reads

$$X(\rho, \phi) \overset{\rho \to -\infty}{\longrightarrow} 2\alpha'\alpha\rho + \mathcal{O}(1). \tag{2.29}$$

Thus, the operator insertion imposes the asymptotic condition that X be linear in ρ, with $\partial_\rho X \to 2\alpha'\alpha$ as $\rho \to -\infty$.

The saddles in the presence of the source are singular at the insertion point. This singular behavior may be regulated by cutting out the neighborhood of the insertion from the world-sheet and introducing an appropriate boundary action there. Let us cut out a small disk d_ε of radius $|z - z'| = \varepsilon$ surrounding z' and deform the action by a boundary term [35, 66]:

$$S(\varepsilon) = S + 2\alpha \int_{\partial d_\varepsilon} \frac{\mathrm{d}\phi}{2\pi}\, X - 2\alpha'\alpha^2 \log(\varepsilon), \tag{2.30}$$

where $\mathrm{d}\phi = \frac{1}{2i}\left(\frac{\mathrm{d}z}{z-z'} - \frac{\mathrm{d}\bar{z}}{\bar{z}-\bar{z}'}\right)$. Then the boundary variation $-\frac{1}{2\pi\alpha'}\int_{\partial d_\varepsilon} \mathrm{d}\phi\, \delta X\, \partial_\rho X$ of S and the variation of the boundary term $2\alpha \int_{\partial d_\varepsilon} \frac{\mathrm{d}\phi}{2\pi}\delta X$ yield the desired boundary equation of motion,

$$\partial_\rho X\big|_{\rho = \log(\varepsilon)} = 2\alpha'\alpha. \tag{2.31}$$

In the limit $\varepsilon \to 0$, one expects the functional integral weighted by the deformed action $e^{-S(\varepsilon)}$ to reproduce the functional integral weighted by $e^{-S}e^{-2\alpha X(z',\bar{z}')}$. The counterterm $-2\alpha'\alpha^2 \log(\varepsilon)$ is included to render the on-shell action finite.

On the plane, the background-charge source $V_{-Q}(z_\infty, \bar{z}_\infty)$ imposes the asymptotic condition at infinity

$$X(z,\bar{z}) \overset{|z|\to\infty}{\longrightarrow} 2\alpha' Q \log|z| + \mathcal{O}(1). \tag{2.32}$$

In the presence of additional insertions $\prod V_{\alpha_j}(z_j, \bar{z}_j)$, the Green function $2\alpha' \sum_j \alpha_j \log|z - z_j|$ satisfies the asymptotic condition only provided

$$\sum_j \alpha_j = Q, \tag{2.33}$$

again reproducing Eqn. 2.19.

As in Eqn. 2.30, the background-charge insertion at the point-at-infinity may be replaced by excising its neighborhood and introducing a boundary term. The action for the linear-dilaton on the plane is therefore given by the $R \to \infty$ limit of [35, 66, 67]

$$S = \frac{1}{2\pi\alpha'} \int_{D_R} \mathrm{d}^2 z\, \partial X \bar{\partial} X - 2Q \int_{\partial D_R} \frac{\mathrm{d}\phi}{2\pi} X + 2\alpha' Q^2 \log(R), \tag{2.34}$$

with D_R a disk of radius R. Note that the prescription amounts to cutting out the source and doubling the extrinsic curvature term in Eqn. 2.11 on the resulting boundary, which ensures that $2 \times \frac{1}{2\pi} \int_{\partial\Sigma} \mathrm{d}\phi \sqrt{\gamma}\mathcal{K} = 2$ produces the Euler characteristic of the sphere rather than the disk. Additional insertions $V_{\alpha_j}(z_j, \bar{z}_j)$ may be included by cutting out disks at $(z_j, \bar{z}_j)$ and supplying additional boundary terms there.

For the most part, we will actually work on the cylinder rather than the plane, and the

asymptotic conditions at the ends of the cylinder satisfying Eqn. 2.24 are

$$X(\rho,\phi) \overset{\rho\to\pm\infty}{\longrightarrow} \pm\alpha' Q\rho + \mathcal{O}(1), \tag{2.35}$$

where $z = e^{\rho+i\phi}$. The cylinder action is then given by the $L\to\infty$ limit of

$$S = \frac{1}{4\pi\alpha'}\int_{-L}^{L} \mathrm{d}\rho \int_0^{2\pi} \mathrm{d}\phi\, \left((\partial_\rho X)^2 + (\partial_\phi X)^2\right) - Q\int_0^{2\pi}\frac{\mathrm{d}\phi}{2\pi}\left(X|_L + X|_{-L}\right) + \alpha' Q^2 L. \tag{2.36}$$

Suppose a primary $e^{-2\alpha X}$ is inserted in the far past on the cylinder. The asymptotic condition is the combination of Eqns. 2.29 and 2.35:

$$X(\rho,\phi) \overset{\rho\to-\infty}{\longrightarrow} 2\alpha'\left(\alpha - \frac{Q}{2}\right)\rho + \mathcal{O}(1). \tag{2.37}$$

Equivalently, the cylinder asymptotic condition Eqn. 2.37 follows from the asymptotic condition Eqn. 2.27 on the plane and the anomalous transformation law Eqn. 2.12 with $e^{2\omega} = \left|\frac{\partial z'}{\partial z}\right|^2 = \frac{1}{|z|^2}$,

$$X'(z',\bar{z}') = X(z,\bar{z}) + \alpha'\frac{Q}{2}\log\left|\frac{\partial z'}{\partial z}\right|^2, \tag{2.38}$$

where $z' = \rho + i\phi = \log z$, and we drop the prime on X'. The effect is again to shift $\alpha \to \alpha - \frac{Q}{2}$.

Note that for $\mathrm{Re}(\alpha) < \frac{Q}{2}$, Eqn. 2.37 sends X to the weak-coupling region, whereas for $\mathrm{Re}(\alpha) > \frac{Q}{2}$ it is mapped to the strong-coupling region. Comparing to the usual mode expansion $X = X_0 - i\alpha' s\rho + \cdots$, one again finds that the operator insertion $e^{-2\alpha X}$ prepares

a state $\Psi(X_0) = e^{isX_0}$ on the cylinder of momentum $s = 2i\left(\alpha - \frac{Q}{2}\right)$.

Finally, we point out that the background-charge factor $V_{-Q/2} = e^{QX}$ that appears in the zero-mode wavefunction may alternatively be understood from the target space string-frame effective action, which includes an overall factor of $e^{-2\Phi}$. Extracting the target space wavefunction from the kinetic term $e^{-2\Phi}(\nabla_X \tilde{\Psi}(X))^2$ requires rescaling $\tilde{\Psi}(X) \to \Psi(X) = e^{-\Phi}\tilde{\Psi}(X)$. For the linear-dilaton, the necessary factor is again $e^{-\Phi} = e^{QX}$.

The preceding discussion has been confined to the free linear-dilaton theory. Our interest in much of the work described in this dissertation will concern the cigar and sine-Liouville sigma-model backgrounds, and three-dimensional cousins thereof, that describe interacting CFTs. However, these backgrounds include limiting regions where the interactions turn off and the free linear dilaton is recovered. Much of the machinery of the free theory therefore continues to be relevant. Before discussing those backgrounds, however, we first consider the Liouville CFT in the next section, which exhibits in a simpler context several features common to these asymptotic linear-dilaton theories.

2.2 Liouville Reflection in the Semi-Classical Limit

In this section, we review relevant details of the Liouville CFT, and we compute the saddle-point expansion of its reflection coefficient in the semi-classical limit as a warm-up to the analogous problem in the $\mathrm{SL}(2,\mathbb{R})/\mathrm{U}(1)$ CFT that we will come to in Sec. 2.4. This saddle-point expansion was originally understood by the authors of [35]. Here, we reproduce the same result using the methods of [68], which reduce the calculation to a quantum mechanics

problem.

2.2.1 Review of Liouville CFT

The free linear-dilaton CFT reviewed in the previous section is ill-defined as a background for string perturbation theory because the effective string coupling $e^{\Phi(X)} = e^{-QX}$ diverges as $X \to -\infty$. It is moreover a non-unitary CFT; the delta-function normalizable spectrum is confined to the complex branch of primaries $\alpha \in \frac{Q}{2} + i\mathbb{R}$, whose OPE will generate operators outside this set that are non-normalizable.

The strong-coupling region may be regulated by turning on a potential barrier $\mu e^{-2b_{\rm L}X}$, with $\mu > 0$ and $\mathrm{Re}(b_{\rm L}) > 0$. Then string configurations for which X becomes large and negative have large actions, and therefore configurations extending too deeply into the strong-coupling region are suppressed in the functional integral. The momentum $b_{\rm L}$ is fixed by demanding that the potential be marginal:[21]

$$b_{\rm L}(Q - b_{\rm L}) = 1, \tag{2.39}$$

whose solution is

$$b_{\rm L} = \frac{Q}{2}\left(1 - \sqrt{1 - \frac{4}{Q^2}}\right). \tag{2.40}$$

[21] In this section we set $\alpha' = 1$ to be consistent with the standard Liouville convention.

The result is the Liouville CFT:[22]

$$S = \frac{1}{4\pi} \int_{\Sigma} \mathrm{d}^2\sigma\sqrt{h}\ \left\{(\nabla X)^2 - Q\mathcal{R}[h]X + 4\pi\mu e^{-2b_{\mathrm{L}}X}\right\}. \tag{2.41}$$

Deforming the linear dilaton by the Liouville potential not only cures the problematic behavior of the string coupling at $X \to -\infty$, but also yields a unitary CFT. The potential completely breaks the anomalous target translation symmetry of the free theory, and the OPE now closes on the complex branch of delta-function normalizable states.

As $X \to \infty$, the Liouville potential vanishes and the free linear dilaton is recovered. One therefore again has scattering solutions of the zero-mode quantum mechanics that behave as plane waves $e^{\pm isX}$ in the free-field region. They are no longer independent, however; the solutions which decay under the potential in the strong-coupling region behave as a linear combination of an incoming wave to the left and a reflected wave to the right in the free-field region,

$$\Psi(X) \overset{X\to\infty}{\longrightarrow} e^{-isX} + R(s)e^{isX}, \tag{2.42}$$

with $R(s)$ the reflection coefficient.

[22] For $Q > 2$, $b_{\mathrm{L}} \in \left(0, \frac{Q}{2}\right)$ lies on the real branch, while for $0 < Q < 2$ $b_{\mathrm{L}} \in \frac{Q}{2} + i\mathbb{R}$ sits on the complex branch. In the latter case V_{L} is complex and oscillatory. However, as an abstract CFT defined by its three-point function (which is known exactly [66,69]), one may analytically continue b_{L} to the right-half of the complex plane [35,66]. The continuation makes sense for $Q < 2$ because b_{L} always has positive real part.

In more detail, consider the zero-mode limit $X = X_0(\rho)$ of Eqn. 2.41:

$$S[X_0] = \int \mathrm{d}\rho \left(\frac{1}{2}\dot{X}_0^2 + 2\pi\mu e^{-2b_{\mathrm{L}}X_0} \right), \tag{2.43}$$

describing the Euclidean mechanics of a particle in the potential

$$V(X_0) = 2\pi\mu e^{-2b_{\mathrm{L}}X_0}. \tag{2.44}$$

The zero-mode wavefunctions are the solutions of the Schrödinger equation,

$$-\frac{1}{2}\Psi''(X_0) + 2\pi\mu e^{-2bX_0}\Psi(X_0) = \frac{s^2}{2}\Psi(X_0). \tag{2.45}$$

The solutions that obey the boundary conditions

$$\Psi_s(X_0) \to \begin{cases} e^{-isX_0} + R(s)e^{isX_0} & X_0 \to \infty \\ 0 & X_0 \to -\infty, \end{cases} \tag{2.46}$$

are Bessel functions

$$\Psi_s(X_0) = \frac{2}{\Gamma\left(-\frac{is}{b_{\mathrm{L}}}\right)} \left(\frac{\pi\mu}{b_{\mathrm{L}}^2}\right)^{-\frac{is}{2b_{\mathrm{L}}}} K_{-\frac{is}{b_{\mathrm{L}}}}\left(\sqrt{\frac{4\pi\mu}{b_{\mathrm{L}}^2}}e^{-b_{\mathrm{L}}X_0}\right). \tag{2.47}$$

$\Psi_s(X_0)$ obeys Eqn. 2.46 with

$$R(s) = \left(\frac{\pi\mu}{b_{\mathrm{L}}^2}\right)^{-\frac{is}{b_{\mathrm{L}}}} \frac{\Gamma\left(\frac{is}{b_{\mathrm{L}}}\right)}{\Gamma\left(-\frac{is}{b_{\mathrm{L}}}\right)}. \tag{2.48}$$

$R(s)$ and $\Psi_s(X_0)$ satisfy the properties $R(s)R(-s) = 1$ and

$$\Psi_s(X_0) = R(s)\Psi_{-s}(X_0). \tag{2.49}$$

One therefore finds vertex operators $V_\alpha = e^{-QX}\Psi_s$ of the CFT, where $s = -2i\left(\alpha - \frac{Q}{2}\right)$, behaving asymptotically as

$$V_\alpha \overset{X\to\infty}{\longrightarrow} e^{-2\alpha X} + R(\alpha)e^{-2(Q-\alpha)X}, \tag{2.50}$$

with the same conformal weights as in Eqn. 2.8. Note that the reflection $\alpha \to Q - \alpha$ of α about $\frac{Q}{2}$ corresponds to $s \to -s$, and Eqn. 2.49 implies

$$V_\alpha = R(\alpha)V_{Q-\alpha}. \tag{2.51}$$

The reflection coefficient written as a function of α becomes

$$R(\alpha) = \left(\frac{\pi\mu}{b_{\mathrm{L}}^2}\right)^{\frac{2}{b_{\mathrm{L}}}\left(\frac{Q}{2}-\alpha\right)} \frac{\Gamma\left(-\frac{2}{b_{\mathrm{L}}}\left(\frac{Q}{2}-\alpha\right)\right)}{\Gamma\left(\frac{2}{b_{\mathrm{L}}}\left(\frac{Q}{2}-\alpha\right)\right)}. \tag{2.52}$$

Eqn. 2.52 is the Liouville reflection coefficient in the quantum-mechanics limit. The exact reflection coefficient of the CFT is known to be [66, 69]

$$R(\alpha) = -\left(\pi\mu\frac{\Gamma(b_{\mathrm{L}}^2)}{\Gamma(1-b_{\mathrm{L}}^2)}\right)^{\frac{2}{b_{\mathrm{L}}}\left(\frac{Q}{2}-\alpha\right)} \frac{\Gamma\left(1-\frac{2}{b_{\mathrm{L}}}\left(\frac{Q}{2}-\alpha\right)\right)}{\Gamma\left(1+\frac{2}{b_{\mathrm{L}}}\left(\frac{Q}{2}-\alpha\right)\right)} \frac{\Gamma\left(1-2b_{\mathrm{L}}\left(\frac{Q}{2}-\alpha\right)\right)}{\Gamma\left(1+2b_{\mathrm{L}}\left(\frac{Q}{2}-\alpha\right)\right)}. \tag{2.53}$$

It satisfies $R(\alpha)R(Q-\alpha) = 1$. Note that the first two factors of Eqn. 2.53 coincide with

Eqn. 2.52 as $b_{\rm L} \to 0$, which we will see is the semi-classical limit.

Thus, whereas the free linear-dilaton background contained independent primaries $e^{-2\alpha X}$ and $e^{-2(Q-\alpha)X}$ of identical conformal weights, in Liouville one finds a single vertex operator V_α that behaves as a superposition of the two in the free-field region. The reflection coefficient is the relative weight of the two terms, and gives the semi-classical amplitude for a string sent in from the weak-coupling region to reflect off the potential and return to weak coupling.

As an abstract CFT quantity, the reflection coefficient characterizes a redundancy in the continued space of CFT operators on the complex α-plane. For $\mathrm{Re}(\alpha) < \frac{Q}{2}$, the first term $e^{-2\alpha X}$ dominates the second $e^{-2(Q-\alpha)X}$ in the $X \to \infty$ limit of V_α. For $\mathrm{Re}(\alpha) > \frac{Q}{2}$, it is the second term that dominates. However, Eqn. 2.51 shows that the CFT operators labeled by α and $Q-\alpha$ are identical, up to rescaling by R. To avoid double-counting, one conventionally labels Liouville vertex operators by α satisfying $\mathrm{Re}(\alpha) < \frac{Q}{2}$, known as the Seiberg bound [47], such that $e^{-2\alpha X}$ is the dominant contribution at infinity. It is impossible to have an operator that asymptotes to $e^{-2\alpha X}$ with $\mathrm{Re}(\alpha) > \frac{Q}{2}$ because it is sub-dominant to its reflection $e^{-2(Q-\alpha)X}$, and both terms are necessarily present to obtain a non-singular solution in the interior.

On the complex branch $\mathrm{Re}(\alpha) = \frac{Q}{2}$, on the other hand, neither exponential dominates the other. The reflection $\alpha \to Q-\alpha$ flips the sign of $\mathrm{Im}(\alpha)$, and one restricts to $\mathrm{Im}(\alpha) > 0$ to avoid the double-counting. The complex and real branches of operators with non-negative conformal weights are then labeled by $\alpha \in \frac{Q}{2} + i\mathbb{R}_+$ and $\alpha \in \left[0, \frac{Q}{2}\right]$.

The asymptotic zero-mode wavefunction for the state prepared by V_α,

$$\Psi_\alpha(X) \overset{X\to\infty}{\longrightarrow} e^{2\left(\frac{Q}{2}-\alpha\right)X} + R(\alpha)e^{-2\left(\frac{Q}{2}-\alpha\right)X}, \tag{2.54}$$

is oscillatory and delta-function normalizable on the complex branch $\alpha \in \frac{Q}{2} + i\mathbb{R}_+$, corresponding to a scattering state with asymptotic momentum s. On the real branch it is exponentially divergent at weak-coupling and therefore non-normalizable. The Liouville Hilbert space of normalizable states is then spanned by the complex branch $\alpha \in \frac{Q}{2} + i\mathbb{R}_+$ [47]. The anomalous momentum conservation law of the free theory is completely broken by the potential, and one obtains a closed OPE algebra and a unitary CFT. The real branch operators with $\alpha \in \left[0, \frac{Q}{2}\right]$, which includes the identity, are nevertheless good local operators of non-negative conformal weight. One can in fact consider the analytic continuation of α to general complex values [35].

Note that with the choice of operator normalization in Eqn. 2.50, the two-point function of V_α is not canonically normalized, but rather proportional to $R(\alpha)$. A canonically normalized primary would be obtained by rescaling by $R(\alpha)^{-1/2}$.

The coefficient μ of the Liouville potential is not a meaningful coupling of the CFT since it may be rescaled by a field redefinition of X. In particular, under the shift $X \to X + \frac{1}{2b_{\mathrm{L}}}\log\mu$, one finds $\mu e^{-2b_{\mathrm{L}}X} \to e^{-2b_{\mathrm{L}}X}$, and thus μ is rescaled to one. The only cost in doing so is that a constant mode of the dilaton $\Phi = -QX \to -QX - \frac{Q}{2b_{\mathrm{L}}}\log\mu$ is introduced. A constant dilaton merely contributes a term $\Phi_0\chi$ to the action, however. It is a trivial improvement

term of the CFT, and its only effect is to rescale correlation functions.[23] In an action with a given μ and Φ_0, only the combination $\mu e^{-2b_{\rm L}\Phi_0/Q}$ is unambiguous.

Relatedly, although the Liouville action takes the form of the free linear-dilaton action deformed by a potential with coefficient μ, Liouville is not a small perturbation of the free theory. The freedom to rescale μ by a field redefinition of X implies that correlation functions are not analytic functions of μ, and one cannot in general write a Liouville correlator as a Taylor expansion in μ with coefficients given by free-theory correlators.

The μ dependence of a correlation function of Liouville primaries may be seen in several ways. By the field redefinition $X = X' - \frac{1}{2b_{\rm L}}\log\mu$ one finds

$$\begin{aligned}\left\langle \prod_j e^{-2\alpha_j X} \right\rangle_\mu &= \int \mathrm{D}X'\, e^{-S_\mu[X']} \prod_j e^{-2\alpha_j X'} \\ &= \int \mathrm{D}X\, e^{-S_{\mu=1}[X]+\frac{Q}{2b_{\rm L}}\chi\log\mu} \prod_j e^{-2\alpha_j X} e^{-2\alpha_j \frac{1}{2b_{\rm L}}\log\mu} \\ &= \mu^{\frac{1}{b_{\rm L}}\left(\frac{1}{2}\chi Q - \sum_j \alpha_j\right)} \left\langle \prod_j e^{-2\alpha_j X} \right\rangle_{\mu=1} . \end{aligned} \tag{2.55}$$

The μ dependence of a correlation function with primary momenta $\{\alpha_j\}$ is therefore given by μ^κ, where [70]

$$\kappa = \frac{1}{b_{\rm L}}\left(\frac{1}{2}\chi Q - \sum_j \alpha_j\right). \tag{2.56}$$

In particular, the correlator is analytic in μ only for $\kappa = N \in \mathbb{N}$.

[23] The scale factor may depend on the insertions in the correlator, however, if as for Liouville primaries they depend on the zero-mode.

Suppose we attempt to expand the Liouville potential around the linear-dilaton background,

$$\left\langle \prod_j e^{-2\alpha_j X} \right\rangle_{\mathrm{L}} = \sum_{N=0}^{\infty} \frac{(-\mu)^N}{N!} \left\langle \prod_j e^{-2\alpha_j X} V_{\mathrm{L}}[X]^N \right\rangle_{\mathrm{LD}}, \tag{2.57}$$

where $V_{\mathrm{L}}[X] = \int \mathrm{d}^2\sigma \sqrt{h}\, e^{-2b_{\mathrm{L}} X}$. The anomalous conservation law of the free theory allows at most one non-zero term in the expansion for compatible values of $\{\alpha_j\}$,

$$N b_{\mathrm{L}} + \sum_j \alpha_j = \frac{1}{2} Q \chi, \tag{2.58}$$

which is again the condition that $\kappa = N$ is a natural number. In other words, for a Liouville correlation function of primaries labeled by $\{\alpha_j\}$, if the quantity Eqn. 2.56 is a natural number then the Liouville correlator is equal to the linear-dilaton correlator with that number of copies of the integrated potential inserted. The zero-mode integral $\int \mathrm{d}x\, e^{2b_{\mathrm{L}}(\kappa - N)x} = \int \mathrm{d}x$ diverges with the target volume, however, and so more precisely the linear-dilaton correlation function with the zero-mode measure omitted computes the residue of the Liouville correlation function at the pole. One could use these data to determine the Liouville correlator with general momenta by "continuation," in the sense that one finds the meromorphic function of $\{\alpha_j\}$ with the given pole structure at those discrete values satisfying $\kappa \in \mathbb{N}$ [66, 67, 69, 71].

For generic $\{\alpha_j\}$, Eqn. 2.58 need not be satisfied, and so every term on the right-hand-side of Eqn. 2.57 would seem to vanish. And yet the Liouville correlator on the left need not be zero. The source of the trouble is the strong-coupling region. Namely, Eqn. 2.57 should be understood more properly as a perturbative expansion in the weak-coupling region of the

Liouville measure in powers of $\mu e^{-2b_{\rm L}X_0}$ [67]:

$$\mathrm{D}X\; e^{-S_{\rm L}[X]}\prod_j e^{-2\alpha_j X} \overset{X_0\to\infty}{\longrightarrow} \mathrm{D}X'\; e^{-S_{\rm LD}[X']}\prod_j e^{-2\alpha_j X'} \times \mathrm{d}X_0\; e^{2b_{\rm L}\kappa X_0}\sum_{N=0}^{\infty}\frac{1}{N!}\left(-\mu e^{-2b_{\rm L}X_0}\right)^N V_{\rm L}[X']^N, \tag{2.59}$$

where we have separated the measure into its zero and non-zero-mode contributions, $X(z,\bar{z}) = X_0 + X'(z,\bar{z})$. Note that whereas μ itself was not uniquely defined, the combination $\mu e^{-2b_{\rm L}X_0}$ is invariant under $X_0 \to X_0+\delta$, $\mu \to e^{2b_{\rm L}\delta}\mu$ and so is a sensible parameter. The expansion is good in the weak-coupling region where the parameter is small, but it does not describe the measure in the strong-coupling region well. To proceed with the expansion for general momenta one would need to introduce a cut-off that regulates the strong-coupling region. The regulator would break the target translation symmetry and eliminate the spurious constraint Eqn. 2.58.

Rather than expanding the potential, one may also study a Liouville correlator by performing the functional integral over the zero-mode outright:

$$\left\langle\prod_j e^{-2\alpha_j X}\right\rangle_\mu = \int \mathrm{D}X'\, e^{-S_{\rm LD}[X']}\prod_j e^{-2\alpha_j X'}\int \mathrm{d}X_0\; e^{2b_{\rm L}\kappa X_0-(\mu V_{\rm L}[X'])e^{-2b_{\rm L}X_0}}. \tag{2.60}$$

The zero-mode integral is a gamma function,

$$\int_{-\infty}^{\infty}\mathrm{d}\xi\; e^{\kappa\xi-\beta e^{-\xi}} = \beta^{\kappa}\Gamma(-\kappa), \qquad \mathrm{Re}(\kappa)<0,\quad \mathrm{Re}(\beta)>0. \tag{2.61}$$

Then for $\mathrm{Re}(\kappa) < 0$, i.e. $\sum_j \mathrm{Re}(\alpha_j) > \frac{1}{2}Q\chi$, one obtains

$$\left\langle \prod_j e^{-2\alpha_j X} \right\rangle_\mu = \frac{\mu^\kappa}{2b_{\mathrm{L}}} \Gamma(-\kappa) \left\langle V_{\mathrm{L}}[X']^\kappa \prod_j e^{-2\alpha_j X'} \right\rangle_{\mathrm{LD},\emptyset} , \tag{2.62}$$

where the latter correlation function is evaluated in the free theory with the zero-mode measure omitted. Since κ is in general a complex number, this expression does not admit an obvious interpretation as a correlation function of local operators, and is defined by the functional integral. When $\mathrm{Re}(\kappa) > 0$, the zero-mode integral over the real line diverges [47], and the integration contour should be deformed to an appropriate complex contour that preserves convergence and analyticity [35], as further discussed below. In particular, for $\kappa \in \mathbb{N}$ Eqns. 2.57 and 2.62 are consistent, the divergence of $\Gamma(-\kappa)$ at its pole coinciding with the target volume divergence of the linear-dilaton zero-mode.

2.2.2 Asymptotic Conditions

Next let us discuss the formulation of asymptotic conditions in Liouville. Much of the machinery of the free theory discussed in Sec. 2.1 continues to apply, with a few caveats. Consider the worldsheet neighborhood of an operator insertion $V_\alpha(z', \bar{z}')$. Suppose $\mathrm{Re}(\alpha) < \frac{Q}{2}$, such that the operator at large $\mathrm{Re}(X)$ is dominated by $e^{-2\alpha X}$, as in the free theory. If one further requires $\mathrm{Re}(\alpha) < 0$, then the free-field Green function Eqn. 2.29 remains a self-consistent solution of the Liouville equation of motion, since it maps the neighborhood of the insertion to $\mathrm{Re}(X) \to \infty$ where the potential is sub-leading. As before, one can cut out the insertion and replace it with the boundary action Eqn. 2.30.

The same considerations as in the free theory require the asymptotic conditions Eqn. 2.32 on the plane or Eqn. 2.35 on the cylinder due to the background charge. These likewise map the insertion point to the weak-coupling region, and the free-field results remain consistent.

When V_α is inserted in the far past on the cylinder, the condition $\mathrm{Re}(\alpha) < 0$ may be relaxed to the Seiberg bound $\mathrm{Re}(\alpha) < \frac{Q}{2}$; the combined effect of V_α and the background charge yield the asymptotic condition Eqn. 2.37, which sends $\mathrm{Re}(X) \to \infty$. One may describe a complex branch insertion similarly by shifting $\alpha \to \alpha - \varepsilon$ with a small regulator $\varepsilon > 0$.

With, for example, insertions of V_α at both ends of the cylinder, with $\mathrm{Re}(\alpha) < \frac{Q}{2}$, one obtains the following action

$$\begin{aligned} S_\alpha =& \frac{1}{4\pi} \int_{-L}^{L} \mathrm{d}\rho \int_{0}^{2\pi} \mathrm{d}\phi \, \left((\partial_\rho X)^2 + (\partial_\phi X)^2 + 4\pi\mu e^{-2b_{\mathrm{L}} X} \right) \\ & - 2\left(\frac{Q}{2} - \alpha\right) \int_0^{2\pi} \frac{\mathrm{d}\phi}{2\pi} \left(X|_{\rho=L} + X|_{\rho=-L} \right) + 4\left(\frac{Q}{2} - \alpha\right)^2 L, \end{aligned} \tag{2.63}$$

with which the functional integral computes the Liouville reflection coefficient $R(\alpha)$ in the limit $L \to \infty$,

$$R(\alpha) = \int_{\mathcal{C}(\alpha)} \mathrm{D}X \, e^{-S_\alpha}. \tag{2.64}$$

We discuss the appropriate choice of integration contour $\mathcal{C}(\alpha)$ in the next sub-section.

We wish to investigate the semi-classical limit of Eqn. 2.64. To do so, it is convenient to

define

$$\tilde{X} \equiv b_{\mathrm{L}} X, \quad \tilde{\mu} \equiv b_{\mathrm{L}}^2 \mu, \quad \eta \equiv b_{\mathrm{L}} \alpha. \tag{2.65}$$

Then the action Eqn. 2.63 for the two-point function of V_α may be written as $S_\alpha = \frac{1}{b_{\mathrm{L}}^2}\tilde{S}$, where

$$\begin{aligned}\tilde{S} =& \frac{1}{4\pi}\int_{-L}^{L} \mathrm{d}\rho \int_0^{2\pi} \mathrm{d}\phi \left((\partial_\rho \tilde{X})^2 + (\partial_\phi \tilde{X})^2 + 4\pi\tilde{\mu} e^{-2\tilde{X}}\right) \\ &- 2\left(\frac{1}{2} - \eta + \frac{1}{2}b_{\mathrm{L}}^2\right)\int_0^{2\pi} \frac{\mathrm{d}\phi}{2\pi}\left(\tilde{X}|_{\rho=L} + \tilde{X}|_{\rho=-L}\right) + 4\left(\frac{1}{2} - \eta + \frac{1}{2}b_{\mathrm{L}}^2\right)^2 L.\end{aligned} \tag{2.66}$$

In the functional integral,

$$R(\eta) = \int_{\mathcal{C}(\eta)} \mathrm{D}\tilde{X}\, e^{-\frac{1}{b_{\mathrm{L}}^2}\tilde{S}}, \tag{2.67}$$

b_{L}^2 plays the role of $\hbar$, with $\tilde{S}$ being order one or higher. Thus, the semi-classical limit is $b_{\mathrm{L}} \to 0$ with $\tilde{\mu}$ held fixed. Moreover, by choosing $\alpha = \frac{\eta}{b_{\mathrm{L}}}$ with η of order one, we have restricted our attention to the reflection coefficient of "heavy" operators, which enter at the same order (namely $\frac{1}{b_{\mathrm{L}}^2}$) as the leading terms in the action. Note that the constraint $\mathrm{Re}(\alpha) < \frac{Q}{2}$ implies that $\mathrm{Re}(\eta) < \frac{1}{2}$ in the $b_{\mathrm{L}} \to 0$ limit.

2.2.3 Saddle-Point Expansion

The semi-classical limit of Eqn. 2.67 was computed by a saddle-point expansion in [35] and matched to the limit of the exact reflection coefficient (Eqn. 2.53). Here, we reproduce the same result using the methods of [68], which are convenient because the calculation is reduced to a particle mechanics problem. In Sec. 2.4 we will apply the same methods to understand the semi-classical limit of the reflection coefficient in the cigar CFT.

We first write down the limit of the exact reflection coefficient [35]. Eqn. 2.53, with the definitions Eqn. 2.65, may be written

$$R(\eta) = -b_{\mathrm{L}}^2 \left(\pi\tilde{\mu}\frac{\gamma(b_{\mathrm{L}}^2)}{b_{\mathrm{L}}^2}\right)^{\frac{1}{b_{\mathrm{L}}^2}\left(1-2\eta+b_{\mathrm{L}}^2\right)} \frac{\gamma\left(-\frac{1}{b_{\mathrm{L}}^2}\left(1-2\eta\right)\right)\gamma\left(2\eta-b_{\mathrm{L}}^2\right)}{\left(1-2\eta+b_{\mathrm{L}}^2\right)^2}, \tag{2.68}$$

where $\gamma(x) = \Gamma(x)/\Gamma(1-x)$.

The asymptotic behavior of the gamma function for large complex values of its argument depends on the direction in the complex plane in which the limit is taken. To $e^{\mathcal{O}(z^{-1})}$, it is given by [35, 72, 73]

$$\Gamma(z) \overset{|z|\to\infty}{\longrightarrow} \begin{cases} e^{\left(z-\frac{1}{2}\right)\log(z)-z+\frac{1}{2}\log(2\pi)+\mathcal{O}(z^{-1})} & \mathrm{Re}(z) > 0 \\ \csc(\pi z) e^{\left(z-\frac{1}{2}\right)\log(-z)-z+\frac{1}{2}\log\left(\frac{\pi}{2}\right)+\mathcal{O}(z^{-1})} & \mathrm{Re}(z) < 0. \end{cases} \tag{2.69}$$

The first line is the usual Stirling approximation, and the second follows from the first in

combination with the identity $\Gamma(z)\Gamma(-z) = -\frac{\pi}{z}\csc(\pi z)$. The asymptotics of $\gamma(z)$ are then

$$\gamma(z) \overset{|z|\to\infty}{\longrightarrow} \begin{cases} \dfrac{2\sin(\pi z)}{z} e^{2z(\log(z)-1)+\mathcal{O}(z^{-1})} & \mathrm{Re}(z) > 0 \\ -\dfrac{\csc(\pi z)}{2z} e^{2z(\log(-z)-1)+\mathcal{O}(z^{-1})} & \mathrm{Re}(z) < 0. \end{cases} \tag{2.70}$$

We obtain, for $\mathrm{Re}(\eta) < \frac{1}{2}$,[24]

$$\begin{aligned} R(\eta) \overset{b_{\mathrm{L}}\to 0}{\longrightarrow} \frac{\pi\tilde{\mu}}{16}\gamma(2\eta)\frac{e^{4\Gamma'(1)\left(\frac{1}{2}-\eta\right)}}{\left(\frac{1}{2}-\eta\right)^3} \\ \times \left(\frac{e^2\pi\tilde{\mu}}{4}\right)^{\frac{2}{b_{\mathrm{L}}^2}\left(\frac{1}{2}-\eta\right)} \left(\frac{1}{2}-\eta\right)^{-\frac{4}{b_{\mathrm{L}}^2}\left(\frac{1}{2}-\eta\right)} \csc\left(\frac{2\pi}{b_{\mathrm{L}}^2}\left(\frac{1}{2}-\eta\right)\right). \end{aligned} \tag{2.71}$$

In the saddle-point expansion, we expect the second line to arise from the leading order $\frac{1}{b_{\mathrm{L}}^2}$ action evaluated on its saddles, and the first line to arise from the fluctuation determinant as well as the order one corrections to the action.

The leading saddle-point expansion is of the form

$$R(\eta) \overset{b_{\mathrm{L}}\to 0}{\longrightarrow} \sum_{\tilde{X}_i} e^{-\frac{1}{b_{\mathrm{L}}^2}(\tilde{S}[\tilde{X}_i]+\mathcal{O}(b_{\mathrm{L}}^2))}. \tag{2.72}$$

Here, $\{\tilde{X}_i\}$ are a subset of solutions to the equations of motion, which are

$$\left(\partial_\rho^2 + \partial_\phi^2\right)\tilde{X} = \tilde{V}'(\tilde{X}) \tag{2.73}$$

[24] $-\Gamma'(1)$ is the Euler-Mascheroni constant.

in the bulk and

$$\partial_\rho \tilde{X}|_{\rho=\pm L} = \pm 2\left(\frac{1}{2} - \eta\right) \tag{2.74}$$

on the boundaries, where $\tilde{V}(\tilde{X}) = 2\pi\tilde{\mu}e^{-2\tilde{X}}$.

Since we allow for complex values of η, clearly the saddles of the functional integral will in general be complex. However, even for real values of η one must sum over complex saddles [35]. The necessity of complexification is familiar from applications of the saddle-point method to asymptotic expansions of ordinary integrals over real variables, where the original real integration contour is typically deformed into a homotopically equivalent sum of steepest-descent contours passing through complex critical points.

The asymptotic expansion of the Gamma function in Eqn. 2.69 may itself be understood as a finite-dimensional example of the saddle-point expansion, since $\Gamma(z)$ may be defined by the integral

$$\Gamma(z) = \int_{\mathcal{C}(z)} \mathrm{d}X\, e^{-(-zX+e^X)}. \tag{2.75}$$

We refer the reader to Appendix C of [35] for a self-contained review, because the problem for the functional integral is in many ways analogous. Briefly, the saddle-points of the "action" $S[X] = -zX + e^X$ are given by $X_N = \log(z) + 2\pi i N$, with $N \in \mathbb{Z}$. The contour $\mathcal{C}(z)$ is given by the real axis for $\mathrm{Re}(z) > 0$, though it must be deformed for $\mathrm{Re}(z) < 0$ to preserve convergence of the integral, as in the discussion of the Liouville zero-mode integral Eqn.

2.61. For $\mathrm{Re}(z) > 0$, $\mathcal{C}(z)$ is homotopic to the steepest-descent contour $\mathcal{C}_0$ through X_0, and one recovers the Stirling formula $e^{-S[X_0]} = e^{z\log(z)-z}$.

Along the imaginary z-axis, however, one encounters what is known as a Stokes wall. There the steepest-descent contour of any saddle-point, which otherwise varies smoothly with z, collides with a neighboring saddle-point. As a result, for values of z just to either side of the imaginary axis, the steepest-descent contour jumps discontinuously. The integration contour $\mathcal{C}(z)$ itself varies smoothly with z, but its expansion in steepest-descent contours changes abruptly upon crossing the Stokes wall, and therefore its asymptotic expansion changes as well. For $\mathrm{Re}(z) < 0$ and $\mathrm{Im}(z) > 0$, $\mathcal{C}(z)$ is instead homotopic to the sum of steepest-descent contours $\sum_{N=0}^{\infty}\mathcal{C}_N$ passing through the saddles X_N. Then the saddle-point expansion yields

$$\begin{aligned}\sum_{N=0}^{\infty} e^{-S[X_N]} =& e^{-S[X_0]}\sum_{N=0}^{\infty} e^{2\pi i z N}\\ &= \csc(\pi z) e^{z\log(-z)-z+\mathcal{O}(z^0)},\end{aligned} \tag{2.76}$$

as in Eqn. 2.69. For $\mathrm{Im}(z) < 0$, the relevant contours are instead $\sum_{N=0}^{\infty}\mathcal{C}_{-N}$, as required for the geometric series to converge.

Thus, the poles of the Gamma function on the negative real axis may be understood as the divergence of the geometric series $\sum_{N=0}^{\infty} e^{2\pi i z N}$ that results from summing over a family of saddles related by complex shifts $X \to X + 2\pi i$. The poles of $\csc\left(\frac{2\pi}{b_{\mathrm{L}}^2}\left(\frac{1}{2}-\eta\right)\right)$ in Eqn. 2.71 will arise from a complex shift symmetry in a similar way [35].

As in the finite-dimensional problem, the saddle-point expansion of a functional integral is performed by deforming the integration contour into a sum of complex cycles [34, 35]. Unlike for a finite-dimensional integral, however, for a functional integral it is in general very challenging to determine the set of steepest-descent cycles that are homotopic to the original contour. In other words, it is at present a hard problem to derive from first principles which complex saddles one should sum over in computing the saddle-point expansion of a functional integral, especially since the necessary set of saddles can jump upon crossing Stokes walls in the parameter space. Since for the problem at hand we know the exact answer and its semi-classical limit, one may identify the set of solutions on which the saddle-point expansion reproduces the known answer [35].

Finally, we have not yet specified the contour $\mathcal{C}(\eta)$ in field space along which the functional integral Eqn. 2.67 is to be performed. In the example of the Gamma function, one starts with a contour along the real axis when z is a positive real number. Then one deforms it as necessary for complex values of z to preserve convergence of the integral and produce an analytic function of z.

By contrast, even for real η the functional integral Eqn. 2.67 over real fields diverges [35, 47]. In the notation of Eqn. 2.61, $\kappa = \frac{2}{b_{\rm L}^2}\left(\frac{1}{2} - \eta\right) + \mathcal{O}(1)$ is positive, and therefore the zero-mode integral over the real axis diverges. Another argument comes from [35]: let $\tilde{X}$ be a real, finite-action configuration, and let $\tilde{X} + a$ be another configuration shifted by a large,

positive real number. Then the action of the latter configuration is given by

$$\tilde{S}[\tilde{X}+a] \overset{a\to\infty}{\longrightarrow} -4a\left(\frac{1}{2}-\eta\right)+\tilde{S}[\tilde{X}]-\tilde{\mu}\int \mathrm{d}\rho\,\mathrm{d}\phi\, e^{-2\tilde{X}}+\mathcal{O}(e^{-2a},b^2). \tag{2.77}$$

Since $\mathrm{Re}(\eta)<\frac{1}{2}$, by making a arbitrarily large the real part of the action may be made arbitrarily negative. This is a region of real field space where $e^{-S}\to\infty$, and therefore the functional integral over real fields cannot converge.

Instead, $\mathcal{C}(\eta)$ must be chosen to be an appropriate complex cycle. By identifying the set of saddles with which the semi-classical limit of the exact result is reproduced, the authors of [35] identified the necessary contour as the sum of steepest-descent contours associated to these complex saddles.

We now proceed with the saddle-point expansion. One must identify the appropriate set of solutions $\{X_i\}$ to the bulk and boundary equations of motion such that Eqn. 2.72 reproduces Eqn. 2.71. It will prove sufficient to consider ϕ-independent trajectories $\tilde{X}(\rho)$, which reduces the question to a mechanics problem with action

$$\begin{aligned}\tilde{S}[\tilde{X}] = &\int_{-L}^{L}\mathrm{d}\rho\left(\frac{1}{2}\dot{\tilde{X}}^2+\tilde{V}(\tilde{X})\right)-2\left(\frac{1}{2}-\eta\right)\left(\tilde{X}(L)+\tilde{X}(-L)\right)\\ &+4\left(\frac{1}{2}-\eta\right)^2 L+\mathcal{O}(b_{\mathrm{L}}^2).\end{aligned} \tag{2.78}$$

The bulk equation of motion Eqn. 2.73,

$$\frac{\mathrm{d}^2\tilde{X}}{\mathrm{d}\rho^2}=\tilde{V}'(\tilde{X}), \tag{2.79}$$

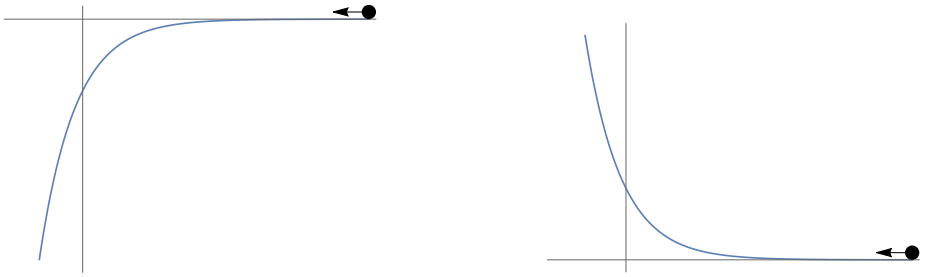

(a) (b)

Figure 2.1: Inverted Potentials. The equation of motion for a zero-mode $\tilde{X}(\rho)$ of the action $\tilde{S}[\tilde{X}]$ describes a particle in an unstable potential with a cliff as $\tilde{X} \to -\infty$ (left). After complexification, however, one finds simple solutions with constant imaginary part $\frac{\pi i}{2} + \pi i N$, on which the potential becomes a stable, repulsive wall (right). The freedom to shift the solutions by $\pi i N$ reflects the complex shift symmetry of the potential, $\tilde{V}(\tilde{X} + \pi i) = \tilde{V}(\tilde{X})$.

describes a particle in the inverted potential $-\tilde{V}(\tilde{X}) = -2\pi\tilde{\mu}e^{-2\tilde{X}}$. In the limit $L \to \infty$, the boundary equations of motion Eqn. 2.74 become the expected asymptotic conditions

$$\tilde{X}(\rho) \overset{\rho\to\pm\infty}{\longrightarrow} \pm 2\left(\frac{1}{2} - \eta\right)\rho + a_{\pm} + \cdots , \tag{2.80}$$

demanding that the particle comes in from and returns to the weak-coupling region with fixed momentum. The sub-leading constants $a_{\pm}$ specify the asymptotic separation $\tilde{X}(\infty) - \tilde{X}(-\infty) = a_+ - a_-$.

Note that the inverted potential is unstable, and a real particle trajectory simply rolls down the hill to $\tilde{X} \to -\infty$ (Fig. 2.1a). Rather, as already mentioned, one must allow for complex-valued saddle points, even for real η. That is, one continues $\tilde{S}[\tilde{X}]$ to a holomorphic functional of maps $\tilde{X} \colon \mathbb{R} \to \mathbb{C}$ into the complex $\tilde{X}$-plane and identifies its critical points.

The simplest solutions have constant imaginary part. Indeed, notice that under the shift $\tilde{X} \to \tilde{X} + \frac{\pi i}{2}$ the potential flips sign. Then the unstable cliff is replaced by a repulsive hill, and one finds solutions describing a particle that rolls up and down the hill (Fig. 2.1b).

Moreover, the potential is invariant under the imaginary shift symmetry $\tilde{V}(\tilde{X}+\pi i)=\tilde{V}(\tilde{X})$. There will consequently be a discrete moduli space of solutions with constant imaginary part $\frac{\pi i}{2}+\pi i N$ for each $N\in\mathbb{Z}$.

One may obtain these solutions explicitly, but note that it is not necessary to do so in order to evaluate their on-shell action. Integrating the equation of motion once produces the energy conservation equation

$$\frac{1}{2}\dot{\tilde{X}}^2-\tilde{V}(\tilde{X})=2\left(\frac{1}{2}-\eta\right)^2, \tag{2.81}$$

with the conserved energy being fixed by the asymptotic condition. Using this equation, we may eliminate $\tilde{V}(\tilde{X})$ from the action,

$$\tilde{S}[\tilde{X}]=\int_{-L}^{L}\mathrm{d}\rho\,\dot{\tilde{X}}^2-2\left(\frac{1}{2}-\eta\right)\left(\tilde{X}(L)+\tilde{X}(-L)\right). \tag{2.82}$$

Letting $\mathscr{C}$ denote the contour traced by a saddle $\tilde{X}(\rho)$, we arrive at

$$\tilde{S}[\tilde{X}]=\int_{\mathscr{C}}\mathrm{d}\tilde{X}\,\sqrt{4\left(\frac{1}{2}-\eta\right)^2+2\tilde{V}(\tilde{X})}-2\left(\frac{1}{2}-\eta\right)\left(\tilde{X}(L)+\tilde{X}(-L)\right), \tag{2.83}$$

the integrand being the velocity function. Note that the square-root has branch points at the turning points of the energy conservation equation, where $-\tilde{V}(\tilde{X}_*+\pi i N)=2\left(\frac{1}{2}-\eta\right)^2$ and the velocity vanishes:

$$\tilde{X}_*=-\log\left(\frac{1}{2}-\eta\right)+\frac{1}{2}\log\left(\pi\tilde{\mu}\right)+\frac{\pi i}{2}. \tag{2.84}$$

One must choose an appropriate branch of the square-root such that the velocity has the correct sign. Then the on-shell action may be computed by evaluating the contour integral for any convenient contour connecting $\tilde{X}(L)$ and $\tilde{X}(-L)$ that avoids the chosen branch cuts.

The explicit solutions may be obtained by separating and integrating the energy conservation equation:

$$\tilde{X}_N(\rho) = \log\cosh\left(2\left(\frac{1}{2}-\eta\right)(\rho+i\rho_0)\right) + \tilde{X}_* + \pi i N. \tag{2.85}$$

Once again, the discrete modulus N reflects the shift symmetry of the potential. The integration constant ρ_0, on the other hand, is a continuous modulus. In the $L\to\infty$ limit, the real part of $i\rho_0$ merely amounts to a reparameterization of ρ, and we therefore take $i\rho_0$ to be pure imaginary. For a given N, by varying ρ_0 one obtains a continuous family of trajectories, such as those with $N=0$ pictured in Fig. 2.2. The trajectory with $\rho_0=0$ is the solution with constant imaginary part $\frac{\pi}{2}$ that rolls up and down the potential hill. As ρ_0 is increased, the asymptotic imaginary parts of the trajectories separate. Within such a family, each saddle necessarily yields the same on-shell action, and the divergent sum over ρ_0 is attributed to the delta-function $\delta(\alpha-\alpha)$ in the two-point function [35]. In varying ρ_0, the action may only change if the trajectory becomes singular, as it does when the asymptotic imaginary separation reaches π. Indeed, we have seen that on the slice $\mathrm{Im}(\tilde{X})=0$, and all shifts thereof by $\pi i\mathbb{Z}$, the inverted potential is an unstable cliff $-e^{-2\tilde{X}}$. In the limit $2\left(\frac{1}{2}-\eta\right)\rho_0\to\frac{\pi}{2}$, the solution approaches a singular trajectory describing a particle with constant imaginary part π that falls down the infinite well and is then ejected from the well with constant imaginary

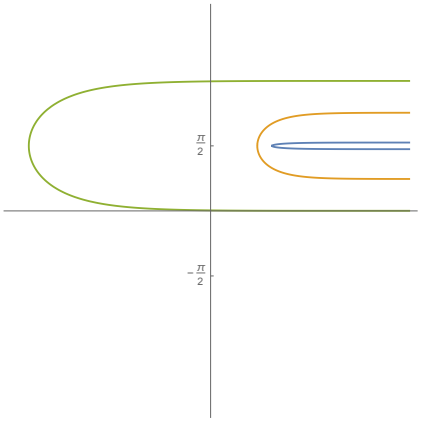

Figure 2.2: Liouville Trajectories. Several examples of solutions in the $N = 0$ family of Eqn. 2.85 are shown, with different values of the continuous modulus ρ_0. The solution with $\rho_0 = 0$ is the simple solution with constant imaginary part $\pi/2$ that rolls up and down the potential shown in Fig. 2.1b—the nearby blue trajectory plotted has a small value of ρ_0. As $2(1/2-\eta)\rho_0$ approaches $\pi/2$, as it almost has for the green curve, the trajectory becomes singular, falling down and climbing back up the cliff at $\mathrm{Im}(\tilde{X}) = 0$ and π shown in Fig. 2.1a.

part 0.

The on-shell action does depend on N, however, due to the shift of the boundary terms:

$$\tilde{S}[\tilde{X}_N] = \tilde{S}[\tilde{X}_0] - 4\pi i \left(\frac{1}{2} - \eta\right) N. \tag{2.86}$$

Let us compute the action $\tilde{S}[\tilde{X}_0]$ of the trajectory with constant imaginary part $\frac{\pi}{2}$ as in Fig. 2.3. The disks indicate the turning points $\tilde{X}_* + \pi i N$, and the dashed lines are a convenient choice of branch cuts of the square-root. The contour has been deformed slightly away from the slice $\frac{\pi i}{2}$, so as to avoid the branch cut.

Either by evaluating the contour integral Eqn. 2.83 or by plugging the explicit solution into Eqn. 2.82, one obtains

$$\tilde{S}[\tilde{X}_0] = -4\left(\frac{1}{2} - \eta\right)\left(\tilde{X}_* - \log(2) + 1\right). \tag{2.87}$$

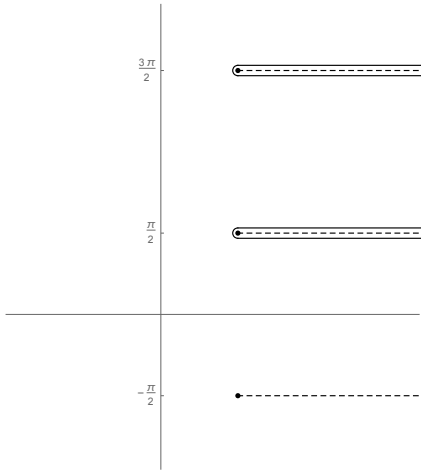

Figure 2.3: Liouville Contours. The on-shell action of a solution $\tilde{X}_N(\rho)$ may be computed by evaluating the contour integral Eqn. 2.83 around the contours shown. The dots represent the turning points $\tilde{X}_* + \pi i N$, which are branch points of the velocity function, and the dashed lines represent a convenient choice of branch cuts. For $\mathrm{Im}(\eta) < 0$, one sums over the contours in the upper-half plane ($N \geq 0$), and for $\mathrm{Im}(\eta) > 0$ one sums over the contours in the lower-half plane ($N \leq -1$).

Its contribution to the saddle-point expansion at order e^{1/b_{L}^2} is then

$$e^{-\frac{1}{b_{\mathrm{L}}^2}\tilde{S}[\tilde{X}_0]} = e^{\frac{2\pi i}{b_{\mathrm{L}}^2}\left(\frac{1}{2}-\eta\right)} \left(\frac{e^2\pi\tilde{\mu}}{4}\right)^{\frac{2}{b_{\mathrm{L}}^2}\left(\frac{1}{2}-\eta\right)} \left(\frac{1}{2}-\eta\right)^{-\frac{4}{b_{\mathrm{L}}^2}\left(\frac{1}{2}-\eta\right)}, \tag{2.88}$$

partly reproducing the second line of Eqn. 2.71. The remaining csc factor is accounted for by summing over the shifted saddles $\tilde{X}_N$ [35]. Observe that, for $\mathrm{Im}(\eta) < 0$,

$$\sum_{N\in\mathbb{Z}_{\geq 0}} e^{\frac{4\pi i}{b_{\mathrm{L}}^2}\left(\frac{1}{2}-\eta\right)N} = \frac{i}{2} e^{-\frac{2\pi i}{b_{\mathrm{L}}^2}\left(\frac{1}{2}-\eta\right)} \csc\left(\frac{2\pi}{b_{\mathrm{L}}^2}\left(\frac{1}{2}-\eta\right)\right), \tag{2.89}$$

the condition on $\mathrm{Im}(\eta)$ ensuring convergence of the sum. In other words, one sums over the contours in the upper-half $\tilde{X}$ plane. The phase in Eqn. 2.89 cancels the unwanted phase in Eqn. 2.88. Together one obtains

$$\sum_{N\in\mathbb{Z}_{\geq 0}} e^{-\frac{1}{b_{\mathrm{L}}^2}\tilde{S}[\tilde{X}_N]} = \left(\frac{e^2\pi\tilde{\mu}}{4}\right)^{\frac{2}{b_{\mathrm{L}}^2}\left(\frac{1}{2}-\eta\right)} \left(\frac{1}{2}-\eta\right)^{-\frac{4}{b_{\mathrm{L}}^2}\left(\frac{1}{2}-\eta\right)} \csc\left(\frac{2\pi}{b_{\mathrm{L}}^2}\left(\frac{1}{2}-\eta\right)\right) e^{\mathcal{O}(1)}, \tag{2.90}$$

reproducing the semi-classical limit Eqn. 2.71 at order $e^{1/b_{\rm L}^2}$.

For $\mathrm{Im}(\eta) > 0$, one instead sums over contours in the lower-half plane,

$$\sum_{N\in\mathbb{Z}_{\leq -1}} e^{\frac{4\pi i}{b_{\rm L}^2}\left(\frac{1}{2}-\eta\right)N} = -\frac{i}{2} e^{-\frac{2\pi i}{b_{\rm L}^2}\left(\frac{1}{2}-\eta\right)} \csc\left(\frac{2\pi}{b_{\rm L}^2}\left(\frac{1}{2}-\eta\right)\right), \tag{2.91}$$

again reproducing the expected result. Note that one should give η a non-zero phase in evaluating the saddle-point expansion to avoid the poles on the real axis.

The order one correction given in the first line of Eqn. 2.71 is expected to arise from the fluctuation determinant around the leading saddles, as well as the order one corrections to the action. It was suggested in [67] that the Liouville potential at small but finite $b_{\rm L}$ should include both $e^{-2b_{\rm L}X}$ and its reflection $e^{-2(Q-b_{\rm L})X}$, the latter being a non-perturbative correction. It would be interesting to understand if this correction contributes to the order one factor of the saddle-point expansion, especially the factor of $\gamma(2\eta)$. More recent work has argued that the action Eqn. 2.41 is not modified, however [74].

In Sec. 2.4, we will investigate the analogous saddle-point expansion of the reflection coefficient for the $\mathrm{SL}(2,\mathbb{R})_k/\mathrm{U}(1)$ CFT. Before coming to that calculation, we first present a review of the CFT in the next section.

2.3 Review of the $\mathrm{SL}(2,\mathbb{R})_k/\mathrm{U}(1)$ CFT

In this section, we review the $\mathrm{SL}(2,\mathbb{R})_k/\mathrm{U}(1)$ CFT that will feature heavily in the remainder of the dissertation. This CFT is a coset of the $\mathrm{SL}(2,\mathbb{R})_k$ WZW model. The group

$\mathrm{SL}(2,\mathbb{R})$ is equivalent to Lorentzian AdS_3, and the WZW model describes a string propagating on that manifold, with the WZW level k corresponding to the AdS length, $l^2_{\mathrm{AdS}} = k l^2_{\mathrm{s}}$. AdS_3 may be described as a solid cylinder with time running along its length, and the coset is defined by gauging this timelike isometry. The result is the unitary $\mathrm{SL}(2,\mathbb{R})_k/\mathrm{U}(1)$ CFT, of central charge

$$c = \frac{3k}{k-2} - 1, \tag{2.92}$$

the first term being the central charge of the $\mathrm{SL}(2,\mathbb{R})_k$ WZW model, less one for the quotient. k is a real number greater than two, which need not be an integer.

In Sec. 3.2 we will review how the $\mathrm{SL}(2,\mathbb{R})_k/\mathrm{U}(1)$ CFT is obtained from the $\mathrm{SL}(2,\mathbb{R})_k$ WZW model by gauging the appropriate symmetry. For now, we will take as given that there exists a CFT of central charge Eqn. 2.92, described by the sigma-model and Virasoro primary spectrum discussed below, and investigate its properties.

2.3.1 The Cigar Sigma-Model

The $\mathrm{SL}(2,\mathbb{R})_k/\mathrm{U}(1)$ CFT admits a sigma-model description, weakly coupled for large k, given by the following metric and dilaton [75]:

$$\mathrm{d}s^2 = \alpha'(k-2)\left(\mathrm{d}r^2 + \frac{1}{\coth^2(r) - \frac{2}{k}}\mathrm{d}\theta^2\right) \tag{2.93a}$$

$$\Phi = \Phi_0 - \frac{1}{2}\log\left(\frac{1}{2}\sinh(2r)\sqrt{\coth^2(r) - \frac{2}{k}}\right). \tag{2.93b}$$

The target space is two-dimensional and has the topology of a disk, with coordinates $r \in [0, \infty)$ and $\theta \sim \theta + 2\pi$. The dilaton is a monotonically-decreasing function of r, with the constant Φ_0 setting its maximal value at the origin: $\Phi|_{r=0} = \Phi_0$. In that neighborhood the geometry is simply $\mathbb{R}^2$ in polar coordinates:

$$\mathrm{d}s^2 = \alpha'(k-2)\left(\mathrm{d}r^2 + r^2\mathrm{d}\theta^2\right) + \mathcal{O}(r^3) \tag{2.94a}$$

$$\Phi = \Phi_0 - \frac{1}{2}\frac{k-1}{k}r^2 + \mathcal{O}(r^3). \tag{2.94b}$$

At large r, on the other hand, the geometry approaches a cylinder of radius $\sqrt{\alpha' k}$, with the dilaton decreasing linearly along its length:

$$\mathrm{d}s^2 = \alpha'(k-2)\mathrm{d}r^2 + \alpha' k\mathrm{d}\theta^2 + \mathcal{O}\left(e^{-2r}\right) \tag{2.95a}$$

$$\Phi = -r + \Phi_0 + \frac{1}{4}\log\left(\frac{16k}{k-2}\right) + \mathcal{O}\left(e^{-2r}\right). \tag{2.95b}$$

The target space therefore resembles a cigar (Fig. 1.4a), with an asymptotic cylinder at large r that caps off at the tip $r = 0$, hence the background is known as the cigar sigma-model. The leading $\mathcal{O}\left(e^{-2r}\right)$ correction to the cylinder metric is $-\frac{4\alpha' k^2}{k-2}e^{-2r}\mathrm{d}\theta^2$, and the corresponding operator $e^{-2r}\partial\theta\bar{\partial}\theta$ is the leading correction to the cylinder background as one heads back toward finite r. It is important to note that although the asymptotic cylinder suggests the sigma-model has a topological winding number, there is no conserved charge because a string that appears to wind the cylinder can unwind at the tip.

For large k the cigar is large and weakly curved,

$$\mathcal{R} = \frac{4}{\cosh^2(r)} \frac{1}{\alpha' k} + \mathcal{O}\left(k^{-2}\right), \tag{2.96}$$

and the sigma-model is weakly coupled in the α' sense. In this limit the background is [32]

$$\mathrm{d}s^2 = \alpha' k \left(\mathrm{d}r^2 + \tanh^2(r)\mathrm{d}\theta^2\right) + \mathcal{O}(k^0) \tag{2.97a}$$

$$\Phi = -\log\cosh(r) + \Phi_0 + \mathcal{O}\left(k^{-1}\right). \tag{2.97b}$$

The action in the weak-coupling limit is then

$$S_{\text{cigar}} = \frac{k}{4\pi} \int_\Sigma \mathrm{d}^2\sigma \sqrt{h} \left\{ (\nabla r)^2 + \tanh^2(r)(\nabla\theta)^2 + \frac{1}{k}\mathcal{R}[h] \left(-\log\cosh r + \Phi_0\right) \right\} \tag{2.98}$$

on a closed worldsheet Σ of metric h_{ab}.

The effective string coupling $g_{\text{s}} = e^{\Phi}$ is determined by the dilaton. The unusual profile $\Phi(r)$ is required by conformal invariance of the curved background. One can check, for example, that Eqn. 2.97 satisfies the leading-order beta function equation

$$\beta_{IJ} = \alpha'(R_{IJ} + 2\nabla_I\nabla_J\Phi) + \mathcal{O}(\alpha'^2) = \mathcal{O}(\alpha'^2). \tag{2.99}$$

Since the dilaton is monotonically decreasing, the string coupling attains its maximum e^{Φ_0} at the tip and decays to zero at large r, which we refer to as the weak-coupling region. The parameter Φ_0 is a modulus of the theory. It reflects the usual freedom to shift the dilaton by a constant, the only effect being to shift the action by $\Phi_0\chi$, with χ the Euler

characteristic of Σ.

2.3.2 The 2D Black Hole

The background Eqn. 2.97 is remarkable because it describes a string in a Euclidean black hole of two-dimensional dilaton-gravity [32]. Namely, from the spacetime perspective, the background is a solution of

$$S_{\text{spacetime}} = -\frac{1}{2\kappa^2}\int \mathrm{d}r\mathrm{d}\theta\sqrt{g}\, e^{-2\Phi}\left(\mathcal{R}[g] + 4\left(\nabla\Phi\right)^2 + \frac{4}{\alpha' k}\right), \tag{2.100}$$

whose equations of motion may be written

$$R_{IJ} + 2\nabla_I\nabla_J\Phi = 0 \tag{2.101a}$$

$$\left(\nabla\Phi\right)^2 - \frac{1}{2}\nabla^2\Phi - \frac{1}{\alpha' k} = 0. \tag{2.101b}$$

The first is again the leading-order beta function equation from the perspective of the world-sheet. The second computes the central charge $c = 2 + 6\alpha'\left((\nabla\Phi)^2 - \frac{1}{2}\nabla^2\Phi\right)$ at large k, $\frac{3k}{k-2} - 1 = 2 + \frac{6}{k} + \mathcal{O}(k^{-2})$.

The interpretation of Eqn. 2.97 as a Euclidean black hole follows by defining the compact coordinate θ as the Euclidean time. Then continuing $\theta = it$ gives the Lorentzian metric in the right wedge of a two-sided black hole (Fig. 2.4a):

$$\mathrm{d}s^2 = \alpha' k\left(\mathrm{d}r^2 - \tanh^2(r)\mathrm{d}t^2\right). \tag{2.102}$$

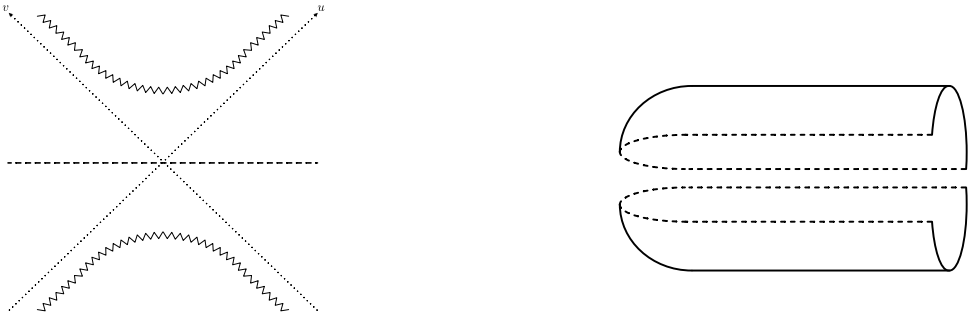

(a) **(b)**

Figure 2.4: The Two-Dimensional Black Hole. The Lorentzian continuation of the Euclidean cigar is a two-sided, eternal black hole. The horizons are the diagonal dotted lines, and the past and future singularities are the zigzag hyperbolas at the bottom and top. The geometry is invariant under time reflection about the dashed line, which enables the construction of the Hartle-Hawking state. The cigar, which has the topology of a disk, is cut in half and glued to the black hole along the fixed line of the reflection symmetry, similar to Fig. 1.2a but resembling the Schwarzschild causal diagram rather than BTZ. This Euclidean cap prepares the state on the dashed line, which is then evolved forward in Lorentzian time.

The geometry approaches flat space at large r, $\mathrm{d}s^2 \to \alpha' k(\mathrm{d}r^2 - \mathrm{d}t^2)$, together with the asymptotically-linear dilaton. The coordinate patch parameterized by r and t ends at the horizon $r = 0$, where the coefficient of $\mathrm{d}t^2$ vanishes. The complete, two-sided black hole may be described in Kruskal coordinates

$$u = e^{-t}\sinh(r), \quad v = -e^{t}\sinh(r), \tag{2.103}$$

in terms of which the metric reads

$$\mathrm{d}s^2 = \alpha' k \frac{\mathrm{d}u\,\mathrm{d}v}{uv - 1}, \tag{2.104}$$

and the dilaton is $\Phi = -\frac{1}{2}\log(1 - uv) + \Phi_0$. The horizon is the locus $uv = 0$, and the singularity is the hyperbola $uv = 1$, whose two branches correspond to the future and past singularities. Note that the singularities correspond to the poles of $\tanh^2(r)$ at $r = \pm\frac{\pi i}{2}$ in

(a) **(b)**

Figure 2.5: Rindler Decomposition. When $\mathbb{R}^2$ in polar coordinates (left) is continued with respect to the angular direction, the result is a wedge of the Rindler decomposition of Minkowski spacetime (right). The Euclidean functional integral over the half-plane prepares the Minkowski vacuum on the dashed line. In angular quantization, the Minkowski vacuum is identified with the thermofield-double state in the two copies of the Hilbert space on the left and right Rindler wedges. The reduced density matrix in a single wedge is a thermal state at the Unruh temperature.

the complexification of the original coordinates.[25] There the coefficient of $\mathrm{d}t^2$ diverges, as does the scalar curvature in Eqn. 2.96, and likewise the dilaton and string coupling. The extended black hole geometry is pictured in Fig. 2.4a. There is of course a second asymptotic boundary in the left wedge. The mass of the black hole is [32]

$$M = \frac{1}{\sqrt{\alpha' k}} e^{-2\Phi_0}. \tag{2.105}$$

In the Euclidean black hole, the horizon bifurcation point corresponds to the tip $r = 0$, where the θ circle shrinks. The geometry in that neighborhood is $\mathbb{R}^2$ (Eqn. 2.94), whose continuation with respect to angular Euclidean time yields Rindler spacetime—the near-horizon geometry of the black hole. Rindler is obtained simply by continuing $\theta = it$ in the plane metric $\mathrm{d}s^2 = \mathrm{d}r^2 + r^2\mathrm{d}\theta^2$ for $\mathbb{R}^2$ in polar coordinates. The resulting Lorentzian metric $\mathrm{d}s^2 = \mathrm{d}r^2 - r^2\mathrm{d}t^2$ describes the right wedge of a two-sided decomposition of Minkowski spacetime, bounded by the Rindler horizon at $r = 0$ where the coefficient of $\mathrm{d}t^2$ vanishes

[25] We point out that the $1/k$ corrections to the $k \to \infty$ metric shift the singularity off the imaginary axis to $r = \pm\coth^{-1}\left(\sqrt{\frac{2}{k}}\right) + \pi i\mathbb{Z} = \frac{\pi i}{2} \pm \sqrt{\frac{2}{k}} + \mathcal{O}(k^{-3/2}) + \pi i\mathbb{Z}$.

(Fig. 2.5).

2.3.3 Spectrum

Returning to the Euclidean theory, we now review its spectrum of Virasoro primaries, which is known exactly thanks to the coset construction from the $\mathrm{SL}(2,\mathbb{R})_k$ WZW model (Sec. 3.2) [75–77]. The Virasoro primaries $\mathcal{O}_{jnw}(z,\bar{z})$ of the coset are labeled by integers n and w and a complex number j, taking the following values:

$$\textbf{(i)} \quad j \in \frac{1}{2} + i\mathbb{R}_+ \tag{2.106a}$$

$$\textbf{(ii)} \quad j_N = \frac{k|w| - |n|}{2} - N \in \left(\frac{1}{2}, \frac{k-1}{2}\right), \quad N \in \mathbb{N}. \tag{2.106b}$$

These two sets are referred to as the complex and real branches of primaries based on the value of j. As in the free linear dilaton and Liouville theories reviewed in Secs. 2.1-2.2, the complex branch primaries correspond to delta-function normalizable scattering states on the cigar with momentum proportional to $\mathrm{Im}(j)$. The integers n and w, meanwhile, correspond to the momentum and winding numbers around the asymptotic cylinder at large r. The real branch primaries with $j = j_N$, on the other hand, correspond to bound states living at the tip of the cigar. These have no analog in the free theory or Liouville. One may also consider the continuation of j to general complex values, including real branch operators for which j is not valued in the discrete set j_N. The latter map to non-normalizable states.

Note that on the complex branch the value of j is independent of the integers n and w, whereas on the real branch n and w determine the allowed values of j up to shifts by the

natural number N, constrained to lie within the interval $\frac{1}{2} < j < \frac{k-1}{2}$. The upper bound $j_N < \frac{k-1}{2}$ ensures positivity of the conformal weights, while the lower bound $j_N > \frac{1}{2}$ ensures normalizability of the wavefunctions. That lower bound implies there may only exist real branch primaries with $k|w| - |n| \geq 1$. In particular, there are none with $w = 0$.

These primaries carry conformal weights

$$h_{jnw} = -\frac{j(j-1)}{k-2} + \frac{(n-kw)^2}{4k}, \qquad \bar{h}_{jnw} = -\frac{j(j-1)}{k-2} + \frac{(n+kw)^2}{4k}. \tag{2.107}$$

Note that the quantity $-j(j-1)$ is a real number not only on the real branch, but also on the complex branch where $-j(j-1) = |j|^2$. On the real branch, it is non-negative for $\frac{1}{2} \leq j \leq 1$ and negative thereafter, its maximal value coinciding with the minimal value on the complex branch. The total conformal weight is non-negative, however. Note also that the spin $h_{jnw} - \bar{h}_{jnw} = -nw$ is appropriately quantized.

Since the sigma-model reduces to the free linear-dilaton $\times$ S^1 background at large r (Eqn. 2.95), the abstract primaries $\mathcal{O}_{jnw}$ may be expanded in free-field primaries in that limit. Define canonically-normalized coordinates,

$$\hat{r} = \frac{1}{Q} r, \quad \hat{\theta} = \sqrt{\alpha' k}\theta, \tag{2.108}$$

in terms of which the asymptotic background is

$$\mathrm{d}s^2 = \mathrm{d}\hat{r}^2 + \mathrm{d}\hat{\theta}^2 \tag{2.109a}$$

$$\Phi = -Q\hat{r}, \tag{2.109b}$$

where

$$Q = \frac{1}{\sqrt{\alpha'(k-2)}}. \tag{2.110}$$

$\hat{\theta}$ is periodic in $2\pi\sqrt{\alpha' k}$. Note that Q goes to zero in the large k limit, in contrast to Liouville where $Q \overset{b_{\mathrm{L}}\to 0}{\longrightarrow} \frac{1}{b_{\mathrm{L}}}$ diverged in the semi-classical limit. In the semi-classical limit of the cigar, the dilaton contribution is sub-leading to the metric.

The Virasoro primaries of the free theory, considered in its own right with $\hat{r}$ permitted to range over the entire real line, are

$$\mathcal{V}_{\alpha p_{\mathrm{L}} p_{\mathrm{R}}}(z,\bar{z}) = e^{-2\alpha\hat{r}(z,\bar{z})} e^{ip_{\mathrm{L}}\hat{\theta}_{\mathrm{L}}(z) + ip_{\mathrm{R}}\hat{\theta}_{\mathrm{R}}(\bar{z})}, \tag{2.111}$$

where p_{L}, p_{R} are valued in the lattice

$$p_{\mathrm{L}} = \frac{n}{\sqrt{\alpha' k}} - \sqrt{\frac{k}{\alpha'}}w, \qquad p_{\mathrm{R}} = \frac{n}{\sqrt{\alpha' k}} + \sqrt{\frac{k}{\alpha'}}w, \qquad n, w \in \mathbb{Z}. \tag{2.112}$$

n is the momentum number around the cylinder and w is (minus) the winding number.[26]

[26] We let w denote the negative of the winding number so that it coincides with the spectral-flow number in $\mathrm{SL}(2,\mathbb{R})_k$, as explained in Sec. 3.2.

Their conformal weights with respect to the free-theory stress tensor

$$T(z) = -\frac{1}{\alpha'}(\partial\hat{r})^2 - Q\partial^2\hat{r} - \frac{1}{\alpha'}(\partial\hat{\theta})^2 \tag{2.113}$$

are

$$h_{\alpha p_{\mathrm{L}} p_{\mathrm{R}}} = \alpha'\alpha(Q-\alpha) + \alpha'\frac{p_{\mathrm{L}}^2}{4}, \qquad \bar{h}_{\alpha p_{\mathrm{L}} p_{\mathrm{R}}} = \alpha'\alpha(Q-\alpha) + \alpha'\frac{p_{\mathrm{R}}^2}{4}. \tag{2.114}$$

The central charge of the Virasoro algebra is

$$c_{\mathrm{LD}\times\mathrm{S}^1} = 2 + 6\alpha' Q^2, \tag{2.115}$$

which reproduces the exact central charge of the coset Eqn. 2.92 when evaluated on Eqn. 2.110.

In the asymptotic region the CFT primary $\mathcal{O}_{jnw}$ may then be expanded in the free-field primaries $\mathcal{V}_{\alpha p_{\mathrm{L}} p_{\mathrm{R}}}$ [75]:

$$\mathcal{O}_{jnw} \overset{\hat{r}\to\infty}{\longrightarrow} \left(e^{-2Q(1-j)\hat{r}} + R(j,n,w)e^{-2Qj\hat{r}}\right) e^{ip_{\mathrm{L}}\hat{\theta}_{\mathrm{L}} + ip_{\mathrm{R}}\hat{\theta}_{\mathrm{R}}}. \tag{2.116}$$

p_{L} and p_{R} are as in Eqn. 2.112; namely, the operator labels n and $-w$ correspond to the momentum and winding numbers around the asymptotic cylinder. j is meanwhile related to

the asymptotic linear-dilaton momentum. $R(j,n,w)$ is the reflection coefficient [44–46]:

$$R(j,n,w) = (\nu(k))^{2j-1}\frac{\Gamma\left(1-\frac{2j-1}{k-2}\right)}{\Gamma\left(1+\frac{2j-1}{k-2}\right)} \times 4^{2j-1}\frac{\Gamma(1-2j)}{\Gamma(2j-1)}\frac{\Gamma\left(j+\frac{|n|-kw}{2}\right)\Gamma\left(j+\frac{|n|+kw}{2}\right)}{\Gamma\left(1-j+\frac{|n|-kw}{2}\right)\Gamma\left(1-j+\frac{|n|+kw}{2}\right)}. \tag{2.117}$$

Semi-classically, as in Liouville, R is the amplitude for a string sent from the weak-coupling region to reflect and return to infinity. As an abstract CFT quantity, it characterizes a redundancy in the space of CFT operators $\mathcal{O}_{jnw}$ when analytically continued to the complex j-plane: operators labeled by j and $1-j$ are identical, up to rescaling by the reflection coefficient. To avoid double-counting operators, one restricts the domain to $\mathrm{Re}(j) > \frac{1}{2}$ or $j \in \frac{1}{2} + i\mathbb{R}_+$ as in Eqn. 2.106.

R satisfies $R(1-j,n,w)R(j,n,w) = 1$. $\nu(k)$ is a j-independent function, analogous to the prefactor $\pi\mu\Gamma(b_{\mathrm{L}}^2)/\Gamma(1-b_{\mathrm{L}}^2)$ appearing in the Liouville reflection coefficient Eqn. 2.53. We will set it to one in what follows.

As recalled at the end of Sec. 2.1, the zero-mode wavefunction for the state prepared by inserting $\mathcal{O}_{jnw}$ in the far past on the cylinder is obtained after rescaling by $e^{-\Phi} = e^{-\Phi_0}\cosh(r)$. For large r, the radial wavefunction is then

$$\Psi_{jnw}(\hat{r}) \overset{\hat{r}\to\infty}{\longrightarrow} \frac{1}{2}e^{-\Phi_0}\left(e^{2Q\left(j-\frac{1}{2}\right)\hat{r}} + R(j,n,w)e^{-2Q\left(j-\frac{1}{2}\right)\hat{r}}\right). \tag{2.118}$$

With $j \in \frac{1}{2}+i\mathbb{R}$, neither exponential dominates the other, the asymptotic radial wavefunction

is oscillatory, and one obtains a delta-function normalizable state. These are the scattering states of Eqn. 2.106a, the two terms in the asymptotic wavefunction describing the incoming and reflected waves at infinity. The asymptotic operator is identified with the linear-dilaton primary $e^{-2\alpha\hat{r}}$ with $\alpha = Q(1-j)$ plus its reflection $e^{-2(Q-\alpha)\hat{r}}$, together with the compact-boson primary of momentum n and winding $-w$. The corresponding free-field weights (Eqn. 2.114), which are invariant under $\alpha \to Q - \alpha$, reproduce the exact weights (Eqn. 2.107).

Away from the complex branch, the first exponential in Eqns. 2.116 and 2.118 dominates the second for $\mathrm{Re}(j) > \frac{1}{2}$. Then, generically, the operator approaches $\mathcal{V}_{\alpha p_{\mathrm{L}} p_{\mathrm{R}}}$ with $\alpha = Q(1-j)$ at weak coupling, the wavefunction diverges exponentially, and the associated state is non-normalizable.

There is an important exception, however, when $R(j,n,w)$ is singular, and this is the manifestation of the bound states. Indeed, on the real branch with $j = j_N$ given by Eqn. 2.106b, one of the two Gamma functions $\Gamma\left(j + \frac{|n| \pm kw}{2}\right)$ in Eqn. 2.117 has a simple pole, depending on the sign of w. For $w > 0$ one has

$$j_N + \frac{|n| - kw}{2} = -N \tag{2.119}$$

and therefore

$$\Gamma\left(j + \frac{|n| - kw}{2}\right) \overset{j \to j_N}{\longrightarrow} \frac{1}{j - j_N} \frac{(-)^N}{N!} + \mathcal{O}(1). \tag{2.120}$$

$\Gamma\left(j_N + \frac{|n| + kw}{2}\right)$ is similarly singular for $w < 0$. The remaining Gamma functions have

additional singularities, but they are not associated to bound states [78].

Thus, for $j = j_N$, it is the reflected component $R(j_N, n, w)e^{-2Qj_N\hat{r}}$ that dominates in the asymptotic region. One obtains a discrete set of operators $\tilde{\mathcal{O}}_{j_N nw}$ defined as the residue of $\mathcal{O}_{jnw}$ as $j \to j_N$ [78]. The zero-mode radial wavefunction decays in the weak-coupling region, corresponding to a normalizable bound state with wavefunction proportional to

$$\Psi_{j_N nw}(\hat{r}_0) \overset{\hat{r}_0\to\infty}{\underset{\propto}{\longrightarrow}} e^{-2Q\left(j_N-\frac{1}{2}\right)\hat{r}_0}. \tag{2.121}$$

In this way, one finds a discrete spectrum of normalizable bound states on Eqn. 2.106b, the lower bound $j_N > \frac{1}{2}$ ensuring the wavefunction decays at infinity.

The simplest bound states have $n = 0$, $w = \mp 1$, and $j = \frac{k}{2} - 1$, which satisfies the upper bound $j < \frac{k-1}{2}$ automatically, and satisfies the lower bound $j > \frac{1}{2}$ for $k > 3$. The asymptotic form of these operators, which we will denote by $\mathcal{W}_\pm$, is

$$\mathcal{W}_\pm \equiv \frac{1}{R}\mathcal{O}_{j=\frac{k}{2}-1,n=0,w=\mp 1} \overset{\hat{r}\to\infty}{\longrightarrow} e^{-\sqrt{\frac{k-2}{\alpha'}}\hat{r}}e^{\pm i\sqrt{\frac{k}{\alpha'}}(\hat{\theta}_{\rm L}-\hat{\theta}_{\rm R})}, \tag{2.122}$$

with radial wavefunction $\Psi_\pm(\hat{r}) \to e^{-Q(k-3)\hat{r}}$. Their sum,

$$\mathcal{O}_{\rm sL} \equiv \mathcal{W}_+ + \mathcal{W}_-, \tag{2.123}$$

is called the sine-Liouville operator [79], and will be important in what follows. It is of conformal weight $(1, 1)$, and one may therefore consider the effect of deforming the CFT by this operator, which we will take up in Sec. 4.4. The wavefunction is normalizable for $k > 3$,

consistent with the lower bound $j > \frac{1}{2}$. For $k < 3$, on the other hand, $j = \frac{k}{2} - 1$ falls below $\frac{1}{2}$, and the wavefunction becomes non-normalizable.

2.3.4 Asymptotic Conditions

The equations of motion following from the action Eqn. 2.98 are

$$\nabla^2 r - \tanh(r)\mathrm{sech}^2(r)(\nabla\theta)^2 + \frac{1}{2k}\mathcal{R}[h]\tanh(r) = 0 \tag{2.124a}$$

$$\nabla^2\theta + 2\mathrm{sech}(r)\mathrm{csch}(r)h^{ab}\nabla_a r\nabla_b\theta = 0. \tag{2.124b}$$

As in the free linear dilaton and Liouville, the curvature coupling contributes source terms on a worldsheet with the plane or cylinder metric. Focusing on the cylinder, the radial equation of motion in the absence of any insertions becomes

$$\partial\bar{\partial}r - \tanh(r)\mathrm{sech}^2(r)\partial\theta\bar{\partial}\theta = -\frac{\pi}{k}\left(\delta(z,\bar{z}) + \delta(z - z_\infty, \bar{z} - \bar{z}_\infty)\right)\tanh(r). \tag{2.125}$$

At large r, we recover the free linear-dilaton equation of motion (Eqn. 2.24),

$$\partial\bar{\partial}\hat{r} = -\pi\alpha' Q\left(\delta(z,\bar{z}) + \delta(z - z_\infty, \bar{z} - \bar{z}_\infty)\right), \tag{2.126}$$

with Green functions

$$\hat{r}(\rho,\phi) \overset{\rho\to\pm\infty}{\longrightarrow} \pm\alpha' Q\rho + \mathcal{O}(1). \tag{2.127}$$

These free Green functions are self-consistent solutions of the full cigar equations of motion in the neighborhood of the source terms because the ends of the cylinder are mapped to the asymptotic region, where the corrections to the linear-dilaton $\times$ S^1 equations of motion are exponentially sub-leading. Then just as before we may write a regulated action for the cigar on a cylinder worldsheet with linear boundary terms at its ends:

$$\begin{aligned} S =& \frac{k}{4\pi} \int_{-L}^{L} \mathrm{d}\rho \int_{0}^{2\pi} \mathrm{d}\phi \, \left((\partial_\rho r)^2 + (\partial_\phi r)^2 + \tanh^2(r) \left((\partial_\rho \theta)^2 + (\partial_\phi \theta)^2 \right) \right) \\ & - \int_{0}^{2\pi} \frac{\mathrm{d}\phi}{2\pi} \left(r|_{\rho=L} + r|_{\rho=-L} \right) + \frac{L}{k}. \end{aligned} \tag{2.128}$$

Next consider the equations of motion in the neighborhood of an insertion $\mathcal{O}_{jnw}(z', \bar{z}')$ away from the curvature singularities. Suppose $\mathrm{Re}(j) > \frac{1}{2}$, with $R(j, n, w)$ regular, such that the operator is dominated by $\mathcal{V}_{Q(1-j),p_\mathrm{L},p_\mathrm{R}}(z', \bar{z}')$ at large $\hat{r}$. The Green functions of the asymptotic linear-dilaton $\times$ S^1 background in the presence of this source are

$$\hat{r}(z, \bar{z}) \overset{|z-z'|\to 0}{\longrightarrow} 2\alpha' Q(1-j) \log|z - z'| + \mathcal{O}(1) \tag{2.129a}$$

$$\hat{\theta}(z, \bar{z}) \overset{|z-z'|\to 0}{\longrightarrow} -\frac{i}{2}\sqrt{\frac{\alpha'}{k}} \left(2n \log|z - z'| - kw \log \frac{z - z'}{\bar{z} - \bar{z}'} \right) + \mathcal{O}(1). \tag{2.129b}$$

Suppose furthermore that $\mathrm{Re}(j) > 1$. Then the neighborhood of the insertion is mapped to $\hat{r} \to \infty$, and once again one obtains a self-consistent solution of the cigar equations of motion.

By contrast, if $j = j_N$, such that $R(j, n, w)$ is singular and the operator approaches $\mathcal{V}_{Qj,p_\mathrm{L}p_\mathrm{R}}$ at large $\hat{r}$, then the free radial Green function in the neighborhood of the (appro-

priately normalized) operator insertion is

$$\hat{r}(z,\bar{z}) \overset{|z-z'|\to 0}{\longrightarrow} 2\alpha' Q j \log|z-z'| + \mathcal{O}(1). \tag{2.130}$$

In this case, even if $\hat{r}$ begins in the asymptotic region, as one approaches the insertion point on the worldsheet $\hat{r}$ is mapped out of the free-field region, and one no longer has a self-consistent solution.

Away from these discrete values, however, the appropriate asymptotic conditions are obtained from the free-field Green functions, and correlation functions with bound state insertions may be obtained by computing the functional integral for generic j and then taking the residue of the result as $j \to j_N$. It is nevertheless interesting to identify an asymptotic condition that describes a bound state insertion directly, rather than as the residue of an ordinary insertion. We return to this problem in Sec. 4.4.1.

If a generic operator is inserted in the far past on the cylinder, then the asymptotic conditions including the effect of the background charge are

$$\hat{r}(\rho,\phi) \overset{\rho\to-\infty}{\longrightarrow} -2\alpha' Q\left(j-\frac{1}{2}\right)\rho + \mathcal{O}(1) \tag{2.131a}$$

$$\hat{\theta}(\rho,\phi) \overset{\rho\to-\infty}{\longrightarrow} -i\sqrt{\frac{\alpha'}{k}}\,(n\rho - ikw\phi) + \mathcal{O}(1). \tag{2.131b}$$

For $\mathrm{Re}(j) > \frac{1}{2}$, the solution is consistent. A complex branch operator may be similarly described by perturbing $j \to j+\varepsilon$ by a small positive regulator.

The ρ dependence of the asymptotic conditions may be enforced as before by linear

boundary terms. The ϕ dependence of $\hat{\theta}$, on the other hand, may be implemented using Lagrange multipliers $\sigma_\pm$. For example, the regulated action for the two-point function of $\mathcal{O}_{jnw}$ and $\mathcal{O}_{j,-n,-w}$ is given by

$$\begin{aligned} S_{jnw} =& \frac{k}{4\pi}\int_{-L}^{L}\mathrm{d}\rho\int_{0}^{2\pi}\mathrm{d}\phi\left((\partial_\rho r)^2+(\partial_\phi r)^2+\tanh^2(r)\left((\partial_\rho\theta)^2+(\partial_\phi\theta)^2\right)\right) \\ &+2\left(\frac{1}{2}-j\right)\int_0^{2\pi}\frac{\mathrm{d}\phi}{2\pi}\left(r|_{\rho=L}+r|_{\rho=-L}\right)+in\int_0^{2\pi}\frac{\mathrm{d}\phi}{2\pi}\left(\theta|_{\rho=L}-\theta|_{\rho=-L}\right) \\ &+k\int_0^{2\pi}\frac{\mathrm{d}\phi}{2\pi}\left(\sigma_+\left(\partial_\phi\theta|_{\rho=L}+w\right)+\sigma_-\left(\partial_\phi\theta|_{\rho=-L}+w\right)\right) \\ &+4\frac{L}{k}\left(j-\frac{1}{2}\right)^2-kw^2L-\frac{L}{k}n^2. \end{aligned} \tag{2.132}$$

Note that the imaginary boundary term for the momentum mode of θ ensures invariance of $e^{-S_{jnw}}$ under $\theta\sim\theta+2\pi$, where $n\in\mathbb{Z}$.

The boundary equations of motion obtained by varying r and $\sigma_\pm$ are

$$\partial_\rho r|_{\rho=\pm L}=\pm\frac{2}{k}\left(j-\frac{1}{2}\right) \tag{2.133a}$$

$$\partial_\phi\theta|_{\rho=\pm L}=-w, \tag{2.133b}$$

while the variation of θ gives

$$\pm\,\partial_\phi\sigma_\pm|_{\rho=\pm L}=\frac{in}{k}+\tanh^2(r)\partial_\rho\theta|_{\rho=\pm L}. \tag{2.134}$$

In the large L limit, Eqn. 2.133a implies the asymptotic condition

$$r \overset{\rho\to\pm\infty}{\longrightarrow} \pm\frac{2}{k}\left(j-\frac{1}{2}\right)\rho, \tag{2.135}$$

as in Eqn. 2.131a. Eqn. 2.133b requires that $\theta \to -w\phi+\theta_0(\rho)$, where $\theta_0(\rho)$ is the zero-mode in the Fourier expansion of $\theta(\rho,\phi)$ around the ϕ circle. This zero-mode is meanwhile fixed by the integral of Eqn. 2.134,

$$\int_0^{2\pi} \mathrm{d}\phi\, \tanh^2(r)\partial_\rho\theta|_{\rho=\pm\infty} = -\frac{2\pi i n}{k}. \tag{2.136}$$

Note that $\tanh^2(r)|_{\rho=\pm\infty}$ goes to one in large L limit. The asymptotic condition on θ is then

$$\theta \overset{\rho\to\pm\infty}{\longrightarrow} -i\frac{n}{k}\rho - w\phi, \tag{2.137}$$

reproducing Eqn. 2.131b.

In other words, Eqn. 2.133b is a Dirichlet condition that requires the non-zero-modes of θ to vanish at the boundaries, while the integral of Eqn. 2.134 is a Neumann condition on the zero-mode. One solves the bulk equations of motion with these boundary conditions, together with the Neumann condition Eqn. 2.133a on r. The Lagrange multipliers are then determined by Eqn. 2.134 up to a zero-mode, which we discard.

The functional integral weighted by $e^{-S_{jnw}}$ computes the reflection coefficient $R(j,n,w)$ in the $L\to\infty$ limit. In the next section, we compute the saddle-point expansion of this integral, restricted to the pure-winding sector for simplicity, and show that there exists a set

of saddles that reproduces the semi-classical limit of the exact reflection coefficient.

2.4 Cigar Reflection in the Semi-Classical Limit

In this section we compute the semi-classical limit of the cigar reflection coefficient by a saddle-point expansion and compare to the large k limit of the exact reflection coefficient (Eqn. 2.117). As in the analogous calculation for Liouville (Sec. 2.2), doing so requires summing over complex saddles, even for real branch operators. We will also find that saddles which hit the black hole singularity contribute to the saddle-point expansion with finite action, and are important for recovering the real branch bound states.

As reviewed in the previous section, the exact reflection coefficient $R(j,n,w)$ of the $\mathrm{SL}(2,\mathbb{R})_k/\mathrm{U}(1)$ CFT is known thanks to work on the $\mathrm{SL}(2,\mathbb{R})_k$ WZW model (and its Euclidean continuation $\mathrm{SL}(2,\mathbb{C})_k/\mathrm{SU}(2)$), and its relation to $\mathrm{SL}(2,\mathbb{R})_k/\mathrm{U}(1)$ via the coset construction [44–46]. $R(j,n,w)$ defines the normalization of the two-point function of the coset primaries $\mathcal{O}_{jnw}$ and $\mathcal{O}_{j,-n,-w}$, with the operator normalization chosen in Eqn. 2.116. Physically, it is the amplitude for a string sent from the weak-coupling region to reflect off the tip of the cigar.

We will focus for simplicity on the pure-winding sector, where $n=0$. Then Eqn. 2.117 simplifies to

$$R(j,w) = 4^{2j-1}\frac{k-2}{\gamma\left(\frac{2j-1}{k-2}\right)}\frac{1}{\gamma(2j)}\gamma\left(j+\frac{1}{2}kw\right)\gamma\left(j-\frac{1}{2}kw\right), \tag{2.138}$$

where $\gamma(z) \equiv \Gamma(z)/\Gamma(1-z)$.

The cigar-sigma model description of the CFT is weakly coupled for large k, and our goal in this section is to compute $R(j,w)$ by a saddle-point expansion in the $k \to \infty$ limit. In order to compare with the same limit of the exact result, let us first determine the large k asymptotics of Eqn. 2.138. To do so, we must first decide how j scales with k. As in the Liouville discussion, we will restrict our attention to heavy operators, whose insertions contribute at the same order in k as the leading terms in the action. We therefore define

$$j = \frac{k\eta}{2}, \tag{2.139}$$

with $\eta = \mathcal{O}(k^0)$. Imposing $\mathrm{Re}(j) > \frac{1}{2}$ requires $\mathrm{Re}(\eta) > \frac{1}{k}$, which relaxes to $\mathrm{Re}(\eta) > 0$ in the large k limit.

Using the gamma function asymptotics Eqns. 2.69-2.70, and assuming without loss of generality that $w > 0$, we obtain

$$\begin{aligned} R(\eta,w) \overset{k\to\infty}{\longrightarrow} & \eta^{-2k\eta}(w+\eta)^{k(w+\eta)} \csc(\pi k\eta) \sin\left(\frac{\pi}{2}k(w+\eta)\right) \\ & \times \begin{cases} \frac{1}{2}(w-\eta)^{k(\eta-w)} \csc\left(\frac{\pi}{2}k(w-\eta)\right) & 0 < \mathrm{Re}(\eta) < w \\ 2(\eta-w)^{k(\eta-w)} \sin\left(\frac{\pi}{2}k(\eta-w)\right) & \mathrm{Re}(\eta) > w \end{cases} \\ & \times \frac{\eta}{(\eta^2-w^2)\gamma(\eta)}. \end{aligned} \tag{2.140}$$

We have kept terms to order k^0 in the exponent. Note that the bound states now correspond to the poles of $\csc\left(\frac{\pi}{2}k(w-\eta)\right)$ at $\eta_N = w - \frac{2N}{k}$. When we compute the saddle-point

expansion, we expect the contribution $\sum e^{-S+\mathcal{O}(k^0)}$ from the order k action evaluated on its saddles to reproduce the first two lines. The last line is order e^{k^0}, which we expect to arise from the fluctuation determinant, as well as the order k^0 corrections to the on-shell action.[27]

The reflection coefficient is computed by the functional integral

$$R(\eta, w) = \int_{\mathcal{C}(\eta)} \mathrm{D}r\mathrm{D}\theta\mathrm{D}\sigma_{\pm}\, e^{-k\tilde{S}_{jw}}, \tag{2.141}$$

with action $k\tilde{S}_{jw} \equiv S_{j,0,w}$ (c.f. Eqn. 2.132):

$$\begin{aligned}\tilde{S}_{jw} =& \frac{1}{4\pi}\int_{-L}^{L}\mathrm{d}\rho\int_{0}^{2\pi}\mathrm{d}\phi\left((\partial_\rho r)^2+(\partial_\phi r)^2+\tanh^2(r)\left((\partial_\rho\theta)^2+(\partial_\phi\theta)^2\right)\right)\\ &-\left(\eta-\frac{1}{k}\right)\int_0^{2\pi}\frac{\mathrm{d}\phi}{2\pi}\left(r|_{\rho=L}+r|_{\rho=-L}\right)+L\left(\eta-1/k\right)^2-w^2L\\ &+\int_0^{2\pi}\frac{\mathrm{d}\phi}{2\pi}\left(\sigma_+\left(\partial_\phi\theta|_{\rho=L}+w\right)+\sigma_-\left(\partial_\phi\theta|_{\rho=-L}+w\right)\right).\end{aligned} \tag{2.142}$$

As discussed in the previous sub-section, the maps r and $\theta \sim \theta + 2\pi$ are defined on a worldsheet cylinder $[-L, L] \times \mathrm{S}^1$ whose length $2L$ is taken to infinity. In this limit, the boundary terms insert the operators $\mathcal{O}_{j=\frac{k\eta}{2},n=0,\pm w}$, as well as the background-charge contributions, on opposite ends of the cylinder, and the functional integral computes the reflection

[27] It has been suggested that the cigar sigma-model is supplemented even at large k by a potential that modifies the background in the neighborhood of the tip [80–82]. It would be interesting to see if the third line of Eqn. 2.140, in particular the factor of $\gamma(\eta)$ which originated in the factor of $\gamma\left(\frac{2j-1}{k-2}\right)$ in Eqn. 2.138, is correctly reproduced by the 1-loop calculation in the pure cigar background. We have not attempted to compute this determinant, however. As mentioned in Sec. 2.2.3, an analogous non-perturbative correction has been proposed in the Liouville background, but recent work [74] has argued that no such modifications are present.

coefficient. In the $k \to \infty$ limit, we would like to evaluate this integral by a saddle-point expansion

$$R(\eta, w) \overset{k\to\infty}{\longrightarrow} \sum_{r_i,\theta_i} e^{-k\tilde{S}_{jw}+\mathcal{O}(k^0)}, \tag{2.143}$$

where $\{r_i, \theta_i\}$ are a subset of solutions of the equations of motion

$$(\partial_\rho^2 + \partial_\phi^2)r - \tanh(r)\mathrm{sech}^2(r)\left((\partial_\rho\theta)^2 + (\partial_\phi\theta)^2\right) = 0 \tag{2.144a}$$

$$(\partial_\rho^2 + \partial_\phi^2)\theta + 2\mathrm{sech}(r)\mathrm{csch}(r)\left(\partial_\rho r\partial_\rho\theta + \partial_\phi r\partial_\phi\theta\right) = 0 \tag{2.144b}$$

in the bulk and

$$\partial_\rho r|_{\rho=\pm L} = \pm\eta \tag{2.145a}$$

$$\partial_\phi\theta|_{\rho=\pm L} = -w \tag{2.145b}$$

$$\int_0^{2\pi} \mathrm{d}\phi\ \tanh^2(r)\partial_\rho\theta|_{\rho=\pm L} = 0 \tag{2.145c}$$

on the boundaries.[28] We have discarded here the contributions from the $\mathcal{O}(k^{-1})$ terms in $\tilde{S}_{jw}$, which contribute to the order one corrections to the saddle-point expansion.

In the limit $L \to \infty$, the boundary equations of motion for r impose the asymptotic

[28] As explained in the previous sub-section, the Lagrange multipliers are then determined on-shell from $\partial_\phi\sigma_\pm = \pm\tanh^2(r)\partial_\rho\theta|_{\rho=\pm L}$ up to a ϕ zero-mode, which we discard. Evaluated on $\theta = -w\phi$, one obtains $\partial_\phi\sigma_\pm = 0$, and we then gauge-fix $\sigma_\pm = 0$.

conditions

$$r \overset{\rho\to\pm\infty}{\longrightarrow} \pm\eta\rho + a_\pm, \tag{2.146}$$

which sends r to the weak-coupling region since $\mathrm{Re}(\eta) > 0$. The integration constants $a_\pm$ are sub-leading, but control the asymptotic separation $r(\infty) - r(-\infty) = a_+ - a_-$.

Applying Eqn. 2.146 in the boundary θ equations of motion allows us to discard the factor of $\tanh^2(r)$ in the large L limit. Then these equations imply the asymptotic condition

$$\theta \overset{\rho\to\pm\infty}{\longrightarrow} -w\phi, \tag{2.147}$$

which demands that θ have winding $-w$ around the ends of the cylinder. The simplest solution sets $\theta = -w\phi$ everywhere, on which the equations of motion reduce to

$$\partial_\rho^2 r - w^2 \tanh(r)\mathrm{sech}^2(r) = 0 \tag{2.148a}$$

$$\partial_\phi r = 0 \tag{2.148b}$$

$$\partial_\rho r|_{\rho=\pm L} = \pm\eta. \tag{2.148c}$$

Thus, in this pure-winding sector the theory reduces to a quantum mechanics problem for $r(\rho)$ with action

$$\tilde{S}[r] = \int_{-L}^{L} \mathrm{d}\rho \left(\frac{1}{2} \left(\frac{\mathrm{d}r}{\mathrm{d}\rho} \right)^2 + V(r) \right) - \eta(r(L) + r(-L)) + \eta^2 L, \tag{2.149}$$

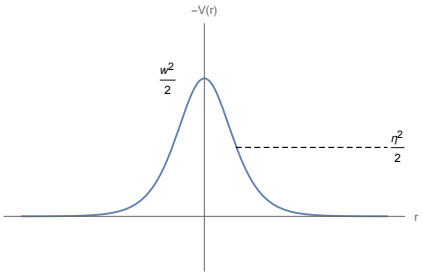

Figure 2.6: Inverted Potential. Restricted to a pure-winding solution $\theta = -w\phi$, the cigar equations of motion describe the mechanics of a particle moving in the inverted potential shown. For η real and less than w, there is a real solution that describes a particle that comes in from $r \to \infty$, rolls partway up the potential hill until it stops at the turning point, and then rolls back out to infinity. The cigar geometry is defined for $r \geq 0$, but to compute the saddle-point expansion of the functional integral we will continue r to the complex plane. Here we draw the potential for the real r slice.

where

$$V(r) = -\frac{1}{2}w^2 \mathrm{sech}^2(r). \tag{2.150}$$

The bulk equation of motion Eqn. 2.148a may be written

$$\frac{\mathrm{d}^2 r}{\mathrm{d}\rho^2} = V'(r), \tag{2.151}$$

describing the mechanics of a particle in the inverted potential $-V(r)$, pictured in Fig. 2.6.

The quantum mechanics of a particle in this potential can in fact be solved exactly, as we review in the next sub-section. We will show that the semi-classical limit of the exact reflection coefficient for the quantum mechanics reproduces that of the CFT at order e^k. We conclude that the saddles with $\theta(\phi) = -w\phi$ and $r = r(\rho)$ are sufficient for reproducing the saddle-point expansion of the coset reflection coefficient, and we do not need to consider more complicated solutions $\theta(\rho, \phi)$ and $r(\rho, \phi)$. Then in the following sub-section we proceed with the saddle-point expansion using these pure-winding configurations.

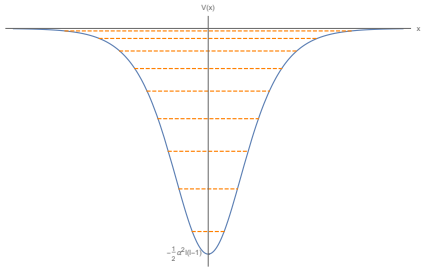

Figure 2.7: The Cigar Quantum Mechanics Potential. The potential for the quantum mechanics that describes the pure-winding sector of the cigar is a well, sometimes called the modified Pöschl-Teller potential.

2.4.1 Quantum Mechanics on the Cigar

The quantum mechanics of a particle in the potential Eqn. 2.150 is exactly solvable.[29] In the literature the potential is usually written in the form

$$V(x) = -\frac{1}{2}\alpha^2 l(l-1)\mathrm{sech}^2(\alpha x). \tag{2.152}$$

with $\alpha > 0$ and $l > 1$. It is a symmetric well of depth $\frac{1}{2}\alpha^2 l(l-1)$, and it vanishes as $x \to \pm\infty$ (Fig. 2.7). It therefore admits both bound states and scattering states. To begin we consider the quantum mechanics on an infinite line, $x \in \mathbb{R}$. The cigar is related to its Z_2 quotient $x \sim -x$.

Consider first the scattering states. We look for solutions of

$$-\frac{1}{2}\psi''(x) + V(x)\psi(x) = \frac{p^2}{2}\psi(x), \tag{2.153}$$

[29] See, for example, Landau and Lifshitz's Quantum Mechanics (Second Edition), Sections 23 and 25. We set $\hbar$ and the mass to one. The potential is often referred to as the modified Pöschl-Teller potential.

behaving asymptotically as

$$\psi(x) \to \begin{cases} e^{ipx} + R(p)e^{-ipx} & x \to -\infty \\ T(p)e^{ipx} & x \to \infty. \end{cases} \tag{2.154}$$

The two linearly independent solutions of this equation are the associated Legendre polynomials $P_{l-1}^{ip/\alpha}(\tanh(\alpha x))$ and $Q_{l-1}^{ip/\alpha}(\tanh(\alpha x))$. The asymptotics of the P function are

$$\begin{aligned} &P_{l-1}^{ip/\alpha}(\tanh(\alpha x)) \\ &\to \begin{cases} \dfrac{i\pi \operatorname{csch}\left(\frac{\pi p}{\alpha}\right)}{\Gamma\left(1+\frac{ip}{\alpha}\right)\Gamma\left(l-\frac{ip}{\alpha}\right)\Gamma\left(1-l-\frac{ip}{\alpha}\right)} e^{ipx} - \dfrac{i\sin(\pi l)\operatorname{csch}\left(\frac{\pi p}{\alpha}\right)}{\Gamma\left(1-\frac{ip}{\alpha}\right)} e^{-ipx} & x \to -\infty \\ \dfrac{1}{\Gamma\left(1-\frac{ip}{\alpha}\right)} e^{ipx} & x \to \infty. \end{cases} \end{aligned} \tag{2.155}$$

The asymptotics of the Q function, on the other hand, contain e^{ipx} and e^{-ipx} at both limits, and must be discarded.

The normalized scattering wavefunction is then

$$\psi(x;p) = -\frac{i}{\pi}\sinh\left(\frac{\pi p}{\alpha}\right)\Gamma\left(1+\frac{ip}{\alpha}\right)\Gamma\left(l-\frac{ip}{\alpha}\right)\Gamma\left(1-l-\frac{ip}{\alpha}\right)P_{l-1}^{ip/\alpha}(\tanh(\alpha x)), \tag{2.156}$$

yielding the reflection and transmission coefficients

$$R(p) = -\frac{1}{\pi}\sin(\pi l)\frac{\Gamma\left(1+\frac{ip}{\alpha}\right)}{\Gamma\left(1-\frac{ip}{\alpha}\right)}\Gamma\left(l-\frac{ip}{\alpha}\right)\Gamma\left(1-l-\frac{ip}{\alpha}\right) \tag{2.157}$$

and

$$T(p) = -\frac{i}{\pi}\sinh\left(\frac{\pi p}{\alpha}\right)\frac{\Gamma\left(1+\frac{ip}{\alpha}\right)}{\Gamma\left(1-\frac{ip}{\alpha}\right)}\Gamma\left(l-\frac{ip}{\alpha}\right)\Gamma\left(1-l-\frac{ip}{\alpha}\right). \tag{2.158}$$

Note this potential has the remarkable property that it is reflectionless when l is an integer; $R(p)$ vanishes due to the factor of $\sin(\pi l)$. In that case, the transmission coefficient may be written

$$T(p)\Big|_{l\in\mathbb{Z}} = \prod_{n=1}^{l-1}\frac{l-n-\frac{ip}{\alpha}}{n-l-\frac{ip}{\alpha}} \tag{2.159}$$

by repeatedly applying the factorial property of the Gamma function, $\Gamma(z+1) = z\Gamma(z)$. In particular, $T(p)$ is a pure phase,

$$|T(p)|^2\Big|_{l\in\mathbb{Z}} = \prod_{n=1}^{l-1}\frac{(l-n)^2+\frac{p^2}{\alpha^2}}{(n-l)^2+\frac{p^2}{\alpha^2}} = 1, \tag{2.160}$$

as required by probability conservation, $|R|^2 + |T|^2 = 1$.

Meanwhile, the bound states are solutions of

$$-\frac{1}{2}\psi''(x) + V(x)\psi(x) = E\psi(x), \tag{2.161}$$

with $-\frac{1}{2}\alpha^2 l(l-1) < E < 0$. They may be obtained from the scattering solutions by continuing $p = i\sqrt{2|E|} \in i\mathbb{R}_+$, so that $\psi(x; i\sqrt{2|E|}) \overset{x\to\infty}{\longrightarrow} Te^{-\sqrt{2|E|}x}$ decays. As $x \to -\infty$,

$$\psi(x; i\sqrt{2|E|}) \overset{x\to-\infty}{\longrightarrow} e^{-\sqrt{2|E|}x} + Re^{\sqrt{2|E|}x}, \tag{2.162}$$

which generically diverges, unless $p = i\sqrt{2|E|}$ is such that R has a pole. At those discrete points, one may hope to find a normalizable bound state proportional to $\frac{1}{R}\psi(x; i\sqrt{2|E|})$.

$R(p)$ has three sets of simple poles due to the three Gamma functions in its numerator. The first, $\Gamma\left(1 + \frac{ip}{\alpha}\right)$, has poles for $p = i\alpha(n+1)$, with n a natural number. These do not correspond to bound states, however, because in the $x \to -\infty$ limit of the P function it is the ratio $\mathrm{csch}\left(\frac{\pi p}{\alpha}\right)/\Gamma\left(1 + \frac{ip}{\alpha}\right)$ that appears, which is regular. The second Gamma function in $R(p)$, $\Gamma\left(l - \frac{ip}{\alpha}\right)$, has poles for $p = -i\alpha(l+n)$, but these do not belong to the domain $i\mathbb{R}_+$, which was necessary for convergence at large x.

It is instead the last Gamma function which is responsible for the bound states, $\Gamma\left(1 - l - \frac{ip}{\alpha}\right)$. The poles are found at

$$p_n = i\alpha(l - 1 - n), \tag{2.163}$$

which belong to $i\mathbb{R}_+$ provided $n < l - 1$. Thus we find the spectrum of bound state energies

$$E_n = \frac{p_n^2}{2} = -\frac{\alpha^2}{2}(l - 1 - n), \quad 0 \leq n < l - 1, \tag{2.164}$$

with wavefunctions

$$\psi_n(x) = P_{l-1}^{-(l-1-n)}(\tanh(\alpha x)). \tag{2.165}$$

Next consider the semi-classical limit. Define

$$\tilde{x} \equiv \alpha x, \quad \tilde{l} \equiv \alpha^2 \sqrt{l(l-1)}, \tag{2.166}$$

in terms of which the Hamiltonian may be written

$$H = \frac{1}{\alpha^2}\left(\frac{1}{2}\left(\frac{\mathrm{d}\tilde{x}}{\mathrm{d}t}\right)^2 + \tilde{V}(\tilde{x})\right), \tag{2.167}$$

where

$$\tilde{V}(\tilde{x}) \equiv -\frac{1}{2}\tilde{l}^2 \mathrm{sech}^2(\tilde{x}). \tag{2.168}$$

Comparing to Eqn. 2.150, we find the same quantum mechanics as the pure-winding sector of the cigar CFT, with the dictionary $w = \tilde{l}$ and $k = \frac{1}{\alpha^2}$.

The semi-classical limit is $\alpha \to 0$ with $\tilde{l}$ fixed. In this limit the bound state spectrum is

$$E_n \to -\frac{\alpha^2}{2}\left(n - \frac{\tilde{l}}{\alpha^2}\right)^2. \tag{2.169}$$

The same semi-classical spectrum may be obtained from the WKB approximation, which says that

$$\int_{-x_*}^{x_*} \mathrm{d}x \sqrt{2(E_n - V(x))} = \pi n, \tag{2.170}$$

where

$$x_* = \frac{1}{\alpha}\cosh^{-1}\left(\sqrt{\frac{\frac{1}{2}\alpha^2 l(l-1)}{-E_n}}\right) \tag{2.171}$$

is the classical turning point, $V(\pm x_*) = E_n$. The integral is

$$\int_{-x_*}^{x_*} \mathrm{d}x\, \sqrt{2(E_n - V(x))} = \pi\left(\sqrt{l(l-1)} - \frac{1}{\alpha}\sqrt{-2E_n}\right), \tag{2.172}$$

from which we obtain

$$E_n \approx -\frac{\alpha^2}{2}\left(n - \sqrt{l(l-1)}\right)^2, \tag{2.173}$$

reproducing the semi-classical limit of the exact spectrum.

As for the scattering states, define

$$p \equiv i\frac{\eta}{\alpha}, \tag{2.174}$$

in terms of which the exact reflection and transmission coefficients may be written

$$R(\eta) = \frac{1}{\pi}\frac{\tilde{l}-\eta}{\eta}\frac{\sin(\pi k\tilde{l})}{\gamma(k\eta)}\Gamma(k(\tilde{l}+\eta))\Gamma(-k(\tilde{l}-\eta)) \tag{2.175}$$

and

$$T(\eta) = -\frac{1}{\pi}\frac{\tilde{l}-\eta}{\eta}\frac{\sin(\pi k\eta)}{\gamma(k\eta)}\Gamma(k(\tilde{l}+\eta))\Gamma(-k(\tilde{l}-\eta)), \tag{2.176}$$

where again $k \equiv \frac{1}{\alpha^2}$. Applying Eqns. 2.69-2.70 we find in the semi-classical limit

$$R(\eta) \overset{k\to\infty}{\longrightarrow} \eta^{-2k\eta}(\tilde{l}+\eta)^{k(\tilde{l}+\eta)} \sin(\pi k\tilde{l}) \csc(\pi k\eta) \tag{2.177}$$
$$\times \begin{cases} -\frac{1}{2}(\tilde{l}-\eta)^{k(\eta-\tilde{l})} \csc\left(\pi k(\tilde{l}-\eta)\right) & 0 < \mathrm{Re}(\eta) < \tilde{l} \\ -i(\eta-\tilde{l})^{k(\eta-\tilde{l})} & \mathrm{Re}(\eta) > \tilde{l} \end{cases}$$
$$\times \sqrt{\frac{\tilde{l}-\eta}{\tilde{l}+\eta}}$$

and

$$T(\eta) \overset{k\to\infty}{\longrightarrow} \eta^{-2k\eta}(\tilde{l}+\eta)^{k(\tilde{l}+\eta)} \tag{2.178}$$
$$\times \begin{cases} \frac{1}{2}(\tilde{l}-\eta)^{k(\eta-\tilde{l})} \csc\left(\pi k(\tilde{l}-\eta)\right) & 0 < \mathrm{Re}(\eta) < \tilde{l} \\ i(\eta-\tilde{l})^{k(\eta-\tilde{l})} & \mathrm{Re}(\eta) > \tilde{l} \end{cases}$$
$$\times \sqrt{\frac{\tilde{l}-\eta}{\tilde{l}+\eta}}.$$

The bound states now correspond to the poles of the $\csc(\pi k(\tilde{l}-\eta))$ factors.

So far we have considered the quantum mechanics on a fully-infinite line. However, the cigar quantum mechanics in Eqn. 2.149 obtained by setting $\theta = -w\phi$ was defined on a half-line. Returning to Eqn. 2.153, the scattering solutions on a half-line are now the linear

combinations of Legendre polynomials that vanish at the origin:

$$\begin{aligned}\psi_{1/2}(x;p) =& 2\frac{\Gamma\left(l-\frac{ip}{\alpha}\right)\Gamma\left(1-l-\frac{ip}{\alpha}\right)}{\Gamma\left(-\frac{ip}{\alpha}\right)}\cos^2\left(\frac{\pi}{2}\left(l+\frac{ip}{\alpha}\right)\right) \\ &\times\left(P_{l-1}^{ip/\alpha}(\tanh(\alpha x))-\frac{2}{\pi}\tan\left(\frac{\pi}{2}\left(l+\frac{ip}{\alpha}\right)\right)Q_{l-1}^{ip/\alpha}(\tanh(\alpha x))\right).\end{aligned} \tag{2.179}$$

They behave as

$$\psi_{1/2}(x;p) \overset{x\to-\infty}{\longrightarrow} e^{ipx}+R_{1/2}(p)e^{-ipx}, \tag{2.180}$$

where the reflection coefficient for the half-line problem is

$$\begin{aligned}R_{1/2}(p) =& 2\frac{\Gamma\left(l-\frac{ip}{\alpha}\right)\Gamma\left(1-l-\frac{ip}{\alpha}\right)}{\Gamma\left(1-\frac{ip}{\alpha}\right)\Gamma\left(-\frac{ip}{\alpha}\right)} \\ &\times\sin\left(\frac{\pi}{2}\left(l-\frac{ip}{\alpha}\right)\right)\cos\left(\frac{\pi}{2}\left(l+\frac{ip}{\alpha}\right)\right)\csc\left(\frac{\pi ip}{\alpha}\right).\end{aligned} \tag{2.181}$$

Alternatively, having already solved the theory on a line, the solution on the half-line is given by its quotient with respect to the reflection symmetry $x \sim -x$. The reflection coefficient $R_{1/2}(p)$ is then the difference of the reflection and transmission coefficients $R(p)$ and $T(p)$,

$$R_{1/2}(p) = R(p) - T(p), \tag{2.182}$$

as can be checked for Eqns. 2.157, 2.158, and 2.181, and the bound state spectrum is given

by the odd solutions

$$E_n = -\frac{\alpha^2}{2}(l-1-n)^2, \quad n = 1,3,5,\ldots < l-1. \tag{2.183}$$

Previously, we identified the bound states with the poles $p_n = i\alpha(l-1-n)$ of $\Gamma\left(1-l-\frac{ip}{\alpha}\right)$. Now we find

$$R_{1/2}(p_n) = \frac{\Gamma(2l-1-n)}{\Gamma(l-n)\Gamma(l-1-n)}\Gamma(-n)\left((-)^n-1\right). \tag{2.184}$$

Whereas $R(p_n) \supset \Gamma(-n)$ was singular for all $n = 0,1,2,\ldots$, the additional factor of $(-)^n - 1$ in $R_{1/2}(p_n)$ eliminates the poles with even n.

Finally, let us compute the semi-classical limit of $R_{1/2}$. With the same notation as before we may write

$$\begin{aligned} R_{1/2}(\eta) =& 2\frac{\tilde{l}-\eta}{\eta}\frac{\Gamma(k(\tilde{l}+\eta))\Gamma(-k(\tilde{l}-\eta))}{\Gamma(k\eta)^2} \\ &\times \sin\left(\frac{\pi}{2}k(\tilde{l}+\eta)\right)\cos\left(\frac{\pi}{2}k(\tilde{l}-\eta)\right)\csc(\pi k\eta). \end{aligned} \tag{2.185}$$

At large k we obtain

$$R_{1/2}(\eta) \overset{k\to\infty}{\longrightarrow} \eta^{-2k\eta}(\tilde{l}+\eta)^{k(\tilde{l}+\eta)} \csc(\pi k\eta) \sin\left(\frac{\pi}{2}k(\tilde{l}+\eta)\right) \tag{2.186}$$
$$\times \begin{cases} -\frac{1}{2}(\tilde{l}-\eta)^{k(\eta-\tilde{l})} \csc\left(\frac{\pi}{2}k(\tilde{l}-\eta)\right) & 0 < \mathrm{Re}(\eta) < \tilde{l} \\ -2i(\eta-\tilde{l})^{k(\eta-\tilde{l})} \cos\left(\frac{\pi}{2}k(\tilde{l}-\eta)\right) & \mathrm{Re}(\eta) > \tilde{l} \end{cases}$$
$$\times \sqrt{\frac{\tilde{l}-\eta}{\tilde{l}+\eta}}.$$

Compared to Eqn. 2.177, the factor of $\csc(\pi k(\tilde{l}-\eta))$ has been replaced by $\csc\left(\frac{\pi}{2}k(\tilde{l}-\eta)\right)$, reflecting the smaller set of bound states.

Looking back at the large k limit of the exact coset reflection coefficient Eqn. 2.140, we find agreement with Eqn. 2.186 to order e^k.[30] We conclude that the restriction to the cigar quantum mechanics $r = r(\rho), \theta = -w\phi$ is sufficient to extract the saddle-point expansion of the reflection coefficient, i.e. $\theta = -w\phi$ is the only saddle of the θ equations of motion that contributes to the expansion.

2.4.2 Complexified Quantum Mechanics

The saddle-point expansion of the coset reflection coefficient has thus reduced to a problem in the quantum mechanics defined by Eqn. 2.149. We wish to identify the appropriate set of solutions of this mechanics that reproduce the semi-classical limit of the exact reflection coefficient (Eqn. 2.140). As in Liouville, the relevant saddles will again be complex, even

[30] Note that the discrepancy between $\cos\left(\frac{\pi}{2}k(\tilde{l}-\eta)\right)$ and $\sin\left(\frac{\pi}{2}k(\tilde{l}-\eta)\right)$ is order e^{k^0}.

when η is real.

Moreover, in light of the abrupt change in Eqn. 2.140 across the line $\mathrm{Re}(\eta) = w$, we anticipate that a Stokes wall in the η-plane is found there. This is not unreasonable, since for η real and less than w there exists a real solution of the equations of motion describing a particle that comes in from $r \to \infty$, rolls partway up the potential until it stops at the turning point, and then rolls back out to infinity. For η greater than w, on the other hand, the particle rolls over the potential and continues to $r \to -\infty$ in the continued field space. At the crossover point, the particle has just enough energy to (asymptotically) reach the top of the hill.

Thus, in computing the saddle-point expansion we expect that we will need to address the domains for $0 < \mathrm{Re}(\eta) < w$ and $\mathrm{Re}(\eta) > w$ separately, and that we will find a different set of contributing saddles in each.

Once again we must specify the contour $\mathcal{C}(\eta)$ in field space along which the functional integral Eqn. 2.141 is to be performed. As in Liouville, even for real η the functional integral over real fields diverges. Repeating the same argument as lead to Eqn. 2.77, consider a finite-action configuration of $(r, \theta, \sigma_\pm)$. Now consider another configuration with $r \to r + a$ shifted by a large, positive real number. Then the action of the latter configuration is given by

$$\tilde{S}_{jw}[r+a] \stackrel{a\to\infty}{\longrightarrow} -2\eta a + \tilde{S}_{jw}[r] + \frac{1}{4\pi}\int \mathrm{d}\rho\,\mathrm{d}\phi\,\mathrm{sech}^2(r)(\nabla\theta)^2 + \mathcal{O}(e^{-2a}, k^{-1}). \tag{2.187}$$

Since $\mathrm{Re}(\eta) > 0$, by making a arbitrarily large the action may be made arbitrarily negative. Thus, the functional integral over real fields cannot converge.

Instead, $\mathcal{C}(\eta)$ must be chosen to be an appropriate complex cycle, which we take to be the sum of the steepest-descent contours that reproduce the correct semi-classical limit. Away from the Stokes walls, the steepest-descent contours themselves vary smoothly with η, as does $\mathcal{C}(\eta)$ in turn. As in the finite-dimensional case, even though the steepest-descent contours jump when η crosses a Stokes wall, $\mathcal{C}(\eta)$ is expected to vary smoothly. Its expansion as a sum of steepest-descent contours changes across the Stokes wall, but the summed contours on either side of the wall should be equivalent up to Cauchy deformation.

Since the original real coordinate $r \geq 0$ of Eqn. 2.149 was valued in a half-line, the relevant complexification is the complex r-plane quotiented by $r \sim -r$. Note that this is a symmetry of the potential Eqn. 2.150. Alternatively, one may compute the saddle-point expansion for the reflection and transmission coefficients of the quantum mechanics before the quotient, and then take their difference to obtain the reflection coefficient in the half-space as in Eqn. 2.182. This is the approach that we will take here. Thus, we regard the action $\tilde{S}[r]$ in Eqn. 2.149 as a holomorphic functional of maps $r\colon \mathbb{R} \to \mathbb{C}$ into the complex r-plane and identify its critical points.[31]

The semi-classical limits Eqns. 2.177- 2.178 of the reflection and transmission coefficients

[31] The transmission coefficient is computed similarly, but with $r(L)$ replaced by $-r(L)$ to fix the momentum at late times to $-\eta$ rather than η.

for the infinite-space quantum mechanics are, in the current notation,

$$R_{\mathrm{QM}}(\eta) \overset{k\to\infty}{\underset{\propto}{\longrightarrow}} \begin{cases} \eta^{-2k\eta}(w+\eta)^{k(w+\eta)}(w-\eta)^{k(\eta-w)} & 0 < \mathrm{Re}(\eta) < w \\ \quad \times \sin(\pi k w)\csc(\pi k\eta)\csc(\pi k(w-\eta)) & \\ \eta^{-2k\eta}(w+\eta)^{k(w+\eta)}(\eta-w)^{k(\eta-w)} & \mathrm{Re}(\eta) > w \\ \quad \times \sin(\pi k w)\csc(\pi k\eta) & \end{cases} \tag{2.188}$$

and

$$T_{\mathrm{QM}}(\eta) \overset{k\to\infty}{\underset{\propto}{\longrightarrow}} \begin{cases} \eta^{-2k\eta}(w+\eta)^{k(w+\eta)}(w-\eta)^{k(\eta-w)}\csc(\pi k(w-\eta)) & 0 < \mathrm{Re}(\eta) < w \\ \eta^{-2k\eta}(w+\eta)^{k(w+\eta)}(\eta-w)^{k(\eta-w)} & \mathrm{Re}(\eta) > w. \end{cases} \tag{2.189}$$

Their difference reproduces the cigar reflection coefficient at order e^k. Thus, our task is reduced to reproducing Eqns. 2.188 and 2.189 by saddle-point expansions for the infinite-space quantum mechanics.

The bulk equation of motion Eqn. 2.151 describes a particle moving in an inverted potential $-V(r)$. One therefore obtains the energy conservation equation,

$$\frac{1}{2}\dot{r}^2 - V(r) = \frac{\eta^2}{2}, \tag{2.190}$$

where $\dot{r} = \frac{\mathrm{d}r}{\mathrm{d}\rho}$. The conserved energy is indeed $\frac{\eta^2}{2}$, as is clear by evaluating the equation at $\rho \to \pm\infty$ and imposing the asymptotic conditions.

Observe that, as a holomorphic function on the complex r-plane, the potential is periodic

in πi:

$$V(r + \pi i) = V(r). \tag{2.191}$$

The turning points, where $-V(r_\pm) = \frac{\eta^2}{2}$ and therefore $\dot{r} = 0$, are given by

$$r_\pm = \pm \cosh^{-1}\left(\frac{w}{\eta}\right), \tag{2.192}$$

as well as all shifts thereof by $\pi i\mathbb{Z}$.

There are also singular points where the potential diverges. $V(r)$ has a double-pole at $r = \frac{\pi i}{2}$,

$$V(r) \overset{r\to\frac{\pi i}{2}}{\longrightarrow} \frac{w^2}{2}\frac{1}{\left(r - \frac{\pi i}{2}\right)^2} + \mathcal{O}(1), \tag{2.193}$$

and likewise at all points $\frac{\pi i}{2} + \pi i\mathbb{Z}$. We point out that $r = \pm\frac{\pi i}{2}$ coincide with the physical singularities of the Lorentzian black hole after continuing θ to Lorentzian time.

Using the energy conservation equation, we may write Eqn. 2.149 as

$$\tilde{S}[r] = \int_{-L}^{L} \mathrm{d}\rho \left(\frac{\mathrm{d}r}{\mathrm{d}\rho}\right)^2 - \eta(r(L) + r(-L)). \tag{2.194}$$

Letting $\mathscr{C}$ denote the contour traced by the solution in the complex r-plane, we may write the action as a contour integral:

$$\tilde{S}[r] = \int_{\mathscr{C}} \mathrm{d}r \, \sqrt{\eta^2 + 2V(r)} - \eta(r(L) + r(-L)). \tag{2.195}$$

Note that the integrand $\sqrt{\eta^2 + 2V(r)} = \dot{r}$ is the velocity function, and one should pick an appropriate branch of the square-root such that the velocity has the correct sign. The turning points $r_\pm + \pi i\mathbb{Z}$ are branch points of the square-root. The double-poles of the potential, meanwhile, lead to simple-poles of the integrand of residue $\pm w$:

$$\pm\sqrt{\eta^2 + 2V(r)} \overset{r\to\frac{\pi i}{2}}{\longrightarrow} \pm\frac{w}{r - \frac{\pi i}{2}} + \mathcal{O}(1). \tag{2.196}$$

The explicit solutions of the bulk equation of motion may be obtained by separating and integrating the energy conservation equation. One finds

$$r(\rho) = \sinh^{-1}\left(\sqrt{\frac{w^2}{\eta^2} - 1}\cosh(\eta(\rho + i\rho_0))\right) + \pi i N_1, \tag{2.197}$$

where ρ_0 is a complex number and N_1 is an integer. ρ_0 is the integration constant that arises in integrating the energy conservation equation. In the limit $L \to \infty$, the real part of $i\rho_0$ is merely a reparameterization of ρ; we therefore take $i\rho_0$ to be pure imaginary. The freedom to shift any solution by $\pi i N_1$ arises from the periodicity of the potential. For each N_1, the continuous modulus ρ_0 parameterizes a family of solutions. The on-shell action is necessarily the same for all trajectories in such a family, unless in varying ρ_0 one encounters a singular solution.[32] The on-shell action does depend on the discrete parameter N_1, however, through the boundary terms.

Since $\sinh^{-1}(z) = \log\left(z + \sqrt{z^2+1}\right)$ is a multi-valued function, one has to pick a branch to define the trajectory. The $\sqrt{z^2+1}$ term leads to square-root branch points at $z = \pm i$, and

[32] The divergent sum over ρ_0 is attributed to the infinite $\delta(j-j)$ factor in the two-point function of $\mathcal{O}_{jnw}$ and $\mathcal{O}_{j,-n,-w}$. [35]

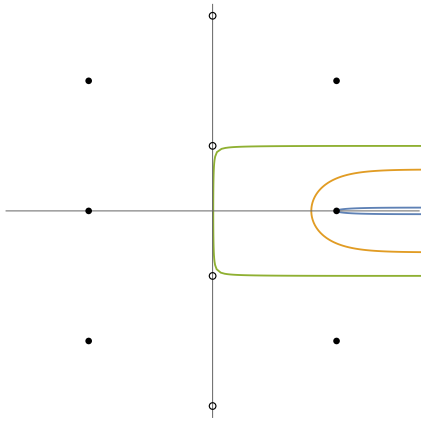

Figure 2.8: A Family of Reflected Solutions. Pictured here are several solutions with η real and less than w, $0 < \rho_0 < \frac{\pi}{2\eta}$, and $N_1 = 0$, obtained from Eqn. 2.197 with the principal branch of $\sinh^{-1}$. The solid disks indicate the turning points and the open circles indicate the singularities. The solution hugging the real axis has ρ_0 just above zero, corresponding to the real solution that rolls up and down the same side of the inverted-potential. All trajectories related by continuously dialing ρ_0 have the same action, unless one hits a singular trajectory in the process. The green solution pictured is nearly singular, with ρ_0 just below $\frac{\pi}{2\eta}$. At that value the trajectory will hit the poles of the potential.

there is a logarithmic branch point at infinity. On the principal branch, the cuts extend along the imaginary axis from i to $i\infty$ and from $-i$ to $-i\infty$, though other choices are convenient depending on the values of the parameters.[33]

Eqn. 2.197 solves the bulk equation of motion, but it remains to check if it satisfies the boundary equations. The velocity function is

$$\dot{r} = \eta \frac{\sqrt{\frac{w^2}{\eta^2} - 1}\sinh(\eta(\rho + i\rho_0))}{\sqrt{\left(\frac{w^2}{\eta^2} - 1\right)\cosh^2(\eta(\rho + i\rho_0)) + 1}}, \tag{2.198}$$

which indeed asymptotes to $\pm\eta$ as $|\rho| \to \infty$. The sign, however, depends on the branch of the square-root in the denominator, which coincides with the branch of the square-root in $\sinh^{-1}(z)$. Depending on the values of the parameters, one obtains either a reflected or

[33] In particular, for complex η the argument of the $\sinh^{-1}$ in Eqn. 2.197 behaves as a spiral at large $|\rho|$ since $\cosh(\eta\rho) \sim e^{\eta|\rho|}$. In that case one has to pick more complicated spiral branch cuts.

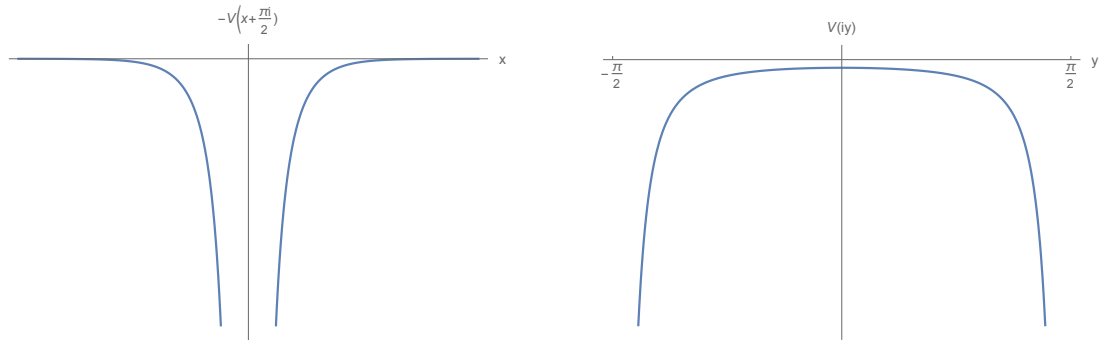

(a) **(b)**

Figure 2.9: Singular Potentials. On the slices $\mathrm{Im}(r) = \frac{\pi}{2}$ (left) and $\mathrm{Re}(r) = 0$ (right), the potential experienced by the particle falls to $-\infty$ at the singular points.

transmitted solution.

For example, several trajectories with η real and less than w, $0 < \rho_0 < \frac{\pi}{2\eta}$, and $N_1 = 0$ are plotted in Fig. 2.8. The solid disks indicate the turning points $r_\pm + \pi i\mathbb{Z}$, and the open circles indicate the singularities $\frac{\pi i}{2} + \pi i\mathbb{Z}$. The blue trajectory that hugs the real axis corresponds[34] to the real solution with $\rho_0 = 0$ for a particle that rolls up and down the potential hill, turning around at r_+. For the green trajectory nearly hitting the poles, on the other hand, ρ_0 is just below $\frac{\pi}{2\eta}$.

Upon reaching $\rho_0 = \frac{\pi}{2\eta}$, the asymptotic imaginary part of the trajectory reaches $\pm\frac{\pi}{2}$, and the saddle becomes singular. The argument of the $\sinh^{-1}$ in Eqn. 2.197 hits the branch points at $\pm i$ at finite ρ. Indeed, the inverted potential on the real slice $\mathrm{Im}(r) = \pm\frac{\pi}{2}$ is an infinite well, $-V\left(x \pm \frac{\pi i}{2}\right) = -\frac{1}{2}w^2\mathrm{csch}^2(x)$, pictured in Fig. 2.9a, and a particle kicked to the left from $x > 0$ falls down the well and hits the singularity. Similarly, on the imaginary axis

[34] In the figure, ρ_0 is deformed slightly away from 0 so that the incoming and outgoing segments of the trajectory do not overlap.

$r = iy$, the potential experienced by y is[35] $V(iy) = -\frac{1}{2}w^2 \sec^2(y)$, which is again singular, as pictured in Fig. 2.9b. Remarkably, we will see that the singular trajectories carry finite action and must be included in the saddle-point expansion to correctly reproduce the semi-classical reflection coefficient. The importance of singular saddles was discussed in closely related contexts in [35, 40].

As explained above, our task is to reproduce the semi-classical reflection and transmission coefficients (Eqns. 2.188-2.189) by saddle-point expansions for the infinite-space quantum mechanics. We address these in turn in the following two sub-sections.

2.4.3 Reflection Coefficient on the Complex r-Plane

We begin with the saddle-point expansion of the reflection coefficient for the complex quantum mechanics on the full r-plane. Let us first compute the action of the real saddle that exists for $0 < \eta < w$. We need to evaluate Eqn. 2.195 for the contour around the positive real axis in Fig. 2.10, which has been slightly deformed away from the real axis so that its incoming and outgoing legs do not overlap. The dashed lines represent a convenient choice of branch cuts of the square-root in the integrand. As before, the solid disks indicate the turning points and the open circles indicate the singularities.

The contribution to the contour integral of the small arc around the turning point vanishes because the integrand is zero there. The contributions of the remaining half-lines above and below the real axis are identical because they sit on opposite sides of the branch cut and

[35] Note that the potential for the imaginary part of the complex coordinate has a relative minus sign, due to the combined factors of i. The equation of motion is $\ddot{y} = \frac{\mathrm{d}}{\mathrm{d}y}\left(\frac{1}{2}w^2 \sec^2(y)\right)$.

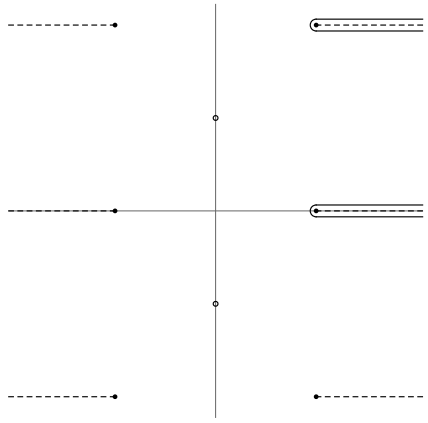

Figure 2.10: Reflected Saddles with Constant Imaginary Part. For η real and less than w, there is a real saddle corresponding to a particle that comes in from $r \to \infty$, rolls partway up the hill until it stops at the turning point, and then rolls back out to infinity. The corresponding contour in the complex r-plane is pictured here, slightly deformed away from being pure real so that the incoming and outgoing segments of the contour do not overlap. Due to the $r \to r + \pi i$ shift symmetry of the complexified problem, one likewise has shifted contours with constant imaginary part πN_1, such as the second contour in the figure with $N_1 = 1$. The dashed lines represent branch cuts of the square-root in Eqn. 2.195.

have opposite orientations, corresponding to the particle coming in from infinity and then going back out to infinity. Each of these two integrals contributes

$$\int_{r_+}^{r(L)} \mathrm{d}r \, \sqrt{\eta^2 + 2V(r)} = \eta \log(\eta) + \frac{w-\eta}{2} \log(w-\eta) - \frac{w+\eta}{2} \log(w+\eta) + \eta r(L), \quad (2.199)$$

in the limit $L \to \infty$. Combined with the boundary term that cancels the linear divergence $\eta r(L)$, we obtain the on-shell action

$$\tilde{S}_0 = 2\eta \log(\eta) + (w-\eta) \log(w-\eta) - (w+\eta) \log(w+\eta). \quad (2.200)$$

The contribution of this solution to the saddle-point expansion is then

$$e^{-k\tilde{S}_0} = \eta^{-2k\eta} (w+\eta)^{k(w+\eta)} (w-\eta)^{k(\eta-w)}. \quad (2.201)$$

This accounts for the first half of Eqn. 2.188 with $0 < \mathrm{Re}(\eta) < w$, leaving the three

trigonometric factors still to be explained.

The simplest of these three factors to understand is $\csc(\pi k\eta)$, which arises by the same mechanism as seen earlier in Liouville due to the shift symmetry of the potential. Even when η is real, one has complex solutions shifted by $\pi i N_1$, for any integer N_1. The contour with $N_1 = 1$ is also shown in Fig. 2.10. Each of these shifted saddles has action $\tilde{S}_0 - 2\pi i\eta N_1$, due to the shift of the boundary terms. One should not sum over all of them, however; the appropriate set depends on the sign of $\mathrm{Im}(\eta)$, which determines whether one obtains a convergent geometric series when $N_1 \in \mathbb{Z}_{\geq 0}$ or when $N_1 \in \mathbb{Z}_{\leq 0}$. For $\mathrm{Im}(\eta) > 0$ one finds

$$\sum_{N_1 \in \mathbb{Z}_{\geq 0}} e^{2\pi i k \eta N_1} = \frac{i}{2} e^{-\pi i k \eta} \csc(\pi k \eta), \tag{2.202}$$

while for $\mathrm{Im}(\eta) < 0$

$$\sum_{N_1 \in \mathbb{Z}_{\leq 0}} e^{2\pi i k \eta N_1} = -\frac{i}{2} e^{\pi i k \eta} \csc(\pi k \eta). \tag{2.203}$$

Since the reflection coefficient has poles on the real η-axis, one should always give η a non-zero phase in computing the saddle-point expansion. Depending on whether η lies above or below the real axis, we must pick one or the other half-infinite set of shifted saddles.

Next consider the factor of $\csc(\pi k(w - \eta))$, which accounts for the bound states of the infinite-space quantum mechanics. We now argue that it is the singular saddles that are responsible for this factor. This requires some explanation, since one ordinarily expects singular configurations to have infinite action and therefore to make no contribution to the

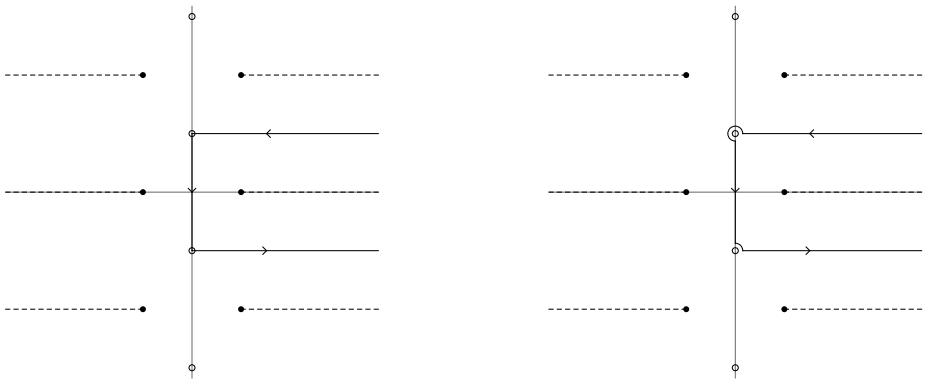

(a) **(b)**

Figure 2.11: Singular Contours. When the asymptotic imaginary part of the reflected contour shown in Fig. 2.8 reaches $\pm\frac{\pi}{2}$, the contour hits the poles of the potential and becomes singular (left). The singular contour must be deformed around the poles of the potential in order to define the action integral Eqn. 2.195. The action of the singular saddle then differs from Eqn. 2.200 by residues. The deformation is not unique, and one must sum over an appropriate set of singular saddles to reproduce the correct semi-classical limit. An example deformation is shown on the right, with action $\tilde{S}_0 - 2\pi i w$.

functional integral. In contrast, the singular saddles in this complexified problem have finite action, and are essential to reproducing the correct semi-classical limit [35, 40].

Consider the singular saddle discussed in the previous sub-section, obtained as the $\rho_0 \to \frac{\pi}{2\eta}$ limit of Eqn. 2.197, with $N_1 = 0$. The contour is shown in Fig. 2.11a. As pictured in Fig 2.9, on the real and imaginary slices $\mathrm{Im}(r) = \pm\frac{\pi}{2}$ and $\mathrm{Re}(r) = 0$, the effective 1-dimensional potential is an infinite well in the neighborhood of the singular points. The speed of the particle subsequently diverges there. However, the remarkable feature of the complexified problem is that the divergent contributions to the action are equal-but-opposite on the real and imaginary segments of the trajectory, the speed of the particle being pure real and pure imaginary in the two cases. One may therefore define the total action by a principal-value type limit.

More precisely, let $z = r - \frac{\pi i}{2}$ be a local coordinate in the neighborhood of the singularity at $r = \frac{\pi i}{2}$. From Eqn. 2.193, the potential has a double-pole there, $V(z) = \frac{w^2}{2}\frac{1}{z^2} + \mathcal{O}(1)$, and

therefore the energy conservation equation in this neighborhood becomes

$$\frac{\mathrm{d}z}{\mathrm{d}\rho} = -\frac{w}{z} + \cdots , \tag{2.204}$$

the minus sign corresponding to the orientation chosen in Fig. 2.11a. The solution near the upper pole is then $z(\rho) = -i\sqrt{2w(\rho+\rho_1)}$, hitting the pole at $\rho = -\rho_1$. The speed-squared is

$$\left(\frac{\mathrm{d}z}{\mathrm{d}\rho}\right)^2 = -\frac{w}{2}\frac{1}{\rho+\rho_1} + \cdots . \tag{2.205}$$

The integrand of the on-shell action thus has a $\frac{1}{\rho}$ type singularity near $r = \frac{\pi i}{2}$, and the integral is[36]

$$\int_{-\rho_1-\varepsilon}^{-\rho_1+\varepsilon} \mathrm{d}\rho \left(\frac{\mathrm{d}z}{\mathrm{d}\rho}\right)^2 = -\frac{w}{2}\left(\pi i + 2\pi i N_2\right), \tag{2.206}$$

with N_2 an integer. The ambiguity in $2\pi i\mathbb{Z}$ amounts to the choice of branch of $\log\rho = \int \frac{\mathrm{d}\rho}{\rho}$. One likewise has a $\frac{1}{\rho}$ singularity in the neighborhood of the lower pole. $\dot{r}^2$ for the complete singular solution with real η is plotted in Fig. 2.12.

[36] The integral $\int_{-a}^{a} \frac{\mathrm{d}\rho}{\rho}$ may be defined by continuing ρ to the complex plane and deforming the contour off the real axis:

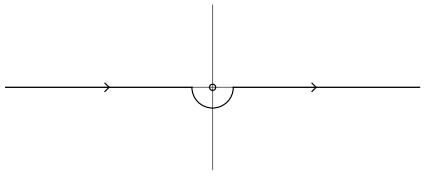

The integral over the counter-clockwise semi-circle about the pole is πi. Discarding it defines the principal-value of the integral, which is zero in this symmetric case. Of course, the deformation of the contour is not unique. One could just as well have deformed it into a clockwise arc above the pole which would instead yield $-\pi i$, or an arc that encircles the pole any number of times. The integral is therefore only defined up to shifts by $2\pi i\mathbb{Z}$, which is equivalently the ambiguity in the choice of branch of $\int \frac{\mathrm{d}\rho}{\rho} = \log(\rho)$.

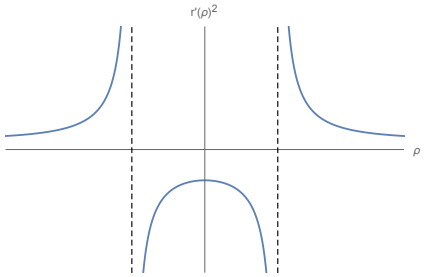

Figure 2.12: Singular Speed-Squared. The speed-squared $\dot{r}^2$ is plotted here for the singular saddle shown in Fig. 2.11a. It has $\frac{1}{\rho}$ type singularities where the contour hits the poles of the potential. The action, which is the integral of $\dot{r}^2$, is finite because $\int_{-\varepsilon}^{\varepsilon} \frac{\mathrm{d}\rho}{\rho}$ may be defined by continuation around the pole. The imaginary part of the integral is ambiguous up to shifts by $2\pi i\mathbb{Z}$, however, corresponding to the choice of how to deform the contour around the poles.

In the formulation of the action as a contour integral in the r-plane, the ambiguity in the action of the singular saddle arises because one must deform the contour in Fig. 2.11a away from the poles at $r = \pm\frac{\pi i}{2}$, and the deformation is not unique. The same integral Eqn. 2.206 in the neighborhood of the pole may be written

$$\int_{-\rho_1-\varepsilon}^{-\rho_1+\varepsilon} \mathrm{d}\rho \left(\frac{\mathrm{d}z}{\mathrm{d}\rho}\right)^2 = -\int_{\mathscr{C}_\varepsilon} \mathrm{d}z\, \frac{w}{z} \tag{2.207}$$

where $\mathscr{C}_\varepsilon$ is a contour that avoids the pole. For example, the integral around the pole at $\frac{\pi i}{2}$ along the contour deformation shown in Fig. 2.11b is $-\frac{3\pi i}{2}w$, corresponding to $N_2 = 1$ in Eqn. 2.206.

The outcome of this discussion is that, in addition to the saddles accounted in Eqns. 2.201-2.203, one has singular saddles of finite action corresponding to contours in the r-plane that wrap the singularities an integer number of times and so differ from $\tilde{S}_0$ by residues. They may be thought of as asymptotic saddles in a fixed topological sector of the functional integral, where the singular points of the potential are excised from the plane, and the configuration space of maps $r\colon [-L, L] \to \{\mathbb{C} - \text{poles}\}$ is divided into homotopy classes labeled by their

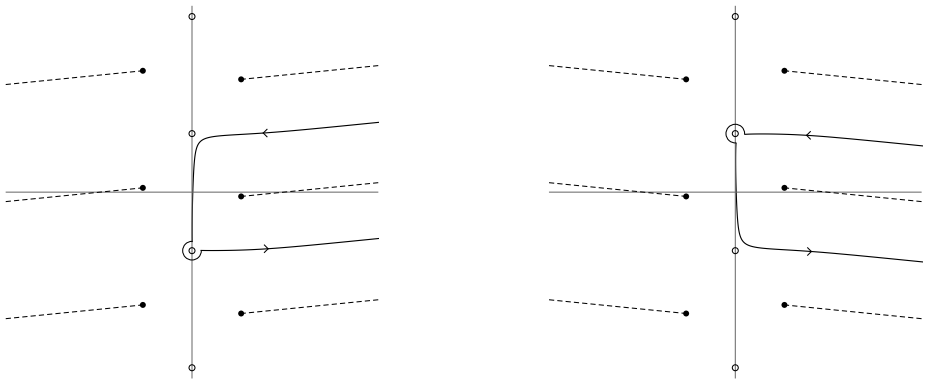

(a) **(b)**

Figure 2.13: Singular Reflected Saddles ($\mathrm{Re}(\eta) < w$). η should be shifted off the real axis for the saddle-point expansion to be well-defined. Compared to Fig. 2.11, η has been given a small positive phase on the left and a small negative phase on the right.

winding numbers around the punctures. As the deformations of the contour around the poles shrink away, one asymptotically approaches an exact solution of the equations of motion, whose action differs from $\tilde{S}_0$ in its imaginary part.

A singular saddle that wraps N_2 times around the pole at $r = \frac{\pi i}{2} + \pi i N_1$ has action $\tilde{S}_0 - 2\pi i \eta N_1 - 2\pi i w N_2$. Figs. 2.13a and 2.13b illustrate such saddles with $N_1 = -1$ and 0, $N_2 = -1$ and 1, and η having a small positive and negative phase, respectively. By summing over saddles with action of the form $\tilde{S}_0 - 2\pi i \eta(N_1 + N_2) + 2\pi i w N_2 = \tilde{S}_0 - 2\pi i \eta N_1 - 2\pi i(\eta - w)N_2$, one may obtain both factors of $\csc(\pi k \eta)$ and $\csc(\pi k(w - \eta))$ required in Eqn. 2.188. We give the precise list of saddles momentarily.

Finally, one must account for the factor of $\sin(\pi k w)$ in Eqn. 2.188. It is again associated to the singular saddles, but it is qualitatively different from the csc factors, corresponding to a two-fold degeneracy of saddles rather than an infinite geometric series. Written in the

form

$$\sin(\pi k w) \propto e^{\pi i k w}(1 - e^{-2\pi i k w}), \tag{2.208}$$

we see that we must sum over two sets of singular saddles, identical except that each contour in one set winds an extra time around the pole. The relative minus sign is due to the orientation of the integration contours, which we will not attempt to determine.

Having explained the mechanism by which each factor in Eqn. 2.188 comes about, let us finally give the list of saddles that reproduces the semi-classical limit for $0 < \mathrm{Re}(\eta) < w$.

For $\mathrm{Im}(\eta) > 0$, the contributing saddles have action

$$\begin{aligned} &\tilde{S}_{N_1 N_2} = \tilde{S}_0 - 2\pi i \eta (N_1 + N_2) + 2\pi i w N_2, \\ &N_1 = 0, 1, 2, \ldots, \ N_2 = 1, 2, 3, \ldots, \end{aligned} \tag{2.209}$$

corresponding to a contour that wraps N_2 times around the pole at $r = -\frac{\pi i}{2} + \pi i (N_1 + N_2)$. Note that $N_1 + N_2 \geq 1$, meaning that all the contours are in the upper-half plane. In addition, one has a second set of saddles with action

$$\begin{aligned} &\tilde{S}'_{N_1 N_2} = \tilde{S}_0 - 2\pi i \eta (N_1 + N_2) + 2\pi i w (N_2 - 1), \\ &N_1 = 0, 1, 2, \ldots, \ N_2 = 1, 2, 3, \ldots, \end{aligned} \tag{2.210}$$

which wrap $N_2 - 1$ times instead. The two sets are weighted with a relative minus sign.

Their contribution to the saddle-point expansion yields at leading order

$$\sum_{\substack{N_1\in\mathbb{Z}_{\geq 0}\\ N_2\in\mathbb{Z}_{\geq 1}}}\left(e^{-k\tilde{S}_{N_1N_2}}-e^{-k\tilde{S}'_{N_1N_2}}\right) \tag{2.211}$$

$$=e^{-k\tilde{S}_0}\sum_{N_1\in\mathbb{Z}_{\geq 0}}e^{2\pi ik\eta N_1}\sum_{N_2\in\mathbb{Z}_{\geq 1}}e^{2\pi ik(\eta-w)N_2}\left(1-e^{2\pi ikw}\right)$$

$$\propto\eta^{-2k\eta}(w+\eta)^{k(w+\eta)}(w-\eta)^{k(\eta-w)}\sin(\pi kw)\csc\left(\pi k\eta\right)\csc\left(\pi k(w-\eta)\right),$$

reproducing Eqn. 2.188. Note that the geometric series converge for $\mathrm{Im}(\eta)>0$. For $\mathrm{Im}(\eta)<0$, the required sum is instead

$$e^{-k\tilde{S}_0}\sum_{N_1\in\mathbb{Z}_{\leq 0}}e^{2\pi ik\eta N_1}\sum_{N_2\in\mathbb{Z}_{\leq -1}}e^{2\pi ik(\eta-w)N_2}\left(1-e^{-2\pi ikw}\right), \tag{2.212}$$

with the same result. These are contours that wrap N_2 or N_2+1 times around the pole at $r=\frac{\pi i}{2}+\pi i(N_1+N_2)$. Note that $N_1+N_2\leq -1$ implies all of the contours are in the lower-half plane.

As forewarned at the beginning of this section, we have not attempted to explain why these are the saddles that contribute to the functional integral, but merely demonstrated that this is the necessary list to reproduce the semi-classical limit of the exact answer. In fact, we take this list as the definition of the contour of the functional integral that computes the reflection coefficient for the quantum mechanics, being given by the sum of the corresponding steepest-descent contours.

So far we have considered the case $0<\mathrm{Re}(\eta)<w$. Next suppose that $\mathrm{Re}(\eta)>w$. In Eqn.

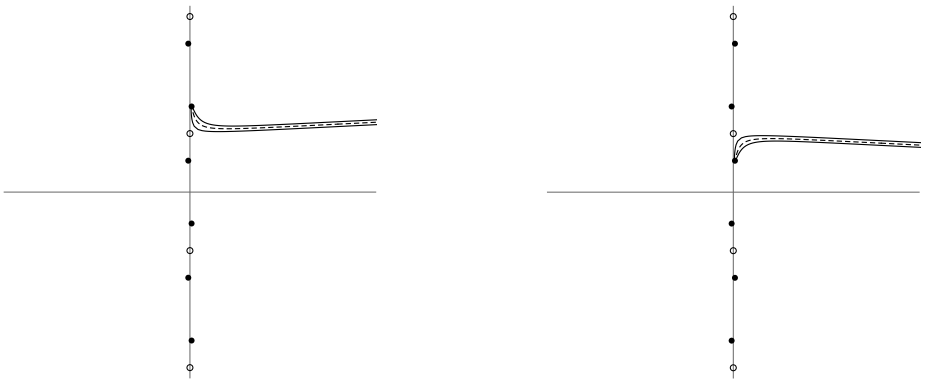

(a) **(b)**

Figure 2.14: Reflected Saddles ($\mathrm{Re}(\eta) > w$). When η is real and greater than w, the only reflected solutions are singular. But one finds non-singular solutions for complex η. On the left η has a small positive phase and on the right it has a small negative phase. The contour is deflected in opposite directions by the pole in the two cases.

2.188, the bound state factor now disappears, because $\frac{\eta^2}{2}$ exceeds the height of the potential. As discussed previously, in light of this abrupt change in the asymptotic expansion of the reflection coefficient, we expect that $\mathrm{Re}(\eta) = w$ corresponds to a Stokes wall, and that the set of contributing saddles jumps for $\mathrm{Re}(\eta) > w$.

When η is real and larger than w, one no longer has a real solution of the equations of motion. The energy of the particle is greater than the height of the potential hill and it rolls over from $r \to \infty$ to $r \to -\infty$, satisfying the boundary conditions for transmission rather than reflection. The only reflected trajectories with η real and greater than w are singular. Once again, η should be given a phase, in which case one finds non-singular trajectories. Figs. 2.14a and 2.14b illustrate reflected solutions for η with a small positive and a small negative phase. As is by now familiar, the set of contributing saddles will depend on whether η lies above or below the real axis.

The action for the contour with $\mathrm{Im}(\eta) > 0$ pictured in Fig. 2.14a is

$$\tilde{S}_0 = 2\eta \log(\eta) - (\eta + w)\log(\eta + w) - (\eta - w)\log(\eta - w) - \pi i(\eta + w). \tag{2.213}$$

The contributing saddles for $\mathrm{Im}(\eta) > 0$ are the shifted saddles of this form in the upper-half plane,

$$\tilde{S}_{N_1} = \tilde{S}_0 - 2\pi i \eta N_1, \quad N_1 = 0, 1, 2, \ldots, \tag{2.214}$$

as well as a second set that wraps the pole at $r = \frac{\pi i}{2} + \pi i N_1$ once,

$$\tilde{S}'_{N_1} = \tilde{S}_{N_1} + 2\pi i w, \quad N_1 = 0, 1, 2, \ldots. \tag{2.215}$$

The two sets are weighted with a relative minus sign, for a total of

$$\begin{aligned} \sum_{N_1 \in \mathbb{Z}_{\geq 0}} \left(e^{-k\tilde{S}_{N_1}} - e^{-k\tilde{S}'_{N_1}} \right) &= e^{-k\tilde{S}_0} \sum_{N_1 \in \mathbb{Z}_{\geq 0}} e^{2\pi i k \eta N_1} \left(1 - e^{-2\pi i k w}\right) \\ &\propto \eta^{-2k\eta} (\eta + w)^{k(\eta+w)} (\eta - w)^{k(\eta-w)} \sin(\pi k w) \csc(\pi k \eta). \end{aligned} \tag{2.216}$$

For $\mathrm{Im}(\eta) < 0$, the necessary saddles are of the form in Fig. 2.14b, but in the lower-half plane. The action for the contour in Fig. 2.14b is

$$\tilde{S}_0 = 2\eta \log(\eta) - (\eta + w)\log(\eta + w) - (\eta - w)\log(\eta - w) - \pi i(\eta - w), \tag{2.217}$$

and the saddle-point expansion is

$$e^{-k\tilde{S}_0}\left(\sum_{N_1\in\mathbb{Z}_{\leq -1}} e^{2\pi i k\eta N_1}\right)\left(1-e^{2\pi i k w}\right). \tag{2.218}$$

This completes the saddle-point expansion of the reflection coefficient for the infinite-space quantum mechanics. Next we turn to the transmission coefficient.

2.4.4 Transmission Coefficient on the Complex r-Plane

The action for the transmission coefficient of the infinite-space quantum mechanics is as in Eqn. 2.195, but with $r(L) \to -r(L)$ so that the velocity at late times is fixed to $-\eta$ rather than η:

$$\tilde{S}[r] = \int_{\mathscr{C}} \mathrm{d}r\, \sqrt{\eta^2 + 2V(r)} - \eta(-r(L) + r(-L)). \tag{2.219}$$

The simplest saddle of Eqn. 2.219 is the real trajectory of a particle with η real and greater than w that rolls over the potential hill, pictured in Fig. 2.15.

The action for this saddle is[37]

$$\tilde{S}_0 = 2\eta\log(\eta) - (\eta+w)\log(\eta+w) - (\eta-w)\log(\eta-w), \tag{2.220}$$

[37]Note that the appropriate branch of the square-root in the integrand of the action should be negative on the real axis, the velocity of the particle always being to the left for this trajectory.

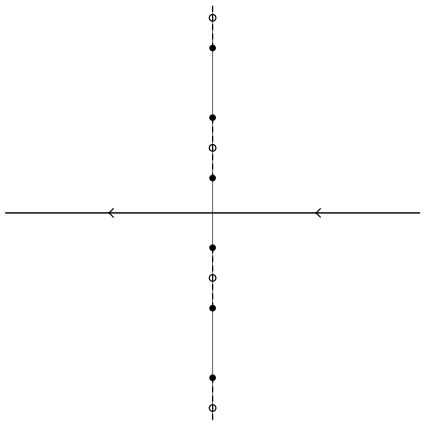

Figure 2.15: Transmitted Saddle ($\eta > w$). For η real and greater than w, there is a real saddle for the transmission coefficient, corresponding to a particle that rolls over the inverted potential from $r \to \infty$ to $r \to -\infty$.

yielding

$$e^{-k\tilde{S}_0} = \eta^{-2k\eta}(\eta + w)^{k(\eta+w)}(\eta - w)^{k(\eta-w)}. \tag{2.221}$$

This reproduces the transmission coefficient Eqn. 2.189 for $\mathrm{Re}(\eta) > w$. Note that although one again has shifted saddles with constant imaginary part πN_1, the action is invariant under the shift. For the same reason, note that the functional integral over real r no longer diverges for the transmission coefficient. Indeed, given that the semi-classical limit of the transmission coefficient is reproduced by a single real saddle for real η, we expect that the contour of integration is real in this case.

When η is real and less than w, the only saddles for the transmission coefficient are singular. Non-singular saddles are obtained for complex η, as pictured in Fig. 2.16.

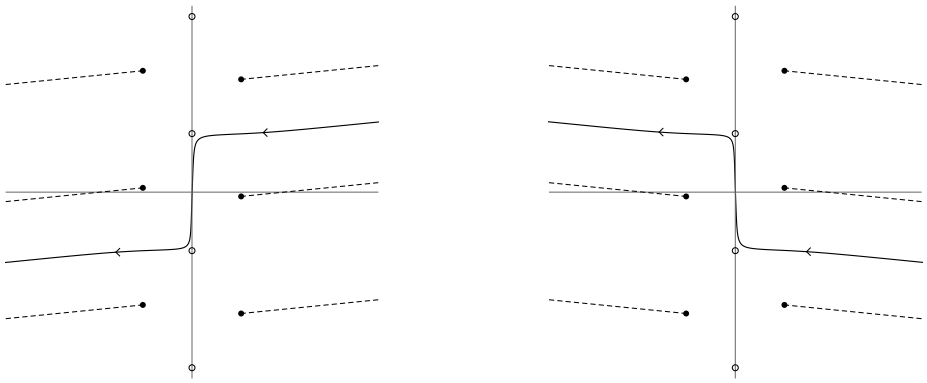

(a) **(b)**

Figure 2.16: Transmitted Saddles ($\mathrm{Re}(\eta) < w$). When η is real and less than w, the only transmitted saddles are singular. Non-singular solutions are found for complex η. On the left η has a small positive phase and on the right it has a small negative phase.

The action for the contour pictured in Fig. 2.16a, where $\mathrm{Im}(\eta) > 0$, is

$$\tilde{S}_0 = 2\eta \log(\eta) - (w+\eta)\log(w+\eta) + (w-\eta)\log(w-\eta) + \pi i(w-\eta), \tag{2.222}$$

which gives

$$e^{-k\tilde{S}_0} = e^{-\pi i k(w-\eta)} \eta^{-2k\eta} (\eta+w)^{k(\eta+w)} (w-\eta)^{k(\eta-w)}. \tag{2.223}$$

The necessary sum is now

$$e^{-k\tilde{S}_0} \sum_{N \in \mathbb{Z}_{\geq 0}} e^{2\pi i k(\eta-w)N} \propto \eta^{-2k\eta} (\eta+w)^{k(\eta+w)} (w-\eta)^{k(\eta-w)} \csc\left(\pi k(w-\eta)\right), \tag{2.224}$$

corresponding to saddles with $\tilde{S}_N = \tilde{S}_0 - 2\pi i \eta N + 2\pi i w N$. As in the reflected case, the shift by $2\pi i w N$ is accounted for by singular saddles that wrap the pole N times. The shift by $2\pi i \eta N$ was previously explained by the change in the boundary action under $r \to r + \pi i N$. As noted a moment ago, however, the boundary action for transmission is invariant under

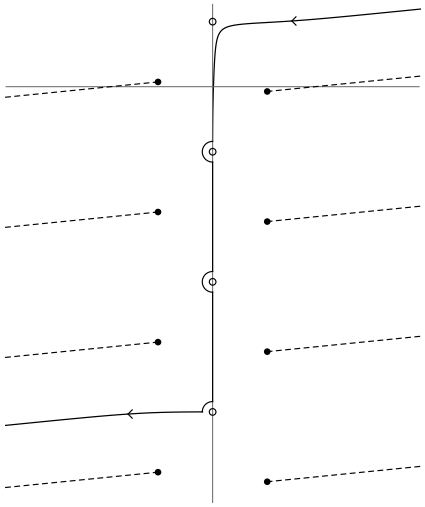

Figure 2.17: Shifted Transmitted Contour. When $\mathrm{Re}(\eta) < w$, one must sum over contours with $r(L) \to r(L) - 2\pi i N$ in order to reproduce the semi-classical limit of the transmission coefficient.

this shift.

Instead, one must consider contours with only one end shifted by $2\pi i N$, as pictured in Fig. 2.17. The integral along the shifted contour is identical to that of Fig. 2.16a; their actions differ only by the shift of the boundary term. By summing over contours of this form, where $r(L) \to r(L) - 2\pi i N$, together with the N-fold wrapping, we obtain the required lattice of actions for Eqn. 2.224.

For $\mathrm{Im}(\eta) < 0$, the action of the saddle pictured in Fig. 2.16b is

$$\tilde{S}_0 = 2\eta \log(\eta) - (w+\eta)\log(w+\eta) + (w-\eta)\log(w-\eta) - \pi i(w-\eta), \tag{2.225}$$

and the saddle-point expansion is

$$e^{-k\tilde{S}_0} \sum_{N \in \mathbb{Z}_{\leq 0}} e^{2\pi i k(\eta - w)N}. \tag{2.226}$$

One has analogous contours as in Fig. 2.17, now with $r(L) \to r(L) - 2\pi i N$ shifted upward.

We do not have a clear rationale for why contours of this form contribute to the saddle-point expansion. Although the contour pictured in Fig. 2.17 is constructed out of the same components as the singular saddles discussed previously, it is not obtained from a limit of smooth saddles, which are always confined to an interval of width πi. For now we merely observe that this is the set which reproduces the semi-classical limit of the exact transmission coefficient, and leave it as an open question to better understand the rules for determining the set of contours that contribute to the saddle-point expansion.

2.5 sine-Liouville Reflection

We conclude this chapter by reviewing the FZZ duality, which gives an alternate Lagrangian description of the $\mathrm{SL}(2,\mathbb{R})_k/\mathrm{U}(1)$ CFT, known as the sine-Liouville background, that is better suited than the cigar description when k is small compared to two. Then we briefly consider what can be said about the saddle-point expansion of the reflection coefficient given by the sine-Liouville functional integral in the limit $k \to 2$.

2.5.1 The FZZ Duality

The $\mathrm{SL}(2,\mathbb{R})_k/\mathrm{U}(1)$ CFT is defined for $k > 2$. We have focused so far on the $k \to \infty$ limit, where the cigar sigma-model provides a weakly-coupled Lagrangian description of the

CFT. In the opposite limit, namely $k-2 \to 0$, the scalar curvature of the cigar diverges,

$$\mathcal{R}_{\text{cigar}} = -\frac{2}{\alpha'}\frac{1}{k-2} + \mathcal{O}((k-2)^0), \tag{2.227}$$

and that description becomes strongly coupled. However, there exists a dual description of the CFT that is better suited at small k known as the sine-Liouville background, and the equivalence of the two Lagrangians is known as the Fateev-Zamolodchikov-Zamolodchikov (FZZ) duality [48, 49].

In the weak-coupling region, the cigar sigma-model approaches the free linear-dilaton $\times$ S^1 background in Eqn. 2.109. As previously discussed, the linear-dilaton $\times$ S^1 itself, with $\hat{r} \in (-\infty, \infty)$ permitted to range over the entire line, is ill-defined because the string coupling diverges as $\hat{r} \to -\infty$. This strong-coupling region is eliminated in the cigar background by ending the geometry at $r = 0$.

In Sec. 2.2, we recalled that the free linear dilaton may alternatively be regulated by turning on the Liouville potential $V_{\mathrm{L}} \propto e^{-2b_{\mathrm{L}}\hat{r}}$ that serves as a barrier, suppressing string configurations which extend too deeply into the strong-coupling region. The Liouville momentum b_{L} was chosen such that the potential is marginal.

The cigar and Liouville $\times$ S^1 backgrounds are identical at large $\hat{r}$ and reproduce the same central charge (Eqn. 2.92). One might ask if they are dual descriptions of the same CFT. The answer is no, as is clear, for example, from the fact that the Liouville $\times$ S^1 theory conserves the string winding number around the cylinder, which is broken in the cigar. There is, however, a close relative of the Liouville $\times$ S^1 background, called sine-Liouville, that is dual

to the cigar, and this is the content of the FZZ duality.

In sine-Liouville, the linear-dilaton$\times$S^1 is instead deformed by $V_{\rm sL} \propto e^{-2b_{\rm sL}\hat{r}}\mathrm{Re}\, e^{i\sqrt{\frac{k}{\alpha'}}(\hat{\theta}_{\rm L}-\hat{\theta}_{\rm R})}$. The potential consists of a Liouville-like radial factor $e^{-2b_{\rm sL}\hat{r}}$, together with the unit-winding operator around the S^1 direction. The presence of the winding operator explicitly breaks the winding number conservation law of the free theory, consistent with winding non-conservation in the cigar. The momentum of the linear-dilaton factor,

$$b_{\rm sL} = \frac{1}{2}\sqrt{\frac{k-2}{\alpha'}}, \tag{2.228}$$

is again chosen such that the potential is weight $(1,1)$,

$$\alpha' b_{\rm sL}(Q - b_{\rm sL}) + \frac{k}{4} = 1, \tag{2.229}$$

$k/4$ being the contribution of the unit-winding operator. At large $\hat{r}$, the potential decays and one recovers the same asymptotic linear-dilaton $\times$ S^1 theory as for the cigar. One thinks of the sine-Liouville background as being built up of a condensate of winding strings on top of the cylinder, as pictured in Fig. 1.4b.

The sine-Liouville action on a closed worldsheet Σ is thus

$$S_{\rm sL} = \frac{1}{4\pi\alpha'}\int_\Sigma \mathrm{d}^2\sigma\sqrt{h}\left\{(\nabla\hat{r})^2 + (\nabla\hat{\theta})^2 + 4\pi\lambda(W_+ + W_-) - \alpha' Q\mathcal{R}[h]\hat{r}\right\}, \tag{2.230}$$

where

$$W_{\pm} = e^{-2b_{\mathrm{sL}}\hat{r}} e^{\pm i\sqrt{\frac{k}{\alpha'}}\left(\hat{\theta}_{\mathrm{L}} - \hat{\theta}_{\mathrm{R}}\right)} \tag{2.231}$$

are the winding ± 1 components of the sine-Liouville potential. λ is a positive constant, analogous to μ in Liouville (Eqn. 2.41).

Note that the duality relates two target spaces of different topologies. In the cigar description the target space is a disk, whose contractible Euclidean time circle lead to the two-sided black hole described in Sec. 2.3.2. In the sine-Liouville description the target space is an annulus, and the analogous continuation with respect to the now non-contractible Euclidean time circle will produce a disconnected Lorentzian geometry. The equivalence of string theory in these two target spacetimes, one connected and one disconnected, is an example of ER = EPR, and is the subject of the second half of the dissertation. Both descriptions share the same asymptotic linear-dilaton $\times$ S^1 region. The leading departure from the free theory at finite r in the cigar is the metric deformation $e^{-2r}\partial\theta\bar{\partial}\theta$, while sine-Liouville results from the potential deformation $e^{-2b_{\mathrm{sL}}\hat{r}} \cos\left(\sqrt{k/\alpha'}(\hat{\theta}_{\mathrm{L}} - \hat{\theta}_{\mathrm{R}})\right)$.

One is again free to add a constant mode Φ_0 to the dilaton, but it may be eliminated by the field redefinition $\hat{r} \to \hat{r} + \frac{\Phi_0}{Q}$, up to a rescaling of λ by $e^{-(k-2)\Phi_0}$. In particular, only the combination $e^{-2\Phi_0}\lambda^{\frac{2}{k-2}}$ is a meaningful parameter of the string theory, which sets the mass of the black hole; we can therefore choose $\Phi_0 = 0$ in the sine-Liouville description.

As in Liouville, although the action Eqn. 2.230 takes the form of the free linear-dilaton$\times \mathrm{S}^1$ deformed by the sine-Liouville potential with coefficient λ, the sine-Liouville background

is not a small perturbation of the free theory due to the freedom to rescale λ by a field redefinition. Correlation functions once again are not analytic functions of λ, and one cannot in general write a sine-Liouville correlator as a Taylor expansion in λ with coefficients computed from the free theory. The non-analytic λ dependence may be evaluated by performing the zero-mode integral over the linear-dilaton coordinate as in Eqn. 2.61. Separating $\hat{r}(z,\bar{z}) = \hat{r}_0 + \hat{r}'(z,\bar{z})$, the functional integral with asymptotic primary insertions $\prod_N e^{-2Q(1-j_N)\hat{r}}\mathcal{S}_N(\hat{\theta})$, where $\mathcal{S}_N$ are S^1 primaries, may be written

$$\begin{aligned}\int \mathrm{D}\hat{r}\mathrm{D}\hat{\theta}\; e^{-S_{\mathrm{sL}}[\hat{r},\hat{\theta}]}\prod_N e^{-2Q(1-j_N)\hat{r}}\mathcal{S}_N \qquad (2.232)\\ = \int \mathrm{D}\hat{r}'\mathrm{D}\hat{\theta}\; e^{-S_{\mathrm{LD}}[\hat{r}']-S_{\mathrm{S}^1}[\hat{\theta}]}\prod_N e^{-2Q(1-j_N)\hat{r}'}\mathcal{S}_N\\ \times\int \mathrm{d}\hat{r}_0\; e^{Q\left(\chi-2\sum_N(1-j_N)\right)\hat{r}_0-\left(\frac{\lambda}{\alpha'}V_{\mathrm{sL}}[\hat{r}',\hat{\theta}]\right)e^{-2b_{\mathrm{sL}}\hat{r}_0}},\end{aligned}$$

where $V_{\mathrm{sL}}[\hat{r}',\hat{\theta}] = 2\int \mathrm{d}^2\sigma\sqrt{h}e^{-2b_{\mathrm{sL}}\hat{r}'}\cos\left(\sqrt{k/\alpha'}(\hat{\theta}_{\mathrm{L}}-\hat{\theta}_{\mathrm{R}})\right)$.

For $\mathrm{Re}(\kappa) < 0$, one obtains

$$\int_{-\infty}^{\infty}\mathrm{d}\hat{r}_0\; e^{2b_{\mathrm{sL}}\kappa\hat{r}_0-\left(\frac{\lambda}{\alpha'}V_{\mathrm{sL}}[\hat{r}',\hat{\theta}]\right)e^{-2b_{\mathrm{sL}}\hat{r}_0}} = \frac{1}{2b_{\mathrm{sL}}}\left(\frac{\lambda}{\alpha'}V_{\mathrm{sL}}[\hat{r}',\hat{\theta}]\right)^{\kappa}\Gamma(-\kappa)\,, \qquad (2.233)$$

where now

$$\kappa = \frac{Q}{2b_{\mathrm{sL}}}\left(\chi - 2\sum_N(1-j_N)\right). \qquad (2.234)$$

When $\mathrm{Re}(\kappa) > 0$, the zero-mode integral over the real line diverges, and must be deformed to a complex contour that preserves convergence and analyticity.

Thus, the sine-Liouville correlation function is reduced to a linear-dilaton $\times \mathrm{S}^1$ correlation function, with the linear-dilaton zero-mode measure omitted, plus κ powers of the integrated sine-Liouville potential:

$$\begin{aligned}\left\langle \prod_N e^{-2Q(1-j_N)\hat{r}} \mathcal{S}_N \right\rangle_{\mathrm{sL}} \\ = \frac{1}{2b_{\mathrm{sL}}} \left(\frac{\lambda}{\alpha'}\right)^{\kappa} \Gamma(-\kappa) \left\langle V_{\mathrm{sL}}[\hat{r},\hat{\theta}]^{\kappa} \prod_N e^{-2Q(1-j_N)\hat{r}} \mathcal{S}_N \right\rangle_{\mathrm{LD}\times\mathrm{S}^1,\emptyset} .\end{aligned} \tag{2.235}$$

On a genus g Riemann surface, one obtains the scaling $\lambda^{\frac{2}{k-2}\left(1-g+\sum_N (j_N-1)\right)}$. The answer is analytic in λ only when κ is a natural number, in which the case the κ insertions of the potential ${V_{\mathrm{sL}}}^{\kappa}$ is most straightforward. The subsequent divergence of the prefactor $\Gamma(-\kappa)$ is attributable to the volume of the non-compact target space.

Observe that the sine-Liouville potential $W_+ + W_-$ coincides with the weak-coupling limit of the previously defined coset operator $\mathcal{O}_{\mathrm{sL}} = \mathcal{W}_+ + \mathcal{W}_-$ (Eqns. 2.122-2.123), hence the common terminology. A conformal perturbation of $\mathrm{SL}(2,\mathbb{R})_k/\mathrm{U}(1)$ by the marginal operator $\mathcal{O}_{\mathrm{sL}}$ is trivial at the level of the CFT—the deformation merely shifts the coefficient λ of the sine-Liouville potential, which may be undone by a field redefinition of $\hat{r}$ at the cost of introducing a dilaton zero-mode. The latter is a trivial improvement term from the perspective of the CFT. As a string background, on the other hand, the deformation by $\mathcal{O}_{\mathrm{sL}}$ is important because it shifts the mass of the black hole. We will explore this point further in Sec. 4.4.

In light of the winding operator in the sine-Liouville potential, it is natural to employ the

T-dual coordinate $\hat{\vartheta} \sim \hat{\vartheta} + 2\pi\sqrt{\frac{\alpha'}{k}}$. The action may then be written

$$S_{\text{sL}} = \frac{1}{4\pi\alpha'} \int_{\Sigma} \mathrm{d}^2\sigma\sqrt{h} \left\{ (\nabla\hat{r})^2 + (\nabla\hat{\vartheta})^2 + 8\pi\lambda e^{-2b_{\text{sL}}\hat{r}} \cos\left(\sqrt{\frac{k}{\alpha'}}\hat{\vartheta}\right) - \alpha' Q\mathcal{R}[h]\hat{r} \right\}. \quad (2.236)$$

As in Liouville, the linear-dilaton factor of the potential $e^{-2b_{\text{sL}}\hat{r}}$ is weakly coupled when b_{sL} is small, i.e. when k is near 2. However, neither the original cylinder radius $\sqrt{\alpha' k}$ nor its T-dual $\sqrt{\alpha'/k}$ is large in that limit, and so the sine-Liouville background is not strictly-speaking weakly coupled there. It is a far better description of the coset for k near 2 than the cigar, however, which becomes infinitely strongly coupled in the limit.

Because the asymptotic conditions for the coset operators discussed in Sec. 2.3.4 in the cigar description mapped the neighborhood of the insertion to the free-field region where the cigar and sine-Liouville backgrounds coincide, the same apply in sine-Liouville. T-dualizing Eqn. 2.131, the asymptotic conditions for an insertion of $\mathcal{O}_{jnw}$ in the far past on the cylinder are

$$\hat{r}(\rho,\phi) \overset{\rho\to-\infty}{\longrightarrow} 2\alpha' Q\left(\frac{1}{2} - j\right)\rho + \mathcal{O}(1) \quad (2.237a)$$

$$\hat{\vartheta}(\rho,\phi) \overset{\rho\to-\infty}{\longrightarrow} iw\sqrt{\alpha' k}\rho + n\sqrt{\frac{\alpha'}{k}}\phi + \mathcal{O}(1). \quad (2.237b)$$

In the previous discussion on the cigar, the (asymptotically) linear dilaton played little role as $k \to \infty$ because Q vanished in the limit. By contrast, Q diverges as $k - 2 \to 0$. The background-charge operators, responsible for the shift by $\frac{1}{2}$ in Eqn. 2.237a, now behave as heavy operators, scaling with the leading-order terms in the action as in the semi-classical

limit of Liouville. Similarly, the $\mathcal{O}_{jnw}$ insertion is itself a heavy operator for j of order one in the $k-2\to 0$ limit.

As an aside, we point out that although Liouville $\times$ S^1, with $Q=1/\sqrt{\alpha'(k-2)}$ and radius $\sqrt{\alpha' k}$, is not equivalent to $\mathrm{SL}(2,\mathbb{R})_k/\mathrm{U}(1)$, it has been conjectured that they are connected by a conformal manifold for $2<k<3$ [49]. A generic point on this conformal manifold would be described by a potential given by the superposition of the Liouville and sine-Liouville potentials. Only the ratio μ/λ of their coefficients is meaningful because one or the other may be scaled away by a field redefinition, so the conformal manifold would be one-dimensional, with Liouville $\times$ S^1 at one end ($\mu/\lambda=\infty$) and $\mathrm{SL}(2,\mathbb{R})_k/\mathrm{U}(1)$ at the other ($\mu/\lambda=0$).

At the pure Liouville$\times\mathrm{S}^1$ point, one expects to find a marginal operator $e^{-2b_{\mathrm{sL}}\hat{r}}\mathrm{Re}\, e^{i\sqrt{\frac{k}{\alpha'}}(\hat{\theta}_{\mathrm{L}}-\hat{\theta}_{\mathrm{R}})}$ which drives one along the conformal manifold toward $\mathrm{SL}(2,\mathbb{R})_k/\mathrm{U}(1)$ under a conformal perturbation. The sine-Liouville momentum $b_{\mathrm{sL}}=\frac{1}{2}\sqrt{\frac{k-2}{\alpha'}}$ is a positive real number and, for $2<k<3$, it satisfies the Seiberg bound $b_{\mathrm{sL}}<\frac{Q}{2}$. Thus, one indeed has a non-normalizable real-branch Liouville$\times\mathrm{S}^1$ primary operator labeled by b_{sL} that approaches the sine-Liouville potential in the weak-coupling region. For $k>3$, however, b_{sL} violates the Seiberg bound. Then it is instead the reflected component $e^{-2(Q-b_{\mathrm{sL}})\hat{r}}$ that dominates in the weak-coupling region, and does not reproduce the sine-Liouville asymptotics.

On the $\mathrm{SL}(2,\mathbb{R})_k/\mathrm{U}(1)$ side, one would similarly expect to find a marginal Liouville op-

erator $e^{-2b_{\rm L}\hat{r}}$, where

$$b_{\rm L} = \frac{1}{2}\left(\frac{1-\sqrt{9-4k}}{\sqrt{\alpha'(k-2)}}\right), \tag{2.238}$$

corresponding to a primary $\mathcal{O}_{jnw}$ with

$$j_{\rm L} = \frac{1}{2}\left(1+\sqrt{9-4k}\right) \tag{2.239}$$

and $n = w = 0$. For $k > 9/4$, one finds $j_{\rm L} \in \frac{1}{2}+i\mathbb{R}$, and the Liouville operator is thus a delta-functional normalizable primary on the complex branch of the $\mathrm{SL}(2,\mathbb{R})_k/\mathrm{U}(1)$ Hilbert space. Though this operator exists even for $k > 3$, beyond that value the $\mathrm{SL}(2,\mathbb{R})_k/\mathrm{U}(1)$ CFT (and its parent $\mathrm{SL}(2,\mathbb{R})_k$ WZW model) undergoes a phase transition [54, 83]. For $2 < k < \frac{9}{4}$, on the other hand, one finds $\frac{1}{2} < j < 1$, and the Liouville operator is a non-normalizable real branch primary.[38] The cross-over point $k = 9/4$ corresponds to the critical string theory for which $c = 26$.

2.5.2 sine-Liouville Limit

We now comment on to what extent one may understand the $k \to 2$ limit of the $\mathrm{SL}(2,\mathbb{R})_k/\mathrm{U}(1)$ reflection coefficient by a saddle-point expansion of the sine-Liouville functional integral.

[38] Presumably it descends from a non-normalizable complementary series primary $|j, m = 0, \bar{m} = 0\rangle \in \mathcal{E}_{j,\alpha=0}$ of $\mathrm{SL}(2,\mathbb{R})_k$, in the terminology of [76].

The action with insertions of $\mathcal{O}_{jnw}$ in the far past and $\mathcal{O}_{j,-n,-w}$ in the far future is

$$\begin{aligned} S_{jnw} =& \frac{1}{4\pi\alpha'}\int_{-L}^{L}\mathrm{d}\rho\int_{0}^{2\pi}\mathrm{d}\phi\left((\partial_\rho\hat{r})^2+(\partial_\phi\hat{r})^2+(\partial_\rho\hat{\vartheta})^2+(\partial_\phi\hat{\vartheta})^2+8\pi\lambda e^{-2b_{\mathrm{sL}}\hat{r}}\cos\left(\sqrt{\frac{k}{\alpha'}}\hat{\vartheta}\right)\right) \\ &-\frac{2}{\sqrt{\alpha'(k-2)}}\left(j-\frac{1}{2}\right)\int_0^{2\pi}\frac{\mathrm{d}\phi}{2\pi}\left(\hat{r}|_{\rho=L}+\hat{r}|_{\rho=-L}\right)-iw\sqrt{\frac{k}{\alpha'}}\int_0^{2\pi}\frac{\mathrm{d}\phi}{2\pi}\left(\hat{\vartheta}|_{\rho=L}-\hat{\vartheta}|_{\rho=-L}\right) \\ &+\int_0^{2\pi}\frac{\mathrm{d}\phi}{2\pi}\left(\sigma_+\left(\partial_\phi\hat{\vartheta}|_{\rho=L}-n\sqrt{\frac{\alpha'}{k}}\right)+\sigma_-\left(\partial_\phi\hat{\theta}|_{\rho=-L}-n\sqrt{\frac{\alpha'}{k}}\right)\right) \\ &+\frac{4}{k-2}\left(j-\frac{1}{2}\right)^2L-kw^2L-\frac{L}{k}n^2. \end{aligned} \tag{2.240}$$

Note that the boundary action for $\hat{\vartheta}$ is well-defined because $w\in\mathbb{Z}$.

Let us again restrict our attention to the $n=0$ sector, where the $k-2\to 0$ limit of the exact reflection coefficient Eqn. 2.138 yields

$$\begin{aligned} R(j,w)\overset{k-2\to 0}{\longrightarrow}& 2^{4\left(j-\frac{1}{2}\right)}\left(j-\frac{1}{2}\right)\frac{\gamma(j+w)\gamma(j-w)}{\gamma(2j)} \\ &\times\left(\frac{e}{2}\frac{k-2}{j-\frac{1}{2}}\right)^{\frac{4}{k-2}\left(j-\frac{1}{2}\right)}\csc\left(\frac{2\pi}{k-2}\left(j-\frac{1}{2}\right)\right), \end{aligned} \tag{2.241}$$

where $j=\mathcal{O}(k^0)$ and $\mathrm{Re}(j)>\frac{1}{2}$. Note that the second line, which is the dominant contribution, is independent of w.

In this limit, the most interesting factor in Eqn. 2.138 is $\gamma\left(\frac{2j-1}{k-2}\right)$, which leads to the csc factor of Eqn. 2.241. The latter arises in the saddle-point expansion from the following shift

symmetry of the sine-Liouville potential:

$$\hat{r} \to \hat{r} + \frac{\pi i}{2b_{\mathrm{sL}}} \tag{2.242a}$$

$$\hat{\vartheta} \to \hat{\vartheta} + \pi\sqrt{\frac{\alpha'}{k}}, \tag{2.242b}$$

under which the linear-dilaton and compact-boson factors of the potential each transform by a sign. By the same argument as before, the functional integral over real $\hat{r}$ diverges and should instead be defined over an appropriate complex cycle. We expect that the cycle will consist of a sum of steepest-descent contours associated to saddles related by the shift symmetry. Under the shift, the action changes by

$$S \to S - \frac{4\pi i}{k-2}\left(j - \frac{1}{2}\right), \tag{2.243}$$

due to the boundary terms. Summing over this discrete moduli space will contribute

$$\sum_{N \in \mathbb{Z}_{\geq 0}} e^{\frac{4\pi i}{k-2}\left(j-\frac{1}{2}\right)N} = \frac{i}{2} e^{-\frac{2\pi i}{k-2}\left(j-\frac{1}{2}\right)} \csc\left(\frac{2\pi}{k-2}\left(j - \frac{1}{2}\right)\right) \tag{2.244}$$

for $\mathrm{Im}(j) > 0$, reproducing the csc in Eqn. 2.241. For $\mathrm{Im}(j) < 0$, one sums over $N \in \mathbb{Z}_{\leq 0}$.

Because the sine-Liouville Lagrangian is not actually weakly coupled, it is more challenging to reproduce the rest of Eqn. 2.241 by the saddle-point expansion. To attempt to extract the $\frac{1}{k-2}$ scaling from the action, one would define

$$\tilde{r} = \sqrt{\frac{k-2}{\alpha'}}\hat{r}, \qquad \tilde{\vartheta} = \sqrt{\frac{k-2}{\alpha'}}\hat{\vartheta}, \qquad \tilde{\lambda} = \frac{k-2}{\alpha'}\lambda, \tag{2.245}$$

in terms of which

$$S_{jw} = \frac{1}{k-2}\Bigg\{ \frac{1}{4\pi}\int_{-L}^{L} \mathrm{d}\rho \int_{0}^{2\pi} \mathrm{d}\phi \left((\partial_\rho \tilde{r})^2 + (\partial_\phi \tilde{r})^2 + (\partial_\rho \tilde{\vartheta})^2 + (\partial_\phi \tilde{\vartheta})^2 + 8\pi\tilde{\lambda} e^{-\tilde{r}} \cos\left(\sqrt{\frac{k}{k-2}}\tilde{\vartheta}\right)\right)$$
$$- 2\left(j-\frac{1}{2}\right)\int_0^{2\pi}\frac{\mathrm{d}\phi}{2\pi}\left(\tilde{r}|_{\rho=L} + \tilde{r}|_{\rho=-L}\right) - iw\sqrt{k(k-2)}\int_0^{2\pi}\frac{\mathrm{d}\phi}{2\pi}\left(\tilde{\vartheta}|_{\rho=L} - \tilde{\vartheta}|_{\rho=-L}\right)$$
$$+ 4\left(j-\frac{1}{2}\right)^2 L - k(k-2)w^2 L\Bigg\}. \tag{2.246}$$

Were the functional in braces $\mathcal{O}((k-2)^0)$, one could proceed with the saddle-point expansion as in the preceding sections. However, the sine-Liouville potential oscillates rapidly in this limit, reflecting the fact that the description is not weakly coupled.

We will not attempt to reproduce the rest of the semi-classical limit using the sine-Liouville description. We point out, however, that the second line of Eqn. 2.241 coincides with the leading terms in the semi-classical limit of the Liouville reflection coefficient (Eqn. 2.71). It was shown in [84] that winding-preserving n-point functions in the $\mathrm{SL}(2,\mathbb{R})_k/\mathrm{U}(1)$ CFT are reproduced by a sum of $2n-2$ point correlation functions in Liouville. In particular, the two-point function of the coset is simply related to the two-point function of Liouville, with a certain dictionary described in [84], and one correspondingly finds that their semi-classical limits are closely related.

3 State Dependence of String Perturbation Theory

Our principal goal in the remainder of this work is to construct examples of string dualities that realize ER = EPR. That is, we will give examples where the theory of a string in a connected target spacetime, such as a two-sided black hole, is equivalent to the theory of a string in a disconnected, but entangled, spacetime. We will describe these dualities in the next chapter. Their formulation, however, requires some lesser-known types of string theories, such as string perturbation theory around a thermofield-double state. In this chapter, we lay the groundwork for constructing such string perturbation theories, emphasizing the case of asymptotic AdS_3 about which the most is understood.

String perturbation theory is often phrased as an expansion around a Lorentzian spacetime solution. However, this is not entirely precise. Even in the non-linear sigma-model approximation at leading order in α', the target space time direction has wrong-sign kinetic terms, and so the definition of the worldsheet functional integral requires the specification

of an appropriate contour in a complexification of the target space. Such contours are string theory analogues of the Schwinger-Keldysh contours familiar from field theory. They consist of Euclidean caps that specify the spacetime state, with the Lorentzian background glued between them.

It is important to emphasize that one needs to specify a spacetime state, and not merely a classical Lorentzian solution, in order to formulate a string perturbation theory. In many applications, it is implicit that one has chosen the spacetime vacuum and so the choice of state may not be stressed. In the examples of ER = EPR we describe in the next chapter, however, that will not be the case. The EPR string theories will be defined around the thermofield-double state in two disconnected copies of the target space. That string perturbation theory is of course different from string theory in the same pair of Lorentzian spacetimes in the factorized vacuum. The choice of state is encoded by the Euclidean caps of the Schwinger-Keldysh contour or, more abstractly, by the unitary CFT one uses to define the Lorentzian theory, and the choice of continuation one makes in doing so.

We begin in Sec. 3.1 by reviewing the geometry of AdS_3 itself, as well as its Euclidean continuation, and the $SL(2,\mathbb{R})_k$ and $SL(2,\mathbb{C})_k/SU(2)$ CFTs that describe a string propagating on those manifolds. Having done so, we then follow-up on the discussion of the cigar background from Sec. 2.3 by describing the coset construction of the $SL(2,\mathbb{R})_k/U(1)$ CFT from $SL(2,\mathbb{R})_k$ in Sec. 3.2. In Sec. 3.3 we come to the formulation of Lorentzian string perturbation theory in various states.

3.1 Review of the $SL(2,\mathbb{R})_k$ and $SL(2,\mathbb{C})_k/SU(2)$ CFTs

In this section we review the $SL(2,\mathbb{R})_k$ and $SL(2,\mathbb{C})_k/SU(2)$ CFTs that describe a string propagating in AdS_3 and Euclidean AdS_3.

3.1.1 Geometry of AdS_3

Let us first review the geometry of AdS_3. Anti de Sitter (AdS) spacetime is the maximally-symmetric vacuum solution of Einstein gravity with negative cosmological constant. Namely, one considers the theory defined by the action

$$S = \frac{1}{2\kappa^2}\int \mathrm{d}^D X\sqrt{-g}(\mathcal{R} - 2\Lambda), \tag{3.1}$$

whose equations of motion are

$$\mathcal{R}_{\mu\nu} = \frac{2\Lambda}{D-2}g_{\mu\nu}. \tag{3.2}$$

When the cosmological constant Λ is a negative number, one writes $\Lambda = -1/l^2_{\mathrm{AdS}}$. Specializing to $D = 3$, which will be the case of interest, one obtains

$$\mathcal{R}_{\mu\nu} = -\frac{2}{l^2_{\mathrm{AdS}}}g_{\mu\nu}. \tag{3.3}$$

(a) AdS_3 **in Cylinder Coordinates.** **(b)** EAdS_3 **in Poincaré Coordinates.**

Figure 3.1

AdS_3 is the simplest solution, given by

$$\mathrm{d}s^2_{\mathrm{AdS}} = l^2_{\mathrm{AdS}} \left(-\cosh^2(r)\mathrm{d}t^2 + \mathrm{d}r^2 + \sinh^2(r)\mathrm{d}\theta^2 \right). \tag{3.4}$$

In these coordinates, it may be thought of as a solid cylinder (Fig. 3.1a), with radial coordinate $r \in [0, \infty)$, angular coordinate $\theta \sim \theta + 2\pi$, and Lorentzian time coordinate $t \in (-\infty, \infty)$ running along its length.

AdS_3 is equivalent to the Lie group $\mathrm{SL}(2, \mathbb{R})$, as may be seen from the parameterization[39]

$$g = e^{i(t+\theta)\mathrm{T}_3} e^{2ir\mathrm{T}_2} e^{i(t-\theta)\mathrm{T}_3} \in \mathrm{SL}(2, \mathbb{R}), \tag{3.5}$$

[39] $e^{\pm 2\pi i \mathrm{T}_3} = -\mathbf{1}$, and therefore g is invariant under both $t \to t + 2\pi$ and $\theta \to \theta + 2\pi$. By $\mathrm{AdS}_3 = \mathrm{SL}(2, \mathbb{R})$, we mean the covering space where t is decompactified.

which yields

$$g = \begin{pmatrix} \sinh(r)\cos(\theta) + \cosh(r)\cos(t) & -\sinh(r)\sin(\theta) + \cosh(r)\sin(t) \\ -\sinh(r)\sin(\theta) - \cosh(r)\sin(t) & -\sinh(r)\cos(\theta) + \cosh(r)\cos(t) \end{pmatrix}, \tag{3.6}$$

where $\mathrm{T}_1 = -\frac{i}{2}\sigma_1$, $\mathrm{T}_2 = -\frac{i}{2}\sigma_3$, and $\mathrm{T}_3 = \frac{1}{2}\sigma_2$ are a basis of $\mathfrak{sl}(2,\mathbb{R})$, satisfying $[\mathrm{T}_i, \mathrm{T}_j] = i\epsilon_{ijk}\eta^{kl}\mathrm{T}_l$, with metric $\eta_{ij} = 2\mathrm{tr}(\mathrm{T}_i\mathrm{T}_j) = \mathrm{Diag}(-1,-1,1)_{ij}$. The AdS_3 metric Eqn. 3.4 is then reproduced by the usual group metric

$$\mathrm{d}s^2_{\mathrm{SL}(2,\mathbb{R})} = \frac{1}{2}l^2_{\mathrm{AdS}}\mathrm{tr}\left(g^{-1}\mathrm{d}g g^{-1}\mathrm{d}g\right). \tag{3.7}$$

The obvious symmetries of Eqn. 3.4 are translations in t and θ. The group structure makes it evident that the full isometry algebra is $\mathfrak{sl}(2,\mathbb{R}) \oplus \mathfrak{sl}(2,\mathbb{R})$, which is six-dimensional. AdS_3 is therefore maximally symmetric, meaning it has as many isometries as $\mathbb{R}^3$.

The Lie algebra $\mathfrak{sl}(2,\mathbb{R}) \oplus \mathfrak{sl}(2,\mathbb{R})$ is equivalent to $\mathfrak{so}(2,2)$. The latter is the Lorentz algebra of $\mathbb{R}^{2,2}$, and indeed AdS_3 may be identified with a hyperboloid embedded in $\mathbb{R}^{2,2}$, just as a sphere S^2 in $\mathbb{R}^3$ inherits the rotation algebra $\mathfrak{so}(3)$ of the embedding space. To understand the embedding, let X^{-1}, X^0, X^1, and X^2 denote coordinates on $\mathbb{R}^{2,2}$, with metric

$$\frac{1}{l^2_{\mathrm{AdS}}}\mathrm{d}s^2_{\mathbb{R}^{2,2}} = -(\mathrm{d}X^{-1})^2 - (\mathrm{d}X^0)^2 + (\mathrm{d}X^1)^2 + (\mathrm{d}X^2)^2. \tag{3.8}$$

As four-dimensional real vector spaces, we may define an isomorphism of $\mathbb{R}^{2,2}$ and $\mathrm{GL}(2,\mathbb{R})$

by

$$g = \begin{pmatrix} X^{-1} + X^1 & X^2 + X^0 \\ X^2 - X^0 & X^{-1} - X^1 \end{pmatrix}. \tag{3.9}$$

Note that

$$-\det(g) = -(X^{-1})^2 - (X^0)^2 + (X^1)^2 + (X^2)^2, \tag{3.10}$$

and therefore $\mathrm{AdS}_3 = \mathrm{SL}(2,\mathbb{R})$ is the subspace of $\mathbb{R}^{2,2}$ laying on the hyperboloid

$$-(X^{-1})^2 - (X^0)^2 + (X^1)^2 + (X^2)^2 = -1. \tag{3.11}$$

The $\mathrm{SO}(2,2)$ isometries of the hyperboloid coincide with the $[\mathrm{SL}(2,\mathbb{R}) \times \mathrm{SL}(2,\mathbb{R})]/\mathrm{Z}_2$ transformations $g \to \Gamma_{\mathrm{L}} g \Gamma_{\mathrm{R}}^{-1}$ of $\mathrm{GL}(2,\mathbb{R})$ that preserve $\det(g) = 1$. The cylinder coordinates of Eqn. 3.5 correspond to the parameterization[40]

$$X^{-1} = \cos(t)\cosh(r) \tag{3.12a}$$

$$X^0 = \sin(t)\cosh(r) \tag{3.12b}$$

$$X^1 = \cos(\theta)\sinh(r) \tag{3.12c}$$

$$X^2 = -\sin(\theta)\sinh(r), \tag{3.12d}$$

with the pullback of the $\mathbb{R}^{2,2}$ metric Eqn. 3.8 reproducing Eqn. 3.4.

[40] Again, the invariance of this parameterization under $t \to t + 2\pi$ reflects the periodicity of t in $\mathrm{SL}(2,\mathbb{R})$, which is decompactified in the covering space AdS_3.

Consider next the Euclidean continuation of AdS_3, obtained from Eqn. 3.4 by continuing $\xi = it$,

$$ds^2_{\text{EAdS}} = l^2_{\text{AdS}} \left(\cosh^2(r)d\xi^2 + dr^2 + \sinh^2(r)d\theta^2\right), \tag{3.13}$$

with $\xi \in (-\infty, \infty)$. This is the manifold Euclidean AdS_3 ($EAdS_3$), and it is the maximally symmetric solution of Einstein's equations in Euclidean signature.

Performing the same continuation in Eqn. 3.5 yields not a group, but a parameterization of the vector space of 2×2 Hermitian matrices with unit determinant and positive eigenvalues. Likewise, the parameterization Eqn. 3.12 becomes

$$X^{-1} = \cosh(\xi)\cosh(r) \tag{3.14a}$$

$$X^1 = \cos(\theta)\sinh(r) \tag{3.14b}$$

$$X^2 = -\sin(\theta)\sinh(r) \tag{3.14c}$$

$$X^3 = \sinh(\xi)\cosh(r), \tag{3.14d}$$

where $X^3 = iX^0$, and

$$g = \begin{pmatrix} X^{-1} + X^1 & X^2 - iX^3 \\ X^2 + iX^3 & X^{-1} - X^1 \end{pmatrix} \tag{3.15}$$

defines an isomorphism of $\mathbb{R}^{1,3}$ and the space of Hermitian matrices. The unit determinant

condition restricts to the hyperboloid

$$-\det(g) = -(X^{-1})^2 + (X^1)^2 + (X^2)^2 + (X^3)^2 = -1, \tag{3.16}$$

and the constraint of positive eigenvalues picks out the sheet $X^{-1} \geq 1$. Thus, EAdS_3 is identified with the upper sheet of a hyperboloid embedded in $\mathbb{R}^{1,3}$. The $\mathrm{SO}(1,3)$ Lorentz symmetry of the hyperboloid now coincides with the $\mathrm{SL}(2,\mathbb{C})/\mathrm{Z}_2$ action $g \to \Gamma g \Gamma^\dagger$ on the space of matrices that preserves the determinant, required to act by conjugation to preserve Hermiticity. This is the familiar identification of $\mathrm{SL}(2,\mathbb{C}) = \mathrm{Spin}(1,3)$ with the double cover of the four-dimensional Lorentz group.[41]

In particular, we find that $\mathfrak{so}(1,3) \simeq \mathfrak{sl}(2,\mathbb{C})$ is the isometry algebra of EAdS_3, where $\mathfrak{sl}(2,\mathbb{C})$ is regarded as a real six-dimensional Lie algebra. Note also that the $\mathfrak{so}(1,3)$ and $\mathfrak{so}(2,2)$ isometry algebras of EAdS_3 and AdS_3 are two real forms of the same complexification $\mathfrak{sl}(2,\mathbb{C}) \oplus \mathfrak{sl}(2,\mathbb{C})$. In AdS/CFT, the former are identified with the boundary CFT_2 global conformal algebras in Euclidean and Lorentzian signature, and the latter is the complexified global conformal algebra.

The action $g \to \Gamma g \Gamma^\dagger$ of $\mathrm{SL}(2,\mathbb{C})$ on the space of 2×2 Hermitian matrices with unit determinant and positive eigenvalues is transitive. The stabilizer of, say, $g = \mathrm{Diag}(1,1)$ is $\mathrm{SU}(2)$. Thus, the vector space, and equivalently EAdS_3, is identified with the coset manifold $\mathrm{SL}(2,\mathbb{C})/\mathrm{SU}(2)$, analogous e.g. to the identification $\mathrm{S}^2 = \mathrm{SO}(3)/\mathrm{SO}(2)$.

Another convenient coordinate system on EAdS_3 is related to the cylinder coordinates of

[41] Or rather its connected component.

Eqn. 3.13 by

$$\sigma = -\xi + \log\cosh r \tag{3.17a}$$

$$\gamma = \tanh(r) e^{\xi + i\theta} \tag{3.17b}$$

$$\bar{\gamma} = \tanh(r) e^{\xi - i\theta}, \tag{3.17c}$$

in terms of which the metric becomes

$$\mathrm{d}s^2_{\mathrm{EAdS}} = l^2_{\mathrm{AdS}} \left(\mathrm{d}\sigma^2 + e^{2\sigma} \mathrm{d}\gamma \mathrm{d}\bar{\gamma} \right). \tag{3.18}$$

These are called Poincarè coordinates (Fig. 3.1b). γ is a complex coordinate, $\bar{\gamma}$ is its complex conjugate, and $\sigma \in (-\infty, \infty)$. At the conformal boundary $r \to \infty$, note that $\gamma \to e^{\xi + i\theta}$ is the usual conformal map between the boundary sphere with complex coordinate γ and the boundary cylinder with complex coordinate $W \equiv \xi + i\theta$.

Having reviewed the geometry of $\mathrm{AdS}_3 = \mathrm{SL}(2,\mathbb{R})$ and $\mathrm{EAdS}_3 = \mathrm{SL}(2,\mathbb{C})/\mathrm{SU}(2)$, we next discuss the $\mathrm{SL}(2,\mathbb{R})_k$ WZW model and $\mathrm{SL}(2,\mathbb{C})_k/\mathrm{SU}(2)$ coset model that describe a string on these manifolds.

3.1.2 $\mathrm{SL}(2,\mathbb{R})_k$ Spectrum

In light of the equivalence $\mathrm{AdS}_3 = \mathrm{SL}(2,\mathbb{R})$, it is natural to describe a string propagating in AdS_3 by the $\mathrm{SL}(2,\mathbb{R})_k$ WZW model [46,76,85–88]. The WZW level k, which is a real number greater than 2, sets the AdS length scale, $l^2_{\mathrm{AdS}} = \alpha' k = l_{\mathrm{s}}^2 k$. AdS_3 has constant negative

curvature $\mathcal{R} = -6/l_{\text{AdS}}^2$, meaning the background defined by the metric Eqn. 3.4 alone is certainly not conformal invariant. In the $\text{SL}(2,\mathbb{R})_k$ WZW model, conformal symmetry on the worldsheet is supported by a B-field that is contributed by the Wess-Zumino term in the WZW action, $\text{tr}\big((g^{-1}\text{d}g)^{\wedge 3} \big) \propto \text{d}B$, with $B \propto \sinh^2(r)\text{d}t \wedge \text{d}\theta$. The dilaton, meanwhile, is a constant, and the central charge is

$$c = \frac{3k}{k-2}. \tag{3.19}$$

One must be careful, however, to define what one means by the $\text{SL}(2,\mathbb{R})_k$ WZW model. The usual WZW action is inadequate; since the metric is Lorentzian, the WZW action includes wrong-sign kinetic terms:

$$\begin{aligned} S = \frac{k}{2\pi}\int \text{d}^2z\big\{ &-\cosh^2(r)\partial t\bar{\partial}t + \partial r\bar{\partial}r + \sinh^2(r)\partial\theta\bar{\partial}\theta \\ &- \sinh^2(r)(\partial t\bar{\partial}\theta - \bar{\partial}t\partial\theta)\big\}. \end{aligned} \tag{3.20}$$

The naive functional integral is therefore divergent and must be defined by a more careful prescription. The ambiguity is meaningful and corresponds to the need to choose a state in spacetime around which one wishes to build a string perturbation theory. The ER = EPR string dualities that we describe in the next chapter will refer to string perturbation theories in various states. The appropriate worldsheet theories are defined by analytic continuation from unitary CFTs, which encode the choice of state. By the $\text{SL}(2,\mathbb{R})_k$ WZW model we mean the theory of a string in AdS_3 in the spacetime vacuum state, which is defined by continuation from the theory with target EAdS_3. We elaborate on this procedure and discuss examples

of different choices of states in Sec. 3.3. Before addressing those generalizations, we first review the spectrum of a string in the AdS_3 vacuum, as constructed in [76].

Observe from Eqn. 3.5 that the obvious isometries of the AdS_3 metric in cylinder coordinates, namely time translations $t \to t + \delta t$ and rotations $\theta \to \theta + \delta\theta$, are implemented in $\mathrm{SL}(2,\mathbb{R})$ by $g \to e^{i\delta t \mathrm{T}_3} g e^{i\delta t \mathrm{T}_3}$ and $g \to e^{i\delta\theta \mathrm{T}_3} g e^{-i\delta\theta \mathrm{T}_3}$. The time translation and rotation generators in the WZW model are therefore the charges $J_0^3 + \bar{J}_0^3$ and $J_0^3 - \bar{J}_0^3$, whose eigenvalues are the spacetime energy and angular momentum. The full list of generators $\{J_0^3, J_0^\pm\} \cup \{\bar{J}_0^3, \bar{J}_0^\pm\}$ of the $\mathfrak{sl}(2,\mathbb{R})_\mathrm{L} \oplus \mathfrak{sl}(2,\mathbb{R})_\mathrm{R}$ isometry algebra, written in the raising/lowering basis, satisfy

$$[J_0^3, J_0^\pm] = \pm J_0^\pm, \quad [J_0^+, J_0^-] = -2J_0^3, \tag{3.21}$$

and similarly for $\bar{J}_0^a$, with $[J_0^a, \bar{J}_0^b] = 0$.

As is usual in WZW models, the target isometry algebra $\mathfrak{sl}(2,\mathbb{R})_\mathrm{L} \oplus \mathfrak{sl}(2,\mathbb{R})_\mathrm{R}$ is extended to a current algebra $\widehat{\mathfrak{sl}}_k(2,\mathbb{R})_\mathrm{L} \oplus \widehat{\mathfrak{sl}}_k(2,\mathbb{R})_\mathrm{R}$:

$$[J_A^3, J_B^3] = -\frac{k}{2} A \delta_{A+B} \tag{3.22a}$$

$$[J_A^3, J_B^\pm] = \pm J_{A+B}^\pm \tag{3.22b}$$

$$[J_A^+, J_B^-] = -2J_{A+B}^3 + kA\delta_{A+B}, \tag{3.22c}$$

J_A^a being the modes of the currents $\{J^a(z)\}_{a=3,\pm}$, $J^a(z) = \sum_{A\in\mathbb{Z}} J_A^a / z^{A+1}$. Likewise one has anti-holomorphic modes $\bar{J}_A^a$ of the currents $\bar{J}^a(\bar{z})$, which satisfy the same algebra and commute with the holomorphic modes. The isometry algebra corresponds to the global

sub-algebra generated by the zero-modes $J^a_0, \bar{J}^a_0$.

The $\mathrm{SL}(2,\mathbb{R})_k$ Hilbert space is organized in representations of this current algebra [76]. These representations come in two varieties. The first are the familiar sort of current algebra representation: one begins with a unitary representation of the global sub-algebra generated by $\left\{J^a_0, \bar{J}^a_0\right\}$, demands it is annihilated by the positive modes $\left\{J^a_A, \bar{J}^a_A\right\}_{A>0}$, and then builds the current-algebra representation by action of the negative modes $\left\{J^a_A, \bar{J}^a_A\right\}_{A<0}$. Unlike the compact case, these representations include states of negative, though bounded-below, conformal weights, as well as states of negative norm. The second variety of representations is less familiar, owing to the non-compactness of $\mathrm{SL}(2,\mathbb{R})$. They arise due to an automorphism of the current algebra, called the spectral-flow automorphism. They again include negative norm states, and in this case the conformal weights need not even be bounded below. These peculiarities are to be expected, in light of the Lorentzian signature of the target space. Combined with an internal CFT of appropriate central charge to cancel the conformal anomaly, one obtains a unitary string spectrum, aside from the usual tachyon, after imposing the Virasoro constraints [76].

The Virasoro modes $\{L_A, \bar{L}_A\}$ are built as usual using the Sugawara construction, and satisfy the Virasoro algebra with central charge Eqn. 3.19. Their commutation relations with the currents modes are

$$[L_A, J^a_B] = -B J^a_{A+B}, \tag{3.23}$$

and likewise for the anti-holomorphic modes. J^a_{-A} with $A > 0$ is a raising operator for L_0

by A units, $[L_0, J^a_{-A}] = AJ^a_{-A}$, and $J^\pm_{-A}$ is a raising/lowering operator for J^3_0 by one unit, $[J^3_0, J^\pm_{-A}] = \pm J^\pm_{-A}$.

Let us first describe the ordinary representations. They are labeled by the global $\mathfrak{sl}(2,\mathbb{R})_{\mathrm{L}} \oplus \mathfrak{sl}(2,\mathbb{R})_{\mathrm{R}}$ representation on which they are built. An $\mathfrak{sl}(2,\mathbb{R})$ representation is labeled by its spin, j, which is related to the quadratic Casimir,

$$c_2 = \frac{1}{2}\left(J^+_0 J^-_0 + J^-_0 J^+_0\right) - (J^3_0)^2, \tag{3.24}$$

by $c_2 = -j(j-1)$. The $\mathfrak{sl}(2,\mathbb{R})$ representations that appear in the $\mathrm{SL}(2,\mathbb{R})_k$ WZW model are called the discrete series, for which j is a positive real number, and the continuous series, for which $j \in \frac{1}{2} + i\mathbb{R}$. We will write the states in a J^3_0-diagonal basis $|j,m\rangle$, where $J^3_0 |j,m\rangle = m |j,m\rangle$.

The discrete-series representations come in two flavors, denoted by $D^\pm_j$, where the $+$ indicates a lowest-weight representation and the $-$ a highest-weight representation. In the former case, one begins with a lowest-weight state $|j,j\rangle$ annihilated by J^-_0, and constructs the remaining states by action of J^+_0:

$$D^+_j = \{|j,m\rangle : m = j, j+1, j+2, \ldots\}. \tag{3.25}$$

Similarly, the highest-weight representation D^-_j is built on a highest-weight state $|j,-j\rangle$

annihilated by J_0^+, with the remaining states constructed by action of J_0^-:

$$D_j^- = \{|j,m\rangle : m = -j, -j-1, -j-2, \ldots\}\,. \tag{3.26}$$

The continuous-series representations, denoted by $C_{j,\alpha}$, consist of an infinite tower of states:

$$C_{j,\alpha} = \{|j,m\rangle : m = \alpha, \alpha \pm 1, \alpha \pm 2, \ldots\}\,. \tag{3.27}$$

α is an additional parameter valued in $[0,1)$. Note that for the discrete-series states, the J_0^3 eigenvalue is equal to j modulo an integer, whereas for the continuous-series states the J_0^3 eigenvalue is unrelated to j.

On a global $\mathfrak{sl}(2,\mathbb{R})$ representation $D_j^\pm$ or $C_{j,\alpha}$ consisting of states $|j,m\rangle$, an $\widehat{\mathfrak{sl}}_k(2,\mathbb{R})$ current-algebra representation is obtained by demanding that these states are primary:

$$J^a_{A>0}\,|j,m\rangle = 0. \tag{3.28}$$

The remaining states of the current-algebra representation are then obtained by action of the negative modes $J^a_{A<0}$. We denote by $\widehat{D}_j^\pm$ and $\widehat{C}_{j,\alpha}$ the current-algebra representations built on the primaries $D_j^\pm$ and $C_{j,\alpha}$. The current-algebra primaries $|j,m\rangle$ are also Virasoro

primary,

$$L_0 \left|j,m\right\rangle = h_j \left|j,m\right\rangle \tag{3.29a}$$

$$L_{A>0} \left|j,m\right\rangle = 0, \tag{3.29b}$$

with conformal weight

$$h_j = -\frac{j(j-1)}{k-2}. \tag{3.30}$$

Note that the quadratic Casimir $c_2 = -j(j-1)$, and by extension h_j, is a positive real number in the continuous series, $c_2 = |j|^2$, whereas it is positive in the discrete series only in the window between zero and one. c_2 is a constant of the representation, and so every primary state $|j,m\rangle$ carries the same conformal weight h_j, independent of m.

The $\widehat{\mathfrak{sl}}_k(2,\mathbb{R})_{\mathrm{L}} \oplus \widehat{\mathfrak{sl}}_k(2,\mathbb{R})_{\mathrm{R}}$ representations of this form that appear in the spectrum of the $\mathrm{SL}(2,\mathbb{R})_k$ WZW model are [76]

$$\mathcal{H}_{\mathrm{SL}(2,\mathbb{R})_k} \supset \bigoplus_{j,\alpha} \begin{cases} \widehat{D}^+_j \otimes \widehat{D}^+_j & j \in \left(\frac{1}{2}, \frac{k-1}{2}\right) \\ \widehat{C}_{j,\alpha} \otimes \widehat{C}_{j,\alpha} & j \in \frac{1}{2} + i\mathbb{R}_+,\ \alpha \in [0,1). \end{cases} \tag{3.31}$$

It will become clear shortly why the highest-weight discrete-series representations are not included here. As usual in WZW models, the relevant representations carry the same spin j on the left and right, as well as the same α in the continuous series. It follows that the difference of the J^3_0 and $\bar{J}^3_0$ eigenvalues is an integer, consistent with the quantization of

angular momentum around the compact cycle of the AdS_3 cylinder, which is generated by $J_0^3 - \bar{J}_0^3$.

Next we discuss the less familiar spectral-flowed representations of the current algebra, denoted by $\widehat{D}_j^{\pm,w}$ and $\widehat{C}_{j,\alpha}^{w}$ with an additional integer label w. These arise due to an automorphism of the $\widehat{\mathfrak{sl}}_k(2,\mathbb{R})$ current algebra called the spectral-flow automorphism. This is a map $J_A^a \to J_A^a[w]$ that preserves Eqn. 3.22:

$$J_A^3[w] = J_A^3 - \frac{k}{2} w \delta_A \tag{3.32a}$$

$$J_A^\pm[w] = J_{A\pm w}^\pm. \tag{3.32b}$$

It is additive, $(J_A^a[w_1])[w_2] = J_A^a[w_1 + w_2]$, and $J_A^a[0] = J_A^a$.

States in spectral-flowed representations transform as ordinary representations under $J_A^a[w]$, with the action of J_A^a then determined by the inverse automorphism

$$J_A^3 = J_A^3[w] + \frac{k}{2} w \delta_A \tag{3.33a}$$

$$J_A^\pm = J_{A\mp w}^\pm[w]. \tag{3.33b}$$

The Virasoro modes, being obtained from the currents by the Sugawara construction, in turn transform under spectral flow:

$$L_A = L_A[w] - w J_A^3[w] - \frac{1}{4} k w^2 \delta_A. \tag{3.34}$$

Thus, the spectral flow of a primary state $|j,m;w\rangle$ transforms under $J^a_A[w]$ as an ordinary primary,

$$J^3_0[w] \quad |j,m;w\rangle = m\,|j,m;w\rangle \tag{3.35a}$$

$$J^\pm_0[w] \quad |j,m;w\rangle \propto |j,m\pm 1;w\rangle \tag{3.35b}$$

$$J^a_{A>0}[w]\,|j,m;w\rangle = 0, \tag{3.35c}$$

with

$$L_0[w] \quad |j,m;w\rangle = h_j\,|j,m;w\rangle \tag{3.36a}$$

$$L_{A>0}[w]\,|j,m;w\rangle = 0. \tag{3.36b}$$

The action of J^a_A and L_A on the same state is then determined by Eqns. 3.33-3.34. In particular, the J^3 and conformal weights are

$$J^3_0\,|j,m;w\rangle = \left(m+\frac{k}{2}w\right)|j,m;w\rangle \tag{3.37a}$$

$$L_0\,|j,m;w\rangle = \left(h_j - wm - \frac{1}{4}kw^2\right)|j,m;w\rangle\,. \tag{3.37b}$$

We will denote by $M = m + \frac{k}{2}w$ the eigenvalue of J^3_0 to distinguish it from the eigenvalue m of $J^3_0[w]$. If w is allowed to be arbitrarily large, as it is in the $\mathrm{SL}(2,\mathbb{R})_k$ spectrum, the conformal weights of these states are unbounded below. This instability is rectified in the full string theory. w may roughly be thought of as a winding number of the string around the θ circle of AdS_3 [76]. Of course, since this cycle is contractible, w is not conserved.

A current algebra primary $|j,m\rangle$ is also Virasoro primary, and from Eqns. 3.33-3.34 it follows that the spectral-flowed state $|j,m;w\rangle$ remains Virasoro primary. With respect to the global sub-algebra, on the other hand, $|j,m;w\rangle$ transforms as a lowest-weight state $|J,M=J\rangle$ for $w>0$:

$$J_0^3\ |j,m;w\rangle = J\,|j,m;w\rangle \tag{3.38a}$$

$$J_0^-\ |j,m;w\rangle = 0 \tag{3.38b}$$

$$c_2\ \ |j,m;w\rangle = -\,J(J-1)\,|j,m;w\rangle\,. \tag{3.38c}$$

Thus, $|j,m;w\rangle$ sits at the bottom of a lowest-weight representation D_J^+ of spin $J=m+\frac{k}{2}w$. For $w<0$, $|j,m;w\rangle \in D_{J'}^-$ is a highest-weight state $|J',M'=-J'\rangle$ of spin $J'=-\left(m+\frac{k}{2}w\right)$.

The complete spectrum of the $\mathrm{SL}(2,\mathbb{R})_k$ WZW model consists of the current-algebra representations built on the lowest-weight discrete-series representations $D_j^+\otimes D_j^+$ for $\frac{1}{2}<j<\frac{k-1}{2}$ and on the continuous-series representations $C_{j,\alpha}\otimes C_{j,\alpha}$ for $j\in\frac{1}{2}+i\mathbb{R}_+$, as well as their associated spectral-flowed representations for all $w\in\mathbb{Z}$ [76]:

$$\mathcal{H}_{\mathrm{SL}(2,\mathbb{R})_k} = \bigoplus_{j,\alpha,w} \begin{cases} \widehat{D}_j^{+,w}\otimes\widehat{D}_j^{+,w} & j\in\left(\frac{1}{2},\frac{k-1}{2}\right),\ w\in\mathbb{Z} \\ \widehat{C}_{j,\alpha}^{w}\otimes\widehat{C}_{j,\alpha}^{w} & j\in\frac{1}{2}+i\mathbb{R}_+,\ \alpha\in[0,1),\ w\in\mathbb{Z}. \end{cases} \tag{3.39}$$

The spectrum does not explicitly list both the lowest-weight and highest-weight discrete-series representations $\widehat{D}_j^{\pm,w}\otimes\widehat{D}_j^{\pm,w}$ because they are not independent. Rather, one has the following isomorphism, which exchanges lowest and highest-weights, shifts the spectral flow

by one unit, and reflects $j \to \frac{k}{2} - j$ [76]:

$$\widehat{D}_j^{-,w} \simeq \widehat{D}^{+,w-1}_{\frac{k}{2}-j}. \tag{3.40}$$

Note that the interval $j \in \left(\frac{1}{2}, \frac{k-1}{2}\right)$ is mapped to itself under the reflection $j \to \frac{k}{2} - j$, so that if j lies in the interval then so does $\frac{k}{2} - j$ and vice-versa.

For example, the representation $\widehat{D}_j^{-,1}$ with one unit of spectral flow is in fact equivalent to the ordinary representation $\widehat{D}^{+}_{\frac{k}{2}-j}$. Under this isomorphism, the spectral-flowed primary states $|j, -j-N; w=1\rangle$ in $\widehat{D}_j^{-,1}$ map to descendent states in $\widehat{D}^{+}_{\frac{k}{2}-j}$:

$$|j, -j-N; w=1\rangle \simeq (J_{-1}^{-})^N \left|\frac{k}{2}-j, \frac{k}{2}-j\right\rangle, \quad N = 0, 1, 2, \ldots. \tag{3.41}$$

The right-hand-side is an $\mathfrak{sl}(2,\mathbb{R})$ lowest-weight state of spin $\frac{k}{2} - j - N$, consistent with the fact that $|j, m; w > 0\rangle$ is lowest-weight state of spin $m + \frac{k}{2}w$. Likewise, their conformal weights

$$h_j - (-j-N) - \frac{1}{4}k = h_{\frac{k}{2}-j} + N \tag{3.42}$$

are identical.

Having now summarized the $\mathrm{SL}(2,\mathbb{R})_k$ WZW model, in the next sub-section we briefly do the same for the $\mathrm{SL}(2,\mathbb{C})_k/\mathrm{SU}(2)$ coset.

3.1.3 $\mathrm{SL}(2,\mathbb{C})_k/\mathrm{SU}(2)$ Spectrum

In light of the identification $\mathrm{EAdS}_3 = \mathrm{SL}(2,\mathbb{C})/\mathrm{SU}(2)$, a string in EAdS_3 may be described by the unitary $\mathrm{SL}(2,\mathbb{C})_k/\mathrm{SU}(2)$ coset WZW model [43, 44, 86–89]. Its action is simplest in Poincaré coordinates [87],

$$S = \frac{k}{2\pi}\int \mathrm{d}^2 z \left(\partial\sigma\bar{\partial}\sigma + e^{2\sigma}\partial\bar{\gamma}\bar{\partial}\gamma\right). \tag{3.43}$$

By the change of variables Eqn. 3.17, one finds in cylinder coordinates[42]

$$S = \frac{k}{2\pi}\int \mathrm{d}^2 z \big\{\partial r\bar{\partial}r + \partial\xi\bar{\partial}\xi + (\partial\xi - i\partial\theta)(\bar{\partial}\xi + i\bar{\partial}\theta)\sinh^2(r)\big\}. \tag{3.44}$$

Eqn. 3.20 is obtained by setting $\xi = it$.

The isometry algebra of EAdS_3 is $\mathfrak{sl}(2,\mathbb{C})$, which is extended to an $\widehat{\mathfrak{sl}}_k(2,\mathbb{C})$ current algebra of the CFT.[43] Its spectrum is then organized in representations of this current algebra, and consists of ordinary representations built atop $\mathfrak{sl}(2,\mathbb{C})$ primaries labeled by their spin j. The spectrum is spanned the complex branch primaries $j \in \frac{1}{2} + i\mathbb{R}_+$ [43, 44, 89].

For applications to string theory, it is convenient to write these representations not in a momentum space basis as in the previous sub-section, but in a function space basis, with the generators implemented by differential operators acting on functions of a complex coordinate

[42] We drop an additional total derivative term $i\tanh(r)(\partial r\bar{\partial}\theta - \bar{\partial}r\partial\theta)$ that corresponds to an exact B-field $\mathrm{d}(\log\cosh(r)\mathrm{d}\theta)$.

[43] Prior to the quotient, one has an $\widehat{\mathfrak{sl}}_k(2,\mathbb{C})_{\mathrm{L}} \oplus \widehat{\mathfrak{sl}}_k(2,\mathbb{C})_{\mathrm{R}}$ current-algebra corresponding to the independent symmetries $g \to \Omega_{\mathrm{L}} g \Omega_{\mathrm{R}}^\dagger$ on the left and right. After the quotient, one is left with a single copy of the symmetry to preserve Hermiticity, $g \to \Omega g \Omega^\dagger$.

x [43, 44]:

$$\mathcal{D}^3 = x\frac{\partial}{\partial x} + j, \qquad \mathcal{D}^+ = \frac{\partial}{\partial x}, \qquad \mathcal{D}^- = x^2\frac{\partial}{\partial x} + 2jx. \tag{3.45}$$

These are the usual global conformal generators familiar from 2D CFT, except that x is not a worldsheet coordinate—indeed, x will be interpreted as a spacetime boundary coordinate in string theory. The primary vertex operators may be written $\Phi_j(z,\bar{z};x,\bar{x})$, where $(z,\bar{z})$ are worldsheet coordinates and $(x,\bar{x})$ parameterize the representation. Their OPEs with the currents are

$$J^a(z)\Phi_j(z',\bar{z}';x,\bar{x}) \sim \frac{\mathcal{D}^a\Phi_j(z',\bar{z}';x,\bar{x})}{z-z'}, \qquad a = 3,\pm, \tag{3.46}$$

and they are again worldsheet scalars of conformal weight h_j. The m basis states described in the previous sub-section are related to the states prepared by these x basis operators via Fourier transformation and continuation.

Near the $\sigma \to \infty$ boundary of EAdS_3, the vertex operators behave for large k as [44, 88]

$$\Phi_j(z,\bar{z};x,\bar{x}) \overset{\sigma\to\infty}{\longrightarrow} e^{-2(1-j)\sigma}\delta^2(\gamma - x) + \frac{1}{\pi}(2j-1)e^{-2j\sigma}|\gamma - x|^{-4j}. \tag{3.47}$$

Accounting for the measure factor $\sqrt{g} = l_{\mathrm{AdS}}^2 e^{2\sigma}$ from the metric Eqn. 3.18, observe that the target wavefunction is delta-function normalizable only for $\mathrm{Re}(j) = \frac{1}{2}$, consistent with the preceding statement that the $\mathrm{SL}(2,\mathbb{C})_k/\mathrm{SU}(2)$ Hilbert space contains only the complex branch states.

Much is known about the $\mathrm{SL}(2,\mathbb{C})_k/\mathrm{SU}(2)$ CFT, as discussed in the references cited. The above are only the essential details that we will require for the applications to follow.

3.2 $\mathrm{SL}(2,\mathbb{R})_k/\mathrm{U}(1)$ From $\mathrm{SL}(2,\mathbb{R})_k$

In Sec. 2.3 we wrote down the cigar sigma-model Lagrangian for the $\mathrm{SL}(2,\mathbb{R})_k/\mathrm{U}(1)$ CFT without justification. In this section we review the coset construction of the CFT by gauging the $\mathrm{SL}(2,\mathbb{R})_k$ WZW model.

The coset is defined by gauging the time-translation isometry along the length of the AdS_3 cylinder generated by $J_0^3+\bar{J}_0^3$ in the WZW model. Promoting $\partial t \to \partial t + A$, $\bar{\partial} t \to \bar{\partial} t + \bar{A}$ in Eqn. 3.20, one obtains the gauged action

$$S \to S + \frac{k}{2\pi}\int \mathrm{d}^2 z \left(J^3 \bar{A} + \bar{J}^3 A - \cosh^2(r) A\bar{A}\right), \tag{3.48}$$

where

$$J^3(z) = -\partial t - \sinh^2(r)\left(\partial t - \partial\theta\right) \tag{3.49}$$

is the holomorphic component of the current for translations in t, and $\bar{J}^3$ is the anti-holomorphic component. Solving the auxiliary equations of motion for $A, \bar{A}$ and evaluating the action on the solution one obtains

$$S_{\text{cigar}} = \frac{k}{2\pi}\int \mathrm{d}^2 z \left(\partial r \bar{\partial} r + \tanh^2(r)\partial\theta\bar{\partial}\theta\right). \tag{3.50}$$

Thus, classically gauging the length of the cylinder produces a disk topology with the cigar metric $\mathrm{d}s^2 = \alpha' k(\mathrm{d}r^2 + \tanh^2(r)\mathrm{d}\theta^2)$, as in Eqn. 2.97a. Quantum mechanically, integrating out the gauge fields produces the dilaton, as necessitated by conformal invariance (Eqn. 2.99), as well as the additional finite k corrections to the background organized in Eqn. 2.93 [75].

We now reproduce the coset spectrum Eqn. 2.106 from the $\mathrm{SL}(2,\mathbb{R})_k$ spectrum Eqn. 3.39. The Virasoro primaries of $\mathrm{SL}(2,\mathbb{R})_k/\mathrm{U}(1)$ descend from those $\mathrm{SL}(2,\mathbb{R})_k$ states which are (i) Virasoro primary, (ii) J^3 and $\bar{J}^3$ primary, and (iii) satisfy the projection $J_0^3 + \bar{J}_0^3 = 0$.

Consider first a current-algebra primary state $|j, m, \bar{m}\rangle$, or more generally its spectral flow $|j, m, \bar{m}; w\rangle$. These states are automatically Virasoro, J^3, and $\bar{J}^3$ primary, with weights given in Eqn. 3.37. Then one need only enforce the projection condition in order for $|j, m, \bar{m}; w\rangle$ to descend to the coset:

$$\left(J_0^3 + \bar{J}_0^3\right)|j, m, \bar{m}; w\rangle = (m + \bar{m} + kw)\,|j, m, \bar{m}; w\rangle = 0. \tag{3.51}$$

For a given w, the weights m and $\bar{m}$ must therefore satisfy

$$m + \bar{m} = -kw. \tag{3.52}$$

Recall that the difference of eigenvalues $J_0^3 - \bar{J}_0^3$ is always an integer, which we will denote

by n, by angular momentum quantization around the AdS_3 cylinder:

$$m - \bar{m} = n. \tag{3.53}$$

Together, we find the allowed values of m and $\bar{m}$ labeled by $w, n \in \mathbb{Z}$:

$$m = \frac{-kw + n}{2}, \quad \bar{m} = \frac{-kw - n}{2}. \tag{3.54}$$

Among the spectral-flowed primaries, we are therefore looking for states of the form

$$\left| j, \frac{-kw + n}{2}, \frac{-kw - n}{2}; w \right\rangle \tag{3.55}$$

in Eqn. 3.39. In the continuous series $\widehat{C}^w_{j,\alpha} \otimes \widehat{C}^w_{j,\alpha}$ one may always find such a state for any $w, n \in \mathbb{Z}$ and $j \in \frac{1}{2} + i\mathbb{R}_+$ by selecting the appropriate value of α. The discrete series is more restrictive, however. We must identify values of j which lie in the physical spectrum $\frac{1}{2} < j < \frac{k-1}{2}$ and are such that $|j, m, \bar{m}\rangle \in D^+_j \otimes D^+_j$ prior to the spectral flow fits in a lowest-weight representation for the given values of $m, \bar{m}$. The latter demands that $m - j$ and $\bar{m} - j$ are natural numbers.

Note first of all that if $w \geq 0$ it is impossible to satisfy the constraint $m + \bar{m} + kw = 0$, because m and $\bar{m}$ are positive numbers for $j > \frac{1}{2}$. If w is negative, one finds solutions of the form [75]

$$\left| j = \frac{k|w| - |n|}{2} - N, \frac{-kw + n}{2}, \frac{-kw - n}{2}; w \right\rangle \in \widehat{D}^{+,w}_j \otimes \widehat{D}^{+,w}_j, \quad w < 0, \tag{3.56}$$

where N is a natural number such that

$$\frac{1}{2} < \frac{k|w| - |n|}{2} - N < \frac{k-1}{2}. \tag{3.57}$$

Note that this bound implies there only exist solutions when $|n| < k|w| - 1$.

For states of this form, one finds

$$m - j = -k\frac{w + |w|}{2} + \frac{n + |n|}{2} + N \tag{3.58}$$

and

$$\bar{m} - j = -k\frac{w + |w|}{2} - \frac{n - |n|}{2} + N, \tag{3.59}$$

and thus for $w < 0$

$$m - j = \begin{cases} n + N & n \geq 0 \\ N & n \leq 0 \end{cases} \qquad \bar{m} - j = \begin{cases} N & n \geq 0 \\ -n + N & n \leq 0 \end{cases} \tag{3.60}$$

As required, the states are such that $m - j, \bar{m} - j \in \mathbb{N}$.

From the perspective of the cigar sigma-model, it would be strange to find asymptotic winding states with only one sign of the winding number. Were we to take $w > 0$, note that the state in Eqn. 3.56 would in fact fit in a highest-weight representation $\widehat{D}_j^{-,w} \otimes \widehat{D}_j^{-,w}$,

which demands $-m-j, -\bar{m}-j \in \mathbb{N}$. Indeed, we find

$$-m-j = k\frac{w-|w|}{2} + \frac{|n|-n}{2} + N \tag{3.61}$$

and

$$-\bar{m}-j = k\frac{w-|w|}{2} + \frac{|n|+n}{2} + N, \tag{3.62}$$

and so for $w > 0$

$$-m-j = \begin{cases} N & n \geq 0 \\ -n+N & n \leq 0 \end{cases} \qquad -\bar{m}-j = \begin{cases} n+N & n \geq 0 \\ N & n \leq 0, \end{cases} \tag{3.63}$$

as required. These states do not appear explicitly in the $\mathrm{SL}(2,\mathbb{R})_k$ spectrum, Eqn. 3.39. However, in light of the isomorphism Eqn. 3.40, they are equivalent to descendent states in $\widehat{D}^{+,w-1}_{\frac{k}{2}-j} \otimes \widehat{D}^{+,w-1}_{\frac{k}{2}-j}$. Their images under the isomorphism are

$$\left(J^-_{-1}[w-1]\right)^{N+\frac{|n|-n}{2}} \left(\bar{J}^-_{-1}[w-1]\right)^{N+\frac{|n|+n}{2}} \left|\frac{k}{2}-j, \frac{k}{2}-j, \frac{k}{2}-j; w-1\right\rangle. \tag{3.64}$$

In summary, we have identified three sets of Virasoro primaries of the $\mathrm{SL}(2,\mathbb{R})_k$ WZW model that descend to Virasoro primaries of the $\mathrm{SL}(2,\mathbb{R})_k/\mathrm{U}(1)$ coset:

- Continuous-series spectral-flowed primary states,

$$\left|j = \frac{1}{2} + is, m = \frac{-kw+n}{2}, \bar{m} = \frac{-kw-n}{2}; w\right\rangle \in \widehat{C}^w_{j,\alpha} \otimes \widehat{C}^w_{j,\alpha}, \tag{3.65}$$

where $w, n \in \mathbb{Z}$, and $\alpha \in [0,1)$ takes the value necessary for $m, \bar{m} = \alpha \bmod \mathbb{Z}$.

- Discrete-series spectral-flowed primary states in lowest-weight representations ($w < 0$) and highest-weight representations ($w > 0$),

$$\left| j_N, m = \frac{-kw+n}{2}, \bar{m} = \frac{-kw-n}{2}; w \right\rangle \in \begin{cases} \widehat{D}^{+,w}_{j_N} \otimes \widehat{D}^{+,w}_{j_N} & w < 0 \\ \widehat{D}^{-,w}_{j_N} \otimes \widehat{D}^{-,w}_{j_N} & w > 0, \end{cases} \tag{3.66}$$

where $j_N = \frac{k|w|-|n|}{2} - N \in \left(\frac{1}{2}, \frac{k-1}{2}\right)$, $N \in \mathbb{N}$, and $w, n \in \mathbb{Z}$.

These are the $\mathrm{SL}(2,\mathbb{R})_k$ parents of the coset states enumerated in Eqn. 2.106. As seen in Sec. 2.3.3, the $\mathfrak{sl}(2,\mathbb{R})$ spin j is related to the linear-dilaton momentum in the asymptotic cylinder region of the cigar, the quantized angular momentum n around the AdS_3 cylinder becomes the momentum around the asymptotic cylinder, and the spectral flow parameter w, which roughly corresponds to the winding number around AdS_3 likewise becomes the winding number around the asymptotic cylinder. The conformal weights of these states with respect to the coset stress tensor are as in Eqn. 2.107, obtained from the $\mathrm{SL}(2,\mathbb{R})_k$ weights Eqn. 3.37b less the U(1) contribution.

We have not proven that this is the complete list of $\mathrm{SL}(2,\mathbb{R})_k$ states which descend to Virasoro primaries of the coset, but this is assured given the independent construction of the coset spectrum from the one-loop partition function in [77].

Finally, we point out that the components $\mathcal{W}_\pm = \mathcal{O}_{j=\frac{k}{2}-1,n=0,w=\mp 1}$ of the sine-Liouville

operator $\mathcal{O}_{\text{sL}} = \mathcal{W}_+ + \mathcal{W}_-$ (Eqn. 2.123) descend from the states [79]

$$\mathcal{W}_\pm = \left| \frac{k}{2} - 1, \pm\frac{k}{2}, \pm\frac{k}{2}; \mp 1 \right\rangle \in \widehat{D}^{\pm,\mp 1}_{\frac{k}{2}-1} \otimes \widehat{D}^{\pm,\mp 1}_{\frac{k}{2}-1}, \tag{3.67}$$

or, under the isomorphism,

$$J^\pm_{-1} \bar{J}^\pm_{-1} |1, \mp 1, \mp 1\rangle \in \widehat{D}^\mp_1 \otimes \widehat{D}^\mp_1. \tag{3.68}$$

In fact, since the $J^3_0, \bar{J}^3_0$ eigenvalues of these states independently vanish (as opposed to merely their sum), the coset states and $\text{SL}(2,\mathbb{R})_k$ states are identical, there being no U(1) factors to strip away. Thus the weights Eqns. 2.107 and 3.37b are identical—namely, $(1,1)$—and $\mathcal{O}_{\text{sL}}$ defines a marginal operator of both $\text{SL}(2,\mathbb{R})_k$ and $\text{SL}(2,\mathbb{R})_k/\text{U}(1)$.

3.3 Schwinger-Keldysh Contours for Lorentzian String Theory

Suppose one wishes to construct a string perturbation theory around a Lorentzian geometry M. Roughly speaking, one often thinks of the worldsheet CFT as a sigma-model[44] into M. However, not only do the target time kinetic terms imply that the functional integral over the real target fields diverges,[45] but moreover the Lorentzian manifold alone is insufficient data—one must also choose a state of semi-classical quantum gravity in spacetime around

[44] Combined with background fields to support conformal symmetry, and a unitary internal CFT to cancel the conformal anomaly.

[45] As we have seen in Ch. 2, the functional integral over real spatial directions can also diverge, such as along the asymptotic linear-dilaton directions encountered there. Along such directions the functional integral should again be defined over a complex cycle in the target space. But that issue is distinct from the divergence of the functional integral over the time coordinate in Lorentzian backgrounds.

which one wishes to construct the perturbation theory.[46] In constructing string perturbation theory in AdS_3, for example, one can choose from a variety of states, such as the global AdS vacuum, an excited state above the vacuum, a thermal or thermofield-double (TFD) state, and so on.

The divergence of the functional integral over Lorentzian target fields and the ambiguity in the choice of state are closely related. The functional integral should instead be defined by continuation from a sigma-model with Euclidean target.[47] Such a continuation is not unique, and the choice one makes encodes the state around which the perturbation theory is defined. Thus, the divergence of the functional integral and the necessity of choosing a state are reconciled by defining the functional integral along a contour in a complexification of the target space. The contour consists of Euclidean caps at either end, which ensure convergence of the functional integral, joined along a Lorentzian excursion in the middle [92–96].

Several such contours in the complex target time plane are pictured in Fig. 3.2. The first computes expectation values in a pure state such as the vacuum, the second in a thermal state, and the third in a TFD state. They share a common Lorentzian section (with two copies thereof in the last example), but correspond to different complexifications of the target time $t_{\rm E} + it$, $t_{\rm E}$ being non-compact in the first and compact in the second and third. Moreover, the periodicity $t_{\rm E} \sim t_{\rm E} + \beta$ in the latter cases is an additional choice, specifying

[46] When computing the string S-matrix in Minkowski spacetime, it is usually implicit that one has chosen the vacuum state. But one could also consider, for example, string perturbation theory in Minkowski spacetime in a thermal state [90, 91], or the HH state of a black hole in asymptotic Minkowski spacetime, and so on.

[47] In this section, we always choose a Euclidean metric on the worldsheet. When we speak of continuing between Lorentzian and Euclidean signatures, we mean with respect to the time coordinate of the target space M.

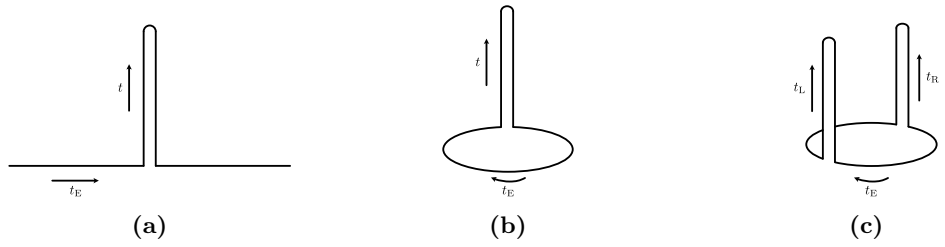

(a) **(b)** **(c)**

Figure 3.2: Schwinger-Keldysh Contours. A Schwinger-Keldysh contour is a contour in the complex time plane that consists of Euclidean caps joined to Lorentzian excursions. The functional integral defined along such a contour computes the expectation value of operators inserted on the Lorentzian section between the initial and final states specified by the Euclidean caps. In field theory, the contour defines the domain on which the fields are defined. In string theory, it is the contour in target space over which the worldsheet functional integral is to be performed. The first contour pictured computes expectation values in a pure state such as the vacuum. The second computes expectation values in a thermal state, and the third in a TFD state.

the inverse temperature of the thermal state.[48]

The continuation is real when the Lorentzian geometry has a Z_2 time-reflection isometry. Moreover the Euclidean and Lorentzian sections share a common zero-time slice—the fixed-point locus of the symmetry—along which they may be glued together to define the contour.

Complex time contours of this form are familiar from ordinary field theory, where they are known as Schwinger-Keldysh contours. In that context, they are contours in the base spacetime, rather than in the target space. Then the contour specifies the domain on which the fields are defined, and the functional integral computes expectation values between the states specified by the caps. The functional integral over the incoming Euclidean cap prepares a state in the Hilbert space of the quantum field theory on the spatial slice to which it is glued. Then the state is evolved forward in Lorentzian time and any desired local operators are inserted. Finally, the Lorentzian segment is reversed and glued to the outgoing Euclidean cap which prepares the outgoing state.

[48]For a black hole, the periodicity of the Euclidean continuation is fixed to obtain a smooth geometry. Then the black hole in the HH state has a fixed temperature. However, a thermal state in e.g. AdS can have any temperature (at least, until the Hagedorn limit).

Such complexified functional integrals may be computed by starting from a Euclidean correlation function and moving the operators to the Lorentzian section by continuing the insertion times in the Euclidean answer. One thinks of cutting open the Euclidean manifold on one or more constant Euclidean time slices and gluing in the Lorentzian excursion. Moreover, one need not continue all of the operator insertions to the Lorentzian section. Operators left on the Euclidean caps prepare different states in which the expectation value is computed.

In string theory, the Schwinger-Keldysh contour becomes a contour in the target space, over which the functional integral that defines the worldsheet CFT is to be performed. Again, one may proceed by starting from a worldsheet correlation function with the Euclidean target and then continuing the vertex operator insertions to the Lorentzian section. Of course, it is not the location of the vertex operator insertion on the worldsheet that one wishes to continue in this case, but rather the quantum numbers that label how the operator transforms under the spacetime symmetries. The Euclidean caps define the state in which the string perturbation theory is constructed, and in the case of AdS_3, the string amplitudes compute expectation values of the boundary CFT_2 in the dual state associated to the caps.[49] One may also construct string theories with different initial and final states, e.g. by fixing different operator insertions on the incoming and outgoing Euclidean sections.

In fact, regarded as a deformation of the Euclidean integration contour in target space, the Lorentzian excursion is contractible. It does not alter the homology cycle of the Euclidean

[49]More precisely, the string amplitudes compute contributions to the boundary CFT expectation values. Depending on whether or not the background is the dominant bulk saddle for a given boundary CFT observable, the corresponding string amplitudes will be the dominant contribution or a sub-dominant correction.

functional integral, and therefore inserting the excursion does not change the integral. One merely takes the Euclidean answer and continues the labels to Lorentzian time.

Although we have phrased the above discussion in the sigma-model approximation, which is convenient for visualizing the target geometry as a complex contour for the functional integral, it is not necessary to resort to a Lagrangian description of the worldsheet CFT. One may begin from an abstract definition of the CFT by its three-point function and OPE, and continue the operator labels to define the Lorentzian string theory. In AdS_3, for example, string theory in various states is constructed by continuation from the unitary $\mathrm{SL}(2,\mathbb{C})_k/\mathrm{SU}(2)$ coset CFT, and various orbifolds thereof, without requiring any reference to a Lagrangian, as we now describe.

In Eqns. 3.4 and 3.13 we defined EAdS_3 by the continuation $\xi = it$ from AdS_3, with $\xi \in (-\infty, \infty)$. The Lorentzian metric is time-independent, and so one may cut it along any spatial slice and glue in a Euclidean cap to prepare a state. Cutting and gluing the two cylinders at $\xi = t = 0$ prepares the global AdS_3 vacuum state.

Alternatively, one could define the Euclidean continuation with compact $\xi \sim \xi + \beta$. The resulting manifold is known as thermal AdS_3 ($\mathrm{TAdS}_3|_\beta = \mathrm{EAdS}_3/\beta\mathbb{Z}$), and has the topology of a solid torus whose non-contractible cycle is parameterized by ξ. Cutting the torus at $\xi = 0$ and gluing in the Lorentzian cylinder prepares a thermal state in AdS_3 at inverse temperature β. More generally, one may slice the torus in half by making cuts at both $\xi = 0$ and $\xi = \beta/2$, and then glue a copy of AdS_3 at each cut. The result is the TFD state in two disconnected copies of AdS_3 (Fig. 3.3a). Tracing over one slice returns the thermal state on

(a) (b)

Figure 3.3: TFD and Factorized Vacuum States in $AdS_3 \cup AdS_3$. Thermal AdS_3, obtained from Euclidean AdS_3 by compactifying the global time coordinate $\xi \sim \xi + \beta$, has the topology of a solid torus. Cutting the torus in half at $\xi = 0$ and $\xi = \beta/2$ and gluing a copy of Lorentzian AdS_3 at each prepares the TFD state in two disconnected copies of AdS_3 (left). By contrast, the factorized vacuum (right) is an unentangled state prepared by cutting $EAdS_3$ in half and gluing it to each copy of AdS_3. In the figure, the $EAdS_3$ half-cylinder has been compactified to a half-ball.

the other, corresponding to sewing one of the cuts back up. Fig. 3.3b shows the same two copies of AdS_3, now with each in its vacuum state. In the figure we have compactified the half-cylinder to the half-ball.

As reviewed in Sec. 3.1, AdS_3 is equivalent to $SL(2,\mathbb{R})$, and to describe a bosonic string in AdS_3 it is natural to take the $SL(2,\mathbb{R})_k$ WZW model for the worldsheet CFT [46, 76, 85–88]. The $SL(2,\mathbb{R})_k$ WZW action is an inadequate definition of the worldsheet CFT, however, for the reasons explained above. Instead one must choose a state, and define the theory by the corresponding continuation from a unitary CFT. The simplest choice is the vacuum state, corresponding to continuation from $EAdS_3 = SL(2,\mathbb{C})/SU(2)$. The $SL(2,\mathbb{C})_k/SU(2)$ coset was studied in [43, 44, 89]. Its continuation to Lorentzian signature, constructed in [46, 76, 85], defines string perturbation theory in AdS_3 in the spacetime vacuum state, as we review in the next sub-section. In the following two sub-sections, we explain the formulation of string theory in AdS_3 in a thermal state and in the asymptotically AdS_3 black hole in the Hartle-Hawking state.

3.3.1 AdS_3 in the Vacuum State

Consider the theory of a string in AdS_3 in the spacetime vacuum state. As reviewed in Sec. 3.1, the isometry algebra of $AdS_3 = SL(2,\mathbb{R})$ is $\mathfrak{sl}(2,\mathbb{R})_L \oplus \mathfrak{sl}(2,\mathbb{R})_R \simeq \mathfrak{so}(2,2)$, which is extended to an $\widehat{\mathfrak{sl}}_k(2,\mathbb{R})_L \oplus \widehat{\mathfrak{sl}}_k(2,\mathbb{R})_R$ current algebra of the worldsheet CFT (Eqn. 3.22). As usual in AdS/CFT, the isometry algebra of the bulk is identified with the global conformal algebra of the dual CFT (BCFT) defined on the spacetime conformal boundary. Namely, the BCFT global conformal generators[50] $\{\mathsf{L}_0, \mathsf{L}_{\mp 1}\} \cup \{\bar{\mathsf{L}}_0, \bar{\mathsf{L}}_{\mp 1}\}$ satisfy the same algebra as the current zero-modes $\{J^3_0, J^\pm_0\} \cup \{\bar{J}^3_0, \bar{J}^\pm_0\}$ (Eqn. 3.21): $[\mathsf{L}_0, \mathsf{L}_{\mp 1}] = \pm \mathsf{L}_{\mp 1}$, $[\mathsf{L}_{-1}, \mathsf{L}_1] = -2\mathsf{L}_0$, and similarly for the anti-holomorphic sector.

Likewise, the $SL(2,\mathbb{C})_k/SU(2)$ coset is equipped with an $\widehat{\mathfrak{sl}}_k(2,\mathbb{C})$ current algebra, whose global sub-algebra $\mathfrak{sl}(2,\mathbb{C}) \simeq \mathfrak{so}(1,3)$ is the isometry algebra of $EAdS_3$ and the global conformal algebra of the BCFT in Euclidean signature. The two current algebras share a common complexification, $\widehat{\mathfrak{sl}}_k(2,\mathbb{C})_L \oplus \widehat{\mathfrak{sl}}_k(2,\mathbb{C})_R$. The complexified global sub-algebra $\mathfrak{sl}(2,\mathbb{C})_L \oplus \mathfrak{sl}(2,\mathbb{C})_R$ is the standard complexification of the global conformal algebra from the perspective of the BCFT, wherein the complex coordinate x and its complex-conjugate $\bar{x}$ on the boundary sphere are promoted to independent complex coordinates, on which the holomorphic and anti-holomorphic dual Virasoro generators act independently.

Whereas string amplitudes in asymptotically flat space compute S-matrix elements, the most natural string amplitudes in AdS compute correlation functions of local operators of the

[50] We denote the worldsheet Virasoro generators by L_n and the BCFT Virasoro generators by L_n.

BCFT, or expectation values thereof in Lorentzian signature. The spectrum of the BCFT is organized in unitary representations of its Virasoro algebra,

$$[\mathsf{L}_n, \mathsf{L}_m] = (n-m)\mathsf{L}_{n+m} + \frac{\mathsf{c}}{12}(n^3 - n)\delta_{n+m}, \tag{3.69}$$

and similarly for $\bar{\mathsf{L}}_n$, with $[\mathsf{L}_n, \bar{\mathsf{L}}_m] = 0$. The central charge is, at large k, [97]

$$\mathsf{c} = \frac{3}{2}\frac{l_{\text{AdS}}}{l_{\text{p}}}. \tag{3.70}$$

where $l_{\text{AdS}} = l_{\text{s}}\sqrt{k}$.

The representations are built on Virasoro primary states labeled by their spins $(J, \bar{J})$, which are positive real numbers. Focusing on the holomorphic factor, a Virasoro primary state $|J, M = J\rangle$ is annihilated by the positive modes $\mathsf{L}_{n>0}$ and is an eigenstate of L_0 with eigenvalue $M = J$. Being annihilated by L_1, it sits at the bottom of a lowest-weight discrete-series representation $D^+_J = \{|J, M\rangle : M \in J + \mathbb{N}\}$ of the global conformal algebra $\mathfrak{sl}(2, \mathbb{C})_{\text{L}}$, the descendent states being obtained by action of L_{-1}, $|J, M\rangle \propto (\mathsf{L}_{-1})^{M-J}\,|J, J\rangle$.

To each global representation D^+_J, one associates by the state-operator map a primary operator $\mathcal{O}_J(x)$ that transforms under $\mathfrak{sl}(2, \mathbb{C})_{\text{L}}$ according to

$$[\mathsf{L}_{-1}, \mathcal{O}_J(x)] = \partial\mathcal{O}_J(x) \tag{3.71a}$$

$$[\mathsf{L}_0, \mathcal{O}_J(x)] = (x\partial + J)\mathcal{O}_J(x) \tag{3.71b}$$

$$[\mathsf{L}_1, \mathcal{O}_J(x)] = (x^2\partial + 2Jx)\mathcal{O}_J(x). \tag{3.71c}$$

$\mathcal{O}_J(x)$ prepares the lowest-weight state when inserted at the origin, $\mathcal{O}_J(0)\,|0\rangle = |J, J\rangle$. By the AdS/CFT dictionary, there is a dual state of a string in AdS_3, which likewise transforms as a lowest-weight state in D_J^+, now with respect to the global $\mathfrak{sl}(2,\mathbb{C})_{\mathrm{L}}$ sub-algebra of the worldsheet current algebra. The descendent states $|J, M\rangle \in D_J^+$ are prepared in the boundary by inserting derivatives of $\mathcal{O}_J(x)$, which are dual to excited string states in the bulk.

Similarly, when inserted at the point-at-infinity, $\mathcal{O}_J(\infty) = \lim_{x\to\infty} x^{2J}\mathcal{O}_J(x)$ prepares a highest-weight state $|J, M = -J\rangle \in D_J^-$. Thus, lowest-weight states may be interpreted as in-states and highest-weight states as out-states.

The string amplitudes, which compute correlation functions of such BCFT operators, are defined by continuation from the $\mathrm{SL}(2,\mathbb{C})_k/\mathrm{SU}(2)$ coset CFT. Recall that the primary operators of $\mathrm{SL}(2,\mathbb{C})_k/\mathrm{SU}(2)$ may be written in a function space basis $\Phi_j(z,\bar{z};x,\bar{x})$, transforming under the current algebra according to Eqn. 3.46. As far as the CFT is concerned, $(x,\bar{x})$ are labels parameterizing the spin j representation of the $\mathfrak{sl}(2,\mathbb{C})$ symmetry inherited from the target isometry algebra. In string theory, $(x,\bar{x})$ are interpreted as the insertion point on the spacetime boundary sphere of a dual BCFT operator $\mathcal{O}_j(x,\bar{x})$ of dual conformal weight (j,j), the transformations Eqn. 3.45 of $\Phi_j(z,\bar{z};x,\bar{x})$ under the isometry algebra coinciding with the transformations Eqn. 3.71 of $\mathcal{O}_j(x,\bar{x})$ under the global BCFT conformal algebra. Although the coset Hilbert space consists only of the complex branch representations $j \in \frac{1}{2} + i\mathbb{R}_+$ [43, 44, 89], j may be continued away from this line [44, 46]. Indeed, these are not the representations of interest for string theory in AdS_3—they correspond to the bosonic string tachyon, and would map to dual representations with complex conformal weights.

Recall from the $\sigma \to \infty$ expansion Eqn. 3.47 that the complex branch was selected by demanding normalizability of the $SL(2,\mathbb{C})_k/SU(2)$ wavefunction. For $\mathrm{Re}(j) < \frac{1}{2}$, the second exponential dominates, and the operator is spread over the boundary sphere. For $\mathrm{Re}(j) > \frac{1}{2}$, however, the first term dominates, and the non-normalizability of the wavefunction is localized at $\gamma = x$, interpreted as a source for an operator of the BCFT on the boundary S^2. Eqn. 3.47 is the standard asymptotic expansion of a solution to the AdS_3 wave equation for a scalar of mass $l^2_{\mathrm{AdS}} m^2 = \Delta(\Delta - 2)$, with a delta-function source at $(x, \bar{x})$ for the dual operator of dimension $\Delta = 2j$. The leading term inserts the source and the sub-leading term is $e^{-2j\sigma}/(2\Delta - d)$ times the two-point function of the dual operator [98].

Thus, for $j > \frac{1}{2}$ one has a map from the worldsheet vertex operator $\Phi_j(z, \bar{z}; x, \bar{x})$ to a primary scalar BCFT operator $\hat{\Phi}_j(x, \bar{x})$ of real conformal weight (j, j) inserted at $(x, \bar{x})$.[51] A string amplitude with many insertions $\Phi_{j_i}(z_i, \bar{z}_i; x_i, \bar{x}_i)$ computes a BCFT correlation function on S^2 with operator insertions at $(x_i, \bar{x}_i)$ of dual conformal weights (j_i, j_i).[52] The vertex operators with $j > \frac{1}{2}$ are non-normalizable from the perspective of the $SL(2,\mathbb{C})_k/SU(2)$ coset, as appropriate for operators that insert delta-function sources on the boundary of Euclidean AdS, and are defined by analytic continuation in j [44, 46]. String amplitudes of two, three, and four primaries were studied in this way in [46].

From BCFT correlation functions on S^2, the boundary insertion points $(x, \bar{x})$ may be continued in the usual way from the Euclidean sphere to the Lorentzian cylinder in order to

[51] More precisely, one has a map from $\Phi_j(z, \bar{z}; x, \bar{x}) \otimes \mathcal{O}_h(z, \bar{z})$, where $\mathcal{O}_h$ is a primary of the internal CFT such that the combined vertex operator is marginal. The construction of the full BCFT Virasoro algebra was discussed in [86–88].

[52] In fact, the string partition function is related to the BCFT generating functional in an ensemble in which the BCFT central charge fluctuates. To obtain a standard CFT with fixed central charge one must perform a Legendre transform of the string partition function, as explained in [99].

(a) **(b)**

Figure 3.4: AdS_3 **Vacuum Schwinger-Keldysh Contour**. String amplitudes for AdS_3 in the spacetime vacuum state compute vacuum expectation values of the dual CFT and are defined by continuation from $SL(2,\mathbb{C})_k/SU(2)$. The Euclidean amplitudes compute BCFT correlation functions on the S^2 conformal boundary of $EAdS_3$, with insertions at the points $(x,\bar{x})$ which labeled the worldsheet vertex operators. The spacetime is complexified and the insertions continued to the Lorentzian section to obtain vacuum expectation values. Though the procedure does not rely on a Lagrangian, one may think of these amplitudes as defined by a worldsheet functional integral along the Schwinger-Keldysh contour in target space shown. A Euclidean cap (in yellow) prepares the AdS_3 vacuum, which is glued to a Lorentzian excursion (in blue) that flows forward and backward in time, and is then glued to the outgoing vacuum cap. String vertex operators insert dual operators on the conformal boundary, indicated by the red $\times$'s. Operators may also be left on the Euclidean caps to define string perturbation theory in AdS_3 in different excited pure states.

define expectation values of the BCFT in the vacuum state (Fig. 3.4). The conformal transformation $(x = e^{\xi+i\theta}, \bar{x} = e^{\xi-i\theta})$ maps the sphere to the Euclidean cylinder, and continuing $\xi \to it$ yields the Lorentzian cylinder $(x = e^{i(t+\theta)}, \bar{x} = e^{i(t-\theta)})$. In doing so, one has continued $(x,\bar{x})$ to independent complex coordinates, and in turn the vertex operator $\Phi_j(z,\bar{z};x,\bar{x})$ is continued to a representation of the complexified current algebra $\widehat{\mathfrak{sl}}_k(2,\mathbb{C})_{\rm L} \oplus \widehat{\mathfrak{sl}}_k(2,\mathbb{C})_{\rm R}$. The original boundary S^2 and the Lorentzian cylinder correspond to two real sections of the complexification. On the worldsheet, one transitions between vertex operators for insertions on the Euclidean sphere or Lorentzian cylinder by restricting the complexified primary $\Phi_j(z,\bar{z};x,\bar{x})$ to the appropriate section.

For example, the two-point amplitude of $\Phi_j(z,\bar{z};x,\bar{x})$ is [46]

$$\left\langle \hat{\Phi}_j(x_1,\bar{x}_1)\hat{\Phi}_j(x_2,\bar{x}_2)\right\rangle = \frac{1}{V_{\rm conf}}\left\langle \Phi_j(z=0;x_1,\bar{x}_1)\Phi_j(z=0;x_2,\bar{x}_2)\right\rangle \propto |x_{12}|^{-4j}, \tag{3.72}$$

as appropriate for a BCFT scalar of dimension $2j$. Making the boundary conformal transformation $\Phi_j(z,\bar{z};x,\bar{x}) \to e^{-2j\xi}\Phi_j(z,\bar{z};\xi,\theta)$, one obtains the standard CFT two-point function for a scalar on the cylinder:

$$\left\langle \hat{\Phi}_j(\xi_1,\theta_1)\hat{\Phi}_j(\xi_2,\theta_2) \right\rangle \propto (\cosh(\xi_{12}) - \cos(\theta_{12}))^{-2j} . \tag{3.73}$$

As expected for a Euclidean correlation function, this expression is non-singular as long as the two insertions are not coincident.

To obtain a Lorentzian expectation value, one slides each insertion to the zero-time slice and then onto the Lorentzian section:

$$\langle 0| \hat{\Phi}_j(t_1,\theta_1)\hat{\Phi}_j(t_2,\theta_2) |0\rangle \propto (\cos(t_{12}) - \cos(\theta_{12}))^{-2j} . \tag{3.74}$$

In doing so, one encounters singularities when one operator hits the lightcone of the other, $t_{12} = \pm\theta_{12}$. Following the usual $i\varepsilon$ prescription to avoid the singularity and obtain a time-ordered expectation value, one replaces $t \to t(1 - i\varepsilon)$. We mostly suppress the $i\varepsilon$'s for notational simplicity.

The perturbative string states of Eqn. 3.39 may be identified with the modes of the boundary position basis vertex operators. For example, the vertex operators $\Phi_{jm\bar{m}}(z,\bar{z})$ for the string states $|j,m,\bar{m}\rangle$ are formally given by the spacetime Fourier transform of

$\Phi_j(z,\bar{z};t,\theta)$:

$$\Phi_{jm\bar{m}}(z,\bar{z}) \propto \int_{-\infty}^{\infty} \mathrm{d}t \int_{0}^{2\pi} \mathrm{d}\theta\, e^{-i(m+\bar{m})t} e^{-i(m-\bar{m})\theta} \Phi_j(z,\bar{z};t,\theta), \tag{3.75}$$

where $m+\bar{m}$ is the spacetime energy and $m-\bar{m}$ is the angular momentum, and similarly for the spectral-flowed operators reviewed below. One may likewise compute string amplitudes of such momentum-basis insertions [46].

When inserted at the origin of the Euclidean section, $\Phi_j(z,\bar{z};x,\bar{x})$ prepares the lowest-weight state $|j,j,j\rangle$ in the representation $D_j^+ \otimes D_j^+$ of the global sub-algebra:

$$\Phi_j(z=0;x=0)\,|0\rangle = |j,j,j\rangle\,. \tag{3.76}$$

This is the bulk string state dual to the BCFT Virasoro primary state of conformal weight (j,j), the latter prepared by the dual operator $\hat{\Phi}_j(x=0)$, both transforming as lowest-weight states of $\mathfrak{sl}(2,\mathbb{C})_{\mathrm{L}} \oplus \mathfrak{sl}(2,\mathbb{C})_{\mathrm{R}}$.[53] The global descendent states $|j,m,\bar{m}\rangle \in D_j^+ \otimes D_j^+$, related to the lowest-weight state by the action of $J_0^+, \bar{J}_0^+$, are prepared by inserting x derivatives of $\Phi_j(z,\bar{z};x,\bar{x})$, and are dual to the global conformal descendents of the BCFT Virasoro primary. In the bulk effective field theory, $|j,j,j\rangle$ is the lowest-energy state of a scalar field of mass[54] $l_{\mathrm{AdS}}^2 m^2 = \Delta(\Delta-2)$ dual to the BCFT scalar primary operator of dimension $\Delta = 2j$.

Of course, the Virasoro primaries of the dual CFT are not all scalars. In addition to the

[53] Again, once combined with an internal operator such that the Virasoro constraints are satisfied.

[54] It is hopefully clear from context when we use m to refer to the mass as opposed to the J_0^3 eigenvalue.

current-algebra primaries $\Phi_j(z,\bar{z};x,\bar{x})$ that prepare lowest-weight states $|j,j,j\rangle \in \widehat{D}^+_j \otimes \widehat{D}^+_j$, one has vertex operators denoted $\Phi^{J\bar{J}}_{jw}(z,\bar{z};x,\bar{x})$ that prepare the spectral-flowed states of Eqn. 3.39 [46]:

$$\Phi^{J\bar{J}}_{jw}(z=0;x=0)\,|0\rangle = \left|j, m = J - kw/2, \bar{m} = \bar{J} - kw/2; w\right\rangle, \quad w > 0. \tag{3.77}$$

These operators are worldsheet Virasoro—but not current-algebra—primaries of conformal weights as in Eqn. 3.37b:

$$h^{J\bar{J}}_{jw} = -\frac{j(j-1)}{k-2} - wJ + \frac{1}{4}kw^2, \qquad \bar{h}^{J\bar{J}}_{jw} = -\frac{j(j-1)}{k-2} - w\bar{J} + \frac{1}{4}kw^2. \tag{3.78}$$

They carry the additional labels[55] $(J,\bar{J})$ specifying their spins with respect to the global $\mathfrak{sl}(2,\mathbb{C})_{\mathrm{L}} \oplus \mathfrak{sl}(2,\mathbb{C})_{\mathrm{R}}$, as well as the spectral-flow label w.

Recall from Eqn. 3.38 that, for $w > 0$, the spectral flow $|j,m,\bar{m};w\rangle$ of a current-algebra primary carries J^3_0 weight $M = m + \frac{k}{2}w$ and transforms as a lowest-weight state $|J, M = J\rangle \in D^+_J$ with respect to $\mathfrak{sl}(2,\mathbb{C})_{\mathrm{L}}$, and similarly for $\mathfrak{sl}(2,\mathbb{C})_{\mathrm{R}}$ with $\bar{M} = \bar{J} = \bar{m} + \frac{k}{2}w$. Thus, each spectral-flowed primary $|j,m,\bar{m};w\rangle$ with $w > 0$ sits at the bottom of a discrete-series representation[56] $D^+_J \otimes D^+_{\bar{J}}$ of the global sub-algebra, and is dual to a BCFT Virasoro primary state of spin $(J,\bar{J})$.[57] Associated to each such lowest-weight string state

[55] For unflowed operators one has $\Phi_j = \Phi^{J=\bar{J}=j}_{j,w=0}$.

[56] Note that, with respect to the global sub-algebra, one obtains a lowest-weight discrete-series representation regardless of whether $|j,m,\bar{m};w\rangle$ came from a spectral-flowed discrete-series $\widehat{D}^{+,w}_j \otimes \widehat{D}^{+,w}_j$ or continuous-series $\widehat{C}^w_{j,\alpha} \otimes \widehat{C}^w_{j,\alpha}$ representation of the current-algebra, as appropriate for a primary of the BCFT. In a continuous-series representation, J and j (and $\bar{J}$ and j) are unrelated, whereas in a lowest-weight discrete-series representation they are related by $j = J - \frac{k}{2}w - \mathbb{N}$.

[57] Once combined with the internal CFT and subjected to the constraints. In particular, $J = m + \frac{k}{2}w$ is not guaranteed to be positive on the spectrum of the $\mathrm{SL}(2,\mathbb{R})_k$ WZW model. It is only after applying the Virasoro constraints that one obtains a physical state of positive $J, \bar{J}$, which maps to a primary of the BCFT.

one has a vertex operator $\Phi^{J\bar{J}}_{jw}(z,\bar{z};x,\bar{x})$ that prepares it. The global descendent states $(J_0^+)^N(\bar{J}_0^+)^{\bar{N}}\,|j,m,\bar{m};w\rangle$ are as before prepared by insertions with derivatives.[58]

For $w<0$, on the other hand, $|j,m,\bar{m};w\rangle$ transforms as a highest-weight state $|J',-J'\rangle\otimes\left|\bar{J}',-\bar{J}'\right\rangle\in D^-_{J'}\otimes D^-_{\bar{J}'}$ of spin $J'=-\left(m+\frac{k}{2}w\right)$, $\bar{J}'=-\left(\bar{m}+\frac{k}{2}w\right)$. As recalled earlier, a lowest-weight state is interpreted as an in-state in the dual CFT, prepared by a spin $(J,\bar{J})$ primary insertion at the origin, whereas a highest-weight state is interpreted as an out-state, prepared by an insertion at infinity. $\Phi^{J\bar{J}}_{jw}(z,\bar{z};x,\bar{x})$, which likewise transforms as a local operator of spin $(J,\bar{J})$ in x-space with respect to the global sub-algebra, also prepares a lowest-weight in-state, and should therefore be labeled by $w>0$ as in Eqn. 3.77. When inserted at infinity, it prepares the highest-weight out-state $\left|j,-\left(J-\frac{k}{2}w\right),-\left(\bar{J}-\frac{k}{2}w\right);-w\right\rangle$ in $D^-_J\otimes D^-_{\bar{J}}$.

The complete spectrum of the $\mathrm{SL}(2,\mathbb{R})_k$ WZW model given in Eqn. 3.39, when combined with a unitary internal CFT and subjected to the Virasoro constraints, yields the unitary spectrum of strings in AdS_3 in the vacuum state [76]. The upper bound on the real branch, $j<\frac{k-1}{2}$, is required to obtain a unitary on-shell spectrum, and ensures compatibility with the spectral-flow isomorphism, which exchanges the upper and lower bounds under $j\to\frac{k}{2}-j$. The spectrum also includes the unflowed complex branch representations $\widehat{C}_{j=\frac{1}{2}(1+is),\alpha}$, whose vertex operators $\Phi_j(z,\bar{z};x,\bar{x})$ do not map to well-defined local operators of the BCFT. These are the bosonic string tachyons, whose spacetime mass $l^2_{\mathrm{AdS}}m^2=-1-s^2$ falls below the

[58] Note that $(J_0^+)^N(\bar{J}_0^+)^{\bar{N}}\,|j,m,\bar{m};w\rangle=(J^+_{-w}[w])^N(\bar{J}^+_{-w}[w])^{\bar{N}}\,|j,m,\bar{m};w\rangle$ transforms as a current-algebra descendent with respect to the unflowed generators, and should not be confused with the state $|j,m+N,\bar{m}+\bar{N};w\rangle$. The latter is the lowest-weight state of its own discrete-series representation, and carries a different worldsheet conformal weight besides.

tachyonic BF bound $l^2_{\text{AdS}}m^2 < -1$ for a scalar in AdS_3 [76, 100].[59]

String amplitudes with spectral-flowed vertex operators were also computed in [46], and may similarly be continued to BCFT expectation values by continuing the boundary insertion points to the Lorentzian cylinder.

For a primary $\Phi^{J\bar{J}}_{jw} \otimes \mathcal{O}_{h\bar{h}}$, with $\mathcal{O}_{h\bar{h}}$ a contribution from the internal CFT, the Virasoro constraint $L_0 - 1 = 0$ may be written

$$J = \frac{1}{4}kw + \frac{1}{w}\left(-\frac{j(j-1)}{k-2} + h - 1\right). \tag{3.79}$$

On the complex branch, j and J are unrelated, and this equation gives a continuous spectrum of spacetime conformal weights parameterized by $\text{Im}(j)$.[60] These are known as "long string" states. They are heavy in the semi-classical limit, J being of order k, and are believed to be a peculiarity of the pure NS background. For the real branch, on the other hand, j and J are related by $j = J - \frac{k}{2}w - N$, with $N \in \mathbb{N}$. Solving the on-shell condition for J then yields a discrete spectrum of spacetime conformal weights [76],

$$J = N + w + \frac{1}{2} + \sqrt{\frac{1}{4} + (k-2)\left(h - 1 - Nw - \frac{1}{2}w(w+1)\right)}. \tag{3.80}$$

[59] We point out that below $k = 3$, at which point it has been argued that the $SL(2,\mathbb{R})_k$ WZW model undergoes a phase transition [54, 83], the real branch spectrum $\frac{1}{2} < j < \frac{k-1}{2}$ falls within the BF window $-1 < l^2_{\text{AdS}}m^2 < 0$ in which two normalizable fall-offs are admissible.

[60] The constraint guarantees J is positive, $-j(j-1) \geq \frac{1}{4}$ being bounded below on the complex branch and $h \geq 0$ being positive by unitarity of the internal CFT. Then Eqn. 3.79 is positive with $k > 2$ and $w > 0$. Note that the constraint, $m + \frac{k}{2}w = \frac{1}{4}kw + \frac{1}{w}\left(-\frac{j(j-1)}{k-2} + h - 1\right)$, is invariant under $w \to -w$ and $m \to -m$. Namely, if $\Phi^{J\bar{J}}_{jw}(z,\bar{z};x,\bar{x}) \otimes \mathcal{O}_{h,\bar{h}}(z,\bar{z})$ prepares a physical lowest-weight in-state $\left|j, J - \frac{k}{2}w, \bar{J} - \frac{k}{2}w; w\right\rangle \otimes |h,\bar{h}\rangle$ when inserted at the origin, then the highest-weight out-state $\left|j, -\left(J - \frac{k}{2}w\right), -\left(\bar{J} - \frac{k}{2}w\right); -w\right\rangle \otimes |h,\bar{h}\rangle$ obtained by inserting the operator at infinity is likewise physical.

These, by constrast, are known as "short string" states, and are the more typical vertex operators.

Next we describe how string perturbation theory in AdS_3 is defined for other choices of the state. Note first of all that one need not continue all the operator insertions in x-space to the Lorentzian section. Leaving an insertion on the Euclidean cap prepares the associated state on the cylinder from the perspective of the BCFT, and defines string perturbation theory in an excited pure state from the perspective of the worldsheet theory.

3.3.2 AdS_3 in a Thermal State

Suppose now that one wishes to study string perturbation theory in AdS_3 in a thermal state. In the BCFT, thermal expectation values are obtained by continuation from Euclidean correlation functions on T^2, the periodicity of the Euclidean time circle fixing the inverse temperature of the state. One constructs the Schwinger-Keldysh contour by cutting the torus at a single time-slice and gluing in the Lorentzian cylinder, or by cutting the torus in half to prepare the TFD state in two copies of the BCFT Hilbert space on a circle.

The TFD state for a theory with Hilbert space $\mathcal{H}(\Sigma)$ is in general defined by

$$|\mathrm{TFD}\rangle = \frac{1}{\mathrm{Tr}_{\mathcal{H}(\Sigma)}(e^{-\beta H})} \sum_n e^{-\beta E_n/2} |n^*\rangle \otimes |n\rangle \in \mathcal{H}(\Sigma) \otimes \mathcal{H}(\Sigma), \tag{3.81}$$

where $\{|n\rangle\}$ is the spectrum of the Hamiltonian H, and the star denotes the action of CPT. It may be prepared by a Euclidean functional integral on $\Sigma \times [0, \beta/2]$, with the two copies of

Σ at the interval boundaries corresponding to the two zero-time slices. Expectation values in this state are computed by the contour sketched in Fig. 3.2c. If we sew up the second cut at $t_E = \beta/2$, we reproduce the thermal state in the single copy of $\mathcal{H}(\Sigma)$ at $t_E = 0$. Indeed, sewing the additional cut corresponds to taking the reduced density matrix in one copy,

$$\mathrm{Tr}_{\mathcal{H}(\Sigma)} |\mathrm{TFD}\rangle \langle \mathrm{TFD}| = \frac{1}{\mathrm{Tr}_{\mathcal{H}(\Sigma)}(e^{-\beta H})} \sum_n e^{-\beta E_n} |n\rangle \langle n| , \tag{3.82}$$

which is the thermal state $e^{-\beta H}$ in $\mathcal{H}(\Sigma)$. The TFD state is a purification of the thermal state, which lifts the mixed thermal state in $\mathcal{H}(\Sigma)$ to a pure state in $\mathcal{H}(\Sigma) \otimes \mathcal{H}(\Sigma)$.

In the bulk, the BCFT state $|\mathrm{TFD}\rangle \in \mathcal{H}(S^1) \otimes \mathcal{H}(S^1)$ is dual to the Hartle-Hawking wavefunctional defined by the gravitational functional integral with thermal boundary conditions at infinity and ending on a spatial slice (or slices) bounded by two circles. Depending on the temperature β^{-1}, this state of bulk gravity is sharply peaked on one of two configurations. For low temperatures one obtains two disconnected copies of AdS_3 (Fig. 3.3a), while for high temperatures one obtains the two-sided, asymptotically-AdS_3 black hole (Fig. 1.2) [23, 25, 101]. The crossover occurs at the Hawking-Page temperature $T_{HP} = \frac{1}{2\pi}$ (in AdS units), where there is a first-order phase transition. In other words, below the Hawking-Page temperature the dominant bulk Euclidean saddle with thermal boundary conditions is $TAdS_3$, whose Euclidean time circle is non-contractible, while at higher temperatures the bulk saddle is the Euclidean black hole, which has the same solid-torus topology but whose Euclidean time direction is now identified with the contractible cycle. The former describes

a thermal gas of strings in AdS_3, which collapses to the black hole at high temperatures.[61]

Thus, depending on β one may think of the bulk dual to the BCFT TFD state as either the bulk TFD state in two disconnected copies of AdS_3 or the Hartle-Hawking (HH) state in the AdS_3 black hole.

Recall that $TAdS_3|_\beta$ is the quotient of $EAdS_3$ that compactifies the cylinder, $\xi \sim \xi + \beta$. The worldsheet theory for a string in $TAdS_3|_\beta$ is then the $J_0^3+\bar{J}_0^3$ orbifold $\beta\mathbb{Z}\backslash \mathrm{SL}(2,\mathbb{C})_k/\mathrm{SU}(2)$. String perturbation theory in a thermal state in AdS_3 is defined by continuation from this orbifold. Its string amplitudes compute the dominant contribution to BCFT T^2 correlation functions below the Hawking-Page temperature. Above the Hawking-Page temperature, the black hole becomes the dominant contribution, which we discuss in the next sub-section.

The quotient preserves two of the six isometries of $EAdS_3$, corresponding to ξ and θ translations. The orbifold projection is

$$e^{i\beta(J_0^3+\bar{J}_0^3)}\Phi_j(z,\bar{z};x,\bar{x})e^{-i\beta(J_0^3+\bar{J}_0^3)} = \Phi_j(z,\bar{z};x,\bar{x}). \tag{3.83}$$

After the boundary conformal transformation $x = e^{\xi+i\theta}$ from the sphere to the cylinder under which $\Phi_j(z,\bar{z};x,\bar{x}) \to e^{-2j\xi}\Phi_j(z,\bar{z};\xi,\theta)$, the projection condition simply enforces periodicity in ξ:

$$\Phi_j(z,\bar{z};\xi,\theta) = \Phi_j(z,\bar{z};\xi+\beta,\theta). \tag{3.84}$$

[61] Until one reaches the Hagedorn temperature, where the theory becomes unstable. Of course, the bosonic string theory is already unstable because of the tachyon. But as the temperature is increased, the thermal circle becomes small and the modes that wind it become lighter. At the Hagedorn temperature, the circle becomes so small that the lightest winding mode becomes tachyonic [54, 90].

Each unflowed primary Φ_j of $SL(2,\mathbb{C})_k/SU(2)$ may be projected to an operator in the untwisted sector of the orbifold by summing over images,

$$\Phi_j(z,\bar{z};\xi,\theta) \to \sum_{n\in\mathbb{Z}} \Phi_j(z,\bar{z};\xi+\beta n,\theta). \tag{3.85}$$

For spectral-flowed operators, one may likewise sum over images of $\Phi^{J\bar{J}}_{jw}(z,\bar{z};x,\bar{x}) \to e^{-J(\xi+i\theta)}e^{-\bar{J}(\xi-i\theta)}\Phi^{J\bar{J}}_{jw}(z,\bar{z};\xi,\theta)$ to obtain a projection-invariant operator:

$$\Phi^{J\bar{J}}_{jw}(z,\bar{z};\xi,\theta) \to \sum_{n\in\mathbb{Z}} \Phi^{J\bar{J}}_{jw}(z,\bar{z};\xi+\beta n,\theta). \tag{3.86}$$

We emphasize that the projection acts on the Euclidean $SL(2,\mathbb{C})_k/SU(2)$ vertex operators and not on the spectrum of Lorentzian string states $|j,m,\bar{m};w\rangle \otimes \left|h,\bar{h}\right\rangle$. The string states are particle-like excitations on top of the AdS_3 background—whether the background is in the vacuum or thermal state does not affect the spectrum of particles.

The correlation functions of the projected primaries Eqns. 3.85-3.86 in the orbifold are obtained by summing over images in the original $SL(2,\mathbb{C})_k/SU(2)$ correlators, and their amplitudes produce the T^2 correlation functions of the BCFT for $\beta > 2\pi$. Correspondingly, the BCFT local operators and correlation functions on T^2 may independently be obtained from the cylinder by summing over images.

The continuation to Lorentzian expectation values in the thermal state is as before. If one cuts the torus at $\xi = 0$ and continues the operators to the Lorentzian section, one obtains string amplitudes in AdS_3 in the thermal state at inverse temperature β. If one makes cuts at

both $\xi = 0$ and $\xi = \beta/2$, one can continue the operator labels to either $\xi = it_{\rm R}$ or $\xi = \frac{\beta}{2} + it_{\rm L}$. The resulting string amplitudes compute expectation values of the continued insertions in two copies of AdS_3 in the TFD state. The corresponding Schwinger-Keldysh contour is obtained by gluing together two copies of Fig. 3.3a. One may also leave insertions on the T^2 Euclidean section to define perturbation theory in a thermal or TFD state deformed by sources.

For example, the two-point amplitude of Φ_j is obtained by summing over images in Eqn. 3.73,[62]

$$\left\langle \hat{\Phi}_j(\xi_1, \theta_1)\hat{\Phi}_j(\xi_2, \theta_2) \right\rangle \propto \sum_{n\in\mathbb{Z}} \left\{\cosh(\xi_{12} + n\beta) - \cos(\theta_{12})\right\}^{-2j} . \tag{3.87}$$

By cutting the torus at $\xi = 0$ and continuing both insertions to the Lorentzian cylinder one obtains the amplitude in a thermal state, [23, 102, 103]

$$\mathrm{tr}\left(e^{-\beta H}\hat{\Phi}_j(t_1, \theta_1)\hat{\Phi}_j(t_2, \theta_2)\right) \propto \sum_{n} \left\{\cos(t_{12} + in\beta) - \cos(\theta_{12})\right\}^{-2j} , \tag{3.88}$$

again suppressing the $i\varepsilon$'s. Alternatively, one could cut the torus at both $\xi = 0$ and $\xi = \beta/2$ preparing the TFD state, and e.g. continue one operator to each side

$$\begin{aligned} &\langle \mathrm{TFD}| \left(1_{\rm L}\otimes\hat{\Phi}_j(t_{\rm R,1}, \theta_1)\right)\left(\hat{\Phi}_j(t_{\rm L,2}, \theta_2) \otimes 1_{\rm R}\right) |\mathrm{TFD}\rangle \\ &\qquad \propto \sum_{n\in\mathbb{Z}} \left\{\cos\left(t_{\rm R,1} - t_{\rm L,2} + i\left(n - 1/2\right)\beta\right) - \cos(\theta_{12})\right\}^{-2j} . \end{aligned} \tag{3.89}$$

[62] Note that by simply replacing each operator by its sum over images, e.g. $\sum_{n,m\in\mathbb{Z}} \langle \mathcal{O}(\xi + n\beta)\mathcal{O}(\xi' + m\beta)\rangle = \sum_{\substack{n-m\in\mathbb{Z} \\ n+m\in\mathbb{Z}}} \langle \mathcal{O}(\xi - \xi' + (n-m)\beta)\mathcal{O}(0)\rangle$, one obtains an extraneous divergent sum $\sum_{n+m}$, which should be discarded.

One may also consider twisted-sector operators of the orbifold, but these are not expected to map to local operators of the BCFT.

3.3.3 The BTZ Black Hole

Above the Hawking-Page temperature, the asymptotically-AdS_3 black hole, known also as BTZ, is the dominant contribution to thermal BCFT expectation values [21–23, 101]. BTZ is a particularly simple black hole because it is a quotient of AdS_3, performed with respect to the $J_0^2 + \bar{J}_0^2$ isometry. The parameterization Eqn. 3.5 diagonalized the action of $J_0^3 \pm \bar{J}_0^3$. To describe the BTZ orbifold, it is therefore more natural to diagonalize $J_0^2 \pm \bar{J}_0^2$ via

$$g = e^{i(\tilde{\Theta}+\tilde{T})\mathrm{T}_2} e^{2i\tilde{R}\mathrm{T}_1} e^{i(\tilde{\Theta}-\tilde{T})\mathrm{T}_2} \in \mathrm{SL}(2,\mathbb{R}), \tag{3.90}$$

where $\tilde{T}, \tilde{\Theta} \in (-\infty, \infty)$ and $\tilde{R} \in (0, \infty)$, yielding

$$g = \begin{pmatrix} e^{\tilde{\Theta}} \cosh(\tilde{R}) & e^{\tilde{T}} \sinh(\tilde{R}) \\ e^{-\tilde{T}} \sinh(\tilde{R}) & e^{-\tilde{\Theta}} \cosh(\tilde{R}) \end{pmatrix}. \tag{3.91}$$

The group metric on Eqn. 3.90 evaluates to

$$\mathrm{d}s^2_{\text{AdS-Rindler}} = l^2_{\text{AdS}} \left(-\sinh^2(\tilde{R})\mathrm{d}\tilde{T}^2 + \mathrm{d}\tilde{R}^2 + \cosh^2(\tilde{R})\mathrm{d}\tilde{\Theta}^2 \right). \tag{3.92}$$

Whereas Eqn. 3.5 covered all of AdS_3, however, these coordinates clearly cover only a patch, which we refer to as AdS_3-Rindler in analogy with the Rindler patch of Minkowski

space. The latter is obtained from flat Euclidean space by continuing with respect to angular Euclidean time, yielding the right wedge of a two-sided decomposition of Minkowski spacetime separated by a coordinate horizon (Fig. 2.5). The metric Eqn. 3.92 is likewise related to the EAdS_3 metric Eqn. 3.13 by continuation not in the length direction of the cylinder but in the angular direction. The result is a wedge of AdS_3 bounded by a coordinate horizon at $\tilde{R} = 0$, where the coefficient $\sinh^2(\tilde{R})$ of $\mathrm{d}\tilde{T}^2$ vanishes.

$\tilde{T}$ translations are implemented in Eqn. 3.90 by $g \to e^{i\delta\tilde{T}\mathrm{T}_2} g e^{-i\delta\tilde{T}\mathrm{T}_2}$, and $\tilde{\Theta}$ translations by $g \to e^{i\delta\tilde{\Theta}\mathrm{T}_2} g e^{i\delta\tilde{\Theta}\mathrm{T}_2}$. These isometries are therefore generated in $\mathrm{SL}(2,\mathbb{R})_k$ by $J_0^2 - \bar{J}_0^2$ and $J_0^2 + \bar{J}_0^2$, respectively. The (non-rotating) BTZ black hole of radius R_s is defined by the $J_0^2 + \bar{J}_0^2$ orbifold that compactifies

$$\tilde{\Theta} \sim \tilde{\Theta} + 2\pi R_\mathrm{s}/l_\mathrm{AdS}. \tag{3.93}$$

In $\mathrm{SL}(2,\mathbb{R})$, this is the identification $g \sim hgh$, with

$$h = e^{2\pi i R_\mathrm{s}\mathrm{T}_2/l_\mathrm{AdS}} = \begin{pmatrix} e^{\pi R_\mathrm{s}/l_\mathrm{AdS}} & 0 \\ 0 & e^{-\pi R_\mathrm{s}/l_\mathrm{AdS}} \end{pmatrix}. \tag{3.94}$$

h is a hyperbolic element of $\mathrm{SL}(2,\mathbb{R})$, meaning that $\mathrm{tr}(h) = 2\cosh(\pi R_\mathrm{s}/l_\mathrm{AdS}) > 2$. The quotient preserves the translation isometries in $\tilde{T}$ and $\tilde{\Theta}$.

The BTZ metric may be expressed in a more Schwarzschild-like form by the coordinate

transformation

$$R = R_{\rm s}\cosh(\tilde{R}), \quad T = \frac{l_{\rm AdS}}{R_{\rm s}}\tilde{T}, \quad \Theta = \frac{l_{\rm AdS}}{R_{\rm s}}\tilde{\Theta}, \tag{3.95}$$

in terms of which Eqn. 3.92 becomes

$$\mathrm{d}s^2_{\rm BTZ} = -(R^2 - R_{\rm s}^2)\mathrm{d}T^2 + \frac{l^2_{\rm AdS}}{R^2 - R_{\rm s}^2}\mathrm{d}R^2 + R^2\mathrm{d}\Theta^2, \tag{3.96}$$

with the BTZ identification $\Theta \sim \Theta + 2\pi$. These coordinates cover the right wedge $R > R_{\rm s}$ of the black hole, which may as usual be extended to a two-sided geometry with left and right asymptotically-AdS_3 regions separated by the horizon (Fig. 3.5a). The mass of the black hole mass is [21, 22]

$$M = \frac{1}{8G_{\rm N}}\frac{R_{\rm s}^2}{l^2_{\rm AdS}}. \tag{3.97}$$

The states of a string in BTZ are given by the $J_0^2 + \bar{J}_0^2$ orbifold of the $\mathrm{SL}(2,\mathbb{R})_k$ spectrum (Eqn. 3.39) with the projection $e^{2\pi i R_{\rm s}/l_{\rm AdS}(J_0^2+\bar{J}_0^2)} = 1$, combined with the twisted sectors that wind the compactified Θ cycle [104–106]. As in Eqn. 3.90, one therefore chooses a basis of $\mathrm{SL}(2,\mathbb{R})_k$ that diagonalizes $J_0^2, \bar{J}_0^2$, which have continuous spectrum. The spectrum of the Hamiltonian $\frac{R_{\rm s}}{l_{\rm AdS}}(J_0^2 - \bar{J}_0^2)$ with respect to the Schwarzschild time T is likewise continuous, as is expected from the bulk effective field theory in the black hole background in the $M_{\rm p} \to \infty$ limit.

Note that in BTZ there is no simple relationship between the perturbative string states

and BCFT primary operators, in contrast to the vacuum theory. In the latter case, for example, the lowest-weight string state $|j,j,j\rangle \in \widehat{D}^+_j \otimes \widehat{D}^+_j$ is prepared on the worldsheet by inserting $\Phi_j(z=0;x=0)$ (Eqn. 3.76). It is dual to the BCFT Virasoro primary state $|j,j,j\rangle \in D^+_j \otimes D^+_j$, likewise transforming in the lowest-weight discrete-series representation of the boundary global conformal algebra, and itself prepared by inserting the dual operator $\hat{\Phi}_j(x=0)$ at the origin of the boundary hemisphere. Both states are eigenstates of the respective bulk and boundary Hamiltonians, global AdS_3 time translations being generated by $J^3_0 + \bar{J}^3_0$, which maps to $\mathsf{L}_0 + \bar{\mathsf{L}}_0$ in the dual. In BTZ, by contrast, a boundary local operator insertion does not prepare an eigenstate of the bulk Hamiltonian $J^2_0 - \bar{J}^2_0$, and one should not expect a simple relationship between bulk string states and BCFT primaries.

The BTZ string theory is again defined by continuation from its Euclidean counterpart. Setting $\tilde{T}_\mathrm{E} = i\tilde{T}$ in Eqn. 3.92 defines the Euclidean BTZ black hole (EBTZ):

$$\mathrm{d}s^2_\mathrm{EBTZ} = l^2_\mathrm{AdS}\left(\sinh^2(\tilde{R})\mathrm{d}\tilde{T}^2_\mathrm{E} + \mathrm{d}\tilde{R}^2 + \cosh^2(\tilde{R})\mathrm{d}\tilde{\Theta}^2\right). \tag{3.98}$$

Near $\tilde{R}=0$, the metric $\tilde{R}^2\mathrm{d}\tilde{T}^2_\mathrm{E} + \mathrm{d}\tilde{R}^2 + \mathrm{d}\tilde{\Theta}^2 + \cdots$ describes the plane in polar coordinates times a circle, and the angle $\tilde{T}_\mathrm{E}$ must be 2π periodic to obtain a smooth solution; the near-horizon Lorentzian geometry is then Rindler $\times$ S^1. Eqn. 3.90 is likewise invariant under $\tilde{T} \to \tilde{T} + 2\pi i$, as $e^{\pm 2\pi \mathrm{T}_2} = -1_{2\times 2}$. The Euclidean Schwarzschild time T_E is periodic in $\beta = 2\pi l_\mathrm{AdS}/R_\mathrm{s}$, which is identified as the inverse Hawking temperature of the black hole in AdS units.

EBTZ at inverse temperature β is therefore a solid torus, with contractible cycle $\tilde{T}_\mathrm{E} \sim$

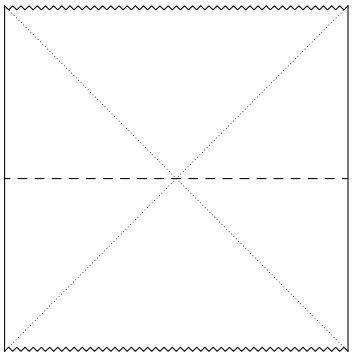

(a) The BTZ Black Hole. The BTZ black hole is the two-sided, asymptotically AdS_3 solution of three-dimensional gravity with negative cosmological constant. It is a quotient of AdS_3, obtained by compactifying $\tilde{\Theta} \sim \tilde{\Theta} + 2\pi R_s/l_{AdS}$ in the coordinates of Eqn. 3.90. The $\tilde{\Theta}$ circle is suppressed in the figure. The geometry is time-dependent, but Z_2 symmetric with respect to the dashed line. This line is the wormhole between the left and right causally disconnected regions. It has the topology of an annulus, with the two circle boundaries corresponding to slices of the asymptotic AdS_3 boundaries.

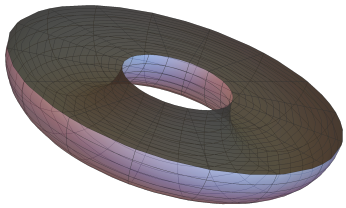

(b) The Hartle-Hawking Cap. The Euclidean continuation of the BTZ black hole is a solid torus, whose contractible cycle is identified with the Euclidean time. Slicing the torus in half across this cycle produces a manifold in the shape of a halved bagel. Its annular boundary is identical to the zero-time slice of the Lorentzian black hole, indicated by the dashed line on the left. Gluing the Euclidean cap to this slice prepares the Hartle-Hawking state in the black hole background, whose reduced density matrix in a single wedge is a thermal state of inverse temperature $2\pi l_{AdS}/R_s$. The purple boundary of the torus prepares the TFD state of the BCFT on the two circle boundaries of the annulus.

Figure 3.5

$\tilde{T}_E + 2\pi$ and non-contractible cycle $\tilde{\Theta} \sim \tilde{\Theta} + 4\pi^2/\beta$. It is identical to the $TAdS_3|_{\tilde{\beta}}$ solid torus at inverse temperature $\tilde{\beta} = 2\pi R_s/l_{AdS} = 4\pi^2/\beta$. When referring to $TAdS_3$, however, it is the non-contractible cycle that one identifies with the Euclidean time as in the previous subsection. Whereas cutting the solid torus in half across its non-contractible cycle prepared the TFD state in two disconnected copies of AdS_3 (Fig. 3.3a), cutting across its contractible cycle produces a Euclidean cap in the shape of a halved bagel, which prepares the Hartle-Hawking (HH) state in the connected black hole (Figs. 3.5b and 1.2a) [23, 26, 27].

The zero-time slice of the two-sided black hole is a wormhole passing between the left and right asymptotically-AdS_3 regions. Topologically, it is an annulus, with the two circle boundaries corresponding to slices of the two AdS_3 boundary cylinders. Although Fig. 3.5a is time dependent with respect to the global Kruskal time that flows vertically, it is symmetric

under time reversal, which is a reflection about the horizontal dashed line in the figure. The existence of this Z_2 symmetry ensures that the Euclidean continuation of the geometry is real, and that the fixed-point locus is common to both the Lorentzian and Euclidean sections. Thus, the two may be cut in half and glued together along this annulus locus to prepare the HH state [23, 26, 27]. This state is a generalized notion of a vacuum for the black hole, and its existence is due to the Z_2 time-reversal symmetry.

Alternatively, the HH state may be thought of as a TFD state with respect to the left and right wedges of the black hole, entangled by the Euclidean cap that evolves between them in angular time (Fig. 4.1a). The reduced density matrix in a single wedge is a thermal state at inverse temperature $\beta = 2\pi l_{\mathrm{AdS}}/R_{\mathrm{s}}$. In this sense, both slicings of the TAdS_3/EBTZ solid torus prepare TFD states, the distinction being that in the first case the spacetime is disconnected while in the second it is connected.

The worldsheet theory for a string in BTZ in the HH state is then similarly obtained by continuation from the $\frac{4\pi^2}{\beta}\mathbb{Z}\backslash\mathrm{SL}(2,\mathbb{C})_k/\mathrm{SU}(2)$ orbifold, but with the continuation now performed with respect to the contractible cycle [104–106]. The equivalence of $\mathrm{EBTZ}|_\beta$ and $\mathrm{TAdS}|_{4\pi^2/\beta}$ shows that the $J_0^3 + \bar{J}_0^3$ and $J_0^2 + \bar{J}_0^2$ orbifolds are identical in the Euclidean case, and we may proceed as in the previous sub-section but with the temperature inverted.

Thus, the projection to the untwisted sector of the orbifold is

$$e^{i\frac{4\pi^2}{\beta}(J_0^3+\bar{J}_0^3)}\Phi_j(z,\bar{z};x,\bar{x})e^{-i\frac{4\pi^2}{\beta}(J_0^3+\bar{J}_0^3)} = \Phi_j(z,\bar{z};x,\bar{x}). \tag{3.99}$$

After the boundary conformal transformation $x = e^{\frac{2\pi}{\beta}(\Theta+iT_{\mathrm{E}})}$, the projection demands peri-

odicity in Θ,

$$\Phi_j\left(z,\bar{z};T_{\rm E},\Theta+2\pi\right)=\Phi_j\left(z,\bar{z};T_{\rm E},\Theta\right), \tag{3.100}$$

and likewise for $\Phi^{J\bar{J}}_{jw}(z,\bar{z};T_{\rm E},\Theta)$. Their correlation functions in the orbifold are again obtained by summing over images, and their string amplitudes compute T^2 correlation functions of the BCFT for $\beta<2\pi$. For example,

$$\begin{aligned}&\left\langle\hat{\Phi}_j(T_{\rm E,1},\Theta_1)\hat{\Phi}_j(T_{\rm E,2},\Theta_2)\right\rangle \\ &\qquad\propto\sum_{n\in\mathbb{Z}}\left\{\cosh\left(\frac{2\pi}{\beta}\left(\Theta_{12}+2\pi n\right)\right)-\cos\left(\frac{2\pi}{\beta}T_{\rm E,12}\right)\right\}^{-2j}.\end{aligned} \tag{3.101}$$

Cutting the torus at $T_{\rm E}=0$ and gluing in the Lorentzian cylinder prepares the thermal state. Continuing both operators gives their thermal expectation value [23, 102, 103]

$$\begin{aligned}&\mathrm{tr}\left(e^{-\beta H}\hat{\Phi}_j(T_1,\Theta_1)\hat{\Phi}_j(T_2,\Theta_2)\right) \\ &\qquad\propto\sum_{n\in\mathbb{Z}}\left\{\cosh\left(\frac{2\pi}{\beta}\left(\Theta_{12}+2\pi n\right)\right)-\cosh\left(\frac{2\pi}{\beta}T_{12}\right)\right\}^{-2j}.\end{aligned} \tag{3.102}$$

Or, making cuts at both $T_{\rm E}=0$ and $\beta/2$ and e.g. continuing an operator to each side,[63]

$$\begin{aligned}&\langle\mathrm{TFD}|\left(1_{\rm L}\otimes\hat{\Phi}_j(T_{\rm R,1},\Theta_1)\right)\left(\hat{\Phi}_j(T_{\rm L,2},\Theta_2)\otimes 1_{\rm R}\right)|\mathrm{TFD}\rangle \\ &\qquad\propto\sum_{n\in\mathbb{Z}}\left\{\cosh\left(\frac{2\pi}{\beta}\left(\Theta_{12}+2\pi n\right)\right)+\cosh\left(\frac{2\pi}{\beta}\left(T_{\rm R,1}+T_{\rm L,2}\right)\right)\right\}^{-2j}.\end{aligned} \tag{3.103}$$

[63] We flip the sign of $T_{\rm L}$ here because the Schwarzschild time Killing vector points in opposite directions on the left and right sides of the black hole.

As in Eqn. 3.75, one may Fourier transform the boundary position space basis of vertex operators to obtain operators of definite BTZ energy and angular momentum. For example,

$$\Phi_{jK\bar{K}}(z,\bar{z}) \propto \int_{-\infty}^{\infty} \mathrm{d}T \int_{0}^{2\pi} \mathrm{d}\Theta e^{-\frac{2\pi i}{\beta}(K-\bar{K})T} e^{-\frac{2\pi i}{\beta}(K+\bar{K})\Theta} \sum_{n\in\mathbb{Z}} \Phi_j(z,\bar{z};T,\Theta+2\pi n), \tag{3.104}$$

where $\frac{2\pi}{\beta}(K \mp \bar{K})$ are the energy and angular momentum. Examples of string amplitudes in this basis are computed in [106]. Absent the sum over images n, one would instead obtain a mode of AdS_3-Rindler.

3.3.4 The 2D Black Hole

Finally, we briefly discuss string perturbation theory in the two-dimensional black hole in the HH state. The two-dimensional Euclidean black hole (Eqn. 2.97) followed from $\mathrm{SL}(2,\mathbb{R})_k$ (or $\mathrm{SL}(2,\mathbb{C})_k/\mathrm{SU}(2)$) by gauging the $J_0^3 + \bar{J}_0^3$ isometry that generates translations along the length of the cylinder (Eqn. 3.50). The Lorentzian black hole is then obtained by continuing in the compact coordinate $\theta = it$ (Eqn. 2.102). Alternatively, recalling the BTZ coordinates on $\mathrm{SL}(2,\mathbb{R})$ describe an AdS_3-Rindler patch (Eqns. 3.90-3.92), likewise related to EAdS_3 by continuation in the compact cycle, one may arrive directly at the two-dimensional Lorentzian black hole by gauging the $J_0^2 + \bar{J}_0^2$ symmetry of $\mathrm{SL}(2,\mathbb{R})_k$ that generates translations in Θ. Then whereas the two-dimensional Euclidean black hole spectrum (Eqn. 2.106) followed from the $\mathrm{SL}(2,\mathbb{R})_k$ spectrum (Eqn. 3.39) by the coset construction that gauged $J_0^3 + \bar{J}_0^3$, the Lorentzian spectrum is obtained by the coset construction with respect to $J_0^2 + \bar{J}_0^2$.

String perturbation theory in the two-dimensional black hole in the HH state is again de-

fined by continuation from the Euclidean black hole. For example, continuing the Euclidean vertex operators $\mathcal{O}_{jn,w=0}$ with $j = \frac{1}{2}(1+is)$ by sending $n \to iE$ yields scattering states in the right wedge.[64] From Eqn. 2.116 one obtains

$$\mathcal{O}_{jE} \overset{r\to\infty}{\longrightarrow} \left(e^{-2(1-j)r} + R(j,E)e^{-2jr}\right) e^{-iEt}, \tag{3.105}$$

with wavefunction

$$\Psi_{jE} \underset{\propto}{\overset{r\to\infty}{\longrightarrow}} \left(e^{isr} + R(j,E)e^{-isr}\right) e^{-iEt}, \tag{3.106}$$

describing an incoming particle in the right wedge that scatters off the black hole horizon. One may likewise construct by continuation vertex operators describing outgoing modes, as well as similar modes in the left wedge, and modes behind the past and future horizons [75].

In the Euclidean theory, one found normalizable bound states at poles of the reflection coefficient. Now $R(j,E)$ is non-singular on the real branch, and one finds only these delta-function normalizable scattering states on the complex branch.[65] These modes do not form a complete set, however. The reason is tied to non-unitarity of the scattering matrix—strings can fall behind the horizon. One can close the OPE by including additional modes, including the operators with $w \neq 0$, but at the cost of sacrificing mutual locality of the vertex operators.

String amplitudes of such scattering operators in the HH state may be obtained by con-

[64] Here E is the energy measured in units of $1/\sqrt{\alpha' k}$, and is conjugate to $t = -i\theta$. The proper time in the large r limit of the metric (Eqn. 2.102) is $-\alpha' k dt^2$.

[65] As in Rindler, the modes are singular at the horizon, $\Psi_{jE} \propto r^{-iE} e^{-iEt}(1 + \mathcal{O}(r^2))$.

tinuation from the corresponding Euclidean amplitudes. The Schwinger-Keldysh contour consists of the two Euclidean caps obtained by halving the cigar (Fig. 2.4b), glued to the zero-time slice of the Lorentzian black hole (Fig. 2.4a), which evolves forward and backward in Lorentzian time. The continuation is more technically challenging than in AdS_3 where one simply continued the boundary insertion point in x-basis worldsheet vertex operators. In momentum basis, one instead computes the Euclidean amplitude as a function of the discrete Matsubara frequencies n, and then continues the result to continuous Lorentzian energies E [75]. The analogous objects in three dimensions are the Fourier modes Eqns. 3.75, 3.104.

4 Stringy ER = EPR

Finally, we apply the machinery developed in the previous chapters to construct examples of string dualities for ER = EPR. The examples are obtained by continuation from the FZZ duality of the $\mathrm{SL}(2,\mathbb{R})_k/\mathrm{U}(1)$ CFT that describes a string in the two-dimensional Euclidean black hole, and similar dualities that we will propose for the $\mathrm{SL}(2,\mathbb{C})_k/\mathrm{SU}(2)$ and $\mathbb{Z}\backslash\mathrm{SL}(2,\mathbb{C})_k/\mathrm{SU}(2)$ CFTs that describe a string in EAdS_3 and EBTZ.

Each of the three Euclidean dualities shares the essential feature that the Euclidean time circle is contractible in one description and non-contractible in the other, with Euclidean time winding conservation violated in the latter case by a condensate of winding strings. Upon continuation then, each gives a string duality realizing ER = EPR. On one side is string theory in a connected spacetime with a horizon in its Hartle-Hawking state, and on the other is string theory in a disconnected union of entangled spacetimes in the thermofield-double state. In the semi-classical limit, the ER description is weakly coupled in the α' sense, and the EPR description is strongly coupled. Both sides may be taken at weak string

coupling, however.[66]

The principal remaining challenge in formulating these continuations is the Lorentzian interpretation of the Euclidean time winding operators that play a critical role in each of the examples. We will argue that these insertions should be treated in angular quantization on the worldsheet—with a corresponding deformation of the moduli space integration contour where necessary—giving rise to a condensate of pairs of entangled, folded strings emanating from the strong-coupling region.

Note that although one could T-dualize the sine-Liouville background, and thereby replace the winding potential with a momentum potential whose Lorentzian interpretation is more straightforward, its continuation would not be dual to the Lorentzian black hole. To obtain a Lorentzian duality, one must continue with respect to the same Z_2 symmetry on both sides of the Euclidean duality. The continuation of the T-dualized sine-Liouville background would instead be dual to the continuation of the so-called trumpet geometry [75], which has a naked singularity where the θ circle of the cigar shrinks.

It may also be possible to construct stringy ER = EPR examples where the winding violation in the non-contractible frame is accomplished by the inclusion of D-branes. Their presence would allow closed strings wrapping the Euclidean time direction to break into pairs of open strings ending on the brane. Given that the EPR side of the duality can be interpreted as describing the constituent objects that make up the black hole, in backgrounds

[66] In the sense that the boundary correlators or scattering amplitudes can be computed in string perturbation theory since they are governed by regions of the target space with tunably-weak string coupling. The target space in the EPR side of the dualities includes a strong-coupling region, however.

with Ramond-Ramond fluxes one would indeed expect to find D-branes. In our examples, however, the dualities only involve closed strings, corresponding to black holes that are made of fundamental strings, and it is the winding potential that is responsible for breaking the symmetry.

In Sec. 4.1 we propose the three-dimensional uplifts of the FZZ duality to the $\mathrm{SL}(2,\mathbb{C})_k/\mathrm{SU}(2)$ and $\mathbb{Z}\backslash\mathrm{SL}(2,\mathbb{C})_k/\mathrm{SU}(2)$ CFTs. In Sec. 4.2 we construct the ER = EPR duality of two-dimensional dilaton-gravity obtained by continuation from the FZZ duality. Here we discuss the idea of angular quantization of the worldsheet CFT, which is essential to understand the state of the folded strings produced by the continuation of the Euclidean time winding condensate. We also discuss the related angular deformation of the contour of integration over the string moduli space that is necessary in the background of Euclidean time winding operators. In Sec. 4.3 we similarly continue the uplifted dualities of asymptotic AdS_3 gravity to obtain two more examples of ER = EPR. Lastly, in Sec. 4.4 we discuss an infinitesimal version of the various dualities in the sense of conformal perturbation theory, which gives two equivalent pictures of shifting the mass of the black hole.

4.1 3D FZZ Dualities

In Secs. 2.3 and 2.5 we reviewed the cigar and sine-Liouville descriptions of the $\mathrm{SL}(2,\mathbb{R})_k/\mathrm{U}(1)$ CFT; the equivalence of the two backgrounds is the content of the FZZ duality. In this section we propose a new duality that may be considered the uplift of FZZ to the EAdS_3 CFT $\mathrm{SL}(2,\mathbb{C})_k/\mathrm{SU}(2)$ (Sec. 3.1), or its EBTZ quotient $\mathbb{Z}\backslash\mathrm{SL}(2,\mathbb{C})_k/\mathrm{SU}(2)$ (Secs. 3.3.2-3.3.3).

The cigar topology, being obtained from EAdS_3 by gauging the translation isometry along the length of the cylinder, may be thought of as a disk sliced from the cylinder (Fig. 1.6a). In the FZZ dual description, the disk topology of the cigar is replaced by the annulus topology of the sine-Liouville cylinder, plus the condensate of winding strings. The two descriptions share the same free linear-dilaton $\times\, \mathrm{S}^1$ limit in the weak-coupling region. Whereas the cigar geometry terminates at the origin of the disk $r = 0$, the sine-Liouville cylinder continues into the strong-coupling region $\hat{r} \to -\infty$, the potential wall instead taking responsibility for reflecting strings away.

It is natural to wonder if there exists a similar duality of the $\mathrm{SL}(2,\mathbb{C})_k/\mathrm{SU}(2)$ and $\mathbb{Z}\backslash\mathrm{SL}(2,\mathbb{C})_k/\mathrm{SU}(2)$ CFTs in which the solid cylinder or torus target space of Eqn. 3.13 with its semi-infinite radial coordinate $r \in [0,\infty)$ is replaced by a fully infinite radial direction $\hat{r} \in (-\infty,\infty)$ and a condensate of winding strings that wrap the resulting non-contractible cycle (Fig. 1.6b). If such a description existed, such that gauging the translation symmetry reproduced the sine-Liouville sigma-model, one would obtain a three-dimensional uplift of the FZZ duality.

One immediately encounters a problem with the above proposal, however, on examining the $\mathrm{SL}(2,\mathbb{C})_k/\mathrm{SU}(2)$ action (Eqn. 3.44). Whereas the cigar and sine-Liouville Lagrangians approach the same free theory at infinity, which may then be deformed by either the cigar-capping or sine-Liouville operators, the EAdS_3 Lagrangian is singular at $r \to \infty$.

This singular asymptotic behavior may be remedied by applying the first-order formal-

ism.[67] Classically, one has the identity of Lagrangians

$$f\partial\bar{W}\bar{\partial}W = \chi\bar{\partial}W + \bar{\chi}\partial\bar{W} - \frac{1}{f}\chi\bar{\chi}, \tag{4.1}$$

the auxiliary equations of motion for $\chi, \bar{\chi}$ setting $\chi = f\partial\bar{W}$ and $\bar{\chi} = f\bar{\partial}W$, which recover the left-hand-side upon substitution. Quantum mechanically, the change of variables introduces a dilaton $\log\sqrt{f}$ from the transformation of the functional integral measure. Thus, the action Eqn. 3.44 may be replaced by

$$S = \frac{k}{2\pi}\int \mathrm{d}^2z \left\{\partial r\bar{\partial}r + \partial\xi\bar{\partial}\xi + \chi(\bar{\partial}\xi + i\bar{\partial}\theta) + \bar{\chi}(\partial\xi - i\partial\theta) - \frac{1}{\sinh^2(r)}\chi\bar{\chi}\right\}, \tag{4.2}$$

together with a dilaton $\Phi = -\log\sinh r + \Phi_0$. This is the cylinder version of the standard Wakimoto form of the action Eqn. 3.43 in Poincarè coordinates [87].[68] χ is a $(1,0)$ form, set to $\chi = \sinh^2(r)\partial\bar{W}$ by the equations of motion, where $W = \xi + i\theta$ is the complex coordinate on the asymptotic cylinder, $W \sim W + 2\pi i$.

Gauging the ξ translation symmetry in Eqn. 3.44 produced the cigar action at leading order (Eqn. 3.50). In the form Eqn. 4.2, the current for ξ translations is $J^3(z) = \partial\xi + \chi$. Then the gauged first-order action becomes

$$S \to S + \frac{k}{2\pi}\int \mathrm{d}^2z \left(J^3\bar{A} + \bar{J}^3A + A\bar{A}\right). \tag{4.3}$$

[67] See e.g. [107, 108] for reviews.

[68] We use χ and W to denote the cylinder-valued first-order coordinates rather than the typical β and γ to avoid confusion with the first-order formalism in Poincarè coordinates.

Classically integrating out $A, \bar{A}$ yields a first-order description of the cigar,[69]

$$S_{\text{cigar}} = \frac{k}{2\pi}\int \mathrm{d}^2 z \left(\partial r \bar{\partial} r + i\chi\bar{\partial}\theta - i\bar{\chi}\partial\theta - \coth^2(r)\chi\bar{\chi}\right), \tag{4.4}$$

and integrating out $\chi, \bar{\chi}$ again reproduces the cigar action.

The presentation Eqn. 4.2 is advantageous because it is non-singular at $r \to \infty$, where the potential $\chi\bar{\chi}/\sinh^2(r)$ goes to zero. In that limit, the gauged action after classically integrating out the gauge fields is then as in Eqn. 4.4 but with $\coth^2(r) \to 1$, and further integrating out the auxiliaries yields the expected asymptotic cylinder background,

$$S_{\text{cigar}} \overset{r\to\infty}{\longrightarrow} \frac{k}{2\pi}\int \mathrm{d}^2 z \left(\partial r \bar{\partial} r + \partial\theta\bar{\partial}\theta\right). \tag{4.5}$$

Thus, Eqn. 4.2 is a preferable description of $\mathrm{SL}(2,\mathbb{C})_k/\mathrm{SU}(2)$ for the purposes of uplifting the FZZ duality because the free theory it approaches at $r \to \infty$ is transparently the uplift of the same limit of the cigar background.

This large r limit of Eqn. 4.2 is a linear-dilaton plus first-order cylinder system. One may define canonically normalized fields

$$\hat{r} = \frac{1}{Q}r, \qquad \hat{W} = \sqrt{\alpha' k}W, \qquad \hat{\chi} = \sqrt{\alpha' k}\left(\chi + \frac{1}{2}\partial\xi\right), \tag{4.6}$$

[69] In this description one has contributions to the dilaton both from the first-order formalism and from integrating out $A, \bar{A}$. Further integrating out $\chi, \bar{\chi}$ eliminates the former contribution, leaving the expected dilaton profile Eqn. 2.97b of the cigar.

such that the asymptotic action appears

$$S_{\mathrm{LD}\times\mathcal{F}(\mathbb{C}/\mathbb{Z})} = \frac{1}{2\pi\alpha'}\int \mathrm{d}^2z\left(\partial\hat{r}\bar{\partial}\hat{r} + \hat{\chi}\bar{\partial}\hat{W} + \hat{\bar{\chi}}\partial\hat{\bar{W}}\right), \quad \Phi(\hat{r}) = -Q\hat{r}. \tag{4.7}$$

We denote by $\mathcal{F}(X)$ the first-order system valued in X; in this case $X = \mathbb{C}/\mathbb{Z}$ is the cylinder $\hat{W} \sim \hat{W} + 2\pi i\sqrt{\alpha' k}$. As before, $Q = 1/\sqrt{\alpha'(k-2)}$ after accounting for quantum corrections. The asymptotic potential $e^{-2r}\chi\bar{\chi}$ in Eqn. 4.2 is the leading correction to the free theory at finite r, analogous to $e^{-2r}\partial\theta\bar{\partial}\theta$ in the cigar.

It is important to understand once more how the gauging of the translation symmetry along the length of the EAdS_3 boundary cylinder is implemented in the description Eqn. 4.7. The holomorphic current $\partial\xi + \chi$ in the unhatted variables becomes $J^3(z) = \hat{\chi} + \frac{1}{4}(\partial\hat{W} + \partial\hat{\bar{W}})$ (after rescaling by $\sqrt{\alpha' k}$ for convenience).[70] Gauging this symmetry of the free linear-dilaton $\times\, \mathcal{F}(\mathbb{C}/\mathbb{Z})$ system is then implemented by

$$S_{\mathrm{LD}\times\mathcal{F}(\mathbb{C}/\mathbb{Z})} \to S_{\mathrm{LD}\times\mathcal{F}(\mathbb{C}/\mathbb{Z})} + \frac{1}{2\pi\alpha'}\int \mathrm{d}^2z\left(J^3\bar{A} + \bar{J}^3 A + A\bar{A}\right), \tag{4.8}$$

which is invariant under $\hat{W} \to \hat{W} + \varepsilon$, $\hat{\bar{W}} \to \hat{\bar{W}} + \varepsilon$, $A \to A - \partial\varepsilon$, $\bar{A} \to \bar{A} - \bar{\partial}\varepsilon$, $\hat{\chi} \to \hat{\chi} + \frac{1}{2}\partial\varepsilon$, and $\hat{\bar{\chi}} \to \hat{\bar{\chi}} + \frac{1}{2}\bar{\partial}\varepsilon$. Integrating out $A, \bar{A}$ and $\chi, \bar{\chi}$, we recover the linear-dilaton $\times\, \mathrm{S}^1$ background.

[70] Note that the appropriate current is not simply $\hat{\chi}$, as might be suggested from the coefficient of $\bar{\partial}\hat{W}$ in Eqn. 4.7. In writing Eqn. 4.7, we have dropped a term $-\frac{i}{2}(\partial\hat{\xi}\bar{\partial}\hat{\theta} - \bar{\partial}\hat{\xi}\partial\hat{\theta})$, which is total derivative in EAdS_3, though one should include it in EBTZ where it contributes a non-trivial B-field. It does not contribute to the equations of motion, but it does contribute $\frac{i}{2}\partial\hat{\theta} = \frac{1}{4}(\partial\hat{W} - \partial\hat{\bar{W}})$ to the holomorphic current for translations in $\hat{\xi} = \mathrm{Re}(\hat{W})$. The correction is important in order to identify the appropriate current whose gauging reproduces the linear-dilaton $\times\, \mathrm{S}^1$ background.

The same subtlety arises in the ordinary complex boson, $\partial X\bar{\partial}X + \partial Y\bar{\partial}Y = \partial\bar{Z}\bar{\partial}Z - i(\partial X\bar{\partial}Y - \bar{\partial}X\partial Y)$, where $Z = X + iY$. The usual holomorphic current for translations in X is ∂X. In the complex description, the corresponding current including the contribution from the exact B-field is $\partial\bar{Z} + i\partial Y = \frac{1}{2}(\partial Z + \partial\bar{Z}) = \partial X$, as desired.

Note that the current in the hatted variables, $\frac{1}{\sqrt{\alpha' k}}\left(\hat{\chi} + \frac{i}{2}\partial\hat{\theta}\right) = \chi + \frac{1}{2}\partial W$, differs from the current $\chi + \partial\xi = \chi + \frac{1}{2}(\partial W + \partial\bar{W})$ in the unhatted variables by $\frac{1}{2}\partial\bar{W}$, which vanishes by the equations of motion. The discrepancy arises because the change of variables Eqn. 4.6 shifts χ by $\partial\xi$, preserving the translational symmetry of ξ under which both χ and $\hat{\chi}$ are invariant, while producing currents that differ by irrelevant terms proportional to the equations of motion.

The $\hat{\chi}\hat{W}$ system is the familiar ($c = 2$) bosonic ghost "$\beta\gamma$" system, except that $\hat{W} \sim \hat{W} + 2\pi i\sqrt{\alpha' k}$ is cylinder-valued. The holomorphic stress tensor is

$$T(z) = -\frac{1}{\alpha'}(\partial\hat{r})^2 - Q\partial^2\hat{r} - \frac{1}{\alpha'}\hat{\chi}\partial\hat{W}, \tag{4.9}$$

whose central charge $3+6\alpha' Q^2$ reproduces the exact central charge $3k/(k-2)$ of $\mathrm{SL}(2,\mathbb{C})_k/\mathrm{SU}(2)$. $\hat{\chi}(z)$ carries conformal weight $(1,0)$ and $\hat{W}(z)$ is dimensionless, where the equations of motion imply $\bar{\partial}\hat{W} = \bar{\partial}\hat{\chi} = 0$. Their OPE is

$$\hat{W}(z)\hat{\chi}(0) \sim \frac{\alpha'}{z}, \tag{4.10}$$

with $\hat{W}(z)\hat{W}(0)$ and $\hat{\chi}(z)\hat{\chi}(0)$ non-singular. The anti-holomorphic sector is analogous.

Having obtained the free-field limit Eqn. 4.7 at the conformal boundary of EAdS_3, we now follow FZZ and attempt to define a dual description by taking the free theory over the infinite $\hat{r}$ line and deforming it by an appropriate uplift of the sine-Liouville potential. As explained following Eqn. 3.67, $\mathrm{SL}(2,\mathbb{R})_k$ and $\mathrm{SL}(2,\mathbb{R})_k/\mathrm{U}(1)$ contain an identical marginal operator $\mathcal{O}_{\mathrm{sL}}$, whose weak-coupling limit in the coset is the sine-Liouville potential (Eqn. 2.122). One may identify the same operator in the continued space of $\mathrm{SL}(2,\mathbb{C})_k/\mathrm{SU}(2)$ operators. We wish to find the asymptotic form of this operator in the linear-dilaton $\times\, \mathcal{F}(\mathbb{C}/\mathbb{Z})$ description of the EAdS_3 boundary. We will therefore search for a marginal operator of the free theory that carries unit winding around $\mathrm{Im}(\hat{W})$ and no momentum, such that it reduces to the familiar sine-Liouville potential upon gauging the symmetry.

The winding operators of the first-order cylinder system are less familiar than those of the ordinary compact boson [109]. From Eqn. 4.10 one obtains

$$\hat{W}(z)e^{\mp\sqrt{\frac{k}{\alpha'}}\int^0 \mathrm{d}z'\,\hat{\chi}+\mathrm{d}\bar{z}'\hat{\bar{\chi}}} \sim \pm\sqrt{\alpha' k}\log(z)e^{\mp\sqrt{\frac{k}{\alpha'}}\int^0 \mathrm{d}z'\,\hat{\chi}+\mathrm{d}\bar{z}'\hat{\bar{\chi}}}, \tag{4.11}$$

and likewise for $\hat{\bar{W}}(\bar{z})$. Thus, $e^{\mp\sqrt{\frac{k}{\alpha'}}\int^0 \mathrm{d}z'\,\hat{\chi}+\mathrm{d}\bar{z}'\hat{\bar{\chi}}}$ carries winding ± 1 with respect to $\hat{\theta} = \frac{1}{2i}(\hat{W} - \hat{\bar{W}})$, while $\hat{\xi} = \frac{1}{2}(\hat{W} + \hat{\bar{W}})$ is single-valued. The integral $\int^0 \mathrm{d}z'\,\hat{\chi} + \mathrm{d}\bar{z}'\hat{\bar{\chi}}$ is evaluated along a contour ending at the origin, where the winding operator is inserted. Demanding that observables be independent of the choice of contour constrains the spectrum of the CFT, such that the integrated expression defines a local operator [109].

This winding operator alone is not annihilated by the current $J^3 = \hat{\chi} + \frac{1}{4}(\partial\hat{W} + \partial\hat{\bar{W}})$, however:[71]

$$\left(\hat{\chi}(z) + \frac{1}{4}\partial\hat{W}(z)\right) e^{\mp\sqrt{\frac{k}{\alpha'}}\int^0 \mathrm{d}z'\,\hat{\chi}+\mathrm{d}\bar{z}'\hat{\bar{\chi}}} \sim \pm\frac{\sqrt{\alpha' k}}{4z}e^{\mp\sqrt{\frac{k}{\alpha'}}\int^0 \mathrm{d}z'\,\hat{\chi}+\mathrm{d}\bar{z}'\hat{\bar{\chi}}}. \tag{4.12}$$

To obtain a winding operator with no momentum along the cylinder one must append the factor $e^{\pm\frac{1}{4}\sqrt{\frac{k}{\alpha'}}(\hat{W}+\hat{\bar{W}})}$, which cancels against the OPE Eqn. 4.12. The OPE of $\hat{W}$ with itself being non-singular, the inclusion of this factor preserves the winding OPE Eqn. 4.11.

Thus, the combination

$$e^{\pm\frac{1}{4}\sqrt{\frac{k}{\alpha'}}(\hat{W}+\hat{\bar{W}})}e^{\mp\sqrt{\frac{k}{\alpha'}}\int \mathrm{d}z'\,\hat{\chi}+\mathrm{d}\bar{z}'\hat{\bar{\chi}}}, \tag{4.13}$$

[71] The last term $\partial\hat{\bar{W}}$ in the current is trivial by the equations of motion, and does not contribute to any OPEs.

or more simply $e^{\mp k \int \mathrm{d}z' \chi + \mathrm{d}\bar{z}' \bar{\chi}}$ in the unhatted variables, carries zero momentum and winding ± 1, as desired. Its conformal weight is $k/4$ on the left and right due to the double-contraction with the stress tensor Eqn. 4.9, just as for the ordinary winding operators $e^{\pm i \sqrt{\frac{k}{\alpha'}} (\hat{\theta}_{\mathrm{L}} - \hat{\theta}_{\mathrm{R}})}$ of the two-dimensional cylinder (Eqn. 2.229).

In fact, Eqn. 4.13 is precisely the dimensional uplift of these ordinary winding operators. Gauging the translation symmetry as in Eqn. 4.8 and solving the auxiliary equations of motion, one finds $\hat{\chi} = \frac{1}{2} \partial \hat{\xi} - i \partial \hat{\theta}$. Evaluating Eqn. 4.13 on this solution yields

$$e^{\pm \frac{1}{2} \sqrt{\frac{k}{\alpha'}} \hat{\xi}} e^{\mp \frac{1}{2} \sqrt{\frac{k}{\alpha'}} \int (\mathrm{d}z' \partial \hat{\xi} + \mathrm{d}\bar{z}' \bar{\partial} \hat{\xi})} e^{\pm i \sqrt{\frac{k}{\alpha'}} \int (\mathrm{d}z' \partial \hat{\theta} - \mathrm{d}\bar{z}' \bar{\partial} \hat{\theta})} = e^{\pm i \sqrt{\frac{k}{\alpha'}} (\hat{\theta}_{\mathrm{L}} - \hat{\theta}_{\mathrm{R}})}, \tag{4.14}$$

the equations of motion of the gauged action implying $\partial \bar{\partial} (\hat{W} - \hat{\bar{W}}) = 0$ and therefore $\hat{\theta}(z, \bar{z}) = \hat{\theta}_{\mathrm{L}}(z) + \hat{\theta}_{\mathrm{R}}(\bar{z})$.

Finally, to this unit winding operator we append the same linear-dilaton primary $e^{-\sqrt{\frac{k-2}{\alpha'}} \hat{r}}$ as in Eqn. 2.231 to obtain a marginal operator. The three-dimensional sine-Liouville potential is then $V_{\mathrm{sL}} \propto W_+ + W_-$, where

$$W_{\pm}(z, \bar{z}) = e^{-\sqrt{\frac{k-2}{\alpha'}} \hat{r}(z, \bar{z})} e^{\pm \frac{1}{4} \sqrt{\frac{k}{\alpha'}} (\hat{W}(z) + \hat{\bar{W}}(\bar{z}))} e^{\mp \sqrt{\frac{k}{\alpha'}} \int^{z, \bar{z}} \mathrm{d}z' \, \hat{\chi} + \mathrm{d}\bar{z}' \hat{\bar{\chi}}}, \tag{4.15}$$

and which reduces to the original two-dimensional sine-Liouville potential upon gauging.

The proposal is that the deformation of the linear-dilaton $\times \mathcal{F}(\mathbb{C}/\mathbb{Z})$ background (Eqn. 4.7) by V_{sL} yields a dual description of $\mathrm{SL}(2, \mathbb{C})_k / \mathrm{SU}(2)$, which is a better description of the CFT when $k - 2$, and therefore the linear-dilaton momentum, is small. If one further

identifies $\hat{W} \sim \hat{W} + 4\pi^2\sqrt{\alpha' k}/\beta_{\rm BH}$ (corresponding to compactifying $\xi \sim \xi + 4\pi^2/\beta_{\rm BH}$), the same deformation of the linear-dilaton $\times\, \mathcal{F}(\mathbb{C}/(\mathbb{Z}\times\mathbb{Z}))$ yields a dual description of the Euclidean black hole CFT $\mathbb{Z}\backslash \mathrm{SL}(2,\mathbb{C})_k/\mathrm{SU}(2)$.

Eqn. 4.15 gives the limiting form of the components $\mathcal{W}_\pm$ of the $\mathrm{SL}(2,\mathbb{C})_k/\mathrm{SU}(2)$ sine-Liouville operator near the conformal boundary of EAdS_3. Recall from Eqn. 3.67 that $\mathcal{W}_\pm$ is obtained from the primary $|k/2-1, \pm k/2, \pm k/2\rangle$ by applying $w = \mp 1$ units of spectral flow. The asymptotic limit of the former is $e^{-(k-2)r}e^{\pm k\xi}$. Spectral flow is meanwhile implemented by the operator $e^{kw\int^z \mathrm{d}z' J^3 + \mathrm{d}\bar{z}'\bar{J}^3} = e^{kw\xi}e^{kw\int^z \mathrm{d}z'\chi + \mathrm{d}\bar{z}'\bar{\chi}}$, where $J^3(z) = \partial\xi + \chi$ [110]. Together, one obtains $\mathcal{W}_\pm \to e^{-(k-2)r}e^{\mp k\int \mathrm{d}z'\chi + \mathrm{d}\bar{z}'\bar{\chi}}$, which is identical to Eqn. 4.15 with the coordinate transformation Eqn. 4.6.

In summary, the proposed duality of $\mathrm{SL}(2,\mathbb{C})_k/\mathrm{SU}(2)$, or its asymptotically-$\mathrm{EAdS}_3$ black hole quotient $\mathbb{Z}\backslash\mathrm{SL}(2,\mathbb{C})_k/\mathrm{SU}(2)$, is as follows. On the one hand one has the familiar description, weakly coupled for large k, of a string propagating in a solid cylinder or torus supported by a B-field:

$$S_{\mathrm{EAdS}_3} = \frac{k}{4\pi}\int_\Sigma \mathrm{d}^2\sigma\sqrt{h}\Big\{(\nabla r)^2 + \cosh^2(r)(\nabla\xi)^2 + \sinh^2(r)(\nabla\theta)^2 - 2\epsilon^{ab}\sinh^2(r)\nabla_a\xi\nabla_b\theta + \frac{\Phi_0}{k}\mathcal{R}[h]\Big\}, \tag{4.16}$$

where $\sqrt{h}\epsilon^{z\bar{z}} = -\sqrt{h}\epsilon^{\bar{z}z} = -i$. In first-order variables (Eqn. 4.2), this background approaches a free linear-dilaton times first-order cylinder system in the $r\to\infty$ limit (Eqn. 4.7). The dual sine-Liouville description is given by the same free theory, defined now with an infinite linear-dilaton direction extending into the strong-coupling region, deformed by the marginal

potential with unit winding and zero momentum,

$$S_{\rm sL} = \frac{1}{4\pi\alpha'}\int_\Sigma \mathrm{d}^2\sigma\sqrt{h}\Big\{(\nabla\hat{r})^2 + 2h^{ab}(\hat{\chi}_a\nabla_b\hat{W} + \hat{\bar{\chi}}_a\nabla_b\hat{\bar{W}}) + 4\pi\lambda(W_+ + W_-) - \alpha' Q\mathcal{R}[h]\hat{r}\Big\}. \tag{4.17}$$

Gauging the translation symmetry in the two descriptions recovers the cigar and two-dimensional sine-Liouville backgrounds, reproducing the original FZZ duality and strongly suggesting the validity of this three-dimensional proposal. We expect there is an analogous supersymmetric duality given by the uplift of the supersymmetric FZZ duality of Hori and Kapustin [55].

This three-dimensional sine-Liouville background shares many similarities with its two-dimensional counterpart. For example, by integrating over the zero-mode one obtains a relation analogous to Eqn. 2.235, where now $\mathcal{S}_N$ denote operators of the first-order system rather than the compact boson. In particular, the correlation functions obey the scaling relation λ^κ, where κ is given in Eqn. 2.234. The same type of scaling is predicted by the dual Wakimoto description of the $\mathrm{SL}(2,\mathbb{C})_k/\mathrm{SU}(2)$ CFT [99,111,112]. Once again the lack of analyticity is due to the freedom to rescale λ by field redefinitions up to shifts of the dilaton zero-mode. In an action with a given coefficient λ and zero-mode Φ_0, the latter may always be eliminated with the former rescaled to $e^{-2b_{\rm sL}\Phi_0/Q}\lambda$.

The $\mathrm{SL}(2,\mathbb{C})_k/\mathrm{SU}(2)$ CFT may alternatively be described in Poincarè coordinates by the linear-dilaton $\times\,\mathcal{F}(\mathbb{C})$ system deformed by the Wakimoto potential $\beta\bar{\beta}e^{-2\sigma}$ [87]. We relabel

here the linear-dilaton field as σ and the first-order fields as β and γ to be consistent with the notation in Eqn. 3.43, which is reproduced upon integrating out $\beta, \bar{\beta}$. If one were to quotient $\gamma \sim \gamma + 2\pi i$ in this description, i.e. replacing $\mathcal{F}(\mathbb{C})$ by $\mathcal{F}(\mathbb{C}/\mathbb{Z})$, one would obtain a singular background with a cusp at $\sigma \to -\infty$ where the transverse Poincarè metric $e^{2\sigma} \mathrm{d}\gamma \mathrm{d}\bar{\gamma}$ shrinks. Continuing with respect to the compact Euclidean time $\mathrm{Im}(\gamma)$ would then yield a thermal state in the Poincarè patch at inverse temperature 2π.

If one deforms this cusp theory by the spectral flow of the Wakimoto operator around the compactified cycle, it is natural to conjecture that an RG flow is initiated back to the $\mathrm{SL}(2,\mathbb{C})_k/\mathrm{SU}(2)$ CFT. The spectral flow in this case preserves the marginal conformal weight of the operator, and introduces winding one around $\mathrm{Im}(\gamma)$. One may further deform the cusp theory by any number of such spectral-flowed operators with any values of spectral flow without changing the endpoint of the RG flow. These flows are reminiscent of discussions of closed string tachyon condensation in string theory [113–120]. By adding all the spectral-flowed operators with particular coefficients, one expects to obtain another description of the $\mathrm{SL}(2,\mathbb{C})_k/\mathrm{SU}(2)$ CFT, as a condensate of winding strings on the thermal Poincarè orbifold. In principle, smoothness of the interior, as encoded in conformal invariance of the worldsheet theory, would determine the coefficients of all of the spectral-flowed operators.

4.2 ER = EPR in 2D Dilaton-Gravity

With our examples of Euclidean ER = EPR CFT dualities in hand—relating a contractible Euclidean time circle in one description to a non-contractible circle plus a con-

densate in the other—we now construct the Lorentzian string theory dualities that follow by continuation.

We begin with the $\mathrm{SL}(2,\mathbb{R})_k/\mathrm{U}(1)$ CFT. For large k this CFT admits a weakly-coupled description given by a string in the cigar-shaped Euclidean black hole of two-dimensional dilaton-gravity, with an asymptotically-linear dilaton (Eqn. 2.98). Cutting the cigar across its contractible θ cycle and continuing yields the conventional description of a string in the 2D Lorentzian black hole in the HH state [75]. String amplitudes computing the S-matrix of particles scattering off the black hole horizon may be obtained by continuation from the Euclidean amplitudes of vertex operators $\mathcal{O}_{jn,w=0}$ under $n \to iE$, where n is the discrete Matsubara frequency of the mode around the compact Euclidean time circle and E is the continuous Lorentzian energy. This is the ER description of the string theory (Fig. 1.2a).

We now turn to the EPR description, corresponding to the string background obtained by continuation from the dual, sine-Liouville description of $\mathrm{SL}(2,\mathbb{R})_k/\mathrm{U}(1)$ (Eqn. 2.230). The sine-Liouville background consists of the free linear-dilaton$\times \mathrm{S}^1$ background (Eqn. 2.109) plus the sine-Liouville potential $4\pi\lambda(W_+ + W_-)$, where $W_\pm$ are the marginal linear-dilaton $\times\, \mathrm{S}^1$ operators with winding ± 1 (Eqn. 2.231). It is a strongly-coupled description of the CFT at large k.

In the asymptotic region $r, \hat{r} \to \infty$ of the cigar and sine-Liouville, the two backgrounds are identical, with the coordinates related by Eqn. 2.108. In that limit, the $\mathrm{SL}(2,\mathbb{R})_k/\mathrm{U}(1)$ Virasoro primaries $\mathcal{O}_{jnw}$ behave as the superposition of linear-dilaton $\times\, \mathrm{S}^1$ primaries given in Eqn. 2.116. To compute an $\mathrm{SL}(2,\mathbb{R})_k/\mathrm{U}(1)$ correlation function of such operators in the

sine-Liouville description, one would insert the corresponding free-field superpositions in the sine-Liouville functional integral.

Let us consider the sine-Liouville potential as a large deformation of the linear-dilaton $\times \mathrm{S}^1$ background, expanding the condensate in powers of the winding operators,

$$\begin{aligned} &\left\langle e^{-\frac{\lambda}{2\alpha'}\int \mathrm{d}^2 z\,(W_+ + W_-)} \cdots \right\rangle_{\mathrm{LD}\times\mathrm{S}^1} \\ &\quad = \sum_{N=0}^{\infty} \frac{1}{(N!)^2} \left(\frac{\lambda}{2\alpha'}\right)^{2N} \left\langle \left(\int \mathrm{d}^2 z\, W_+(z,\bar{z})\right)^N \left(\int \mathrm{d}^2 z'\, W_-(z',\bar{z}')\right)^N \cdots \right\rangle_{\mathrm{LD}\times\mathrm{S}^1} , \end{aligned} \tag{4.18}$$

where the ellipses stand for additional operator insertions $\prod_i e^{-2Q(1-j_i)\hat{r}} e^{in_i\theta}$. Note that the winding conservation law of the free background demands that an equal number of W_+ and W_- factors contribute in each term.[72] We wish to understand the Lorentzian string theory defined by continuation from each term in this expansion, which we refer to as the EPR microstate string backgrounds.[73]

Note that Eqn. 4.18 is not a perturbative expansion around the linear-dilaton $\times\, \mathrm{S}^1$ background, however. As recalled in Sec. 2.5.1, and as discussed in the analogous context of Liouville in Sec. 2.2.1, because λ may be rescaled by field redefinitions, there is no sense in which it is a small parameter. As a result, sine-Liouville correlation functions are not in general analytic in λ, but rather scale with λ^κ as in Eqn. 2.235, where κ is the function of the primary momenta $\{j_i\}$ given in Eqn. 2.234. In the special case that $\kappa \in 2\mathbb{N}$, however, one does

[72] We restrict our attention here to non-winding S^1 primaries that, with $j = \frac{1}{2}(1+is)$, continue to ordinary scattering states of the black hole.

[73] Note, however, that these continued backgrounds describe the thermally entangled microstates. We will not discuss string backgrounds for the pure EPR microstates, though it would be interesting to do so.

obtain an analytic function[74] proportional to $\lambda^\kappa \Gamma(-\kappa) \langle \left(\int W_+\right)^{\kappa/2} \left(\int W_-\right)^{\kappa/2} \cdots \rangle_{\mathrm{LD}\times \mathrm{S}^1, \emptyset}$.

Correspondingly, for compatible values of the momenta $\{j_i\}$, one finds in Eqn. 4.18 a single term consistent with the anomalous momentum conservation law of the linear dilaton (Eqn. 2.19),

$$2N b_{\mathrm{sL}} + Q \sum_i (1 - j_i) = \frac{1}{2} Q \chi. \tag{4.19}$$

This is simply the condition that $\kappa = 2N$, reproducing the preceding result. The zero-mode integral collapses to $\int \mathrm{d}\hat{r}_0$, which diverges with the volume of the target and is reflected in the pole of the gamma function. The free-theory correlators therefore compute the residues of sine-Liouville correlation functions at these poles [121]. Correlation functions for general momenta could be in principle be obtained by continuation from these residues computed from the free theory, by determining the meromorphic function with the corresponding pole structure, as in Liouville [66, 67, 69, 71].

For generic values of $\{j_i\}$, including the scattering states of interest for the black hole, the anomalous conservation law need never be satisfied, and each linear-dilaton $\times$ S^1 correlation function on the right-hand-side of Eqn. 4.18 appears to vanish. Yet sine-Liouville admits no such anomalous conservation law, the translation symmetry of the target linear-dilaton direction being completely broken by the potential, and exact CFT correlation functions of operators that violate Eqn. 4.19 certainly need not vanish.

The same puzzle arose in the discussion surrounding Eqn. 2.57 for Liouville. As explained

[74] Or, rather, the residue at the pole of the gamma function is an analytic function of λ.

there, the source of the trouble is the strong-coupling region, and Eqn. 4.18 should more properly be interpreted as defining a perturbative expansion of the sine-Liouville measure in powers of $\lambda e^{-2b_{\rm sL}\hat{r}_0}$, where $\hat{r}_0$ is the zero-mode of $\hat{r}$:

$$\begin{aligned}
&\mathrm{D}\hat{r}\mathrm{D}\theta\; e^{-S_{\rm sL}[\hat{r},\theta]}\prod_i e^{-2Q(1-j_i)\hat{r}}e^{in_i\theta} \qquad (4.20)\\
&\quad\overset{\hat{r}_0\to\infty}{\longrightarrow}\; \mathrm{D}\hat{r}'\mathrm{D}\theta\; e^{-S_{\mathrm{LD}\times\mathrm{S}^1}[\hat{r}',\theta]}\prod_i e^{-2Q(1-j_i)\hat{r}'}e^{in_i\theta}\\
&\qquad\times \mathrm{d}\hat{r}_0\; e^{2b_{\rm sL}\kappa\hat{r}_0}\sum_{N=0}^{\infty}\frac{1}{(N!)^2}\left(\frac{\lambda e^{-2b_{\rm sL}\hat{r}_0}}{2\alpha'}\right)^{2N}\left(\int W_+[\hat{r}',\theta]\right)^N\left(\int W_-[\hat{r}',\theta]\right)^N.
\end{aligned}$$

Whereas λ itself is not a small parameter, the combination $\lambda e^{-2b_{\rm sL}\hat{r}_0}$ is invariant under $\hat{r}_0 \to \hat{r}_0+\delta$, $\lambda \to e^{2b_{\rm sL}\delta}\lambda$, and gives a perturbative expansion about the weak-coupling region.

To proceed more carefully for general momenta, one should introduce a regulator that controls the strong-coupling region. In the zero-mode integral Eqn. 2.233 that lead to Eqn. 2.235, one could introduce a hard cut-off $\hat{r}_{\rm c}$ on the lower bound of the integral and attempt to understand the limit as $\hat{r}_{\rm c}\to-\infty$. The regulator will break the anomalous momentum conservation law of the free background, eliminating the spurious constraint Eqn. 4.19. Alternatively, rather than this hard cut-off step function $\Theta(\hat{r}_0-\hat{r}_{\rm c})$, one could employ a soft cut-off by inserting $\exp\left(-e^{-2b_{\rm sL}(\hat{r}_0-\hat{r}_{\rm c})}\right)$ in the integral, which behaves similarly but varies smoothly. Then Eqn. 2.233 becomes

$$\int_{-\infty}^{\infty}\mathrm{d}\hat{r}_0\; e^{2b_{\rm sL}\kappa\hat{r}_0-\left(\frac{\lambda}{\alpha'}V_{\rm sL}[\hat{r}',\hat{\theta}]+e^{2b_{\rm sL}\hat{r}_{\rm c}}\right)e^{-2b_{\rm sL}\hat{r}_0}} = \frac{1}{2b_{\rm sL}}\left(\frac{\lambda}{\alpha'}V_{\rm sL}[\hat{r}',\hat{\theta}]+e^{2b_{\rm sL}\hat{r}_{\rm c}}\right)^{\kappa}\Gamma\left(-\kappa\right). \qquad (4.21)$$

Writing $\varepsilon = e^{2b_{\rm sL}\hat{r}_{\rm c}}$, such that $\varepsilon \to 0$ when $\hat{r}_{\rm c} \to -\infty$ meaning that the regulator is removed, the regulated version of Eqn. 2.235 is

$$\begin{aligned}\left\langle \prod_N e^{-2Q(1-j_N)\hat{r}} \mathcal{S}_N \right\rangle_{{\rm sL},\varepsilon} \\ = \frac{1}{2b_{\rm sL}} \Gamma(-\kappa) \left\langle \left(\frac{\lambda}{\alpha'} V_{\rm sL}[\hat{r},\hat{\theta}] + \varepsilon \right)^{\kappa} \prod_N e^{-2Q(1-j_N)\hat{r}} \mathcal{S}_N \right\rangle_{{\rm LD}\times {\rm S}^1,\emptyset} .\end{aligned} \tag{4.22}$$

One may now attempt to expand the free-field correlator in powers of $\frac{1}{\varepsilon}$ by writing

$$\left(\frac{\lambda}{\alpha'} V_{\rm sL} + \varepsilon \right)^{\kappa} = \varepsilon^{\kappa} \sum_{M=0}^{\infty} \binom{\kappa}{M} \left(\frac{\lambda}{\alpha'} \frac{V_{\rm sL}}{\varepsilon} \right)^{M} , \tag{4.23}$$

where $\binom{\kappa}{M}$ is the generalized binomial coefficient. In this way, one more properly obtains as in Eqn. 4.18 an expansion for sine-Liouville correlation functions as a sum over free-theory correlators with integer powers of the integrated potential inserted. This expansion may diverge, in general. The situation is similar to conformal perturbation theory, where one expands an exactly marginal deformation $e^{-\lambda \int \mathcal{O}}$, obtaining a series with finite radius of convergence. In that case the expansion is suppressed by factors of $\frac{1}{M!}$, whereas the binomial coefficients in Eqn. 4.23 fall off less rapidly. Thus, the above expansion may only be an asymptotic series, which we speculate may be Borel resummable. We have not attempted to verify this, however.

We will not pursue further the explicit implementation of the regulator here. Our goal is not to offer a new computational framework for obtaining string amplitudes in the black hole, but to give an abstract understanding of the string backgrounds corresponding to the

thermal EPR microstates. To that end, we now consider the Lorentzian continuation of the string background defined by each term in Eqn. 4.18.

Consider first the free linear-dilaton $\times$ S^1 itself, i.e. $N = 0$. This is the flat space solution of the dilaton-gravity equations of motion (Eqn. 2.101). The target cylinder has the topology of an annulus, which, when halved and glued to its Lorentzian continuation with respect to the S^1, prepares a Schwinger-Keldysh contour for the disconnected union of two copies of linear-dilaton $\times$ time in the TFD state (Fig. 1.5a).

As in the Euclidean background, each Lorentzian spatial slice extends from a weak-string-coupling limit at $\hat{r} \to \infty$ to a strong-coupling region $\hat{r} \to -\infty$. The two asymptotic weak-coupling regions are identical to the left and right asymptotic regions of the two-sided black hole. But whereas the left and right regions of the black hole are connected in the interior at the horizon, the two copies of linear-dilaton $\times$ time are disconnected, with strong-coupling boundaries in their interiors instead of horizons.

Each remaining term in the expansion Eqn. 4.18 inserts N pairs of W_+, W_- operators on top of the linear-dilaton $\times$ S^1 background. Thus, upon continuation they will introduce deformations of the TFD state in the disconnected union of linear-dilaton $\times$ time. Because the $W_\pm$ are winding operators around the Euclidean time circle, however, the Lorentzian interpretation of these deformations is not immediately obvious.

Moreover, there is a problem of mutual locality that arises in attempting to continue $n \to iE$ in the insertions represented by the ellipses in Eqn. 4.18. Namely, the winding and

momentum operators of the compact boson obey an OPE

$$e^{in\theta(z,\bar{z})}e^{\pm ik\tilde{\theta}(0)} \sim \left(\frac{z}{\bar{z}}\right)^{\pm n/2} e^{in\theta(0)\pm ik\tilde{\theta}(0)}. \tag{4.24}$$

When the momentum operator circles the winding insertion at the origin ($z \to e^{2\pi i}z, \bar{z} \to e^{-2\pi i}\bar{z}$), the OPE coefficient transforms by a factor $e^{\pm 2\pi i n}$. Then the operator algebra is well-defined only for $n \in \mathbb{Z}$, which is of course the expected momentum quantization of the compact boson. It follows that by continuing the momentum labels $n \to iE$ in a linear-dilaton $\times$ S^1 correlator with a given number of $W_\pm$ insertions, one will in general obtain a multi-valued function on the worldsheet. In order to define string perturbation theory in the EPR microstates obtained by continuation from each term in the expanded background, we must establish how to compute a well-defined string amplitude by integrating such an apparently multi-valued expression over the moduli space.

We address these questions in the following two sub-sections. We first show that each pair of W_+, W_- insertions introduces on top of the disconnected linear-dilaton $\times$ S^1 background a pair of strings in a TFD state in the sense of angular quantization on the worldsheet (Fig. 1.7a). Each string is folded, with its ends in the strong-coupling region, and each folded string is entangled with its pair, with one in the left and one in the right copy of the spacetime (Fig. 1.5a). We then argue that the multi-valued correlation functions obtained by continuation from the linear-dilaton $\times$ S^1 should be integrated over a deformed contour in a complexification of the string moduli space on which they are single-valued in order to obtain amplitudes in the background of such entangled, folded strings.

4.2.1 Angular Quantization

One sometimes obtains a target space picture in string theory by adopting the "static" gauge after choosing a flat metric on the worldsheet, in order to fix the residual conformal gauge redundancy that remains within the full diffeomorphism $\times$ Weyl gauge redundancy of the functional integral. In static gauge, the target Euclidean time coordinate is fixed to the worldsheet time coordinate ρ in the sense of radial quantization, where $z = e^{\rho+i\phi}$. This choice is unacceptable in the background of Euclidean time winding operators, however. For example, in the neighborhood of a winding ± 1 insertion at the origin on the worldsheet, the target Euclidean time $\theta \sim \theta + 2\pi$ should obey

$$\theta \overset{\rho\to-\infty}{\longrightarrow} \pm\phi. \tag{4.25}$$

Rather than the static gauge $\theta = \rho$, one may instead adopt an angular gauge condition $\theta = \pm\phi$, in which the compact coordinate ϕ is viewed as the worldsheet Euclidean time direction.

We are therefore motivated to treat the neighborhood of Euclidean time winding insertions on the worldsheet in angular rather than the usual radial quantization. In this section we elaborate on this quantization scheme. In fact, the following is a pure CFT discussion, independent of the application to Lorentzian string theory that we ultimately have in mind, and which we return to at the end of the sub-section.

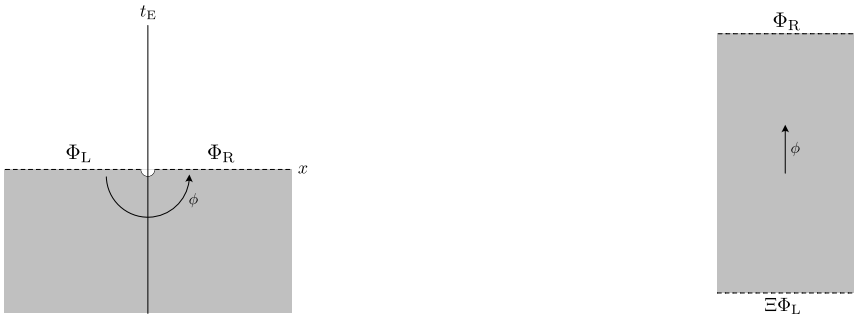

(a) **(b)**

Figure 4.1: The Minkowski Vacuum and the Rindler TFD. The Euclidean functional integral over the lower-half plane prepares the Minkowski vacuum state on the $t_E = 0$ slice (left). The same functional integral may be interpreted as a Euclidean transition amplitude between states on the negative and positive x-axis, with the angular direction ϕ interpreted as Euclidean time (right). Then the Minkowski vacuum is equivalent to the TFD state in the angularly quantized Hilbert space $\mathcal{H}_L \otimes \mathcal{H}_R$. In the same way, the HH state for the two-sided black hole may be interpreted as a TFD state with respect to the left and right wedges. The reduced density matrix in a single wedge is a thermal state of inverse Hawking temperature β_{BH}.

The basic idea of angular quantization is familiar[75] from the functional integral derivation of the Unruh effect in Rindler spacetime [124]. Consider a field theory on $\mathbb{R}^2$, with the flat metric $ds^2 = dt_E^2 + dx^2$. The functional integral over the lower-half plane prepares the Minkowski vacuum state $|\Omega\rangle$ in the Hilbert space of the theory on the x-axis (Fig. 4.1a). It is a wavefunctional, $\Psi_\Omega[\Phi(x)] = \langle\Phi|\Omega\rangle$, that takes field data $\Phi(x)$ on the fixed t_E slice and returns the value of the functional integral over the lower-half plane with that boundary condition.

Let $x = e^\rho \cos(\phi)$, $t_E = e^\rho \sin(\phi)$ define cylinder coordinates, in terms of which $ds^2 = e^{2\rho}\left(d\rho^2 + d\phi^2\right)$. The lower-half plane may be foliated by radial lines at fixed ϕ, rather than horizontal lines at fixed t_E. Then the same functional integral admits an alternative Hilbert space interpretation as a transition amplitude between a state on the negative x-axis and a state on the positive x-axis, with Euclidean time evolution given by rotation in ϕ (Fig.

[75] See e.g. [122, 123] for useful reviews.

4.1b):

$$\langle \Phi | \Omega \rangle = \langle \Phi_{\mathrm{R}} | \, e^{-\pi R} \Xi \, | \Phi_{\mathrm{L}} \rangle \, . \tag{4.26}$$

We have divided the field data $\Phi(x)$ into $\Phi_{\mathrm{L}}(x)$ on the negative x-axis and $\Phi_{\mathrm{R}}(x)$ on the positive x-axis. R generates rotations in ϕ, and Ξ is the CPT operator which maps the Hilbert space on the left to the Hilbert space on the right.

Inserting a complete set of eigenstates of R, the transition amplitude may be written

$$\langle \Phi_{\mathrm{R}} | \, e^{-\pi R} \Xi \, | \Phi_{\mathrm{L}} \rangle = \langle \Phi_{\mathrm{L}} | \otimes \langle \Phi_{\mathrm{R}} | \left(\sum_i e^{-\pi \omega_i} \, | i^* \rangle \otimes | i \rangle \right) , \tag{4.27}$$

where $| i^* \rangle = \Xi^\dagger \, | i \rangle$. Thus, the Minkowski vacuum $| \Omega \rangle$ on the slice $t_{\mathrm{E}} = 0$ is equivalent to the TFD state in $\mathcal{H}_{\mathrm{L}} \otimes \mathcal{H}_{\mathrm{R}}$:

$$| \Omega \rangle = \sum_i e^{-\pi \omega_i} \, | i^* \rangle \otimes | i \rangle \, . \tag{4.28}$$

More precisely, the Hilbert space on the line does not factorize into a product of left and right Hilbert spaces due to divergences associated to degrees of freedom in the neighborhood of the origin. The vacuum in the full spacetime does define a state on the von Neumann operator algebra in both Rindler wedges.

When $\mathbb{R}^2$ is continued with respect to $t_{\mathrm{E}} = it$, one obtains standard coordinates on Minkowski space, with metric $\mathrm{d}s^2 = -\mathrm{d}t^2 + \mathrm{d}x^2$. Then expectation values in the vacuum

state may be computed by cutting the Euclidean functional integral on $\mathbb{R}^2$ at $t_{\mathrm{E}} = 0$, gluing in the Minkowski plane, and continuing operator insertions to the Lorentzian section.

Instead continuing with respect to $\phi = i\mathfrak{t}$, one obtains the right wedge of the Rindler decomposition of Minkowski spacetime (Fig. 2.5b). In particular, $x = e^{\rho}\cosh(\mathfrak{t})$ and $t = e^{\rho}\sinh(\mathfrak{t})$, and therefore the coordinates ρ and $\mathfrak{t}$ cover the region $x > |t|$, bounded by the Rindler horizon. The relation between the Rindler coordinates on the right wedge and the full Minkowski spacetime is analogous to the relation between Schwarzschild coordinates on the right wedge of a black hole and the extended two-sided black hole. One may similarly define Rindler coordinates in the remaining wedges. Lines of constant ρ are hyperbolas $x^2 - t^2 = \text{const.}$, and lines of constant $\mathfrak{t}$ are straight lines through the origin, $t/x = \text{const.}$ Translation in $\mathfrak{t}$ is an isometry, timelike in the right and left wedges (though with opposite orientations), and spacelike in the top and bottom wedges. It corresponds to the boost isometry in the original Minkowski coordinates.

Because ϕ is 2π periodic, when a Euclidean functional integral on $\mathbb{R}^2$ is cut at $\phi = 0$ (i.e. the positive x-axis) and operator insertions are continued to the right Rindler wedge $\phi \to i\mathfrak{t}$, one obtains an expectation value in a thermal state at inverse temperature 2π. This is the Unruh effect: the reduced density matrix of the Minkowski vacuum in the right (or left) Rindler wedge is a thermal state. Indeed, from Eqn. 4.28 one obtains $\mathrm{tr}_{\mathcal{H}_{\mathrm{L}}}\left(|\Omega\rangle\langle\Omega|\right) = e^{-2\pi R}$. By slicing the Euclidean functional integral at both $\phi = 0$ and $\phi = \pi$, one may continue operators to either the left or right Rindler wedges, and so obtain expectation values in $\mathcal{H}_{\mathrm{L}} \otimes \mathcal{H}_{\mathrm{R}}$ in the TFD state.

(a) **(b)**

Figure 4.2: Radial and Angular Slicings. The same Euclidean functional integral on a sphere may be assigned different Hilbert space interpretations by choosing different foliations. In radial quantization (left), one slices the sphere into circles centered at the poles. Each circle is a spatial slice, and Euclidean time flows along the radial direction transverse to the slices. Then the functional integral over the sphere computes the inner-product of the states prepared by the operator insertions at the poles in the Hilbert space e.g. on the equatorial circle. In angular quantization, the spatial slices are instead radial lines connecting the poles, and Euclidean time flows along the angular direction. Then the same two-point function on the sphere computes the thermal trace in the angularly quantized Hilbert space on the dashed line. Given a point on the sphere, its spatial slice in radial quantization is the orbit of the rotation generator, and its Euclidean time evolution is the orbit of the dilation generator. In angular quantization, the roles of the two symmetries are exchanged.

The thermal state $e^{-2\pi R}$ and its TFD purification are simple examples of states in an angularly quantized Hilbert space. The angular quantization that we propose in what follows generalizes this construction by allowing operator insertions at one or both asymptotic endpoints of the spatial slices.

CFTs are usually treated in radial quantization. That is, when one refers to the Hilbert space of a 2D CFT, one typically means the Hilbert space $\mathcal{H}(\mathrm{S}^1)$ on a circle, corresponding to a slice of the cylinder $\mathrm{S}^1 \times \mathbb{R}$ with Lorentzian time running along its length. One has an isomorphism between this Hilbert space and the space of local operators at a point. Each local operator is mapped to a state on the circle by the Euclidean functional integral over a hemisphere glued to the circle slice, with the operator inserted at the pole. And each state may be mapped to its corresponding local operator by a conformal transformation that shrinks the circle to a point.

Thus, a Euclidean CFT correlation function on S^2, such as the two-point function illus-

trated in Fig. 4.2a, may be cut, e.g. on the equator, and interpreted as an inner-product in the radially quantized Hilbert space on that circle:

$$\langle \mathcal{O}(0)\mathcal{O}'(\infty)\rangle_{S^2} = \langle \mathcal{O}'|\mathcal{O}\rangle_{\mathcal{H}(S^1)} \,. \tag{4.29}$$

The Euclidean functional integral over the southern hemisphere prepares the state associated to the operator insertion at the south pole, and the integral over the northern hemisphere prepares the state associated to the operator at the north pole. By sewing up the cut on the dashed circle, the functional integral on the sphere computes the inner-product of these two states. One may also insert the Lorentzian cylinder at the cut, and by continuing additional operator insertions to the Lorentzian section one may compute their expectation value between the two states.

In that continuation, Euclidean time evolution is defined by the dilation symmetry of the CFT, which scales the local complex coordinate $z \to \lambda z$ centered at the operator insertion at the pole (and therefore translates the cylinder time coordinate $\log|z| \to \log|z| + \log\lambda$). The slices of the sphere at fixed Euclidean time are circles centered at the poles. In this foliation, given a point on the sphere, its spatial slice is the orbit of the rotation generator around the poles, and its Euclidean time evolution flows along the orbit of the dilation generator.

This foliation is not unique, however. Let us instead slice the sphere in radial lines connecting the poles as in Fig. 4.2b, and define Euclidean time evolution by rotation. In this slicing, the roles of the dilation and rotation generators are exchanged: the spatial slice on which a point lies is its orbit under dilation, and Euclidean time runs along the orbit of

rotation.

Then the Euclidean functional integral over the sphere with the radial cut prepares a thermal state $e^{-2\pi R} \in \mathcal{H}_{\mathcal{O}\mathcal{O}'}(\mathbb{R})$ in the Hilbert space of angular quantization on the dashed line, where the subscripts label the operator insertions at the poles. The same two-point function, obtained by sewing up the cut, is therefore assigned a different interpretation in this quantization scheme—it is a thermal trace in $\mathcal{H}_{\mathcal{O}\mathcal{O}'}(\mathbb{R})$:

$$\langle \mathcal{O}' | \mathcal{O} \rangle_{\mathcal{H}(\mathrm{S}^1)} = \mathrm{tr}_{\mathcal{H}_{\mathcal{O}\mathcal{O}'}(\mathbb{R})} \left(e^{-2\pi R} \right) . \tag{4.30}$$

One may continue additional operator insertions with respect to $\phi \to i\mathrm{t}$, corresponding to gluing in a Rindler wedge at the cut, and so obtain expectation values of operators in Rindler spacetime in this thermal state. And one may cut the sphere in half to define the TFD state in two copies of $\mathcal{H}_{\mathcal{O}\mathcal{O}'}(\mathbb{R})$ (Fig. 1.7a). By continuing additional operator insertions via $\phi \to i\mathrm{t}_\mathrm{R}$ or $\phi \to \pi + i\mathrm{t}_\mathrm{L}$, one obtains an expectation value in the TFD state in the left and right Rindler wedges.

One way to regulate the UV divergences associated to the left/right split of the Hilbert space here is to end the Rindler wedges at a boundary with appropriate boundary conditions. In the Euclidean functional integral this corresponds to excising a small neighborhood of the insertion point of the operator being treated in angular quantization [125], as in the discussion of asymptotic conditions in Ch. 2. In the limit that the regulator is removed, the boundary conditions become the asymptotic conditions associated to the inserted operator. Of course, the regulator breaks conformal symmetry, which is only restored in the limit.

Let us now apply this machinery to the linear-dilaton $\times$ S^1 background with insertions of $W_\pm$ operators in order to understand the deformations they introduce on top of the $\mathbb{R}^{1,1}\cup\mathbb{R}^{1,1}$ string theory upon continuation. The Hilbert space $\mathcal{H}_{\mathcal{O}\mathcal{O}'}(\mathbb{R})$ is defined by the asymptotic conditions imposed by the insertions $\mathcal{O},\mathcal{O}'$ at the ends of the line. For a $W_\pm$ insertion, these asymptotic conditions follow from Eqn. 2.131 with $\alpha = b_{\rm sL}$,[76]

$$\hat{r} \overset{\rho\to-\infty}{\longrightarrow} \sqrt{\alpha'(k-2)}\rho, \tag{4.31}$$

together with the winding condition Eqn. 4.25. Note in particular that the neighborhood of the insertion point is mapped to the strong-coupling region $\hat{r}\to-\infty$ in spacetime.[77]

Consider the leading term $N=1$ on top of the linear-dilaton $\times$ S^1 string background in Eqn. 4.18, with a pair of winding operators W_+, W_- inserted on CP^1. Let $W_+(0)$ be fixed at the origin and $W_-(\infty)$ at the point-at-infinity using the global conformal redundancy of the string worldsheet (Fig. 1.7a). In the neighborhood of each of the two insertions, the string is mapped to the strong-coupling region as it wraps the Euclidean spacetime cylinder with unit winding. In between, the worldsheet extends along the cylinder toward finite string coupling before folding back on itself (Figs. 1.5b and 1.7b).

When the Euclidean spacetime annulus is halved to prepare the TFD state on the two zero-time slices $t_{\rm R}=0$ at $\theta=0$ and $t_{\rm L}=0$ at $\theta=\pi$, one finds a pair of entangled folded

[76] When the operator insertion coincides with a curvature singularity, the asymptotic condition is modified by a contribution from the linear-dilaton background charge. But the correction is sub-leading in the large k limit because $Q\sim\frac{1}{\sqrt{k}}$.

[77] More precisely, the asymptotic condition fixes the derivative $\partial_\rho\hat{r}$ in the neighborhood of the operator insertion, and Eqn. 4.31 may be shifted by a constant. This constant shift may be an imaginary number, since in general the saddles of the functional integral may be complex. The asymptotic condition nevertheless implies $\mathrm{Re}(\hat{r})\to-\infty$, meaning that the string is sent to the strong-coupling region.

strings, one on each spatial slice, emanating from the strong-coupling region (Fig. 1.5a). The respective folded strings are the images of the worldsheet spatial slices—in the sense of angular quantization—at $\phi = 0$ and $\phi = \pi$. The pre-image of the halved embedded worldsheet that connects the two folded strings across the target Euclidean cap is the halved worldsheet shown in Fig. 1.7a, bounded by $\phi = 0$ and π. Thus, the pair of folded strings are prepared in the worldsheet TFD state in two copies of the angularly quantized Hilbert space, $\mathcal{H}_{+-}(\mathbb{R}) \otimes \mathcal{H}_{+-}(\mathbb{R})$.

When the angular gauge condition $\theta = \phi$ is continued with respect to the target and angularly quantized worldsheet (i.e. $\theta = it_{\rm R}$ and $\phi = i\mathfrak{t}_{\rm R}$, and $\theta = \pi + it_{\rm L}$ and $\phi = \pi + i\mathfrak{t}_{\rm L}$), one may think of the folded strings as evolving along their respective Lorentzian spacetimes, with both ends continuing to asymptote to the strong-coupling boundaries.[78]

Ideas relating Euclidean time winding operators and folded string solutions were previously explored in [126]. In that context, the folded strings emanated from the weak-coupling region. Here we extend the connection between Euclidean time winding operators and folded strings from the $c = 1$ analysis of [126, 127] to the true black hole regime of $k > 3$.

Using the tools described in Ch. 2, the asymptotic conditions can be implemented by a boundary condition on an excised neighborhood of the operator insertion, in the limit that the boundary shrinks away. The linear-dilaton $\times$ S^1 with W_+ and W_- insertions at the origin

[78] For an ordinary insertion $e^{in\theta}$, on the other hand, the asymptotic condition $\theta \to -i\frac{\alpha'}{R^2} n\rho$ becomes $t \to E\mathfrak{t}$ after continuing $\theta = it$, $\rho = i\mathfrak{t}$, and $n = i\frac{R^2}{\alpha'}E$ in the usual sense of radial quantization.

and point-at-infinity is described by the $L \to \infty$ limit of the action[79]

$$S = \frac{1}{4\pi\alpha'} \int_{-L}^{L} \mathrm{d}\rho \int_{0}^{2\pi} \mathrm{d}\phi \left\{ (\partial_\rho \hat{r})^2 + (\partial_\phi \hat{r})^2 + (\partial_\rho \hat{\theta})^2 + (\partial_\phi \hat{\theta})^2 \right\} \tag{4.32}$$
$$+ 2\left(b_{\mathrm{sL}} - \frac{Q}{2}\right) \int_{0}^{2\pi} \frac{\mathrm{d}\phi}{2\pi} \left(\hat{r}|_L + \hat{r}|_{-L}\right) + \int_{0}^{2\pi} \frac{\mathrm{d}\phi}{2\pi} \left\{ \sigma_+ (\partial_\phi \hat{\theta}|_L - R) + \sigma_- (\partial_\phi \hat{\theta}|_{-L} - R) \right\}.$$

Then the boundary equations of motion,

$$\partial_\rho \hat{r}|_{\rho=\pm L} = \mp 2\alpha' \left(b_{\mathrm{sL}} - \frac{Q}{2}\right) \tag{4.33a}$$

$$\partial_\phi \hat{\theta}|_{\rho=\pm L} = R, \tag{4.33b}$$

imply the asymptotic conditions in the $L \to \infty$ limit. $\sigma_\pm$ are Lagrange multipliers that implement the winding condition around S^1.

Similarly, for $N > 1$ each pair of W_+, W_- insertions may be thought of as introducing an additional pair of folded strings to the background in the TFD state of angular quantization (Fig. 4.4a). Then the exponentiated sine-Liouville potential amounts in the Lorentzian continuation to a condensate of folded strings emanating from strong coupling on top of the disconnected union of two copies of linear-dilaton × time.

Angular quantization should be understood as applying to the neighborhood of each pair of winding operators, and a genus-zero string diagram with $2N$ such insertions is analogous to a diagram with $2N$ loops of open strings (i.e. $2N$ holes). The associated process is

[79] Here we choose the cylinder metric, which is responsible for the background-charge shifts of the boundary terms by $-Q/2$. These terms are unimportant in the large k limit, however. One should also add an L-dependent counterterm to render the on-shell action finite.

the amplitude of ordinary closed string scattering states to interact with N pairs of folded strings in a state defined by the associated Euclidean functional integral. This also includes interactions by string exchange between the folded strings.

The folded string worldsheets we describe here are somewhat formal in the sense that there is no such saddle of the linear-dilaton $\times$ S^1 functional integral—e.g. the two-point function of W_+ and W_- alone vanishes by the anomalous conservation law. To obtain interesting saddles one must of course insert additional operators, which will connect to the folded string asymptotic conditions at strong coupling and fill in the solution in the interior. As discussed earlier, in general one must also regulate the linear-dilaton to suppress its strong-coupling region.

Alternatively, one may consider the continued sine-Liouville background itself without expanding the condensate. Here it is the sine-Liouville potential that regulates the strong-coupling region. In this context, one may interpret the physics of the condensate by considering the effect of introducing an additional pair of $\mathcal{W}_\pm$ insertions on top of it. Then the asymptotic conditions associated to these insertions must be modified from Eqns. 4.25 and 4.31 because those map the string out of the weak-coupling region where the free-field description is no longer valid. However, the free-field asymptotic conditions do show that a string initially found at large $\hat{r}$ will head toward strong coupling at the rate $\sqrt{\alpha'(k-2)}$ and with winding ± 1 as one begins to approach the insertion point on the worldsheet. Then in the weak-coupling regions one will again find a pair of folded strings, with their ends headed toward strong coupling. The state of the pair of strings is again the TFD state of angular

quantization on the worldsheet, formally defined by the Euclidean functional integral on a hemisphere with insertions of $\mathcal{W}_+$ and $\mathcal{W}_-$ on its boundary. In other words, one has added another pair of folded strings on top of the full EPR background, whose ends dissolve into the condensate at strong coupling.

To properly define the state of the folded strings, one should include the contribution from the bc gauge-fixing ghost system. Given a weight $(1,1)$ Virasoro primary operator of the matter CFT such as $W_\pm$, one forms a physical operator $W_\pm c\bar{c}$ of the full string background by including a factor $c\bar{c}$ from the ghosts. In radial quantization, this operator prepares the BRST invariant state $|W_\pm c\bar{c}\rangle = |W_\pm\rangle \otimes |{\downarrow\downarrow}\rangle \in \mathcal{H}(S^1)$ of the linear-dilaton $\times$ S^1 $\times$ bc $\times$ $\bar{b}\bar{c}$ CFT, where $|{\downarrow}\rangle$ is the bc vacuum state of ghost number $-1/2$ prepared by $c(0)$.

In angular quantization, with $W_+c\bar{c}$ and $W_-c\bar{c}$ inserted at the poles of CP^1, one obtains the TFD state in two copies of $\mathcal{H}_{+-}(\mathbb{R}) \otimes \mathcal{H}_{cc}(\mathbb{R}) \otimes \mathcal{H}_{\bar{c}\bar{c}}(\mathbb{R})$, where $\mathcal{H}_{cc}(\mathbb{R})$ is the angularly quantized Hilbert space of the bc CFT with c insertions at either end, and likewise for $\mathcal{H}_{\bar{c}\bar{c}}(\mathbb{R})$. To define the latter Hilbert spaces, it is convenient to recall that the $bc \times \bar{b}\bar{c}$ CFT is itself equivalent to a linear-dilaton of complex background charge $Q_X = 3i/\sqrt{2\alpha'}$ [128]. On the one hand, one has the ghost CFT of central charge $c_{bc} = -26$, with holomorphic stress tensor

$$T_{bc}(z) = -(\partial b)c - 2b\partial c, \tag{4.34}$$

and with OPEs

$$b(z)c(0) \sim \frac{1}{z}, \qquad b(z)b(0),\ c(z)c(0) \sim 0, \tag{4.35}$$

and the analogous anti-holomorphic formulas. The dual description is a linear dilaton $X(z,\bar{z}) = X(z) + \bar{X}(\bar{z})$ with holomorphic stress tensor

$$T_X(z) = -\frac{1}{\alpha'}(\partial X)^2 - Q_X \partial^2 X \tag{4.36}$$

and OPE

$$X(z)X(0) \sim -\frac{\alpha'}{2}\log z. \tag{4.37}$$

The fields are related by the identifications

$$b(z) = e^{i\sqrt{\frac{2}{\alpha'}}X(z)}, \qquad c(z) = e^{-i\sqrt{\frac{2}{\alpha'}}X(z)}, \tag{4.38}$$

and similarly for the anti-holomorphic fields. In particular, the linear-dilaton central charge $c_X = 1 + 6\alpha' Q_X^2$ reproduces -26. b and c transform with conformal weights $(2,0)$ and $(-1,0)$ with respect to T_{bc}, and $e^{\pm i\sqrt{\frac{2}{\alpha'}}X}$ carry the same weights with respect to T_X.

To ensure fractional powers of b and c do not appear, X must be compact with periodicity $2\pi\sqrt{\alpha'/2}$ [129]. There is no contradiction with the presence of the linear dilaton, however, because the background charge Q_X is complex; though the dilaton action $-\frac{Q_X}{4\pi}\int \mathrm{d}^2\sigma\sqrt{h}\,\mathcal{R}X$ is not invariant under the shift, its variation is a multiple of $2\pi i$, and therefore the functional integral measure is well-defined.

The bc equations of motion imply the classical conservation of the ghost-number current $J(z) = -bc$, with respect to which c carries ghost number $+1$ and b carries ghost number

-1. Then the identifications Eqn. 4.38, taking care to account for the implied normal ordering, yield $J = -i\sqrt{\frac{2}{\alpha'}}\partial X$. X therefore corresponds to the bosonization of the ghost-number current, the ghost-number symmetry of the bc description mapping to the translation symmetry in X of the linear-dilaton description.

The ghost-number symmetry is anomalous due to the mismatch in the number of c and b zero-modes on a worldsheet of genus g, which, by the Riemann-Roch theorem, is $\dim\{c_0\} - \dim\{b_0\} = 3-3g$. Then the functional integral measure $\mathrm{D}c\,\mathrm{D}b \supset \prod\{\mathrm{d}c_0\}\{\mathrm{d}b_0\}$ carries charge $-(3-3g)$ under the symmetry, and the charges of any insertions must sum to $3-3g = \frac{3}{2}\chi$ to obtain a non-zero correlation function, where $\chi = 2-2g$ is the Euler characteristic of the worldsheet. Correspondingly, the target translation symmetry of X in the linear-dilaton background is anomalous (Eqn. 2.19). With $\alpha_b = -i/\sqrt{2\alpha'}$ for a b insertion and $\alpha_c = +i/\sqrt{2\alpha'}$ for a c insertion, the linear-dilaton anomalous conservation law likewise ensures that a correlator with N_c insertions of $e^{-i\sqrt{\frac{2}{\alpha'}}X}$ and N_b insertions of $e^{i\sqrt{\frac{2}{\alpha'}}X}$ may be non-zero only if $N_c - N_b = \frac{3}{2}\chi$.

The anomaly also implies that the ghost-number current is not a Virasoro primary, and therefore under the conformal map $z = e^w$ between the plane and cylinder, the transformed current is given not by $\tilde{J}(w) = zJ(z)$ but by $\tilde{J}(w) = zJ(z) - \frac{3}{2}$. Then the ghost-number charges of a state on the cylinder and a local operator on the plane differ by $-3/2$, accounting for the discrepancy between the ghost-number 1 operator c and the ghost-number $-1/2$ vacuum state $|{\downarrow}\rangle$ it prepares. The corresponding anomaly in the linear-dilaton current was likewise responsible for the shifted momentum of states proportional to the background

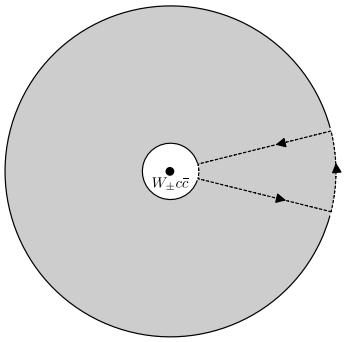

Figure 4.3: BRST Invariance. The physical vertex operator $W_\pm c\bar{c}$ is BRST invariant and prepares a BRST invariant state in the sense of radial quantization. The thermal state of angular quantization prepared with an asymptotic insertion of $W_\pm c\bar{c}$ is likewise BRST invariant. With the neighborhood of the insertion excised from the worldsheet and replaced by the appropriate asymptotic conditions on the resulting boundary circle, the BRST current vanishes on the circle in the limit that it shrinks away. Because the line integral of the current around the dashed loop shown vanishes by current conservation, it follows that the BRST charges measured on the two radial slices are identical.

charge (Eqn. 2.6).

The equivalence of the $bc \times \bar{b}\bar{c}$ CFT and the linear-dilaton X makes the construction of the TFD state in two copies of the Hilbert space $\mathcal{H}_{cc}(\mathbb{R}) \otimes \mathcal{H}_{\bar{c}\bar{c}}(\mathbb{R})$ of angular quantization analogous to the TFD in two copies of $\mathcal{H}_{+-}(\mathbb{R})$. The asymptotic condition Eqn. 4.31 for a $W_\pm$ insertion at the end of the line is replaced by

$$X \overset{\rho\to-\infty}{\longrightarrow} i\sqrt{2\alpha'}\rho, \tag{4.39}$$

or $X \to -i\sqrt{\frac{\alpha'}{2}}\rho$ when combined with the background-charge contribution in the far past on the cylinder. Along with the linear-dilaton $\times$ S^1 action Eqn. 4.32, one has the bosonized ghost action

$$S_X = \frac{1}{4\pi\alpha'}\int_{-L}^{L} \mathrm{d}\rho \int_0^{2\pi} \mathrm{d}\phi \left\{(\partial_\rho X)^2 + (\partial_\phi X)^2\right\} + 2\left(\alpha_c - \frac{Q_X}{2}\right)\int_0^{2\pi}\frac{\mathrm{d}\phi}{2\pi}\left(X|_L + X|_{-L}\right). \tag{4.40}$$

The combination $W_\pm c\bar{c}$ is BRST invariant in the operator sense, and prepares a BRST

invariant state on the circle in the sense of radial quantization. The thermal (and TFD) state in the Hilbert space of angular quantization is likewise BRST invariant. Indeed, consider the integral of $j_{\rm BRST}$ around the dashed loop shown in Fig. 4.3, where $j_{\rm BRST} = e^{-i\sqrt{\frac{2}{\alpha'}}X}\left(T_{\hat{r}} + T_{\hat{\theta}} + T_X\right)$ [130]. The grey annulus represents the worldsheet with the neighborhood of the origin and point-at-infinity excised and replaced by the asymptotic conditions on their boundaries. The integral around the closed loop vanishes by conservation of the current, and therefore the difference in the charges evaluated along the two radial line segments equals the integrals of the current over the two circular arcs. The latter vanish in the limit $L \to \infty$ because the conformal weight of the excised insertion was zero. That is, when the linear-dilaton $\times$ S^1 stress tensor $T_{\hat{r}} + T_{\hat{\theta}}$ (Eqn. 2.113) is evaluated on the asymptotic conditions Eqns. 4.25, 4.31 one obtains

$$T_{\hat{r}} + T_{\hat{\theta}} \overset{z\to 0}{\longrightarrow} \frac{1}{z^2}, \tag{4.41}$$

whereas on the ghost asymptotic condition Eqn. 4.39 one finds

$$T_X \overset{z\to 0}{\longrightarrow} -\frac{1}{z^2}. \tag{4.42}$$

Together therefore, $j_{\rm BRST} \to 0$. It follows that the BRST charge in the sense of angular quantization commutes with the Hamiltonian (i.e. the rotation generator), and therefore the thermal state of angular quantization associated to $W_{\pm}c\bar{c}$ is BRST invariant.[80]

[80] In principle, a trace defined with the BRST invariant density matrix we construct here should be computable by summing over BRST invariant states in the angularly quantized Hilbert space. In the classical limit, [126] found there were no solutions with vanishing stress energy. However, the $T = 0$ condition in the linear-dilaton theory is not itself a classically conformally invariant equation, necessitating a fully quantum treatment.

4.2.2 Mutual Locality and the String Moduli Contour

We now address the question of mutual locality that arises in attempting to continue the labels of vertex operator insertions in a given term in the expansion Eqn. 4.18 from their Euclidean Matsubara frequencies n to Lorentzian energies E. Namely, the OPE Eqn. 4.24 of a compact boson primary operator $e^{in\theta(z,\bar{z})}$ of momentum n with a unit-winding operator $e^{\pm ik\tilde{\theta}(z,\bar{z})}$ is single-valued on the z-plane only for integral n. It follows that a correlation function where these insertions approach one another will behave as $(z/\bar{z})^{\pm n/2} = e^{\pm in\phi}$, whose continuation $e^{\mp E\phi}$ is a multi-valued function of ϕ. Thus, a correlation function with a given number of winding operators and scattering operators will generically yield a multi-valued function of z upon continuation. This multi-valuedness appears to be an obstacle to defining Lorentzian string perturbation theory for the EPR thermal microstates obtained by continuation from each term of Eqn. 4.18.

On the one hand, one could evaluate a Lorentzian string amplitude for a given N by first computing the Euclidean amplitude with $n \in \mathbb{Z}$—i.e. integrating the Euclidean correlation function over the moduli space—and only then continuing $n \to iE$ in the final answer. In principle, this is a satisfactory definition of string perturbation theory in each of the EPR microstates. However, we would like to give a fully Lorentzian prescription for computing EPR string amplitudes directly from the apparently multi-valued correlation functions of winding operators and scattering operators.

The multi-valuedness of the continued linear-dilaton $\times$ S^1 correlation functions is not in

and of itself problematic, as these are not the objects of interest in string perturbation theory. Rather, the worldsheet CFT correlation functions serve to produce a measure on the string moduli space, which, when integrated, yields the desired string amplitude. The relevant conditions on the measure are then that it should be single-valued along the integration contour and such that the integral converges.

We will argue that the continued correlation functions should be integrated along a deformed contour in a complexification of the moduli space for which these conditions are satisfied.

The necessity of complexification and deformation of the integration contour is in fact encountered already in ordinary string backgrounds, though it is not always described in that language [131]. The deformation is required to avoid divergences that appear at points in the moduli space corresponding to the collision of two operator insertions on the worldsheet. For example, the Virasoro-Shapiro amplitude for tree-level $2 \to 2$ tachyon scattering in flat spacetime is typically expressed as an integral over the complex plane with three marked points, corresponding to summing over the insertion point $(z, \bar{z})$ of one operator, with the other three being fixed at arbitrary points using the conformal redundancy. The integral over the z-plane diverges whenever the momenta are above the threshold set by the tachyon mass, due to singularities when the integrated operator approaches the fixed insertions [132]. In this example, it so happens that the amplitude may be defined by evaluating the integral over z in an unphysical region where it does converge and then continuing the answer to the physical region. But more generally, the naive integral over the moduli space may never

converge, and so a more systematic approach is necessary.

As explained in [131], to obtain a finite string amplitude one complexifies the moduli space, corresponding in the $2 \to 2$ example to treating the coordinates $(z, \bar{z})$ of the integrated operator as independent complex coordinates $(z, \tilde{z})$. The original moduli space is the section $\tilde{z} = \bar{z}$ on which $\tilde{z}$ coincides with the complex conjugate of z. An appropriate integration contour for the sum over moduli may then be taken to be the usual cycle $\tilde{z} = \bar{z}$ almost everywhere, but with a small disk neighborhood of each of the fixed insertions where the original integral diverged replaced by the Lorentzian cylinder of radial quantization. In general one must also ascend to a cover of the complexified moduli space on which the integrand is single-valued.

In the neighborhood of the origin, for example, one continues $(z = e^{\rho+i\phi}, \bar{z} = e^{\rho-i\phi})$ to independent complex coordinates, and replaces the original contour (on which ρ and ϕ were real) by continuing $\rho = \rho_0 + i\mathfrak{t}$ in a small neighborhood $|z| < e^{\rho_0}$ of the insertion. $\mathfrak{t}$ is the worldsheet Lorentzian time in the sense of radial quantization, and so the deformation effectively glues the Lorentzian cylinder at $\mathfrak{t} = 0$ to the z-plane with an excised disk along the boundary circle $|z| = e^{\rho_0}$. The singular neighborhood of the collision point at the origin is thereby removed from the integration contour, and one instead integrates along $\mathfrak{t} \in (-\infty, 0]$. ϕ remains real on this contour.

In a string background with Euclidean time winding operator insertions, we conjecture that Lorentzian string amplitudes should be defined with an analogous angular rather than radial contour deformation. That is, in the neighborhood of a point on the moduli space

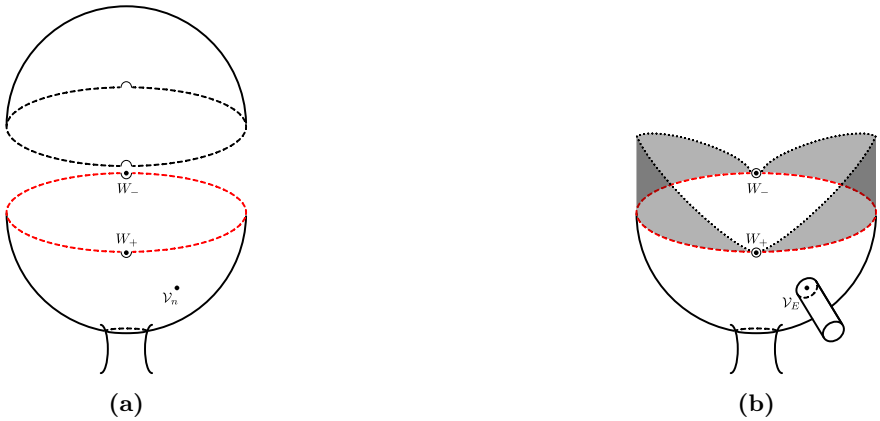

Figure 4.4: The Contour of Angular Quantization. Near any pair of W_+, W_- insertions on the worldsheet of a linear-dilaton $\times$ S^1 string diagram, one may slice their neighborhood as shown on the left. The upper cap prepares a pair of folded strings in the TFD state of angular quantization, which is glued to the rest of the worldsheet below. In computing a string amplitude of linear-dilaton $\times$ time including Euclidean time winding insertions, one must choose a deformed contour of integration in evaluating the sum over moduli. On the right is sketched the contour used to evaluate the integral of a Lorentzian scattering operator. When the integrated insertion approaches another ordinary operator, the contour is deformed along the Lorentzian cylinder of radial quantization according to the prescription of [131]. When it approaches a winding operator, the Euclidean cap that prepared the TFD state of folded strings is replaced by the pair of Rindler diamonds shown and glued along the red zero-time slice. The radial deformation prevents two scattering insertions from colliding, while the angular deformation prohibits a scattering operator from looping around a winding operator.

where a momentum operator and a winding operator collide, the original contour is replaced not with the Lorentzian cylinder of radial quantization, but with a Rindler wedge (or wedges) of angular quantization. In this case it is ρ that remains real while $\phi = i\mathfrak{t}$ is continued.[81] The contour is sketched in Fig. 4.4b, referring to the portion of the moduli integral over the insertion point of an ordinary scattering operator. Whereas the radial deformation prevents two scattering insertions from colliding, the angular deformation prevents a scattering insertion from looping around a winding insertion.

With this deformation, the measure obtained from a linear-dilaton $\times$ S^1 correlation function after continuing $n \to iE$, which was multi-valued on the original moduli space $\tilde{z} = \bar{z}$, becomes single-valued on the new contour in the complexification. In particular, the con-

[81] It would also be interesting to understand the appropriate contour deformation when two Euclidean time winding operators collide.

tinuation of the problematic OPE coefficient $e^{\mp E\phi}$ that followed from Eqn. 4.24 is now a single-valued and oscillatory function $e^{\mp iE\mathfrak{t}}$ of $\mathfrak{t}$.

For example, consider the two-point function in the $N = 1$ background of $e^{-2Q(1-j)\hat{r}}e^{in\theta}\mathcal{O}_h$ and $e^{-2Q(1-j)\hat{r}}e^{-in\theta}\mathcal{O}_h$, where $\mathcal{O}_h$ is an internal primary of weight h. Using the conformal gauge redundancy, fix the winding operators at the origin and point-at-infinity, and fix one of the momentum operators at $z = 1$. The insertion point of the remaining momentum operator is to be integrated. To avoid the need for a regulator, let us for simplicity pick $j = \frac{k-1}{2}$, such that Eqn. 4.19 is satisfied.[82] Continuing $n \to iE$, the internal weight h is chosen to satisfy the on-shell condition,

$$-\frac{j(j-1)}{k-2} - \frac{E^2}{4k} + h = 1. \tag{4.43}$$

The moduli space contour over which the location of the unfixed momentum operator is to be integrated is shown in Fig. 4.4b.

4.3 ER = EPR in Asymptotic AdS_3 Gravity

Next we consider the examples of ER = EPR for asymptotic AdS_3 gravity obtained by continuation from the dual descriptions of the $SL(2,\mathbb{C})_k/SU(2)$ and $\mathbb{Z}\backslash SL(2,\mathbb{C})_k/SU(2)$ CFTs. These examples are in several respects simpler than in two-dimensional dilaton-gravity.

[82] Albeit this is not a scattering operator, for which j would lie on the complex branch. When we discuss the AdS_3 duality in the next section, however, it will be the real branch j's that are of physical interest.

For large k, the weakly-coupled description of $\mathrm{SL}(2,\mathbb{C})_k/\mathrm{SU}(2)$ is of a string in a solid cylinder geometry (Eqn. 3.13) supported by a B-field (Eqn. 4.16). A Virasoro primary operator $\Phi^{J\bar{J}}_{jw}(z,\bar{z};\xi_0,\theta_0)$ is labeled by a point (ξ_0,θ_0) on the spacetime conformal boundary, where a delta-function source for the dual BCFT primary operator of conformal weight $(J,\bar{J})$ is inserted. Because EAdS is effectively a box, string amplitudes do not compute an S-matrix, but rather correlation functions in the dual CFT of such operator insertions [46, 86–88].

In the weakly-coupled description of $\mathbb{Z}\backslash\mathrm{SL}(2,\mathbb{C})_k/\mathrm{SU}(2)$, the length $\xi \sim \xi + \tilde{\beta}$ is compactified to form a solid torus geometry. Untwisted vertex operators of the orbifold may be obtained from the primaries $\Phi^{J\bar{J}}_{jw}(z,\bar{z};\xi_0,\theta_0)$ by summing over images in ξ_0 to enforce periodicity, and the string amplitudes of such operators compute BCFT correlation functions on the spacetime boundary T^2.

In the dual description of $\mathrm{SL}(2,\mathbb{C})_k/\mathrm{SU}(2)$ (Eqn. 4.17), which is strongly coupled for large k, the EAdS_3 solid cylinder is replaced by the first-order cylinder system $\mathcal{F}(\mathbb{C}/\mathbb{Z})$ and an infinite linear-dilaton direction (Eqn. 4.7), deformed by the three-dimensional sine-Liouville potential $4\pi\lambda(W_+ + W_-)$, where $W_\pm$ wind the now non-contractible θ cycle of the $W = \xi + i\theta \in \mathbb{C}/\mathbb{Z}$ cylinder (Eqn. 4.15). After writing the EAdS_3 action in first-order form (Eqn. 4.2), the two backgrounds coincide in the weak-coupling region, where the vertex operators $\Phi^{J\bar{J}}_{jw}(z,\bar{z};\xi_0,\theta_0)$ asymptote to a superposition of linear-dilaton $\times\,\mathcal{F}(\mathbb{C}/\mathbb{Z})$ operators. For an unflowed operator, for example, transforming Eqn. 3.47 to cylinder coordinates one

finds for $j > 1/2$,[83]

$$\Phi_j(z,\bar{z};\xi_0,\theta_0) \to e^{-2Q(1-j)\hat{r}}\delta(\xi-\xi_0)\sum_{n\in\mathbb{Z}}\delta(\theta-\theta_0-2\pi n) + \text{sub-leading}. \tag{4.44}$$

Inserting these linear-dilaton $\times\, \mathcal{F}(\mathbb{C}/\mathbb{Z})$ operators in the sine-Liouville functional integral, one may in principle compute $\mathrm{SL}(2,\mathbb{C})_k/\mathrm{SU}(2)$ correlation functions in the dual description. The dual description of $\mathbb{Z}\backslash\mathrm{SL}(2,\mathbb{C})_k/\mathrm{SU}(2)$ is the same, but with the first-order cylinder $\mathcal{F}(\mathbb{C}/\mathbb{Z})$ replaced by the torus $\mathcal{F}(\mathbb{C}/(\mathbb{Z}\times\mathbb{Z}))$, corresponding to compactifying $\xi = \mathrm{Re}(W)$.

When the EAdS_3 cylinder is cut and continued with respect to the Euclidean time coordinate ξ along its length, the Schwinger-Keldysh contour prepares the spacetime vacuum state in AdS_3. Then continuing the operator labels $\xi_0 \to it_0$ in the Euclidean string amplitudes yields BCFT expectation values of local operator insertions on the Lorentzian boundary cylinder in the dual vacuum state of radial quantization. When $\xi \sim \xi + \tilde{\beta}$ is compactified, continuing with respect to ξ defines string theory two copies of AdS_3 in the bulk TFD state of inverse temperature $\tilde{\beta}$.

Performing the same continuation in the sine-Liouville background yields a dual description of string perturbation theory in AdS_3 in the vacuum or thermal state. This is the better description of these theories when $k-2$ is a small number.

Our interest in the context of ER = EPR, however, is the continuation with respect to the compact Euclidean time coordinate θ—contractible in the original description and non-contractible in the dual, where the condensate is responsible for breaking the winding

[83] Here ξ, θ are sigma-model fields of the first-order system and ξ_0, θ_0 are labels for the boundary insertion point.

symmetry.

When the original description of $\mathrm{SL}(2,\mathbb{C})_k/\mathrm{SU}(2)$ is continued with respect to $\theta \to iT$, the Schwinger-Keldysh contour prepares the TFD state in a connected pair of AdS_3-Rindler wedges (Eqn. 3.92), and the continued string amplitudes compute expectation values of the BCFT in its TFD state in two copies of the angularly quantized Hilbert space on a line. After the $\xi \sim \xi + \tilde{\beta}$ orbifold, the same continuation of $\mathbb{Z}\backslash\mathrm{SL}(2,\mathbb{C})_k/\mathrm{SU}(2)$ prepares the HH state in the two-sided BTZ black hole of inverse Hawking temperature $\beta = 4\pi^2/\tilde{\beta}$.[84] In both cases, one obtains the theory of a string in a connected, two-sided geometry with a horizon. These are the ER descriptions of string theory in AdS_3-Rindler and BTZ.

The θ continuation of the dual backgrounds defines the EPR description of each of these two string theories. As in Eqn. 4.18, we treat the sine-Liouville potential as a large deformation of the free theory, now being the linear-dilaton $\times\, \mathcal{F}(\mathbb{C}/\mathbb{Z})$, or $\mathcal{F}(\mathbb{C}/(\mathbb{Z}\times\mathbb{Z}))$, background. At leading order, continuing $\theta = \mathrm{Im}(W)$ yields the Schwinger-Keldysh contour for the TFD state in two copies of linear-dilaton $\times\, \mathcal{F}(\mathbb{R}^{1,1})$ or $\mathcal{F}(\mathbb{R}\times\mathrm{S}^1)$ (Fig. 1.5a).

The remaining terms in the expansion insert pairs of W_+, W_- operators on top of the free-field Euclidean background, and in turn introduce deformations of the spacetime TFD state upon continuation. As in the two-dimensional case, we interpret each set as inserting a pair of folded strings emanating from the strong-coupling region in the TFD state of angular quantization on the worldsheet. The asymptotic conditions defining a $W_\pm$ insertion are as

[84] The black hole coordinates from Sec. 3.3.3 are obtained by rescaling $\Theta = \frac{\beta}{2\pi}\xi$, which is the non-contractible cycle of periodicity 2π, and $T_\mathrm{E} = \frac{\beta}{2\pi}\theta$, which is the contractible cycle of periodicity β.

in Eqn. 4.31 in the linear-dilaton direction, and, from Eqn. 4.11,

$$W(z) \overset{z\to 0}{\longrightarrow} \pm \log(z) \tag{4.45a}$$

$$\bar{W}(\bar{z}) \overset{\bar{z}\to 0}{\longrightarrow} \pm \log(\bar{z}). \tag{4.45b}$$

Or, in terms of $\xi = \frac{1}{2}(W + \bar{W})$ and $\theta = \frac{1}{2i}(W - \bar{W})$,

$$\xi \overset{\rho\to -\infty}{\longrightarrow} \pm\rho \tag{4.46a}$$

$$\theta \overset{\rho\to -\infty}{\longrightarrow} \pm\phi. \tag{4.46b}$$

Thus, with $W_+(0)$ and $W_-(\infty)$ fixed on CP^1, the worldsheet is mapped to the strong-coupling region with unit winding in the neighborhood of each insertion, while $\xi \to \mp\infty$. In between, the string formally extends partway toward finite $\hat{r}$ before folding back toward strong-coupling, while ξ ranges over the real line. When the target is halved to prepare the spacetime TFD state, one finds on the left and right zero-time slices a folded string emanating from the strong-coupling region and extended along the ξ direction (Fig. 4.5).

The same asymptotic conditions describe the sine-Liouville potential in the Euclidean black hole. Although Eqn. 4.46a may at first appear to be in tension with the compactification of ξ, recall that in these variables the current with respect to which the orbifold is performed is not simply ξ's conjugate variable χ, but $\chi + \partial\xi$, and the second term introduces an additional twist. As a result it is not obvious at a glance that the asymptotic condition respects the orbifold projection, but one is guaranteed as much because the operators $W_\pm$

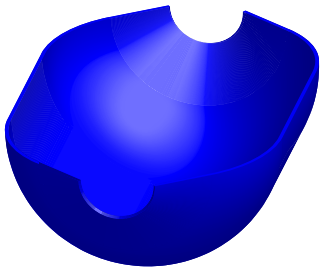

Figure 4.5: Folded Strings in EAdS_3. The spacetime image of the halved worldsheet from Fig. 1.7a with a pair of $W_\pm$ insertions is shown. The inner semicircles correspond to the strong-coupling region $\hat{r} \to -\infty$ of the linear-dilaton, the θ direction winds around these circles, and the ξ direction extends along the depth of the figure. The left and right boundaries are folded strings extending from the strong-coupling region partway toward finite $\hat{r}$ before falling back to strong coupling, while ξ ranges from minus infinity to infinity. The folded strings live on the zero-time slices $\theta = t_\mathrm{R} = 0, \theta = it_\mathrm{L} + \pi = \pi$ of the Lorentzian continuation.

are invariant.

Unlike the two-dimensional linear-dilaton $\times$ S^1 background, where the winding and continued scattering operator insertions were mutually non-local (Eqn. 4.24) and required the Rindler deformation of the moduli contour discussed in the previous section, the boundary position basis vertex operators admitted by the AdS_3 asymptotics do not suffer from this issue of mutual locality with the winding operators that appear in the expanded background. Indeed, the Euclidean boundary position basis vertex operators are manifestly periodic in Euclidean time, and the Lorentzian vertex operators, being defined by continuation, likewise respect the imaginary time periodicity. Explicitly, the relevant OPE to check is between[85] the winding operators $e^{\mp\sqrt{\frac{k}{\alpha'}}\int^{(z,\bar{z})} \mathrm{d}z'\hat{\chi}(z')+\mathrm{d}\bar{z}'\hat{\bar{\chi}}(\bar{z}')}$ of the first-order system and the delta-function

[85] The additional factors of Eqns. 4.15 and 4.44 are not relevant to the mutual locality question.

operators

$$\sum_{n\in\mathbb{Z}}\delta^2\left(\hat{W}(z)-\hat{W}_0-2\pi i\sqrt{\alpha' k}n\right) \tag{4.47}$$
$$\propto\sum_{n\in\mathbb{Z}}\int \mathrm{d}p\, e^{\frac{i}{2}\left(p-i\frac{n}{\sqrt{\alpha' k}}\right)\left(\hat{W}(z)-\hat{W}_0\right)}e^{\frac{i}{2}\left(p+i\frac{n}{\sqrt{\alpha' k}}\right)\left(\hat{\bar{W}}(\bar{z})-\hat{\bar{W}}_0\right)},$$

which are conveniently expressed via their inverse Fourier transform. Using Eqn. 4.10, one finds the OPE

$$e^{\frac{i}{2}\left(p-i\frac{n}{\sqrt{\alpha' k}}\right)\left(\hat{W}(z)-\hat{W}_0\right)}e^{\mp\sqrt{\frac{k}{\alpha'}}\int^0 \mathrm{d}z'\hat{\chi}(z')} \tag{4.48}$$
$$= z^{\pm\frac{i}{2}\sqrt{\alpha' k}\left(p-i\frac{n}{\sqrt{\alpha' k}}\right)}e^{\frac{i}{2}\left(p-i\frac{n}{\sqrt{\alpha' k}}\right)\left(\hat{W}(0)-\hat{W}_0\right)\mp\sqrt{\frac{k}{\alpha'}}\int^0 \mathrm{d}z'\hat{\chi}(z')}(1+\mathcal{O}(z)),$$

and similarly for the anti-holomorphic factors. Together, the $z,\bar{z}$ dependence of the pre-factors is

$$z^{\pm\frac{i}{2}\sqrt{\alpha' k}\left(p-i\frac{n}{\sqrt{\alpha' k}}\right)}\bar{z}^{\pm\frac{i}{2}\sqrt{\alpha' k}\left(p+i\frac{n}{\sqrt{\alpha' k}}\right)}=|z|^{\pm i\sqrt{\alpha' k}p}\left(\frac{z}{\bar{z}}\right)^{\pm n/2}, \tag{4.49}$$

which is single-valued and oscillatory, regardless of whether $\hat{W}_0,\hat{\bar{W}}_0$ sit on the Euclidean or Lorentzian section. Then the only $i\varepsilon$ prescription necessary to define Lorentzian string amplitudes with vertex operator insertions in the boundary position basis is the usual prescription that replaces the target Lorentzian time insertion point $T\to T(1-i\varepsilon)$, as expected from the perspective of the dual CFT, and required to identify the branch of the continued of Euclidean string amplitudes appropriate for time-ordered expectation values.

Of course, if one wishes to compute string amplitudes in the momentum basis rather than

the boundary position basis (Eqns. 3.75, 3.104), an analogous mutual locality issue as in the two-dimensional case will arise, and the Rindler deformation of the moduli integration contour will again be necessary.

Unlike the two-dimensional black hole, in AdS_3 the short-string vertex operators of interest include the real branch of j, and the unregulated expansion Eqn. 4.18 is of greater practical utility. For the two-point function of $\Phi_j(z,\bar{z};\xi_0,\theta_0)$, for example, the solution of the compatibility condition Eqn. 4.19 at genus zero is

$$j_N = \frac{1}{2}\left((k-2)N+1\right). \tag{4.50}$$

In e.g. the $N=1$ background, one finds a compatible correlator for $j=\frac{k-1}{2}$.[86] Then one could compute

$$\begin{aligned}&\langle\Phi_j(z_0,\bar{z}_0;\xi_0,\theta_0)\Phi_j(z_1,\bar{z}_1;\xi_1,\theta_1)\rangle_{\mathrm{SL}(2,\mathbb{C})_k/\mathrm{SU}(2)} \\ &= \left(\frac{\lambda}{2\alpha'}\right)^2\left\langle \mathcal{V}_{j,\xi_0,\theta_0}(z_0,\bar{z}_0)\mathcal{V}_{j,\xi_1,\theta_1}(z_1,\bar{z}_1)\int \mathrm{d}^2z_+\mathrm{d}^2z_-\; W_+(z_+,\bar{z}_+)W_-(z_-,\bar{z}_-)\right\rangle_{\mathrm{LD}\times\mathcal{F}(\mathbb{C}/\mathbb{Z})},\end{aligned} \tag{4.51}$$

where $\mathcal{V}_{j,\xi_i,\theta_i}$ is given by the right-hand-side of Eqn. 4.44. To extract the correlator for general j one would, as in Liouville, determine the meromorphic function whose poles coincide with the free-theory correlators of j_N.

To compute the string amplitude obtained from Eqn. 4.51, one would fix $z_+=0$, $z_-=\infty$, and $z_1=1$, and integrate over z_0. No contour deformation is necessary in this basis. One must also tensor the operators with an internal CFT scalar primary $\mathcal{O}_h$ of conformal weight

[86] Curiously, this coincides with the upper bound of the discrete-series spectrum.

h, chosen such that the on-shell condition is satisfied,

$$-\frac{j(j-1)}{k-2}+h=1. \tag{4.52}$$

4.4 Infinitesimal FZZ Dualities

We end by discussing an "infinitesimal" interpretation of the FZZ duality, its three-dimensional uplift, and their Lorentzian continuations. This interpretation is based on the isomorphism Eqn. 3.40 that relates the spectral-flowed components $\mathcal{W}_{\pm}$ of the sine-Liouville operator (Eqn. 3.67) to unflowed current-algebra descendents (Eqn. 3.68), as identified by the authors of [79]. We apply their identification of these vertex operators to discuss an infinitesimal version of each duality in the sense of conformal perturbation theory around the $\mathrm{SL}(2,\mathbb{R})_k/\mathrm{U}(1)$ or $\mathbb{Z}\backslash\mathrm{SL}(2,\mathbb{C})_k/\mathrm{SU}(2)$ CFTs: there are two semi-classical descriptions of perturbations by the sine-Liouville operator which shift the mass of the black hole. In the unflowed description of the perturbation, the value of the dilaton zero-mode is shifted. In the flowed description, the perturbation introduces a condensate of strings that wrap the horizon. These strings are the constituent objects that make up the black hole, and so its mass is shifted under the deformation.

As reviewed in Secs. 2.3.3 and 3.2, the $\mathrm{SL}(2,\mathbb{R})_k$ and $\mathrm{SL}(2,\mathbb{R})_k/\mathrm{U}(1)$ CFT spectra share a marginal operator $\mathcal{O}_{\mathrm{sL}}=\mathcal{W}_{+}+\mathcal{W}_{-}$, normalizable[87] for $k>3$ and non-normalizable for $2<k<3$. One may likewise identify $\mathcal{O}_{\mathrm{sL}}$ in the continued spectrum of $\mathrm{SL}(2,\mathbb{C})_k/\mathrm{SU}(2)$

[87] Delta-function normalizable in the $\mathrm{SL}(2,\mathbb{R})_k$ case.

operators, again (delta-function) normalizable for $k > 3$. The sine-Liouville potential is the limiting form of $\mathcal{O}_{\rm sL}$ near the weak-coupling boundary in the various sigma-model descriptions of these CFTs.

The sine-Liouville Lagrangians for these CFTs make evident that a conformal perturbation by $\mathcal{O}_{\rm sL}$ is trivial at the CFT level. The deformation merely shifts the coefficient λ of the sine-Liouville potential, which may be undone by a field redefinition that shifts $\hat{r}$ by a constant. Then the perturbation leaves the same sine-Liouville background, except that the dilaton has been shifted by a constant, resulting from the linear-dilaton in $\hat{r}$. The latter is a trivial improvement term of the CFT, the only effect being to multiply the functional integral by $e^{-\delta\Phi_0\chi}$, where χ is the worldsheet Euler characteristic.

In the string theory, however, $e^{-2\Phi_0}\lambda^{\frac{2}{k-2}}$ controls the mass of the black hole, which is deformed under the perturbation. That the perturbation is normalizable for $k > 3$ implies that the black hole mass may fluctuate [133, 134].[88]

Consider first the $\mathrm{SL}(2,\mathbb{R})_k/\mathrm{U}(1)$ case. The infinitesimal duality will equate two descriptions of the perturbation by $\mathcal{O}_{\rm sL}$ in the cigar sigma-model at large k. In one description, the deformation shifts the value Φ_0 of the dilaton at the tip of the cigar, and in the other it introduces a condensate of strings that wrap the tip. The next two sub-sections explain the origins of these two equivalent descriptions of the sine-Liouville deformation.

[88] For $2 < k < 3$ the CFTs likely no longer admit a black hole interpretation [83].

4.4.1 The Winding Condensate

Consider a perturbation of the $\mathrm{SL}(2,\mathbb{R})_k/\mathrm{U}(1)$ CFT by the sine-Liouville operator, $\varepsilon \int \mathrm{d}^2 z\, \mathcal{O}_{\mathrm{sL}}$. In conformal perturbation theory, the deformation is expanded in powers of ε:

$$e^{-\varepsilon \int (\mathcal{W}_+ + \mathcal{W}_-)} = \sum_{N_1,N_2=0}^{\infty} \frac{(-\varepsilon)^{N_1+N_2}}{N_1! N_2!} \left(\int \mathcal{W}_+ \right)^{N_1} \left(\int \mathcal{W}_- \right)^{N_2}. \tag{4.53}$$

At large k, $\mathcal{W}_\pm$ is a heavy operator that changes the behavior of the saddles of the functional integral. To understand the behavior of the saddles in the neighborhood of these insertions, we wish to identify an asymptotic condition for $\mathcal{W}_\pm$ in the cigar description of the CFT.

As discussed in Sec. 2.3.4, the asymptotic conditions in Eqn. 2.131 describing an operator insertion $\mathcal{O}_{jnw}$ of $\mathrm{SL}(2,\mathbb{R})_k/\mathrm{U}(1)$ in the far past on the cylinder assume a generic value of j, with $\mathrm{Re}(j) > \frac{1}{2}$, on which $R(j,n,w)$ is non-singular. The string is mapped to the free-field region in the neighborhood of the operator insertion, and thus the free-field asymptotic condition is a self-consistent solution of the cigar equations of motion. On the bound state spectrum j_N, however, which includes the sine-Liouville operator, R has simples poles, and one must be more careful. In that case, it is the reflected term in Eqn. 2.116 that dominates in the weak coupling region, $\frac{1}{R}\mathcal{O}_{jnw} \to \mathcal{V}_{Qj,p_{\mathrm{L}},p_{\mathrm{R}}}$, and the free-field asymptotic condition flips sign,

$$r \overset{\rho\to-\infty}{\longrightarrow} \frac{2}{k}\left(j - \frac{1}{2}\right)\rho. \tag{4.54}$$

This asymptotic condition maps the string out of the free-field region and is inconsistent.

This agrees with the fact that the bound states are normalizable, and do not extend out to infinity in r.

The linear solution (Fig. 4.6) is a saddle for the two-point function of the linear-dilaton primaries $e^{-2(1-j)r}$ and e^{-2jr}, sending the string to $r \to \infty$ and $r \to -\infty$ in the neighborhoods of the two respective operators. In the cigar, of course, the geometry ends at $r = 0$, and in the vicinity of the tip the free cylinder equations of motion are modified by the curvature of the cigar. One would like to understand how the free trajectory is corrected once the string leaves the free-field region, and thereby obtain an asymptotic condition for the bound state insertion. We will argue that the string worldsheet asymptotically wraps the tip of the cigar.

Because the neighborhood of the bound state insertion is mapped out of the free-field region, the large r expansion e^{-2jr} of the operator is insufficient to determine the requisite asymptotic condition. The radial dependence of the vertex operator on the full cigar was obtained in [75]:[89] [90]

$$\begin{aligned} &\frac{4^{j-1}}{\Gamma(2j-1)}\frac{\Gamma(j+m)\Gamma(j-\bar{m})}{\Gamma(1+m-\bar{m})} \\ &\times \sinh^{m-\bar{m}}(r)\cosh^{-(m+\bar{m})}(r){}_2F_1(j-\bar{m},1-j-\bar{m};1+m-\bar{m};-\sinh^2(r)) \\ &\overset{r\to\infty}{\longrightarrow} e^{-2(1-j)r} + 4^{2j-1}\frac{\Gamma(1-2j)}{\Gamma(2j-1)}\frac{\Gamma(j+m)\Gamma(j-\bar{m})}{\Gamma(1-j+m)\Gamma(1-j-\bar{m})}e^{-2jr}, \end{aligned} \tag{4.55}$$

where $m = \frac{1}{2}(-kw+n)$ and $\bar{m} = \frac{1}{2}(-kw-n)$, as in Eqn. 3.66. Note that the reflection

[89] This expression holds for $m \geq \bar{m}$ (i.e. $n \geq 0$). Note that the reflection coefficient is invariant under $w \to -w$. For $m \leq \bar{m}$ one sends $m \to -m$ and $\bar{m} \to -\bar{m}$, which is equivalent to flipping the signs of n and w. Then it is the absolute value of n that appears in the reflection coefficient, as in Eqn. 2.117.

[90] To obtain the wavefunction, one would multiply by $\cosh(r)$ as described in Sec. 2.3.3.

coefficient reproduces the second line of Eqn. 2.117.[91]

Recalling that the hypergeometric series terminates when its first or second argument is a non-positive integer, we find that the hypergeometric function is a finite order polynomial in $\sinh^2(r)$ on the bound state spectrum. On the lowest-weight states, $j - \bar{m} = -N$, this is evident from Eqn. 4.55, where the hypergeometric function yields an order N polynomial in $\sinh^2(r)$. On the highest-weight states, $j + m = -N$, it becomes evident after applying the hypergeometric fractional transformation rule

$$\begin{aligned} &{}_2F_1(j - \bar{m}, 1 - j - \bar{m}; 1 + m - \bar{m}; -\sinh^2(r)) \\ &\quad = \cosh^{2(m+\bar{m})}(r) {}_2F_1(j + m, 1 - j + m; 1 + m - \bar{m}; -\sinh^2(r)). \end{aligned} \tag{4.56}$$

In the pure-winding sector ($n = 0$) one obtains on the bound state spectrum $j_N = \frac{k|w|}{2} - N$,

$$\mathcal{O}_{j_N, n=0, w} \propto \operatorname{sech}^{k|w|}(r) {}_2F_1\left(-N, -k|w| + N + 1; 1; -\sinh^2(r)\right). \tag{4.57}$$

For $N = 0$ the hypergeometric function is 1, for $N = 1$ it is $1 + (-k|w| + 2)\sinh^2(r)$, and so on.

These operators consist of a heavy factor $\operatorname{sech}^{k|w|}(r)$, which enters at the same order as the leading terms in the action, times a light factor, which is sub-leading. The heavy factor inserts a source in the leading equations of motion and therefore affects the form of

[91] It is unclear to us if the missing factor from the first line of Eqn. 2.117, which is of order one in the large k limit, is due to a non-perturbative correction to the cigar background as has been suggested in the literature [80–82], or if it is a perturbative correction. See Ft. 27.

the saddles. The light factor, by constrast, is merely evaluated on the leading saddles and contributes to the sub-leading correction in the saddle-point expansion. Moreover, since the heavy factor is independent of N, the behavior of the saddle for any bound state insertion is independent of N.[92] Our principal interest is in the components of the sine-Liouville operator, for which $N = 1$ and $w = \pm 1$. Let us choose $w = -1$; the case $w = 1$ is analogous.

Since the asymptotic condition for $\mathcal{O}_{j=\frac{k}{2}-N,n=0,w=-1}$ is independent of N, we may in fact set $N = 0$. This state is not part of the physical spectrum, of course. In fact, it is rather special in the continued space of states; it is in a sense a reflection of the identity operator [76]. Note first of all that its conformal weight is zero. In the coset construction from $\mathrm{SL}(2,\mathbb{R})_k$, $\mathcal{O}_{j=\frac{k}{2},n=0,w=-1}$ descends from the state

$$\left| j = \frac{k}{2}, m = \frac{k}{2}, \bar{m} = \frac{k}{2}; w = -1 \right\rangle \in \widehat{D}^{+,w=-1}_{\frac{k}{2}} \otimes \widehat{D}^{+,w=-1}_{\frac{k}{2}}. \tag{4.58}$$

$\left| j = \frac{k}{2}, m = \frac{k}{2}, \bar{m} = \frac{k}{2} \right\rangle$ is known as the spectral flow operator [46, 76] because its product with another operator imparts one unit of spectral flow. By flowing this state backward by one unit as in Eqn. 4.58, one obtains a trivial operator of J^3_0, $\bar{J}^3_0$, and conformal weight zero. Under the isomorphism Eqn. 3.40, it maps to the trivial highest-weight state $\left| j' = 0, m' = 0, \bar{m}' = 0; w' = 0 \right\rangle$.

To understand the asymptotic condition associated to this operator, return to the cigar quantum mechanics Eqn. 2.149, obtained after choosing a pure-winding configuration $\theta = \phi$. The inverted potential $-V(r) = \frac{1}{2}\mathrm{sech}^2(r)$ is a hill of height $\frac{1}{2}$, as shown in Fig. 2.6. For

[92] We have assumed here that N is of order one in the large k limit, else the order N polynomial in $\sinh^2(r)$ would no longer be a light operator.

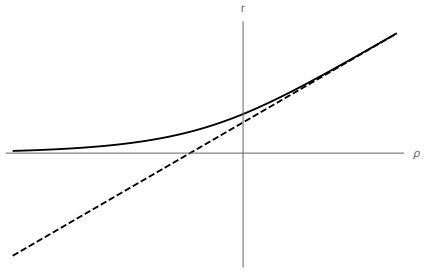

Figure 4.6: The Cigar Wrapping Saddle. When $j = j_N$ lies on the bound state spectrum Eqn. 2.106b, the reflection coefficient is singular, and it is the otherwise sub-leading term e^{-2jr} in Eqn. 2.116 that describes the operator $\mathcal{O}_{jnw}$ in the asymptotic region. The free field Green function, shown by the dashed line, maps the string out of the free field region and must be modified. The complete solution for $|w| = 1$ and $n = 0$ is $\theta = \pm\phi$, $r = \sinh^{-1}(e^{\rho})$. The neighborhood of the bound state insertion wraps the tip of the cigar, with $r \to e^{\rho}$ asymptotically approaching $r = 0$. The leading saddle is independent of N, which enters in the sub-leading correction to the saddle-point approximation.

generic real values of $\eta < 1$, one obtained real solutions describing a particle that comes in from infinity with speed η, rolls partway up the hill to a height of $\frac{1}{2}\eta^2$, and then rolls back to infinity. For $\eta = 1$, corresponding to $j = \frac{k}{2}$, the particle has just enough energy to asymptotically approach the top of the potential at $r = 0$. It does not return to infinity, but rather wraps the tip of the cigar, taking infinite time to do so.

This cigar wrapping solution is

$$r(\rho) = \sinh^{-1}(e^{\rho}), \tag{4.59}$$

shown in Fig. 4.6, with limiting behavior

$$r(\rho) \to \begin{cases} e^{\rho} & \rho \to -\infty \\ \\ \rho & \rho \to \infty. \end{cases} \tag{4.60}$$

As expected from Eqn. 4.54 with $j = \frac{k}{2}$, in the asymptotic region the solution approaches the free-field Green function $r \to \rho$. Eqn. 4.59 gives the completion of the solution beyond

the free-field region.

The asymptotic conditions

$$r \overset{\rho\to-\infty}{\longrightarrow} e^{\rho} \tag{4.61}$$

$$\theta \overset{\rho\to-\infty}{\longrightarrow} \phi, \tag{4.62}$$

describe a string that wraps the tip of the cigar. Since the bound state operators for $N \neq 0$ differ at sub-leading order, we claim that this is the appropriate asymptotic condition for any N of order one, including $\mathcal{W}_+$. The asymptotic condition for $\mathcal{W}_-$ is the same, but with $\theta \to -\phi$. Observe that this is simply the holomorphic map that sends the worldsheet coordinate $z = e^{\rho}e^{i\phi}$ to the target coordinate $Z = re^{i\theta}$ in the neighborhood of the tip of the cigar, where the geometry is $\mathbb{R}^2$. As usual, one may shift ρ by a continuous modulus $i\rho_0$ that changes the angle at which the trajectory approaches the origin in the complex r-plane, and one may moreover consider solutions shifted by $\pi i\mathbb{Z}$.

Note that $\dot{r} \to r$ as $\rho \to -\infty$ and $\dot{r} \to 1$ as $\rho \to \infty$. This configuration is therefore a saddle of the action

$$\begin{aligned} S =& \frac{k}{4\pi}\int_{-L}^{L} \mathrm{d}\rho \int_{0}^{2\pi} \mathrm{d}\phi \left((\partial_\rho r)^2 + (\partial_\phi r)^2 + \tanh^2(r)\left((\partial_\rho\theta)^2 + (\partial_\phi\theta)^2\right)\right) \\ &+ k\int_{0}^{2\pi}\frac{\mathrm{d}\phi}{2\pi}\left(-r|_{\rho=L} + \frac{1}{2}r^2|_{\rho=-L}\right) \\ &+ k\int_{0}^{2\pi}\frac{\mathrm{d}\phi}{2\pi}\Big(\sigma_+\left(\partial_\phi\theta|_{\rho=L} - 1\right) + \sigma_-\left(\partial_\phi\theta|_{\rho=-L} - 1\right)\Big) + \mathcal{O}(k^0), \end{aligned} \tag{4.63}$$

with radial boundary equations of motion

$$\partial_\rho r|_{\rho=L} = 1 \tag{4.64a}$$

$$\partial_\rho r|_{\rho=-L} = r|_{\rho=-L}. \tag{4.64b}$$

The on-shell action is $S = -k\log(2)$.

Thus, one may interpret the cigar-wrapping configuration as a saddle for the two-point function of $\mathcal{O}_{j=\frac{k}{2}-N,n=0,w=\pm1}$. In the special case when $N = 0$, this is a trivial operator. Then the r^2 boundary term yields the identity operator in the limit that it shrinks away, and one may alternatively interpret the configuration as a saddle for the one-point function. For $N \neq 0$, one inserts the light factor of the operator at the boundary and the insertion becomes non-trivial.

Since the reflection coefficient is singular, the sum over complex saddles may diverge with the free-field boundary condition specified by the linear boundary term at $\rho = L$. Our primary interest is not in the cigar wrapping saddle itself, however, but in the tip wrapping asymptotic condition $\dot{r} \to r$ for the bound states.

Having established the asymptotic conditions that describe $\mathcal{W}_\pm$ insertions in the cigar sigma-model, we may now return to the interpretation of the sine-Liouville deformation in conformal perturbation theory (Eqn. 4.53). In the neighborhood of each $\mathcal{W}_\pm$ insertion, the asymptotic condition implies that the image of the string worldsheet asymptotically wraps the tip of the cigar with winding ±1 (Fig. 4.7a). In this way, the conformal perturbation by

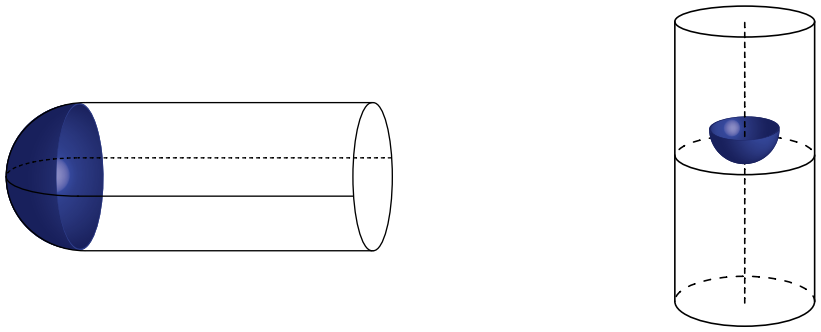

(a) (b)

Figure 4.7: sine-Liouville Asymptotic Conditions. The spacetime image of the string worldsheet in the neighborhood of a $\mathcal{W}_+$ insertion is shown in the cigar description of $\mathrm{SL}(2,\mathbb{R})_k/\mathrm{U}(1)$ (left) and the cylinder description of $\mathrm{SL}(2,\mathbb{C})_k/\mathrm{SU}(2)$ (right).

$\mathcal{O}_{\mathrm{sL}}$ introduces a condensate of strings that wrap the horizon.

4.4.2 The Dilaton-Shifting Operator

The dual semi-classical description of the perturbation follows from the isomorphism (Eqns. 3.67-3.68) [79]

$$\left|\frac{k}{2}-1,\pm\frac{k}{2},\pm\frac{k}{2};\mp 1\right\rangle \simeq J^{\pm}_{-1}\bar{J}^{\pm}_{-1}\left|1,\mp 1,\mp 1;0\right\rangle . \tag{4.65}$$

For example, $J^{-}_{-1}\left|j=1,m=1;w=0\right\rangle$ carries zero J^3_0 charge, is of holomorphic conformal weight one, and is a lowest-weight state of $\mathfrak{sl}(2,\mathbb{R})_{\mathrm{L}}$, consistent with the properties of $|k/2-1,-k/2;1\rangle$. The latter belongs to the normalizable spectrum for $k>3$, such that $j=k/2-1$ satisfies the lower bound $j>1/2$. The former likewise belongs to the spectrum for $k>3$, such that $j=1$ satisfies the upper bound $j<\frac{k-1}{2}$, the spectral-flow isomorphism $j\to k/2-j$ exchanging the upper and lower bounds.

The sine-Liouville operator $\mathcal{O}_{\rm sL}$ is the sum of the $w = \mp 1$ operators on the left of Eqn. 4.65. Let us denote by $\mathcal{O}_\Phi$ the sum on the right.[93] The isomorphism identifies the two. On a flat worldsheet, the vertex operator for $\mathcal{O}_\Phi$ in the cigar description is, at large k [55],

$$\mathcal{O}_\Phi(z,\bar{z})\big|_{\rm flat} = \frac{k}{2\pi}\mathrm{sech}^2(r)\left(\partial r\bar{\partial}r + \tanh^2(r)\partial\theta\bar{\partial}\theta\right). \tag{4.66}$$

Recalling the cigar metric Eqn. 2.97a, this operator is evidently a metric deformation. Namely, adding to the cigar action $\varepsilon\int \mathrm{d}^2z\,\mathcal{O}_\Phi$ results in a sigma-model with shifted metric

$$\mathrm{d}s^2[\varepsilon] = \alpha' k\left(\mathrm{d}r^2 + \tanh^2(r)\mathrm{d}\theta^2\right)\left(1+\varepsilon\mathrm{sech}^2(r)\right). \tag{4.67}$$

The deformed metric is in fact related to the original metric by a reparameterization $\tilde{r} = r + \frac{1}{2}\varepsilon\tanh(r)$:

$$\mathrm{d}s^2[\varepsilon] = \alpha' k\left(\mathrm{d}\tilde{r}^2 + \tanh^2(\tilde{r})\mathrm{d}\theta^2\right) + \mathcal{O}(\varepsilon^2). \tag{4.68}$$

On a curved worldsheet, the deformation by $\mathcal{O}_\Phi$ must simultaneously transform the dilaton $\Phi \to \Phi[\varepsilon] = -\log\cosh(\tilde{r}) + \tilde{\Phi}_0 + \mathcal{O}(\varepsilon^2)$ so as to preserve the conformal symmetry of the background:

$$\Phi[\varepsilon] = -\log\cosh(r) + \Phi_0 - \frac{1}{2}\varepsilon\tanh^2(r) + \varepsilon\delta\Phi_0 + \mathcal{O}(\varepsilon^2). \tag{4.69}$$

We have also allowed for the deformation to shift the zero-mode $\Phi_0 \to \tilde{\Phi}_0 = \Phi_0 + \varepsilon\delta\Phi_0$,

[93] One could also consider the marginal operator defined by the differences of these operators, but this deformation breaks worldsheet parity [55].

Eqn. 2.99 placing no constraint on the constant mode of the dilaton. Since the operator is normalizable at large k, one expects the deformation to vanish at large r, from which we infer that $\delta\Phi_0 = \frac{1}{2}$. Then the vertex operator for $\mathcal{O}_\Phi$ is given by

$$\mathcal{O}_\Phi(z,\bar{z}) = \operatorname{sech}^2(r)\left(\frac{k}{2\pi}\left(\partial r\bar{\partial}r + \tanh^2(r)\partial\theta\bar{\partial}\theta\right) + \frac{1}{16\pi}\mathcal{R}[h]\right). \tag{4.70}$$

The deformation of the cigar sigma-model by $\varepsilon\int \mathrm{d}^2z\,\mathcal{O}_\Phi$ is thus again almost trivial. By the field redefinition $r \to \tilde{r}$ one may undo the deformation, up to a shift $\Phi_0 \to \Phi_0 + \frac{\varepsilon}{2}$ of the value of the dilaton at the tip. This is a trivial improvement term from the perspective of the CFT. In the string theory, however, Φ_0 sets the mass of the black hole (Eqn. 2.105), which is shifted under the perturbation, $\delta M = -\varepsilon M$.

Thus, the identification Eqn. 4.65 leads to an infinitesimal form of the FZZ duality, relating superficially different marginal deformations of the cigar that shift the mass of the black hole. One description simply shifts the value of the dilaton at the tip of the cigar, while the dual description introduces a condensate of winding strings that wrap the tip.

For a black hole of a given mass M, one may formally apportion the mass between the value of the dilaton at the tip and the strength of the condensate—as for Φ_0 and λ in the sine-Liouville description, neither of the two parameters is independently meaningful. One may always trade away the contribution from the condensate in favor of a shifted value of the dilaton by applying the duality. The black hole may therefore be described by the pure cigar background Eqn. 2.97 of mass Eqn. 2.105 with the condensate turned off, just as one may set the constant mode of the dilaton to zero in the sine-Liouville background Eqn.

2.230. Alternatively, one may trade Φ_0 in favor of the condensate. Then as in the sine-Liouville description one may think of the black hole as being made up of winding strings. The conformal perturbation adds additional strings and so increases the black hole mass.

The same isomorphism Eqn. 4.65 between $\mathcal{O}_{\mathrm{sL}}$ and $\mathcal{O}_\Phi$ holds in three dimensions, and therefore the duality of $\mathrm{SL}(2,\mathbb{C})_k/\mathrm{SU}(2)$ and its black hole quotient $\mathbb{Z}\backslash\mathrm{SL}(2,\mathbb{C})_k/\mathrm{SU}(2)$ admits a similar infinitesimal interpretation. The BTZ black hole mass (Eqn. 3.97) scales with $1/G_{\mathrm{N}}$, which, in three-dimensional gravity goes as $G_{\mathrm{N}} \propto l_{\mathrm{p}} \propto g_{\mathrm{s}}^2 l_{\mathrm{s}}$. Thus, $M \propto e^{-2\Phi_0}$ as in the two-dimensional black hole. A conformal perturbation by $\mathcal{O}_\Phi$ again shifts the constant mode of the dilaton, and in turn the mass. To understand the dual interpretation, one needs the asymptotic conditions for $\mathcal{W}_\pm$ in EAdS_3. The asymptotic conditions Eqn. 4.61 in the cigar followed from the $\rho \to -\infty$ limit of the cigar-wrapping saddle $r = \sinh^{-1}(e^\rho)$, $\theta = \pm\phi$. This configuration may be uplifted to a solution of the $\mathrm{SL}(2,\mathbb{C})_k/\mathrm{SU}(2)$ equations of motion with

$$\xi = \pm\frac{1}{2}\log(1+e^{2\rho}). \tag{4.71}$$

We conjecture that the asymptotic condition for $\mathcal{W}_\pm$ in EAdS_3 and the Euclidean black hole is then as in Eqn. 4.61, together with $\xi \to \pm\frac{1}{2}e^{2\rho}$, up to shifts by a constant. Then the perturbation by $\mathcal{O}_{\mathrm{sL}}$ again introduces a condensate of horizon-crossing strings, the horizon now corresponding to the one-dimensional locus $r = 0$ (Fig. 4.7b).

4.4.3 Infinitesimal Lorentzian Dualities

Lastly, we briefly consider the Lorentzian continuation of these infinitesimal dualities. Each identifies two equivalent descriptions of the effect of a conformal perturbation by the sine-Liouville operator $\mathcal{O}_{\text{sL}} = \mathcal{W}_+ + \mathcal{W}_-$ (Eqn. 2.123) in the ER description of the respective CFTs. In one description, the deformation introduces a condensate of strings that wrap the Euclidean horizon $r = 0$, and in the other the constant mode of the dilaton is shifted. The black hole mass is in turn shifted under the deformation, in the case of $\text{SL}(2,\mathbb{R})_k/\text{U}(1)$ and $\mathbb{Z}\backslash\text{SL}(2,\mathbb{C})_k/\text{SU}(2)$.

The conformal perturbation deforms the Euclidean background that defines the Lorentzian string theory upon continuation. Expanding the perturbation as in Eqn. 4.53, a superposition of $\mathcal{W}_\pm$ insertions is introduced on the worldsheet. Note that, in contrast to Eqn. 4.18, we are now treating the perturbation as an expansion around the exact CFT background as opposed to the free-field background. In particular, the winding number need not be conserved.

In the cigar, the asymptotic conditions Eqn. 4.61 for $\mathcal{W}_\pm$ map the neighborhood of the insertion point to the tip as pictured in Fig. 4.7a. On the $\theta = 0$ fixed-time slice, one finds a string with one end at the tip of the cigar, and likewise on the $\theta = \pi$ slice. When the cigar is cut in half across its θ cycle to prepare the HH state of the black hole, the $\mathcal{W}_\pm$ insertion therefore adds a pair of entangled strings in the TFD state of $\mathcal{H}_{\pm,1}(\mathbb{R}) \otimes \mathcal{H}_{\pm,1}(\mathbb{R})$, one in the left wedge and one in the right, each with one end pinned at the horizon bifurcation

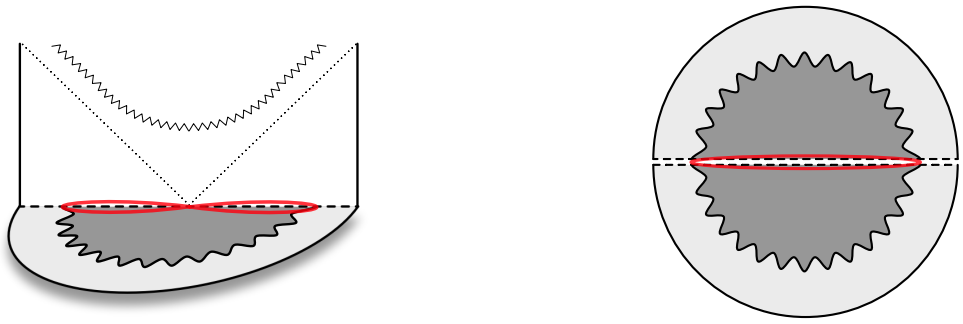

(a) (b)

Figure 4.8: The Infinitesimal Duality. When the $\mathrm{SL}(2,\mathbb{R})_k/\mathrm{U}(1)$ or $\mathbb{Z}\backslash\mathrm{SL}(2,\mathbb{C})_k/\mathrm{SU}(2)$ Euclidean black hole CFT is deformed by a marginal operator known as the sine-Liouville operator—so-called because its free-field limit is the sine-Liouville potential—a condensate of strings that wrap the Euclidean horizon is introduced (right). The red loop is a spatial slice of string, corresponding to the image of the dashed line in Fig. 1.7a bounding the worldsheet TFD state with a pair of winding insertions. It may be thought of as a pair of folded strings emanating from the horizon, contrasted with the disconnected folded strings emanating from the strong-coupling region in the EPR description (Fig. 1.5b and 1.7b). When continued to the Lorentzian ER string theory, one finds a pair of folded strings joined at the horizon bifurcation point in an entangled state. The deformation introduces a condensate of such strings, and the infinitesimal duality asserts that the same effect is described by shifting the constant mode of the dilaton. In both descriptions the mass of the black hole is in turn shifted.

point. Or, with a pair of $\mathcal{W}_+, \mathcal{W}_-$ insertions as in Fig. 1.7a, one finds on the spacetime zero-time slice a pair of folded strings emanating from the horizon in the TFD state of $\mathcal{H}_{+-}(\mathbb{R}) \otimes \mathcal{H}_{+-}(\mathbb{R})$, as sketched in Fig. 4.8a. These folded strings should be compared with those emanating from the strong-coupling region of the EPR background (Fig. 1.5a)—in the ER description they end on the horizon while in the EPR description they dissolve into the condensate. One may think of the deformation as adding to the condensate of strings that make up the black hole and thus shifting the mass. The dual dilaton-shifting description of course shifts the mass as well.

In $\mathrm{SL}(2,\mathbb{C})_k/\mathrm{SU}(2)$ or $\mathbb{Z}\backslash\mathrm{SL}(2,\mathbb{C})_k/\mathrm{SU}(2)$ the picture is similar. The $\mathcal{W}_\pm$ insertions again add pairs of strings to the AdS_3-Rindler or BTZ backgrounds with one or both ends on the horizon bifurcation locus, the strings now extending in the ξ direction as well due to the additional asymptotic condition $\xi \to \pm\frac{1}{2}e^{2\rho}+\text{const.}$ (Eqn. 4.71). The conformal perturbation

by $\mathcal{O}_{\rm sL}$ introduces a condensate of such strings.

These horizon-bound strings, and their strong-coupling-bound EPR counterparts, resemble the open strings conjectured in [135, 136] to account for the black hole entropy. It would be very interesting to understand how to compute the entropy in these string backgrounds. Our work may also be relevant to understanding entanglement entropy in string theory, related to ideas discussed in [137, 138].

References

[1] M. Van Raamsdonk, "Comments on quantum gravity and entanglement," arXiv:0907.2939 [hep-th].

[2] M. Van Raamsdonk, "Building up spacetime with quantum entanglement," Gen. Rel. Grav. **42** (2010) 2323–2329, arXiv:1005.3035 [hep-th]. [Int. J. Mod. Phys.D19,2429(2010)].

[3] V. E. Hubeny, M. Rangamani, and T. Takayanagi, "A Covariant holographic entanglement entropy proposal," JHEP **07** (2007) 062, arXiv:0705.0016 [hep-th].

[4] J. Maldacena and L. Susskind, "Cool horizons for entangled black holes," Fortsch. Phys. **61** (2013) 781–811, arXiv:1306.0533 [hep-th].

[5] S. Ryu and T. Takayanagi, "Holographic derivation of entanglement entropy from AdS/CFT," Phys. Rev. Lett. **96** (2006) 181602, arXiv:hep-th/0603001.

[6] S. Ryu and T. Takayanagi, "Aspects of Holographic Entanglement Entropy," JHEP **08** (2006) 045, arXiv:hep-th/0605073.

[7] A. Einstein and N. Rosen, "The Particle Problem in the General Theory of Relativity," Phys. Rev. **48** (1935) 73–77.

[8] A. Einstein, B. Podolsky, and N. Rosen, "Can quantum mechanical description of physical reality be considered complete?," Phys. Rev. **47** (1935) 777–780.

[9] S. Hawking, "Particle Creation by Black Holes," Commun. Math. Phys. **43** (1975) 199–220. [Erratum: Commun.Math.Phys. 46, 206 (1976)].

[10] S. W. Hawking, "Breakdown of Predictability in Gravitational Collapse," Phys. Rev. D **14** (1976) 2460–2473.

[11] J. D. Bekenstein, "Black holes and entropy," Phys. Rev. D **7** (1973) 2333–2346.

[12] J. D. Bekenstein, "Generalized second law of thermodynamics in black hole physics," Phys. Rev. D **9** (1974) 3292–3300.

[13] W. Israel, "Event horizons in static vacuum space-times," Phys. Rev. **164** (1967) 1776–1779.

[14] W. Israel, "Event horizons in static electrovac space-times," Commun. Math. Phys. **8** (1968) 245–260.

[15] L. Susskind, "The World as a hologram," J. Math. Phys. **36** (1995) 6377–6396, arXiv:hep-th/9409089.

[16] J. D. Bekenstein, "A Universal Upper Bound on the Entropy to Energy Ratio for Bounded Systems," Phys. Rev. D **23** (1981) 287.

[17] G. 't Hooft, "Dimensional reduction in quantum gravity," Conf. Proc. C **930308** (1993) 284–296, arXiv:gr-qc/9310026.

[18] J. M. Maldacena, "The Large N limit of superconformal field theories and supergravity," Int. J. Theor. Phys. **38** (1999) 1113–1133, arXiv:hep-th/9711200 [hep-th]. [Adv. Theor. Math. Phys.2,231(1998)].

[19] S. S. Gubser, I. R. Klebanov, and A. M. Polyakov, "Gauge theory correlators from noncritical string theory," Phys. Lett. **B428** (1998) 105–114, arXiv:hep-th/9802109 [hep-th].

[20] E. Witten, "Anti-de Sitter space and holography," Adv. Theor. Math. Phys. **2** (1998) 253–291, arXiv:hep-th/9802150 [hep-th].

[21] M. Banados, C. Teitelboim, and J. Zanelli, "The Black hole in three-dimensional space-time," Phys. Rev. Lett. **69** (1992) 1849–1851, arXiv:hep-th/9204099 [hep-th].

[22] M. Banados, M. Henneaux, C. Teitelboim, and J. Zanelli, "Geometry of the (2+1) black hole," Phys. Rev. **D48** (1993) 1506–1525, arXiv:gr-qc/9302012 [gr-qc]. [Erratum: Phys. Rev.D88,069902(2013)].

[23] J. M. Maldacena, "Eternal black holes in anti-de Sitter," JHEP **04** (2003) 021, arXiv:hep-th/0106112 [hep-th].

[24] W. Israel, "Thermo field dynamics of black holes," Phys. Lett. A **57** (1976) 107–110.

[25] S. W. Hawking and D. N. Page, "Thermodynamics of Black Holes in anti-De Sitter Space," Commun. Math. Phys. **87** (1983) 577.

[26] J. B. Hartle and S. W. Hawking, "Path Integral Derivation of Black Hole Radiance," Phys. Rev. **D13** (1976) 2188–2203.

[27] J. B. Hartle and S. W. Hawking, "Wave Function of the Universe," Phys. Rev. **D28** (1983) 2960–2975. [Adv. Ser. Astrophys. Cosmol.3,174(1987)].

[28] N. Bao, J. Pollack, and G. N. Remmen, "Wormhole and Entanglement (Non-)Detection in the ER=EPR Correspondence," JHEP **11** (2015) 126, arXiv:1509.05426 [hep-th].

[29] D. Berenstein and A. Miller, "Can Topology and Geometry be Measured by an Operator Measurement in Quantum Gravity?," Phys. Rev. Lett. **118** no. 26, (2017) 261601, arXiv:1605.06166 [hep-th].

[30] D. Berenstein and A. Miller, "Superposition induced topology changes in quantum

gravity," JHEP **11** (2017) 121, arXiv:1702.03011 [hep-th].

[31] D. L. Jafferis, "Bulk reconstruction and the Hartle-Hawking wavefunction," arXiv:1703.01519 [hep-th].

[32] E. Witten, "On string theory and black holes," Phys. Rev. **D44** (1991) 314–324.

[33] E. Witten, "A New Look At The Path Integral Of Quantum Mechanics," arXiv:1009.6032 [hep-th].

[34] E. Witten, "Analytic Continuation Of Chern-Simons Theory," AMS/IP Stud. Adv. Math. **50** (2011) 347–446, arXiv:1001.2933 [hep-th].

[35] D. Harlow, J. Maltz, and E. Witten, "Analytic Continuation of Liouville Theory," JHEP **12** (2011) 071, arXiv:1108.4417 [hep-th].

[36] R. Balian, G. Parisi, and A. Voros, "Quartic Oscillator," in Feynman Path Integrals, pp. 337–360. 1978.

[37] A. Voros, "The return of the quartic oscillator. the complex wkb method," Annales de l'I.H.P. Physique thorique **39** no. 3, (1983) 211–338. http://eudml.org/doc/76217.

[38] A. Cherman, D. Dorigoni, and M. Unsal, "Decoding perturbation theory using resurgence: Stokes phenomena, new saddle points and Lefschetz thimbles," JHEP **10** (2015) 056, arXiv:1403.1277 [hep-th].

[39] A. Behtash, G. V. Dunne, T. Schfer, T. Sulejmanpasic, and M. nsal, "Complexified path integrals, exact saddles and supersymmetry," Phys. Rev. Lett. **116** no. 1, (2016) 011601, arXiv:1510.00978 [hep-th].

[40] A. Behtash, G. V. Dunne, T. Schfer, T. Sulejmanpasic, and M. nsal, "Toward PicardLefschetz theory of path integrals, complex saddles and resurgence," Ann. Math. Sci. Appl. **02** (2017) 95–212, arXiv:1510.03435 [hep-th].

[41] T. Fujimori, S. Kamata, T. Misumi, M. Nitta, and N. Sakai, "Nonperturbative contributions from complexified solutions in $\mathbb{C}P^{N-1}$models," Phys. Rev. **D94** no. 10, (2016) 105002, arXiv:1607.04205 [hep-th].

[42] A. Behtash, G. V. Dunne, T. Schaefer, T. Sulejmanpasic, and M. nsal, "Critical Points at Infinity, Non-Gaussian Saddles, and Bions," JHEP **06** (2018) 068, arXiv:1803.11533 [hep-th].

[43] J. Teschner, "On structure constants and fusion rules in the SL(2,C) / SU(2) WZNW model," Nucl. Phys. **B546** (1999) 390–422, arXiv:hep-th/9712256 [hep-th].

[44] J. Teschner, "Operator product expansion and factorization in the H+(3) WZNW model," Nucl. Phys. **B571** (2000) 555–582, arXiv:hep-th/9906215 [hep-th].

[45] A. Giveon and D. Kutasov, "Comments on double scaled little string theory," JHEP **01** (2000) 023, arXiv:hep-th/9911039 [hep-th].

[46] J. M. Maldacena and H. Ooguri, "Strings in AdS(3) and the SL(2,R) WZW model. Part 3. Correlation functions," Phys. Rev. **D65** (2002) 106006, arXiv:hep-th/0111180 [hep-th].

[47] N. Seiberg, "Notes on quantum Liouville theory and quantum gravity," Prog. Theor. Phys. Suppl. **102** (1990) 319–349.

[48] "V. Fateev, A. Zamolodchikov and Al. Zamolodchikov, unpublished,".

[49] V. Kazakov, I. K. Kostov, and D. Kutasov, "A Matrix model for the two-dimensional black hole," Nucl. Phys. **B622** (2002) 141–188, arXiv:hep-th/0101011 [hep-th].

[50] L. Eberhardt, M. R. Gaberdiel, and R. Gopakumar, "Deriving the AdS_3/CFT_2 correspondence," JHEP **02** (2020) 136, arXiv:1911.00378 [hep-th].

[51] M. R. Gaberdiel and R. Gopakumar, "Tensionless string spectra on AdS_3," JHEP **05** (2018) 085, arXiv:1803.04423 [hep-th].

[52] L. Eberhardt, M. R. Gaberdiel, and R. Gopakumar, "The Worldsheet Dual of the Symmetric Product CFT," JHEP **04** (2019) 103, arXiv:1812.01007 [hep-th].

[53] G. Giribet, C. Hull, M. Kleban, M. Porrati, and E. Rabinovici, "Superstrings on AdS_3 at $\| = 1$," JHEP **08** (2018) 204, arXiv:1803.04420 [hep-th].

[54] M. Berkooz, Z. Komargodski, and D. Reichmann, "Thermal AdS(3), BTZ and competing winding modes condensation," JHEP **12** (2007) 020, arXiv:0706.0610 [hep-th].

[55] K. Hori and A. Kapustin, "Duality of the fermionic 2-D black hole and N=2 liouville theory as mirror symmetry," JHEP **08** (2001) 045, arXiv:hep-th/0104202 [hep-th].

[56] J. S. Schwinger, "Brownian motion of a quantum oscillator," J. Math. Phys. **2** (1961) 407–432.

[57] L. Keldysh, "Diagram technique for nonequilibrium processes," Zh. Eksp. Teor. Fiz. **47** (1964) 1515–1527.

[58] N. Itzhaki, "Stringy instability inside the black hole," JHEP **10** (2018) 145, arXiv:1808.02259 [hep-th].

[59] A. Giveon and N. Itzhaki, "Stringy Black Hole Interiors," JHEP **11** (2019) 014, arXiv:1908.05000 [hep-th].

[60] A. Giveon and N. Itzhaki, "Stringy Information and Black Holes," JHEP **06** (2020)

117, arXiv:1912.06538 [hep-th].

[61] A. Giveon, N. Itzhaki, and U. Peleg, "Instant Folded Strings and Black Fivebranes," JHEP **08** (2020) 020, arXiv:2004.06143 [hep-th].

[62] K. Attali and N. Itzhaki, "The Averaged Null Energy Condition and the Black Hole Interior in String Theory," Nucl. Phys. B **943** (2019) 114631, arXiv:1811.12117 [hep-th].

[63] N. Itzhaki and L. Liram, "A stringy glimpse into the black hole horizon," JHEP **04** (2018) 018, arXiv:1801.04939 [hep-th].

[64] K. P. Yogendran, "Horizon strings and interior states of a black hole," Phys. Lett. B **750** (2015) 278–281, arXiv:1808.05748 [hep-th].

[65] K. P. Yogendran, "Closed Strings in the 2D Lorentzian Black Hole," arXiv:1808.10109 [hep-th].

[66] A. B. Zamolodchikov and A. B. Zamolodchikov, "Structure constants and conformal bootstrap in Liouville field theory," Nucl. Phys. **B477** (1996) 577–605, arXiv:hep-th/9506136 [hep-th].

[67] J. Teschner, "Liouville theory revisited," Class. Quant. Grav. **18** (2001) R153–R222, arXiv:hep-th/0104158 [hep-th].

[68] D. L. Jafferis and E. Schneider, "Semi-Classical Analysis of the String Theory Cigar," arXiv:2004.05223 [hep-th].

[69] H. Dorn and H. J. Otto, "Two and three point functions in Liouville theory," Nucl. Phys. **B429** (1994) 375–388, arXiv:hep-th/9403141 [hep-th].

[70] V. G. Knizhnik, A. M. Polyakov, and A. B. Zamolodchikov, "Fractal Structure of 2D Quantum Gravity," Mod. Phys. Lett. A **3** (1988) 819.

[71] P. Di Francesco and D. Kutasov, "World sheet and space-time physics in two-dimensional (Super)string theory," Nucl. Phys. B **375** (1992) 119–170, arXiv:hep-th/9109005.

[72] M. V. Berry, "Infinitely many stokes smoothings in the gamma function," Proceedings of the Royal Society: Mathematical and Physical Sciences (1990-1995) **434** no. 1891, (1991) 465–472.

[73] S. Pasquetti and R. Schiappa, "Borel and Stokes Nonperturbative Phenomena in Topological String Theory and c=1 Matrix Models," Annales Henri Poincare **11** (2010) 351–431, arXiv:0907.4082 [hep-th].

[74] A. Kupiainen, R. Rhodes, and V. Vargas, "The DOZZ Formula from the Path Integral," JHEP **05** (2018) 094, arXiv:1803.05418 [hep-th].

[75] R. Dijkgraaf, H. L. Verlinde, and E. P. Verlinde, "String propagation in a black hole geometry," Nucl. Phys. **B371** (1992) 269–314.

[76] J. M. Maldacena and H. Ooguri, "Strings in AdS(3) and SL(2,R) WZW model 1.: The Spectrum," J. Math. Phys. **42** (2001) 2929–2960, arXiv:hep-th/0001053 [hep-th].

[77] A. Hanany, N. Prezas, and J. Troost, "The Partition function of the two-dimensional black hole conformal field theory," JHEP **04** (2002) 014, arXiv:hep-th/0202129 [hep-th].

[78] O. Aharony, A. Giveon, and D. Kutasov, "LSZ in LST," Nucl. Phys. **B691** (2004) 3–78, arXiv:hep-th/0404016 [hep-th].

[79] A. Giveon, N. Itzhaki, and D. Kutasov, "Stringy Horizons II," JHEP **10** (2016) 157, arXiv:1603.05822 [hep-th].

[80] D. Kutasov, "Accelerating branes and the string/black hole transition," arXiv:hep-th/0509170 [hep-th].

[81] A. Giveon, N. Itzhaki, and D. Kutasov, "Stringy Horizons," JHEP **06** (2015) 064, arXiv:1502.03633 [hep-th].

[82] A. Giveon and N. Itzhaki, "String theory at the tip of the cigar," JHEP **09** (2013) 079, arXiv:1305.4799 [hep-th].

[83] A. Giveon, D. Kutasov, E. Rabinovici, and A. Sever, "Phases of quantum gravity in AdS(3) and linear dilaton backgrounds," Nucl. Phys. **B719** (2005) 3–34, arXiv:hep-th/0503121 [hep-th].

[84] S. Ribault and J. Teschner, "H+(3)-WZNW correlators from Liouville theory," JHEP **06** (2005) 014, arXiv:hep-th/0502048 [hep-th].

[85] J. M. Maldacena, H. Ooguri, and J. Son, "Strings in AdS(3) and the SL(2,R) WZW model. Part 2. Euclidean black hole," J. Math. Phys. **42** (2001) 2961–2977, arXiv:hep-th/0005183 [hep-th].

[86] J. de Boer, H. Ooguri, H. Robins, and J. Tannenhauser, "String theory on AdS(3)," JHEP **12** (1998) 026, arXiv:hep-th/9812046 [hep-th].

[87] A. Giveon, D. Kutasov, and N. Seiberg, "Comments on string theory on AdS(3)," Adv. Theor. Math. Phys. **2** (1998) 733–782, arXiv:hep-th/9806194 [hep-th].

[88] D. Kutasov and N. Seiberg, "More comments on string theory on AdS(3)," JHEP **04** (1999) 008, arXiv:hep-th/9903219 [hep-th].

[89] K. Gawedzki, "Noncompact WZW conformal field theories," in New symmetry principles in quantum field theory., pp. 0247–274. 1991.

arXiv:hep-th/9110076 [hep-th].

[90] J. J. Atick and E. Witten, "The Hagedorn Transition and the Number of Degrees of Freedom of String Theory," Nucl. Phys. **B310** (1988) 291–334.

[91] G. T. Horowitz and J. Polchinski, "Selfgravitating fundamental strings," Phys. Rev. D **57** (1998) 2557–2563, arXiv:hep-th/9707170.

[92] P. Horava and C. J. Mogni, "String Perturbation Theory on the Schwinger-Keldysh Time Contour," Phys. Rev. Lett. **125** no. 26, (2020) 261602, arXiv:2009.03940 [hep-th].

[93] P. Horava and C. J. Mogni, "Large-N Expansion and String Theory Out of Equilibrium," arXiv:2008.11685 [hep-th].

[94] P. Horava and C. J. Mogni, "Keldysh Rotation in the Large-N Expansion and String Theory Out of Equilibrium," arXiv:2010.10671 [hep-th].

[95] K. Skenderis and B. C. van Rees, "Real-time gauge/gravity duality: Prescription, Renormalization and Examples," JHEP **05** (2009) 085, arXiv:0812.2909 [hep-th].

[96] K. Skenderis and B. C. van Rees, "Real-time gauge/gravity duality: Prescription, Renormalization and Examples," JHEP **05** (2009) 085, arXiv:0812.2909 [hep-th].

[97] J. Brown and M. Henneaux, "Central Charges in the Canonical Realization of Asymptotic Symmetries: An Example from Three-Dimensional Gravity," Commun. Math. Phys. **104** (1986) 207–226.

[98] I. R. Klebanov and E. Witten, "AdS / CFT correspondence and symmetry breaking," Nucl. Phys. B **556** (1999) 89–114, arXiv:hep-th/9905104.

[99] J. Kim and M. Porrati, "On the central charge of spacetime current algebras and correlators in string theory on AdS_3," JHEP **05** (2015) 076, arXiv:1503.07186 [hep-th].

[100] P. Breitenlohner and D. Z. Freedman, "Stability in Gauged Extended Supergravity," Annals Phys. **144** (1982) 249.

[101] E. Witten, "Anti-de Sitter space, thermal phase transition, and confinement in gauge theories," Adv. Theor. Math. Phys. **2** (1998) 505–532, arXiv:hep-th/9803131 [hep-th].

[102] E. Keski-Vakkuri, "Bulk and boundary dynamics in BTZ black holes," Phys. Rev. D **59** (1999) 104001, arXiv:hep-th/9808037.

[103] D. Birmingham, I. Sachs, and S. N. Solodukhin, "Relaxation in conformal field theory, Hawking-Page transition, and quasinormal normal modes," Phys. Rev. D **67** (2003) 104026, arXiv:hep-th/0212308.

[104] M. Natsuume and Y. Satoh, "String theory on three-dimensional black holes," Int. J. Mod. Phys. **A13** (1998) 1229–1262, arXiv:hep-th/9611041 [hep-th].

[105] S. Hemming and E. Keski-Vakkuri, "The Spectrum of strings on BTZ black holes and spectral flow in the SL(2,R) WZW model," Nucl. Phys. **B626** (2002) 363–376, arXiv:hep-th/0110252 [hep-th].

[106] S. Hemming, E. Keski-Vakkuri, and P. Kraus, "Strings in the extended BTZ space-time," JHEP **10** (2002) 006, arXiv:hep-th/0208003 [hep-th].

[107] A. S. Losev, A. Marshakov, and A. M. Zeitlin, "On first order formalism in string theory," Phys. Lett. B **633** (2006) 375–381, arXiv:hep-th/0510065.

[108] N. A. Nekrasov, "Lectures on curved beta-gamma systems, pure spinors, and anomalies," arXiv:hep-th/0511008.

[109] E. Frenkel and A. Losev, "Mirror symmetry in two steps: A-I-B," Commun. Math. Phys. **269** (2006) 39–86, arXiv:hep-th/0505131.

[110] R. Argurio, A. Giveon, and A. Shomer, "Superstrings on AdS(3) and symmetric products," JHEP **12** (2000) 003, arXiv:hep-th/0009242.

[111] A. Giveon and D. Kutasov, "Notes on AdS(3)," Nucl. Phys. B **621** (2002) 303–336, arXiv:hep-th/0106004.

[112] G. Giribet and C. A. Nunez, "Correlators in AdS(3) string theory," JHEP **06** (2001) 010, arXiv:hep-th/0105200.

[113] J. L. F. Barbon and E. Rabinovici, "Remarks on black hole instabilities and closed string tachyons," Found. Phys. **33** (2003) 145–165, arXiv:hep-th/0211212.

[114] J. L. F. Barbon and E. Rabinovici, "Closed string tachyons and the Hagedorn transition in AdS space," JHEP **03** (2002) 057, arXiv:hep-th/0112173.

[115] G. T. Horowitz and E. Silverstein, "The Inside story: Quasilocal tachyons and black holes," Phys. Rev. D **73** (2006) 064016, arXiv:hep-th/0601032.

[116] J. A. Harvey, D. Kutasov, E. J. Martinec, and G. W. Moore, "Localized tachyons and RG flows," arXiv:hep-th/0111154.

[117] G. T. Horowitz, "Tachyon condensation and black strings," JHEP **08** (2005) 091, arXiv:hep-th/0506166.

[118] E. Silverstein, "Singularities and closed string tachyons," in 23rd Solvay Conference in Physics: The Quantum Structure of Space and Time. 2, 2006. arXiv:hep-th/0602230.

[119] A. Adams, X. Liu, J. McGreevy, A. Saltman, and E. Silverstein, "Things fall apart:

Topology change from winding tachyons," JHEP **10** (2005) 033, arXiv:hep-th/0502021.

[120] A. Adams, J. Polchinski, and E. Silverstein, "Don't panic! Closed string tachyons in ALE space-times," JHEP **10** (2001) 029, arXiv:hep-th/0108075.

[121] T. Fukuda and K. Hosomichi, "Three point functions in sine-Liouville theory," JHEP **09** (2001) 003, arXiv:hep-th/0105217.

[122] D. Harlow, "Jerusalem Lectures on Black Holes and Quantum Information," Rev. Mod. Phys. **88** (2016) 015002, arXiv:1409.1231 [hep-th].

[123] E. Witten, "APS Medal for Exceptional Achievement in Research: Invited article on entanglement properties of quantum field theory," Rev. Mod. Phys. **90** no. 4, (2018) 045003, arXiv:1803.04993 [hep-th].

[124] W. G. Unruh and N. Weiss, "Acceleration Radiation in Interacting Field Theories," Phys. Rev. **D29** (1984) 1656.

[125] K. Ohmori and Y. Tachikawa, "Physics at the entangling surface," J. Stat. Mech. **1504** (2015) P04010, arXiv:1406.4167 [hep-th].

[126] J. M. Maldacena, "Long strings in two dimensional string theory and non-singlets in the matrix model," JHEP **09** (2005) 078, arXiv:hep-th/0503112.

[127] B. Balthazar, V. A. Rodriguez, and X. Yin, "Long String Scattering in c = 1 String Theory," JHEP **01** (2019) 173, arXiv:1810.07233 [hep-th].

[128] D. Friedan, E. J. Martinec, and S. H. Shenker, "Conformal Invariance, Supersymmetry and String Theory," Nucl. Phys. B **271** (1986) 93–165.

[129] E. P. Verlinde and H. L. Verlinde, "Chiral Bosonization, Determinants and the String Partition Function," Nucl. Phys. B **288** (1987) 357.

[130] A. D'Adda, M. A. Rego Monteiro, and S. Sciuto, "BRST Invariant N - Reggeon Vertex With Bosonized Ghosts," Nucl. Phys. B **294** (1987) 573–594.

[131] E. Witten, "The Feynman $i\epsilon$ in String Theory," JHEP **04** (2015) 055, arXiv:1307.5124 [hep-th].

[132] J. Polchinski, String theory. Vol. 1: An introduction to the bosonic string. Cambridge Monographs on Mathematical Physics. Cambridge University Press, 12, 2007.

[133] N. Seiberg and S. H. Shenker, "A Note on background (in)dependence," Phys. Rev. D **45** (1992) 4581–4587, arXiv:hep-th/9201017.

[134] J. L. Karczmarek, J. M. Maldacena, and A. Strominger, "Black hole non-formation in

the matrix model," JHEP **01** (2006) 039, arXiv:hep-th/0411174.

[135] L. Susskind, "Some speculations about black hole entropy in string theory," arXiv:hep-th/9309145.

[136] L. Susskind and J. Uglum, "Black hole entropy in canonical quantum gravity and superstring theory," Phys. Rev. D **50** (1994) 2700–2711, arXiv:hep-th/9401070.

[137] E. Witten, "Open Strings On The Rindler Horizon," JHEP **01** (2019) 126, arXiv:1810.11912 [hep-th].

[138] A. Dabholkar, "Strings on a cone and black hole entropy," Nucl. Phys. B **439** (1995) 650–664, arXiv:hep-th/9408098.

[139] Y. Hikida and V. Schomerus, "The FZZ-Duality Conjecture: A Proof," JHEP **03** (2009) 095, arXiv:0805.3931 [hep-th].

[140] A. Maloney, A. Strominger, and X. Yin, "S-brane thermodynamics," JHEP **10** (2003) 048, arXiv:hep-th/0302146 [hep-th].

[141] A. Almheiri, X. Dong, and B. Swingle, "Linearity of Holographic Entanglement Entropy," JHEP **02** (2017) 074, arXiv:1606.04537 [hep-th].

[142] P. Gao, D. L. Jafferis, and A. C. Wall, "Traversable Wormholes via a Double Trace Deformation," JHEP **12** (2017) 151, arXiv:1608.05687 [hep-th].

[143] S. Collier, P. Kravchuk, Y.-H. Lin, and X. Yin, "Bootstrapping the Spectral Function: On the Uniqueness of Liouville and the Universality of BTZ," arXiv:1702.00423 [hep-th].

[144] N. Vilenkin and A. Klimyk, Representation of Lie Groups and Special Functions, Volume 1: Simplest Lie Groups, Special Functions and Integral Transforms. 1991.

[145] G. Giribet, "Scattering of low lying states in the black hole atmosphere," Phys. Rev. **D94** no. 2, (2016) 026008, arXiv:1606.06919 [hep-th]. [Addendum: Phys. Rev.D94,no.4,049902(2016)].

[146] R. Ben-Israel, A. Giveon, N. Itzhaki, and L. Liram, "On the black hole interior in string theory," JHEP **05** (2017) 094, arXiv:1702.03583 [hep-th].